# Quantitative Investigation of Univariate Time Series Behavior in Financial Markets

YAOYUE TANG

Supervisor: Michael Harré
Associate Supervisor: Itai Einav

A thesis submitted in fulfilment of
the requirements for the degree of
Doctor of Philosophy

School of Computer Science
Faculty of Engineering
The University of Sydney
Australia

1 August 2024

## Statement of originality

This is to certify that to the best of my knowledge, the content of this thesis is my own work. This thesis has not been submitted for any degree or other purposes.

I certify that the intellectual content of this thesis is the product of my own work and that all the assistance received in preparing this thesis and sources have been acknowledged.

Date: 31 July 2024

Yaoyue Tang

## Authorship attribution statement

This thesis includes materials that have been previously published or submitted for publication.

Chapter 2 of this thesis is published as: Karina Arias-Calluari, Morteza. N. Najafi, Michael S. Harré, Yaoyue Tang, Fernando Alonso-Marroquin, 'Testing stationarity of the detrended price return in stock markets', *Physica A: Statistical Mechanics and its Applications*, Volume 587, 2022, 126487, ISSN 0378-4371, https://doi.org/10.1016/j.physa.2021.126487.

I co-designed the data analysis with the co-authors, collaborated with the co-authors in analyzing the data, contributed to writing Sections I, III, and Appendix C, and the interpretation of the results was incorporated into the conclusion.

Chapter 3 of this thesis is submitted as: Yaoyue Tang, Karina Arias-Calluari, Michael S. Harré, Fernando Alonso-Marroquin, 'Stylized Facts of High-Frequency Bitcoin Time Series', arXiv preprint arXiv:2402.11930.

I designed the study, conducted the analysis, and wrote the manuscript.

Chapter 4 of this thesis is published as: Yaoyue Tang, Fatemeh Gharari, Karina Arias-Calluari, Fernando Alonso-Marroquin, Morteza. N. Najafi, 'Variable-order porous media equations: Application on modeling the S&P500 and Bitcoin price return', *Physical Review E*, 109, 024310, https://doi.org/10.1103/PhysRevE.109.024310

I am the first author of this paper, and I co-designed the study with the co-authors, collaborated with the co-authors on the analysis of both the stock market and cryptocurrency, and wrote the related sections.

Chapter 5 of this thesis is ready to be submitted as a publication.

I designed the study, conducted the analysis, and co-wrote the related sections.

In addition to the statements above, in cases where I am not the corresponding author of a published item, permission to include the published material has been granted by the corresponding author.

Date: 31 July 2024
Yaoyue Tang

As the supervisor for the candidature upon which this thesis is based, I can confirm that the authorship attribution statements above are correct.

Date: 31 July 2024
Dr. Michael Harré

# Abstract

This thesis contributes to a growing body of work in statistical analysis of univariate time series in financial markets, bridging the conventional markets, such as the S&P500 index, with emerging digital assets like Bitcoin cryptocurrency. The research focuses on understanding the effects of deterministic factors and market volatility.

We first develop governing equations to describe the S&P500 price return, utilizing a $q$-Gaussian diffusion process that exhibits fractional, non-linear diffusion characteristics. This approach decomposes time series into deterministic trends and stochastic fluctuations. The application of this $q$-Gaussian model provides a better fit for describing return fluctuations.

The comparative analysis extends to Bitcoin price returns, revealing stylized facts similar to conventional markets, including heavy tails, self-similarity, volatility clustering, and short-time autocorrelation. The $q$-Gaussian process effectively describes the anomalous diffusion in Bitcoin price returns, presenting a power-law decay in terms of volatility against diffusion time.

The temporal evolution of exponents characterizing anomalous characteristics is explored, deriving a specific category of solutions for variable order nonlinear Fokker-Planck equations, formulated as variable order $q$-Gaussian functions. The variable order diffusion process is governed by the Central Limit Theorem, transitioning from a $q$-Gaussian to a Gaussian distribution over time, providing a more robust model for real-world financial systems.

Finally, this thesis investigates non-stationary effects in price return for both markets. Results highlight that localized stationarity can be achieved by truncating the time series into segments, and for each segment, removing the trend and volatility of the price return is required. Moreover, we demonstrate that external events can significantly impact market statistics.

## Acknowledgements

I express my deepest gratitude to my supervisor, Dr. Michael Harré, for the support, guidance, and expertise, which has been invaluable throughout the entire process of this thesis. Thank you for all your ideas, discussions, compassion, and care you have shown.

Many thanks to Prof. Constantino Tsallis, for providing me with the opportunity to participate in the conference in Brazil, where inspiring discussions added different perspectives to this thesis.

Many thanks to Dr. Fernando Alonso-Marroquin, Dr. Morteza Nattagh-Najafi, Prof. Itai Einav, Dr. Benjy Marks, Dr. Faham Tahmasebinia, Prof. Tim Wilkinson, for sharing their knowledge and insights during my academic journey.

Many thanks to Dr. Karina Arias-Calluari, for her kind heart, extensive knowledge, unwavering support, and indispensable mentoring every step of the way.

To my research group and friends Dr. Leonardo Crespo, Dr. Miaoyan Pang, Dr. David Riley, Dr. Jiale Zhu, Chen Chen, Weiyi Wang, Fiona Fong, Honey Thomas, Andrés Escobar, Jacob Elmasry, Dr. Yutaka Tsumura, Jiawe Tu and everyone in room 101 and 322, for the collaborative spirit, and for the joyful moments we shared.

To my family, my mom Deng Ming, my aunt Deng Ying, and my cousin Pan Ran, for the unconditional loving support, for constantly believing in my abilities, and for the understanding and hope you always had towards me.

A special thanks to Yong King Yau, Dough, and Bobo, for your patience, support, and company, for enduring my crankiness, and for encouraging me through the hard times.

Finally to myself for not giving up, despite all the struggles.

# Contents

# List of Figures

CHAPTER 1

# Introduction

---

This thesis focuses on exploring the statistical properties of univariate time series found in financial economics, namely the price returns. It aims at understanding and analyzing the trends and patterns in price return over time, both in the traditional stock market represented by the S&P500 index and the digital asset of Bitcoin cryptocurrency. The financial market is a dynamic system where buyers and sellers engage in interactions and respond to external information, which leads to the agreement of the price for assets (Mantegna and Stanley 1999). These interactive trading activities result in a continuous time, discrete event, stochastic arrival process of index values, which are pre-processed into evenly-spaced discrete time intervals that are analyzed in this work. Modeling market price changes is always of great interest to researchers. Analyzing the time series of price fluctuations can provide a better understanding of the properties of asset returns and allow us to develop predictive models and test the applications of the models to empirical data.

The price of a financial asset fluctuates over time, giving rise to a stochastic process, which is a statistical concept used to describe the evolution of a random variable over time. Various models have been proposed to describe the stochastic process. In recent years, the market has seen fluctuations on more significant scales, necessitating a comparative empirical study of its statistical characteristics across varying periods. This thesis analyzes the properties of price returns for two financial time series. Most financial studies focus on price returns instead of prices of assets for two reasons. Firstly, since the size of the investment does not affect price changes, returns can provide a complete and consistent summary of the investment opportunity (Campbell et al. 1997). Secondly, returns present more attractive statistical properties than prices, including stationarity (Campbell et al. 1997).

The organization of this chapter is as follows. Section 1.1 reviews the historical foundations of statistical methods in financial economics. Section 1.2 provides insight into the current state of this field of study, presenting more recent results related to market dynamics of both the S&P500 and Bitcoin price returns. Section 1.3 discusses some open questions in financial economics and how they are addressed in this thesis. This includes stochastic diffusion equations derived to describe the price return, the comparative analysis of the statistical properties of Bitcoin and the S&P500, the time-dependent diffusion model for the evolution of the probability distribution function (PDF) of price return, as well as the comparative analysis of the stationarity of Bitcoin and the S&P500 price return.

## 1.1 Historical foundations of financial fluctuations

There exists an open question among academics and investors: *To what extent can the preceding historical record of a stock's price be used to meaningfully estimate the future statistical properties of a market index?* This question has persisted for a long time, and various models have been proposed with different capabilities in describing price fluctuations in the market.

Pioneering work in the field of financial modeling dates back to Louis Bachelier in 1900. Bachelier (Bachelier 1900) introduced the first option pricing model for speculative markets in his doctoral thesis, using a Brownian motion model. The Brownian motion model is named after the British botanist Robert Brown, who observed the random trajectories of pollen immersed in water (Brown 1828a; Brown 1828b). The random movements of particles from regions of high concentration to low concentration without external force result in the diffusion process, which ultimately yields a state of uniform dispersion through the gradual blending (Metzler et al. 1999; Metzler and Klafter 2000). In 1905, the work of Einstein (Einstein 1905) established a mathematical model conceptualizing Brownian motion as a random trajectory characterized by a mean square displacement: $\langle(\Delta x)^2\rangle = 2dDt$, where $\Delta x$ is the displacement of the Brownian particle in a certain time interval $t$, $d$ is the spatial dimension and $D$ is the diffusion coefficient (Vainstein et al. 2006). Einstein then deduced the famous Einstein-Stokes relation (Einstein 1908; Einstein 1956) to define the diffusion constant $D$ using Avogadro's number with suggestions for the experimental verification of his theory. The outcomes of Einstein's research resulted in an early confirmation of the molecular theory of matter, where the French physicist Jean Baptiste Perrin experimentally determined Avogadro's number. Perrin was awarded the Nobel Prize in Physics in 1926 in recognition of his contributions.

The Brownian motion model, also known as the Einstein-Wiener process (Renn 2005) is one of the most important models in the theory and application of stochastic processes. It describes the diffusion process using the differential equation:

$$\frac{\partial P(x,t)}{\partial t} = D\frac{\partial^2 P(x,t)}{\partial x^2}, \tag{1.1}$$

where $x$ is the random variable, $t$ is the time interval, $D$ is the diffusion coefficient, and $P(x,t)$ is the time-dependent probability density function (PDF) governing the distribution of the random variable $x$. The solution to the differential equation leads to a normal (Gaussian) distribution for the PDF:

$$P(x,t) = \frac{1}{\sqrt{2Dt}}g\left(\frac{x}{\sqrt{2Dt}}\right),\ g(x) = \frac{1}{\sqrt{\pi}}e^{-x^2}. \tag{1.2}$$

Besides the contributions of Einstein, Langevin (Langevin 1908) proposed a distinct and innovative approach to describe Brownian motion by using the concept of a stochastic force (Metzler et al. 2014). Langevin's approach is based on what is nowadays called the stochastic differential equation, or Langevin equation, given by:

$$m\frac{dv}{dt} = -\lambda v + \eta(t), \tag{1.3}$$

where $m$ is the mass of the particle, $v$ is the velocity, $\lambda$ is the damping coefficient, and $\eta(t)$ is the noise term that follows the Gaussian normal distribution. In its application to financial time series, the Langevin equation can be written as:

$$\frac{dx}{dt} = \mu(x,t) + \sigma(x,t)\eta(t), \tag{1.4}$$

where $x$ represents the price return, $\mu$ is the mean values of the return, and $\sigma$ is the standard deviation of return.

The Brownian motion model holds fundamental importance in modern approaches to stochastic process modeling. However, it was later found to be inadequate to describe financial markets. Empirical studies of financial markets have found that price changes more closely follow a stable Paretian power-law distribution, with infinite variance (Mandelbrot and Taylor 1967). Therefore, alternative models were proposed to improve their ability to capture the statistical characteristics of the markets.

Since Louis Bachelier introduced the Gaussian distribution model for speculative market price fluctuations, more attention has been given to price changes in commodity and stock markets. Empirical evidence supporting the Gaussian distribution model includes the study of Kendall (Kendall and Hill 1953) where he observed “approximately" normal distribution in the price change for Chicago wheat and British common stocks. However, with the analysis performed on the abundant empirical data accumulated, the distributions of price changes were found to be “peaked” at the center, and extreme tails are higher than normal distributions. Mandelbrot (Mandelbrot 1963) analyzed the price fluctuation of the cotton price changes between 1816 and 1958 and found that the tail behavior is a power-law distribution with an exponent of $\alpha = 1.7$. He proposed the substitution of the Gaussian distribution with another set of probability laws, known as the “stable Paretien”, which was initially defined in the work of Paul Lévy (Lévy 1954; Gnedenko and Kolmogorov 1968; I cite this as an English version of the derivations). The Lévy stable distribution model is a generalization of the Brownian motion model, and the slope of the tails is characterized with the parameter $\alpha \in (0, 2]$ (Mandelbrot 1963). This study is the first acknowledgment of fat-tailed distributions in financial economics, and the fat tails indicate a higher likelihood of extreme events than the predictions made by a normal distribution (Stanley et al. 2002; Stoyanov et al. 2011). Lévy stable processes follow a generalized central limit theorem, and the shape of the probability distribution of Lévy stable processes presents power-law tails. The Lévy-stable distribution is given as the inverse Fourier transform of the characteristic function:

$$f(x;\alpha,\beta,\rho,\mu) = \frac{1}{2\pi}\int_{-\infty}^{\infty}\phi(t;\alpha,\beta,\rho,\mu)e^{-ixt}dt, \tag{1.5}$$

where $\phi(t)$ is given in Sec. 34 in the book of Gnedenko and Kolmogorov (Gnedenko and Kolmogorov 1968) as:

$$\phi(t;\alpha,\beta,\rho,\mu) = \exp(it\mu - |\rho t|^{\alpha}(1 - i\beta\mathrm{sgn(t)}\Phi)). \tag{1.6}$$

where $\alpha \in (0, 2)$, $\beta \in [-1, 1]$ is the skewness parameter that measures the asymmetry of the distribution, $\rho \in (0, \infty)$ is the scale parameter, and $\mu \in (-\infty, \infty)$ is the location parameter. Here $\alpha$ is the characteristic exponent of the distribution, measuring the magnitude of the extreme tail of the distribution, and $\alpha = 2$ recovers the Gaussian distribution.

Mandelbrot derived a simplified version for the PDF of Lévy stable distribution, given by (Mandelbrot 1967):

$$P_{\alpha}(x) = \frac{1}{\pi}\int_{0}^{\infty}\exp(-\gamma t^{\alpha})\cos(tx)\,dt, \tag{1.7}$$

where $P_{\alpha}(x)$ is the stationary PDF of random variable $x$, $t$ is the time interval, $\gamma$ is a scale parameter, and $\alpha \in (0, 2)$ is the characteristic exponent of the distribution, measuring the magnitude of the extreme tail of the distribution.

An important characteristic of the Lévy stable distribution is its infinite variance, indicating the non-Gaussian nature of the probability distribution of empirical data. Bachelier's Brownian motion model assumes that the price returns are random variables with statistically independent and identical distributions, following a Gaussian distribution with zero mean and finite variance. Some important properties of the Brownian motion model include statistical stationarity and self-similarity in the price increments. Stationarity in price return indicates a condition where samples of Brownian motion, taken over equal time increments, exhibit a constant mean and standard deviation. Self-similarity indicates that samples of Brownian motion have the statistical characteristic that a scaling in time is equivalent to a scaling in state space. The Lévy stable distribution model preserves the principles of stationarity and self-similarity. Additionally, it takes into account characteristics such as fat-tailed return distributions and the presence of long-term dependence (Mandelbrot 1997). Further investigations have also shown that empirical distributions of financial returns (and log-returns) often deviate from the normal Gaussian distribution, displaying pronounced heavy tails (Cont 2001). Mandelbrot's subsequent analysis on wheat price in Chicago, railroad stocks price, and exchange rates reported power-law tails with $\alpha \in [1, 2]$ (Mandelbrot 1967). Another study examining the daily log returns on thirty stocks in the Dow Jones Industrial Average also reported long-tailed distributions with $\alpha < 2$ (Fama 1963), indicating that the Lévy stable distribution offers a more accurate representation of the data compared to the Gaussian distribution.

The Lévy distribution is well-suited for financial markets as it can capture abrupt changes in the market. These changes signify that markets present higher risks compared to what is described by a Gaussian distribution model. Following the study of Mandelbrot, Mantegna and Stanley (Mantegna and Stanley 1994) introduced the truncated Lévy flight (TLF) where the arbitrarily large steps of a Lévy flight are eliminated, and the tails become approximately exponential. The truncated Lévy flight exhibits finite variance and allows a slow convergence to a Gaussian distribution, as implied by the Central Limit Theorem (Matacz 1997; Kamaruzaman et al. 2013). Results demonstrate a well-defined crossover between Lévy and Gaussian regimes with increased time intervals (Mantegna and Stanley 1994). Inspired by these results, Koponen (Koponen 1995) derived an analytical form for the characteristic function of a truncated Lévy distribution with an exponential cutoff in the tails. These theoretical results have led to several empirical studies, all supporting the TLF as a simple and effective model for financial data (Ncheuguim et al. 2014; Mantegna and Stanley 1995; Mantegna and Stanley 1996; Mantegna and Stanley 1997).

In 1973, a pricing model for financial markets that considers the impact of time and risk factors was formulated. This is the Black-Scholes model that has significantly influenced contemporary financial theory. Although the Brownian motion model was widely acknowledged, its applicability is constrained by the potential occurrence of negative values in stock prices within this model. Furthermore, the risk premia were not adequately addressed in the Brownian motion model. Therefore, an alternative form of the Brownian motion model was introduced as a significant advancement in financial price modeling. This non-negative variation is known as the geometric Brownian motion model proposed by Black and Scholes in 1973 (Black and Scholes 1973). The Black-Scholes equation (BSE) was introduced as the governing equation of the price evolution of a European call option (Black and Scholes 1973). The BSE is a partial differential equation (PDE) that is regarded as the fundamental framework for mainstream contemporary financial asset modeling. The BSE describes the following relationship:

$$\frac{\partial V}{\partial t} + \frac{1}{2}\sigma^2 S^2 \frac{\partial^2 V}{\partial S^2} = rV - rS\frac{\partial V}{\partial S}, \tag{1.8}$$

where $V$ is the price of the option, $S$ is the price of the underlying asset, $\sigma$ is the standard deviation of the returns of $S$, $r$ is the annual interest rate. In contrast to Bachelier's model, where the price fluctuations follow a Gaussian distribution, the distributions by the Black-Scholes model are replaced with log-normal distribution. Under the framework of geometric Brownian motion, the differences between logarithmic prices are Gaussian distributed. A stochastic process $S_t$ following the geometric Brownian motion satisfies the stochastic differential equation:

$$dS_t = \mu S_t dt + \sigma S_t dW_t, \tag{1.9}$$

where $W_t$ is the Brownian motion, $\mu$ stands for the drift and $\sigma$ is the volatility. $S_t$ follows a log-normal distribution, and the PDF of $S_t$ is given by:

$$P(x) = \frac{1}{x\sigma\sqrt{2\pi}}\text{exp}(-\frac{(\text{log}x - \mu)^2}{2\sigma^2}). \tag{1.10}$$

The Black-Scholes model suggests that financial instruments will exhibit a log-normal distribution of prices as they follow a random walk process with a consistent drift and volatility. The BSE provides a theoretical estimate for the price of European-style options. It illustrates that the option has a distinct price determined by the security's risk and its expected return. The Nobel Prize in Economics in 1997 was awarded to to Merton and Scholes for their contributions to the Black-Scholes model. The pioneering work of Black and Scholes offers a framework for option pricing, which allows traders and investors to determine the price of an option through a definitive structured methodology that has been tested. Moreover, it enabled risk management more efficiently, allowing investors to assess potential returns as well as understand vulnerabilities within their investment portfolio.

The models widely used in the 20th century hold the belief that the contribution of each individual day to the changes in price is negligible (Mandelbrot 2001). Modern portfolio theory aims to optimize returns while maintaining a given level of risk, and it considers significant price drops in the market to be very unlikely or impossible to incorporate (Mandelbrot 1999). However, empirical evidence has contradicted this notion, as there have been a considerable number of sudden and substantial changes in the market (Sornette 2003). Moreover, the extent of price movements, whether large or small, may remain relatively stable for a year, and then experience a sudden increase in variability for an extended period of time (Mandelbrot 2001). Mandelbrot (Mandelbrot 1963) identified the clustering characteristic in volatility, denoting the tendency for significant fluctuations in prices to cluster together, leading to a sustained pattern of the amplitude of price variations. Therefore, the incorporation of an alternative model becomes necessary to include a more realistic depiction of market risks. Empirical evidence of the market has suggested that volatility clustering in the financial market may lead to the long-range memory of the volatility time series (Oh et al. 2008; Niu and Wang 2013). This long-range memory can be detected using the Hurst exponent, $H$ (Lo 1991; Granero et al. 2008). Hurst exponent is introduced initially in hydrology by Harold Edwin Hurst (Hurst 1951) for reservoir control for the Nile River Dam. Hurst exponent is connected with the autocorrelation of time series, and it quantifies the relative tendency of a time series to regress to the mean, or to cluster in a certain direction (Kleinow 2002). The range of Hurst exponent is $0 < H < 1$, where values within $0 < H < 0.5$ indicate anti-correlation time series and $0.5 < H < 1$ denote persistence with long memory effects (Kale and Butar Butar 2011; Sánchez-Granero et al. 2012). This long-range memory has been observed to exhibit a connection with scaling and fractal behavior (Mandelbrot 1982; Samorodnitsky et al. 2007).

Mandelbrot (Mandelbrot 1982) studied fractal geometry in coastlines and the distribution of galaxies, suggesting the possible implications of fractals in financial economics. Fractal structures, also known as scale-invariant structures, are widely found in geology (Mandelbrot 1982; Turcotte 2003), natural waves (Addison 1997), neuronal and physiological responses (Kantelhardt et al. 2002c; Ihlen 2012). In these instances, the structure demonstrates a fragmented nature and replicates its geometric form on smaller intervals or subdivisions of the object or signal (Chen et al. 2016a). A fractal system is usually described by a scale-invariant parameter called fractal dimension ($D$) (Mandelbrot 1982), which is related to the Hurst exponent, $H$. The model proposed in 1997 is considered in continuous time and comprises a Brownian motion that follows a 'multifractal trading time' (Mandelbrot 1997). This model is known as the fractional Brownian motion (fBm) model for $H \neq 1/2$, and it recovers the Brownian motion with $H = 1/2$. The fBm process is defined as (Mandelbrot and Van Ness 1968):

$$B_H(t) = \frac{1}{\Gamma(H + \frac{1}{2})} \int_0^t (t - \tau)^{H-1/2} dB(\tau), \tag{1.11}$$

where $H$ is the Hurst exponent in $(0, 1)$, $B(\tau)$ is a white noise.

A fractal market model implies that fluctuations of a stock or currency exhibit a similar pattern when a market chart is enlarged or reduced to fit the same time and price scale, and it presents both self-similarity and long-range dependence (Mandelbrot 1997). The fractional Brownian model provides a more realistic prediction of price fluctuations in the market by estimating the probability of market changes. Similar to the classical Brownian motion, the distribution pattern of a fractional Brownian motion also follows a Gaussian distribution, without heavy tails (Evertsz 1995). The primary difference between the fractional Brownian motion model and a classical Brownian motion model lies in the fact that the increments in the classical Brownian motion model are independent, whereas the increments in the fractional Brownian motion model are not. Instead, it shows long-range dependence and is indicated in the power-law autocorrelation with varying values of $H$. When $0 < H < 1/2$, the autocorrelation of the increments is negative, whilst the autocorrelation of the increments is positive when $1/2 < H < 1$. In comparison to the proposed models in terms of price change $\Delta x$ over a time increment $\Delta t$, the classical Brownian motion model uses $\Delta x = \sqrt{\Delta t} = \Delta t^{1/2}$, the Lévy stable model gives $\Delta x \sim \Delta t^{1/\alpha}$, and the fractional Brownian motion model uses $\Delta x \sim \Delta t^{H}$, with all the exponents being time-invariant.

In financial market modeling, the evolution of the probability distribution function (PDF) is of great interest. A notable contribution to the field of stochastic motion theory was made by Smoluchowski (Smoluchowski 1916), who proposed the Smoluchowski equation to describe the movement of a diffusive particle under the influence of an external drag force field. Smoluchowski's work is also known as the Fokker-Planck equation, which can be used to describe the evolution of stochastic systems. It is a partial differential equation that describes the temporal evolution of the PDF, given by (Plastino and Plastino 1995; Risken 1996; Salinas 2001; Frank 2005; Oliveira et al. 2019):

$$\frac{\partial}{\partial t}P(x,t) = -\frac{\partial}{\partial x}[\mu(x,t)P(x,t)] + \frac{1}{2}\frac{\partial^2}{\partial x^2}[D(x,t)P(x,t)] \tag{1.12}$$

where $\mu$ is the drift coefficient, $D$ is the diffusion coefficient, and $P(x,t)$ is the probability density of the random variable $x$. PDFs derived from the linear Fokker-Planck equation typically follow a Gaussian distribution, which often fails to describe the financial market, especially when considering the heavy-tailed non-Gaussian distribution model of the markets (Aljethi and Kılıçman 2023). Alternatively, the non-linear Fokker-Planck equation was proposed with fractional derivatives as a generalization of the linear model to describe the time evolution of the PDF of price return (Borland 2002a; Borland 2002b), given by:

$$\frac{\partial}{\partial t}[P(x,t)]^{\mu} = -\frac{\partial}{\partial x}\mu(x,t)[P(x,t)]^{\mu} + D\frac{\partial^2}{\partial x^2}[P(x,t)]^{\nu} \tag{1.13}$$

where $\mu = 1$ is commonly used for simplicity. Various values of $\nu$ have been observed in different systems (Tsallis and Bukman 1996), and here we follow the Tsallis nonextensive thermostatistics (Tsallis 1988; Tsallis et al. 2003), where the diffusion equation can be written as:

$$\frac{\partial P(x,t)}{\partial t} = D\frac{\partial^2 P(x,t)^{2-q}}{\partial x^2}, \ q \in [-\infty, 3) \tag{1.14}$$

The solution of the diffusion equations leads to the following PDF:

$$P(x,t) = \frac{1}{\sqrt{3-q}(Dt)^{\frac{1}{3-q}}} g_q\left(\frac{x}{\sqrt{3-q}(Dt)^{\frac{1}{3-q}}}\right),$$
$$g_q(x) = \frac{1}{C_q}e_q(-x^2), \quad e_q(x) = [1+(1-q)x]^{\frac{1}{1-q}}, \ Cq = \sqrt{\frac{\pi}{q-1}}\frac{\Gamma((3-q)/(2(q-1)))}{\Gamma(1/(q-1))}, \tag{1.15}$$

which is a $q$-Gaussian distribution with fat-tails for $q > 1$. For the special case when $q = 1$, the $q$-Gaussian distribution aligns with the Gaussian distribution, and this recovers the standard Black-Scholes stock-price model. The $q$-Gaussian distribution follows a generalized $q$-Central Limit Theorem, which is defined with correlated random variables. This is different from the classical Central Limit Theorem, which requires the random variables to be independent (Umarov et al. 2008; Umarov and Constantino 2022).

Tsallis nonextensive thermostatistics was introduced in 1988 as a basis for generalizing the standard statistical mechanics (Tsallis 1988), and it was later found to be a suitable model for the financial market. Whilst the geometric Brownian motion model and Lévy stable model had some success in describing market price movements, empirical evidence shows that there are some cases where these models are inadequate, and the slope of the power-law tails falls outside Lévy regime (Müller et al. 1990; Lux 1996; Gopikrishnan et al. 1998; Stanley et al. 2000). For instance, Gopikrishnan *et al.* (Gopikrishnan et al. 1998) analyzed data from three major US stock markets over a two-year period and identified a tail slope of $\alpha = 3.1 \pm 0.03$ for the positive tail and $\alpha = 2.84 \pm 0.12$ for the negative tail. Another study conducted two independent analyses with large-scale data (Plerou et al. 1999). The datasets used for the analyses consist of 40 million records covering a two-year period of 1994 to 1995 for all trades at the three major U.S. stock markets (the New York Stock Exchange (NYSE), the American Stock Exchange (AMEX), and the National Association of Securities Dealers Automated Quotation (Nasdaq)), as well as 35 million daily records for approximately 16,000 companies over a longer period of 35 years from 1962 to 1996 (Plerou et al. 1999). The findings of this study revealed that the distribution tails can be described by a power-law decay. This decay was characterized by an exponent ranging from $2.5 < \alpha < 4$, which falls outside the stable Lévy regime of $0 < \alpha < 2$ (Plerou et al. 1999). These findings underscore the necessity of alternative distribution models for a more accurate description of market behavior. As a response, Tsallis's $q$-Gaussian distribution model was proposed and applied to the empirical analysis of financial markets as an improved fit to return distributions(Tsallis 1988; Borland 1998; Tsallis et al. 2003). Later, a unified model was proposed for the distributions with asymptotic power-law decay called the $(q, \alpha)$-stable distribution, with $(1, \alpha)$-stable recovers the standard Lévy distribution and $(q, 2)$-stable corresponds to the $q$-Gaussian distribution (Umarov et al. 2010; Tsallis and Arenas 2014; Umarov and Constantino 2022). Empirical evidence has demonstrated that the $q$-Gaussian distribution model with fat tails at $q > 1$ is capable of effectively modeling real data (Borland 2002a; Borland 2002b).

In this section, we reviewed the historical developments of financial modeling since 1900, covering the significant breakthroughs in producing accurate descriptions of market fluctuations. The development of these models set the cornerstones for modern financial economics. In the next section, we will review more recent developments in financial modeling, as well as the applications of the models to empirical data, providing insight into the research focus of this thesis.

## 1.2 Current state of financial modeling

In recent years, a substantial research effort has been devoted to modeling the distribution of market returns, considering their non-linearity and non-stationarity characteristics.

The $q$-Gaussian distribution has been applied to model empirical data and has demonstrated itself as a suitable option for describing the financial market. Borland found that using $q = 1.5$, the $q$-Gaussian distribution model presents a good fit to the empirical distribution of price returns for S&P500 (Borland 2002b). More recent studies support the application of the $q$-Gaussian distribution model. Tsallis (Tsallis 2017) explored the $q-$statistics and the application on finance and economics by exploring the 10 top-volume stocks in the NYSE and in NASDAQ in 2001. Results present that $q-$Gaussian distribution can well-describe the log return of financial time series with $q = 1.4$. Ruiz (Ruiz and Marcos 2018) analyzed return distributions of the 100 companies traded on NYSE in 1998–1999 and found that the cumulative distribution of the absolute normalized returns can be described by the $q$-Gaussian distribution. Their result found that $q = 1.53$ for small time intervals, gradually decreasing to $q = 1.35$ at large time intervals (Ruiz and Marcos 2018). A study analyzing the S&P500 price return over a 22-year period also found that the $q$-Gaussian probability distribution function can well describe the S&P500 price return (Alonso-Marroquin et al. 2019). This study measured the non-Gaussian anomalous diffusion with the height of PDF, in which $P_{max} \sim t^{1/\alpha}$. Results show that the diffusion process can be characterized into two regimes, in which $\alpha = 1.26 \pm 0.04$ for a strong superdiffusion regime at small time intervals, and transits to a weak superdiffusion regime with $\alpha = 1.79 \pm 0.01$ at large time intervals (Alonso-Marroquin et al. 2019).

The application of non-linear Fokker-Planck equation in stock market time series to describe the anomalous diffusion process was improved by introducing a fractionalization scheme to the model, considering self-similarity of the time series (Gharari et al. 2021). Fractional calculus extends the meaning of derivatives of integral order $d^n y/dx^n$ to a positive real order. Riemann and Liouville attributed to the earliest systematic studies on fractional calculus and presented the so-called Riemann-Liouville fractional derivative (Ross 1974; Oldham and Spanier 1974; Samko et al. 1993). In recent decades, research on fractional calculus has shown its application in diverse scientific fields, including physics, chemistry, engineering, social sciences, and finance (Ross 1974). It can be used to model phenomena with memory or long-range dependence. The applications of fractional calculus range from diffusion and advection phenomena, to optimal control of fractional dynamic systems and to finance and economics (Ross 1974). Various derivatives for fractionalizing the PDE and these methods have shown their applications in financial modeling. In particular, the Karugampola fractional derivative operator has found its application in constructing the fractional porous media equation (PME), which can serve as the governing equation for analyzing the detrended price return of the S&P500 index (Alonso-Marroquin et al. 2019; Gharari et al. 2021; Arias-Calluari et al. 2021). However, the diffusion equations with constant order parameters may present limited validity in describing some diffusion processes, for example, the diffusion process in a porous medium. In financial analysis, more recent empirical evidence shown that constant order fractional partial equation does not fully capture the market dynamics. Analysis of stochastic fluctuations in the S&P500 price return found that the diffusion process can be described as a superdiffusive self-similar $q$-Gaussian process. The anomalous diffusion exponent $\alpha$ at small time intervals is found to be $\alpha > 2$ and $q > 1$, slowly converging to $\alpha \to 2, q \to 1$ (Arias-Calluari et al. 2021). These findings imply the necessity of models with variable order fractional derivatives for a more accurate description of the market dynamics.

In the preceding sections, we summarize the results of the extensive analysis conducted on conventional financial assets. With technological advances becoming integral to our personal and professional lives, digital assets have become more popular and valuable. The emergence of investable digital assets has captured the attention of both investors and academics. This thesis focuses on the comparative analysis between the conventional stock market, the S&P500, and the new digital asset, Bitcoin cryptocurrency. Bitcoin was first introduced by Satoshi Nakamoto in 2008 (Nakamoto 2008) and has expanded significantly, especially within the past five years. Cryptocurrencies operate by bypassing trusted third parties, such as traditional financial institutions, and instead rely on peer-to-peer networking and cryptography (Mukhopadhyay et al. 2016). This structure is known as the decentralized feature of cryptocurrency and is supported by the public ledger called the blockchain technology (Mukhopadhyay et al. 2016). The novelty of cryptocurrencies leads to immediate research interest in terms of the safety, ethical, and legal aspects of Bitcoin (Marian 2013; Brito et al. 2014; Böhme et al. 2015; Hendrickson and Luther 2017; Gross et al. 2017; Corbet et al. 2019). From a financial economics viewpoint, this new digital asset is also of great interest. The Efficient Market Hypothesis (EMH) was tested on cryptocurrency by measuring the Hurst exponent of the time series. The Efficient Market Hypothesis (EMH) postulates a capital market is efficient if it accurately and comprehensively incorporates all available information to determine security prices (Fama 1970; Malkiel 1989). Fama (Fama 1970) differentiates among three variants of efficiency, and the most commonly examined one is the weak efficiency form, in which the investors are unable to use historical data to predict future returns. The weak form EMH has been examined in the traditional assets (Kristoufek and Vosvrda 2014a), but less attention is given to Bitcoin (Urquhart 2016). The Hurst exponent ($H$) has gained considerable attention in empirical examinations of financial time series, particularly in the assessment of efficiency in financial markets and stock indices (Rejichi and Aloui 2012; Mynhardt et al. 2014; Kristoufek and Vosvrda 2014b). It serves as a metric for market memory due to its association with power-law autocorrelation (Gneiting and Schlather 2004; Vogl 2023). Market memory offers the potential for predicting future prices by analyzing past market behaviors. Markets characterized by limited or negligible memory exhibit higher randomness, suggesting unpredictability and thereby implying market efficiency. Therefore, a Hurst exponent approaching 0.5 substantiates market efficiency, while deviations from 0.5 suggest decreasing market efficiency (Mynhardt et al. 2014). The findings indicate that cryptocurrency markets tend to exhibit a general level of inefficiency (Urquhart 2016; Zhang et al. 2018b). Specifically for Bitcoin, the first study on the market efficiency of Bitcoin examined daily closing prices from 2010 to 2016, and reported the R/S Hurst exponent of $H = 0.353$ for the entire time period, rejecting the weak-form informational efficiency hypothesis (Urquhart 2016). However, when dividing the time series into two segments, from 2010 to 2013 and from 2013 to 2016, the R/S Hurst exponent shifts from $H = 0.363$ to $H = 0.406$, i.e. the Hurst exponent is a complex, non-stationary feature of markets as they evolve over time (Urquhart 2016). Subsequent investigations supported this claim through diverse testing methodologies, utilizing datasets encompassing various time intervals and frequencies (Kurihara and Fukushima 2017; Jiang et al. 2018; Caporale et al. 2018; Zhang et al. 2018a; Noda 2021). Employing a dataset of Bitcoin's returns from 2011 to 2017 using the DFA method for obtaining the Hurst exponent, another study highlighted that the Hurst exponent underwent notable changes as time progressed (Bariviera et al. 2017). In the early years of Bitcoin's existence, from 2011 to 2014, the average Hurst exponent was approximately $H = 0.6$, whereas after 2014, it dropped to $H = 0.5$ and fluctuated between [0.45, 0.55] (Bariviera et al. 2017). More recent studies in the cryptocurrency market have focused on changes in market efficiency before and after a significant event, namely the outbreak of the COVID-19 pandemic, yet the empirical evidence is bifurcated. Some studies assert that Bitcoin's growing efficiency with $H$ shifted from 0.6134 before to 0.5129 after Covid (Mnif et al. 2020; Mnif and Jarboui 2021). Conversely, some reported increased inefficiency after the pandemic. One study used the adjusted magnitude of market inefficiency (AMIM) criteria (Le Tran and Leirvik 2020) with a rolling window, and measured how often the markets are efficient throughout the considered period. They reported that Bitcoin was efficient for $65.9\%$ of the time in the pre-pandemic period, and only $4.19\%$ of the time in the post-pandemic period (Montasser et al. 2022). Specifically, a synthesis of empirical evidence points towards a scenario where Bitcoin experiences escalated inefficiency in the short term, coupled with signs of regained efficiency in the long term (Kakinaka and Umeno 2022).

Other research on cryptocurrency focuses on examining the price dynamics of cryptocurrency, as well as cross-correlations of cryptocurrency prices with other financial assets. Price fluctuations in cryptocurrency are more significant than those in traditional markets, indicating that the cryptocurrency market is more volatile with higher risk. Some studies examine price fluctuations of cryptocurrency through the interconnections between various cryptocurrencies and between cryptocurrency and exogenous classical market prices, including the stock market, gold, and crude oil prices (Conrad et al. 2018; Ciaian et al. 2018; Ariya et al. 2020; Klein et al. 2018). Studies observed strong connections between various cryptocurrency markets (Conrad et al. 2018; Ciaian et al. 2018), an inverse relationship between THB/USD exchange rate and Bitcoin prices (Ariya et al. 2020), and a significant positive correlation with gold price (Klein et al. 2018). Others focus on investigating price dynamics of cryptocurrency through the statistical characteristics of the market. These recurring statistical patterns, often termed 'stylized facts,' are consistently observed across diverse times and markets and serve as key summaries of market behavior (Cont 2001; Chakraborti et al. 2011). The concept of stylized facts, initially introduced in macroeconomics to describe statistical patterns characterizing macroeconomic growth over extended periods and diverse countries (Kaldor 1961), has become widely adopted in financial economics. The significance of analyzing stylized facts lies in establishing the foundation for the development of theoretical models and constructing econometric theories (Rydén et al. 1998; Liesenfeld and Jung 2000; Andersson 2001; Carnero 2004; Bulla and Bulla 2006; Malmsten and Teräsvirta 2010; Chakraborti et al. 2011). Examinations of Bitcoin and other cryptocurrencies reveal characteristics such as fat-tailed distributions, pronounced skewness and kurtosis, high volatility, and short-time return autocorrelations (Hu et al. 2019; De Sousa Filho et al. 2021; Cremaschini et al. 2023; Ghosh et al. 2023; Zhang et al. 2018a). Most of the literature focuses on daily price returns, yet it is noteworthy that these characteristics may differ when assessed using data of higher frequency. For instance, an analysis of Bitcoin's intraday returns identified a decline in volatility over time (Bariviera et al. 2017). Moreover, studies using higher frequency data have shown that the return distributions of Bitcoin exhibit heavier tails (De Sousa Filho et al. 2021). Considering the significant impact of high-frequency traders who exploit the rapid advancement in computing power, especially in the cryptocurrency market (Wen et al. 2022), investigating the intraday features of cryptocurrency time series emerges as a crucial endeavor. Furthermore, current literature examines the stylized facts of cryptocurrency mostly in a qualitative fashion, yet lacks a quantitative examination of these properties. In this thesis, we investigate the stylized facts of Bitcoin in terms of high-frequency intraday returns and conduct a comparative analysis of the statistical characteristics against the conventional market S&P500 price return.

This section summarizes more recent research findings focusing on financial economic modeling, as well as on the novel digital asset, cryptocurrency. The following section will introduce the focus of this thesis by briefly introducing the main idea of each chapter.

## 1.3 Contributions of this thesis

In summary, the aim of this thesis is to answer the following research questions: (1) Given the distinctive market formation process in Bitcoin, how do the statistical characteristics differ from those of conventional stock markets? (2) How can we derive a generalized non-linear fractional Fokker-Planck equation with variable orders that can be used as governing equations of the financial market? (3) How can the non-stationary effect of the market returns be considered in describing the PDF of returns? (4) Does the extent of non-stationarity vary among different types of financial assets and across different time periods?

To address these questions, this thesis begins by proposing a governing equation for stock market indexes in Chapter 2. The governing equation is formulated using a generalized porous media equation with drift considering the non-stationarity characteristics of market dynamics. We perform the Detrended Fluctuation Analysis on the S&P500 price return, and test the stationarity of the detrended price return following the Wiener–Khinchin theorem (Arias-Calluari et al. 2022).

In Chapter 3, we examine the stylized facts of Bitcoin price return. Stylized facts have been extensively studied in traditional financial markets, yet less attention has been given to new digital assets. Analyzing the stylized facts can establish the foundation for developing theoretical forecasting models and constructing econometric theories (Chakraborti et al. 2011). Since the market formation is significantly different in cryptocurrency market, a quantitative analysis comparing the statistical characteristics between cryptocurrency and conventional financial assets is necessary. Moreover, studies have found that some market measurements, such as the Hurst exponent, can change with different time periods. Therefore, this thesis investigates the stylized facts of Bitcoin price return across different time periods and explores the changes in the statistical characteristics (Tang et al. 2024a).

Chapter 4 derives the solutions to the variable order non-linear fractional Fokker-Planck equations. Since the constant order diffusion models are sometimes inadequate to describe the dynamics of the complex market system, variable order equations can provide more accurate models for price fluctuations. The variable order $q$-Gaussian functions are used and tested for the application to both conventional financial markets and cryptocurrency (Tang et al. 2024b).

To address the last research question in this thesis, we conducted a comparative analysis of the stationarity for both the S&P500 and Bitcoin price return in Chapter 5. By comparing the extent to which the stationarity is maintained with different detrending and normalizing parameters, we assess localized stationarity against global stationarity across various time periods.

The organization of this thesis is as follows. Chapter 2 derives the stochastic differential equation and tests the stationarity of the detrended S&P500 price return. Chapter 3 investigates the statistical characteristics of Bitcoin price return in terms of the 'stylized facts', and compares those to the observed properties in the S&P500 price return. In Chapter 4, we develop a solution of the non-linear porous media equation, with time-dependent exponents, and test the application to modeling the S&P500 and Bitcoin price return. In Chapter 5, the empirical comparison between the stationarity for Bitcoin and the S&P500 is conducted, exploring the local non-stationarity across different time periods. Finally, the conclusion section is presented, covering the significant findings of this research and suggesting possible directions for future research. (The appendices from the original publications are incorporated into their respective chapters, following the structure of the publications.)

CHAPTER 2

# Testing stationarity of the detrended price return in stock markets

---

The basis of the decomposition of the stock market indexes into a stochastic part and a drift term started with the BSE and its modified versions. Extensive research has been performed following the BSE to describe the price fluctuations, yet the limitation exists that the BSE assumes that the price return follows a Gaussian distribution. This limitation can be resolved by proposing a different stochastic process to model the price fluctuations. Empirical evidence has shown that $q$-Gaussian distribution is a good candidate.

This chapter proposes a generalized porous media equation with drift as the governing equation for stock market indexes. The proposed governing equation can be expressed as a Fokker-Plank equation (FPE) with a non-constant diffusion coefficient. The governing equation accounts for non-stationary effects and describes the time evolution of the probability distribution function (PDF) of the price return. By applying Ito's Lemma, the FPE is associated with a stochastic differential equation (SDE) that models the time evolution of the price return in a fashion different from the classical Black-Scholes equation. Both FPE and SDE account for a deterministic trend and a stochastic $q$-Gaussian noise. The presented model is validated using the intraday price return of the S&P500 index for a 25-year period. We show that the price return becomes stationary by normalizing the detrended data set. The normalization of the data is calculated by subtracting the trend and then dividing it by the standard deviation of the detrended price return. The stationarity test follows the Wiener–Khinchin theorem, which represents the power spectral density of a time series in terms of its Fourier transform of autocorrelation. Additionally, this paper presents the multifractal analysis for the detrended and normalized price return to describe the Hurst exponent dynamics over the dataset.

## 2.1 Introduction

Complex dynamic systems encountered in business (Box 2013), financial markets (Nava et al. 2016), genetics (Gu, Zhou et al. 2010; Peng et al. 1994), neuroscience (Márton et al. 2014; Oliveira Filho et al. 2019), biomedicine (Huang et al. 1998; Chua et al. 2010), ocean dynamics (Gay-Balmaz and Holm 2018) and seismology (Marano 2019) generate non-stationary time series. A time series is non-stationarity when it is non-identically distributed throughout their full length of time (Mandelbrot and Hudson 2010; Bahri and Sharples n.d.). In stock markets, these type of time series are simple price return (Politi et al. 2012; Nava et al. 2016; Bahri and Sharples n.d.; Maganini et al. 2018), volatility of index price (Roman et al. 2008) and stock market index (Ponta et al. 2019; Lan et al. 2010). In the statistical analysis of financial markets, the non-stationarity time series that is extensively analyzed is the simple price return, which is an arithmetical difference (Lan et al. 2010). For price return, the non-stationarity is produced by the non-constant activity during a trading day and the heterogeneity of market participants (Clara-Rahola et al. 2017; Nava et al. 2016).

The non-stationary time series are difficult to analyze because the process remains in a non-equilibrium state. Consequently, their models do not achieve optimal forecasting and control (Box 2013; Schmidt 2011). Therefore, it is challenging to obtain an accurate model that can be used to calculate the probability of future value based on initial conditions.

In recent years, extensive research has been devoted to model the index price return distributions considering its statistical features, and non-stationarity characteristics (Meng et al. 2015; Ahn et al. 2018; Meng et al. 2016). The Black–Scholes equation have been the governing equation to describe the characteristics of the stock return distribution (Marathe and Ryan 2005; Björk and Hult 2005; Chen et al. 2016b). This important model used the Geometric Brownian Motion (GBM) to model the index price return. However, it fails to capture the non-Gaussian properties of the price return (Chen et al. 2016b), negative skewness (Ahn et al. 2018), and negative values obtained from recent events (Walker 2020). As a result, different models started to appear, applying modifications or generalizations to the GBM. The Fractional Brownian Motion (FBM) (Ali and AL-Qazaz 2020), the Mixed Fractional

Brownian Motion (MFBM) as a combination of the Brownian motion with the FBM (Rao 2016), the Generalized Mixed Fractional Brownian Motion (GMFBM) (He and Chen 2014; Thäle 2009), and Fokker Planck Equation (Borland 2002a). These new models capture better the characteristic features of the index price return. However, some of them were developed considering a neutral risk assumption (He and Chen 2014; Michael and Johnson 2003). As an alternative to these traditional stock return models, an increasing number of quantum models have also been applied to study the stochastic dynamics of stock prices. The most well-known are; the Quantum Spatial-periodic Harmonic model (QSH) (Meng et al. 2015), the Quantum Brownian Motion model (QBM) (Meng et al. 2016), and the Quantum Harmonic Oscillator model (QHO) (Ahn et al. 2018). An advantage of these models is that they incorporate the market uncertainty (risk), although they have been derived from the stochastic equation of a Brownian process.

The contribution of this paper is the presentation of a simpler but more effective governing equation to model the non-stationarity of price return. This governing equation is constructed based on the decomposition of the time-series by a deterministic part or trend and a stochastic part or q-gaussian noise. The stochastic part adequately represents the stylized facts of the financial time series such as the fat-tailed distribution, aggregational normality and self-similarity with finite variance. Therefore, the stochastic part can be modeled by a self-similar q-Gaussian distribution centered on zero. To validate our governing equation, the trend of the S&P500 index data is removed by applying a moving average method (MA) based on the Kurtosis evaluation. By applying an arithmetical difference to the detrended S&P500 index data, the detrended price return is calculated. The detrended price return exhibits fat tails, short-term correlation and volatility clustering. The volatility clustering effect represents a non-constant standard deviation over the full length of the time series (Schmidt 2011). As a consequence, the detrended price return is non-identically distributed, and therefore, non-stationary. To remove the volatility clusters, we divided the detrended price return by the standard deviation, i.e. it was “standardized”. This process is called “normalization of the data set". We show that the normalized price return is a stationary process by applying the power spectral density theory. Hence, the detrended and normalized price return is identically distributed throughout their full length of time holding finite and time-invariant values of mean and variance.

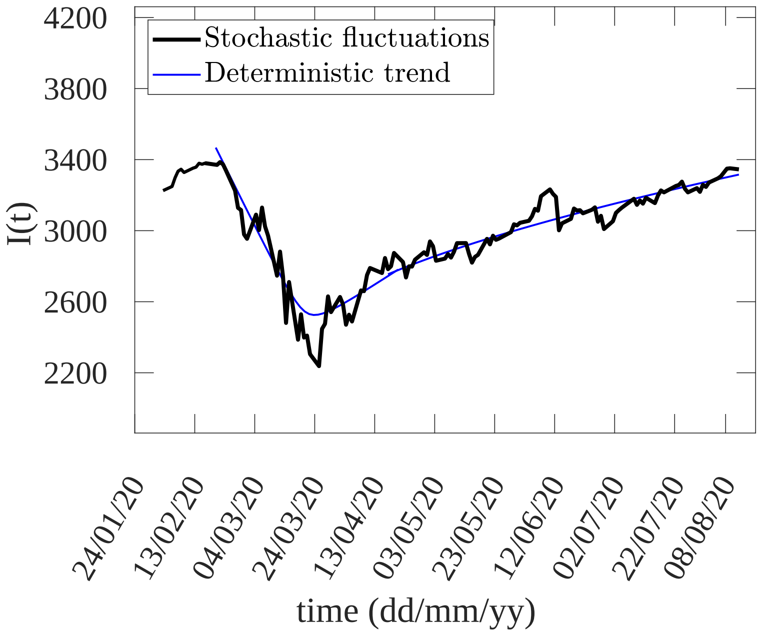


FIGURE 2.1: Schematic plot of a downward and upward swing in the S&P500. The index is decomposed into a deterministic trend (blue) and stochastic fluctuations (black).

Additionally, this paper presents the scaling analysis of the detrended price return and the normalized price return by estimating the Hurst exponent $H$ (Kantelhardt et al. 2002b). Time series are classified as monofractal or multifractal depending on how the Hurst exponent varies over several orders of magnitude (Gu and Zhou 2006). A time series is called monofractal if the Hurst exponent is constant for all the orders of magnitude, otherwise, it is called multifractal (Telesca et al. 2004).

This chapter is divided into four parts: In Section 2.2, the governing equation of the simple price return is presented. Section 2.3 presents a straightforward way to detrend the stock market price, based on the optimization of a moving window via the kurtosis evaluation. Then, the normalized price return is obtained right after dividing the detrended price return by the standard deviation. In Section 2.4, we perform the tests on the normalized price return to show that it is stationary. The test verifies that the power spectrum of the time series equals the Fourier transform of its autocorrelation (Witt et al. 1998; Ivanov et al. 2009) Section V, is based on the evaluation of the Hurst exponent in terms of the orders of the statistical moments of the time series. We provide the details of the Hurst exponent calculation and the characterization of the detrended price return. Finally, the conclusions and perspectives of this work are presented in Section 2.6.

## 2.2 Governing equation of price return

The conventional approach to option pricing analysis leads to the classical Black-Scholes equation or non-linear Black-Scholes equation (BSE) as the governing equation of price return (Barles and Soner 1998). A limitation of the BSE is the assumption that stock prices follow a geometric Brownian motion pattern, ignoring that prices can have sustained trends and even can reach negative values in the real indexes (Walker 2020). Our governing equation covers BSEs' limitations, allowing the price to fluctuate in a particular direction (trend) and incorporates stochastic or q-Gaussian noise. The q-Gaussian noise is a better descriptor of the fluctuations in stock markets (Alonso-Marroquin et al. 2019). For this analysis, the price return at time $t$ is defined as (Mantegna and Stanley 1995; Johnson et al. 2003; Voit 2005):

$$X(t_0, t) = I(t_0 + t) - I(t_0), \tag{2.1}$$

where $I(t_0)$ is the stock market index at time $t_0$, and $I(t)$ is the stock market index for any time $t > t_0$.

We assume that the stock market index $I(t)$ can be decomposed into a deterministic trend $\overline{I}(t)$ and a stochastic time series $I^*(t)$:

$$I(t) = \overline{I}(t) + I^*(t). \tag{2.2}$$

Then, the price return $X(t)$ is split into a deterministic $\overline{X}(t)$ component and stochastic or q-Gaussian noise $x(t)$:

$$X(t) = \overline{X}(t) + x(t), \tag{2.3}$$

where $\overline{X}(t) = \overline{I}(t_0 + t) - \overline{I}(t_0)$ and $x(t) = I^*(t_0 + t) - I^*(t)$. This equation can be written as a Stochastic Differential Equation (SDE)

$$dX(t) = d\overline{X}(t) + dx(t), \tag{2.4}$$

where $d\overline{X}(t) = \overline{I}(t+dt) - \overline{I}(t_0)$ and $dx(t) = I^*(t+dt) - I^*(t)$, and $dt$ is an infinitesimal time. Our aim is to find the components of this SDE. Based on previous work (Alonso-Marroquin et al. 2019), we postulate that the probability density function (PDF) of the detrended price return $x(t)$ is described by the functional form :

$$P(x,t) = \frac{1}{(Dt)^{1/\alpha}} \left[ g_q \left( \frac{x}{(Dt)^{1/\alpha}} \right) \right] \tag{2.5}$$

where $D$, $q$ and $\alpha$ are time-dependent fitting exponents, and $g_q(x)$ is the function so-called normalized q-Gauss distribution function. This distribution function is often used in the non-extensive statistical mechanics, because allows the generalization of Boltzmann entropy. The $g_q(x)$ is defined as: (Ruiz and Marcos 2018):

$$g_q(x) = \frac{1}{C_q} \left[ 1 - (1-q)x^2 \right]^{\dfrac{1}{1-q}}, \tag{2.6}$$

The normalization constant $C_q$ for $1 < q < 3$ is given by:

$$Cq = \sqrt{\frac{\pi}{q-1}} \frac{\Gamma((3-q)/(2(q-1)))}{\Gamma(1/(q-1))}. \tag{2.7}$$

Then, we apply the following change of variable $T = t^{\xi}$, where $\xi = \dfrac{3-q}{\alpha}$, in the governing equation of $P(x,t)$ [Eq.(12) from (Alonso-Marroquin et al. 2019)]. The corresponding Partial Differential Equation (PDE) is:

$$\frac{\partial P}{\partial T} = D^{\xi} \frac{\partial^2 P^{2-q}}{\partial x^2}, \tag{2.8}$$

where the difussion term is $D^{\xi}$. By applying Eqs. (2.3), (2.5),and (2.6), the PDF of price return $P(X,T)$ is:

$$P(X,T) = \frac{1}{(D^{\xi}T)^{1/(\xi\alpha)}} \frac{1}{C_q} \left[ 1 - (1-q) \frac{[X - \overline{X}(T)]^2}{(D^{\xi}T)^{2/(\xi\alpha)}} \right]^{\dfrac{1}{1-q}}. \tag{2.9}$$

Then, the chain rule is applied to obtain the governing equation of $P(X, T)$.

$$\begin{aligned}\frac{\partial^2}{\partial^2 x} &= \frac{\partial^2}{\partial^2 X} \\ \frac{\partial}{\partial T} &= \frac{1}{\xi} t^{1-\xi} \frac{\partial}{\partial t} + \frac{\partial \overline{X}(T)}{\partial T} \frac{\partial}{\partial X}\end{aligned} \tag{2.10}$$

By replacing Eq(2.10) in Eq(2.8), the general PDE can be defined considering that $\frac{t^{1-\xi}}{\xi} = \frac{\partial t}{\partial T}$ as:

$$\frac{\partial P}{\partial T} = D^{\xi} \frac{\partial^2 P^{2-q}}{\partial X^2} - \frac{\partial \overline{X}(T)}{\partial T} \frac{\partial P}{\partial X}. \tag{2.11}$$

The term $D^{\xi}$ is the diffusive parameter, which is independent on $X$. Consequently, a comparison between Eq(2.11) with the linear Fokker-Planck equation (LFPE) is made. The LFPE is :

$$\frac{\partial P(X,T)}{\partial \tau} = -\frac{\partial (D_1 P(X,T))}{\partial x} + \frac{\partial^2 (D_2 P(X,T))}{\partial x^2}, \tag{2.12}$$

After that, the diffusion coefficient in the LFPE is defined as: $D_2 = D^{\xi} P(X,T)^{1-q}$ . By replacing Eq(2.9) into this equation, we obtain an explicit expression for diffusion coefficient of the LFPE:

$$D_2 = D^{2/\alpha} C_q^{q-1} T^{(q-1)/(3-q)} \left[1 - \frac{(1-q)[X - \overline{X}(T)]^2}{(D^{\xi} T)^{2/(3-q)}}\right] \tag{2.13}$$

and the drift term is:

$$D_1 = \frac{\partial \overline{X}(t)}{\partial T} \tag{2.14}$$

The drift term is the overall direction of the index price showing particular tendencies (trend). The trend is associated with the systematic risk response, where external events can produce a change of trend direction (Arias-Calluari et al. 2022). This feature implies that future price changes are dependent on past values and therefore it is possible to develop a forecast in the short term with some degree of confidence.

The Fokker–Planck equation in Eq. (2.12) is used to obtain the probability distribution of price return at any time. The stochastic differential equation (SDE) represents the dynamics of price

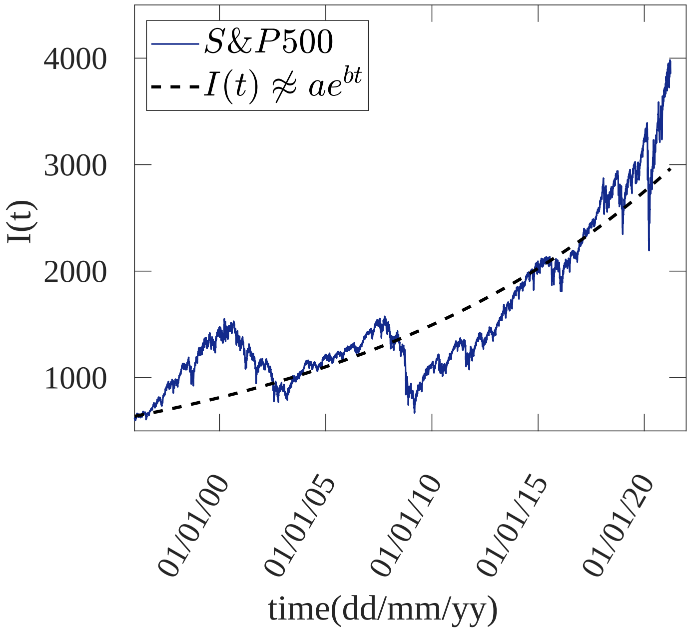


FIGURE 2.2: (Stock market index $I(t)$ of S&P500 in the period of 02/01/96 to 30/03/21 (more than 25 years). Considering the GBM in Eq. (2.16), the deterministic part is modeled to find the trend of the S&P500. As a result, the fitted line $ae^{bt}$ is an approximation of the S&P500 data trend, where $a = (9.845 \pm 0.7) \times 10^{-51}$ and $b = (1.668 \pm 0.001) \times 10^{-4}$. We note that when this approximated trend is subtracted, the fluctuations will not form a normal distribution function. This rules out the validity of Eq. (2.16).

return as a function of time (Vasconcelos 2004). The SDE can be obtained by applying the Itō Lemma (Vasconcelos 2004) in Eq.(2.12):

$$dX_T = \mu(T)dT + \sigma(X,T)dW_T, \tag{2.15}$$

with drift $\mu(T) = D_1(T)$ and variance $\sigma^2(X,T) = 2D_2(X,T)$. The function $W_T$ is the Gaussian noise, and the term $\sigma(X,T)dW_T$ corresponds to q-Gaussian noise. The interpretation of our SDE is that in a small time interval, $dT$, the price return changes its value due two effects. The first one is related with the drift $D_1$ that depends on time only. The second is the diffusion term $D_2$ that depends on time and price return.

The SDE in Eq. (2.15) is different from the Geometrical Brownian Motion (GBM) (Tsay 2005):

$$dI_T = \mu I_T dT + \sigma\, I_T dB_T, \tag{2.16}$$

where, $\mu$ and $\sigma$ values are constants, and $B_T$ is the standard Brownian noise. The GBM is the basic model for stock price dynamics in the Black-Scholes framework (Vasconcelos 2004; Björk and Hult 2005). If we consider the approximation, $dZ_T = dI_T/I_T$, where $Z_T$ is a logarithmic difference of the stock market index $Z(t_0, t) = \ln\left[\frac{I(t_0+t)}{I(t_0)}\right]$. Then, Eq. (2.16) can be simplified as $Z_T = \mu dT + \sigma\, dB_T$. The solution of this equation is an exponential growth superposed by a normally distributed Brownian process (Vasconcelos 2004; Björk and Hult 2005). This solution constitutes a rough approximation of the price return, as shown in Figure 2.2. In some studies, the log-return $Z_T$ is often used for technical analysis because it is close to the percentage price change (Ren et al. 2018; Gopikrishnan et al. 1999; Cao et al. 2017), a concept often used to neutralize most of the non-stationary effects (Mandelbrot 1997; Cont and Tankov 2004; Jondeau et al. 2007). One of the key properties of the GBM approach to modeling asset prices is that prices will not go negative, an assumption that may not be reasonable given recent events in some asset markets. Some examples are crude oil's price fall and the bankruptcy of some assets of global energy companies, which had reached negative values (Walker 2020). Additionally, in the GBM, it is assumed that the natural logarithmic of price return follows the Brownian motion with drift and that the price return has a normal distribution (Vasconcelos 2004). However, price returns or log price returns have been modeled by a q-Gaussian distribution function (Xu and Beck 2016). Thus, the stochastic differential equation, Eq.(2.15), could potentially model this behavior better than the standard GBM.

## 2.3 Detrending time series

In the previous section, we postulated that the time series of the price return can be decomposed into a deterministic time series and q-Gaussian noise. In what follows, we validate this hypothesis by performing an analysis of the S&P500 index. The analyzed data corresponds to a time frame from January 1st, 1996 to March 31th, 2021 with a frequency of one minute.

The S&P500 stock market index data was obtained from the Thomson Reuters Corporation (Corporation 2020). Before the analysis, few artifacts were removed from the data (Corporation 2012; plummets 2000; Ferreira and Karali 2015), as explained in the Appendix 2.A).

The Moving Average is a widely known method to remove the trend in time series (Hansun 2013; Gu, Zhou et al. 2010; Alonso-Marroquin et al. 2019). Many variations and implementations have been developed by researchers, but its underlying purpose remains, which is to determine the trend. Despite new models, the MA method is still considered as a good option for detrending the data due to its easiness, objectiveness, reliability, and usefulness (Hansun 2013).

The MA is a common average within a time window size that is shifted forward until the end of the data set (Hansun 2013). Each point in the time series data is equally weighted. The arithmetic centered moving average has been the most widely used MA case (Gu, Zhou et al. 2010).

The MA method offers different options for its calculation. The first option is regarding how the time window will be shifted until the end of the data. For this analysis, it has been used an overlapped or rolling window. These windows are extended over an interval $[t,\ \ t+t_w]$, where the consecutive window is incremented by one time point to: $[t+1,\ \ t+t_w+1]$. The $t_w$ represents the size of the time window. The second option is choosing the polynomial order $k$ for fitting each time segment for the detrending process. The original MA uses $k=0$, which represents an unweighted mean (Alessio et al. 2002). The option $k=1$ is used in other studies when the focus is on the local trend (particular tendency per window) (Peng et al. 1994). These options were tested and applied in the index price $I(t)$. In our analysis, there is no major difference between $k=0$ and $k=1$, so $k=0$ was used.

### 2.3.1 Optimal time window

The size of the time window, $t_w$, is the key parameter to obtain stationary detrended data. The distribution of the data set of each window $t_w$ should be self-similar, without outliers (extreme events), but with time-dependant standard deviation. Xu et al. (Xu and Beck 2016)

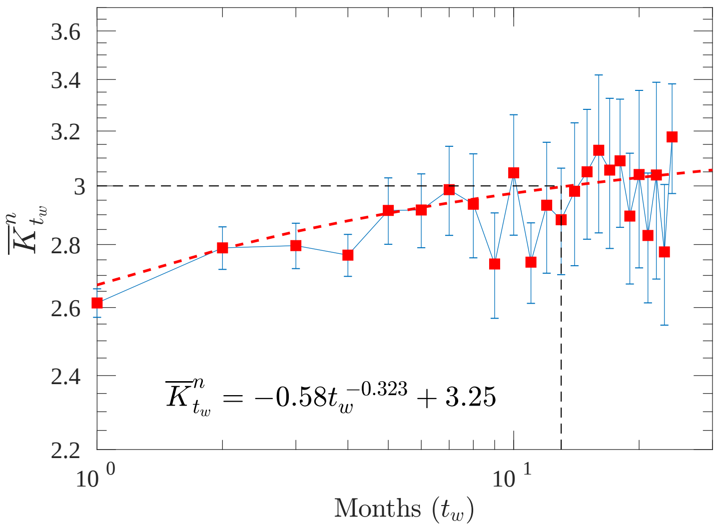


FIGURE 2.3: Optimal window size $t_w$ that will be used for the Moving Average. The $\overline{K}^n_{tw} = 3$ yields a time window of $13 \pm 1$ months. The smaller time window, $t_w$, is chosen to preserve data features that tend to attenuate with longer time windows. The blue bars are graphical representations of the standard error of $\overline{K}^n_{tw}$ data in average per $t_w$

applied the kurtosis definition to compare each distribution of the data set of each window $t_w$. The kurtosis of a time series $X$ is defined as the fourth standardized moment, defined as the relation between central moments $\langle u^n \rangle$ of order $n$, where $u = X - \langle X \rangle$,

$$K = \frac{\langle u^4 \rangle}{\langle u^2 \rangle^2}, \tag{2.17}$$

where the delimiters $\langle \, \rangle$ denotes time average for each particular time window.

The optimal time window should satisfy the condition of Kurtosis equals three to obtain an optimum time window size such that for a given data set, the distribution in each window is as close as possible to a Gaussian distribution (Buonocore et al. 2019). Additionally, a Kurtosis equals three implies a time series in which extreme or outlier events are improbable to occur, with a skewness equals to zero. The skewness is defined as a normalized third-order moment of the PDF. As a consequence, the time series remains symmetric around its mean value (Labit et al. 2007).

Before applying the MA method, we developed a preliminary process to choose an optimal time window $t_w$. We used a range of values between $1$ to $25$ months as a possible time window. For each possible $t_w$ value, the total length of $N$ of the time series is split into non-overlapping time windows. The total length of $N$ is often not a multiple of the time window, $t_w$. Consequently, the number of segments is defined by rounding them to the nearest lower integer $\lfloor n = N/t_w \rfloor$. Next, the kurtosis in each $j^{th}$ window is calculated, where $j = 1, 2, 3, 4.....n$. and averaged for the $n$ windows as follows;

$$\overline{K}_{t_w}^{n} = \frac{1}{n}\sum_{j=1}^{n} K_{t_w}(j), \tag{2.18}$$

where $\overline{K}_{t_w}^{n}$ denotes the average over the $n$ windows. Figure 2.3 presents the results of $\overline{K}_{t_w}^{n}$. The optimal window size is $13 \pm 1$ months. The time window assumed for the MA analysis is $12$ months. The smaller value of time window, $t_w$, is chosen because it will preserve features of the data such as peak height and width, which is usually attenuated with a longer time window $t_w$.

### 2.3.2 Calculation of trend and fluctuating part

The non-stationary time series of the stock market index $I(t)$ is decomposed into a trend $\tilde{I}(t)$ and a stochastic part $I^*(t)$,

$$I^*(t) = I(t) - \overline{I}(t). \tag{2.19}$$

The trend $\overline{I}(t)$ is constructed for the index price of S&P500 applying MA method with $k = 0$ and considering overlapped windows of $t_w = 12$ months. This process is constructed based on a weighted sum or average of each time window. Considering that the time windows for $t < \frac{t_w}{2}$ and $t > N - \frac{t_w}{2}$ are truncated, we identified three cases to calculate the moving average that depends on the position of the moving window (Xu et al. 2005):

• For $t < \frac{t_w}{2}$:

$$\overline{I}(t) = \frac{2}{t_w + 2t} \sum_{k=-t+1}^{\lceil (t_w-1)/2 \rceil} I(t+k) \tag{2.20}$$

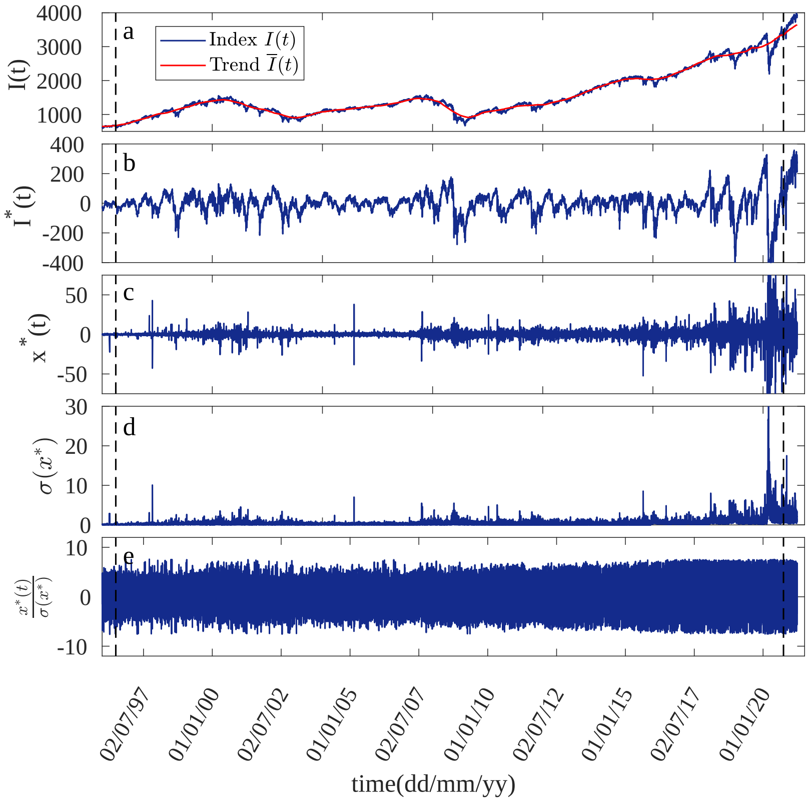


FIGURE 2.4: (a) Trend obtained after applying the MA analysis for a time window of 12 months for S&P500 data. (b) Detrend price $I^*(t)$ after subtracting the trend shown in subfigure 4-a. (c) Detrended price return, $x^*(t)$, obtained from the differences between adjacent elements of $I^*(t)$. (d) The standard deviation is obtained from an overlapping or rolling window of 1 hour. Within a time period of 1 hour, the time-dependence of the standard deviation is captured before it dissipates. (e) The subfigure represents the normalized price return. The normalization of the detrended price return is calculated by dividing the data set by the standard deviation previously calculated as $\sigma(x^*)$.

- For $\frac{t_w}{2} < t < N - \frac{t_w}{2}$:

$$\overline{I}(t) = \frac{1}{t_w} \sum_{k=-\lfloor (t_w-1)/2 \rfloor}^{\lceil (t_w-1)/2 \rceil} I(t+k) \tag{2.21}$$

- For $t > N - \frac{t_w}{2}$:

$$\overline{I}(t) = \frac{2}{2N - 2t + t_w} \sum_{k=-\lfloor (t_w-1)/2 \rfloor}^{\lceil N-t \rceil} I(t+k), \tag{2.22}$$

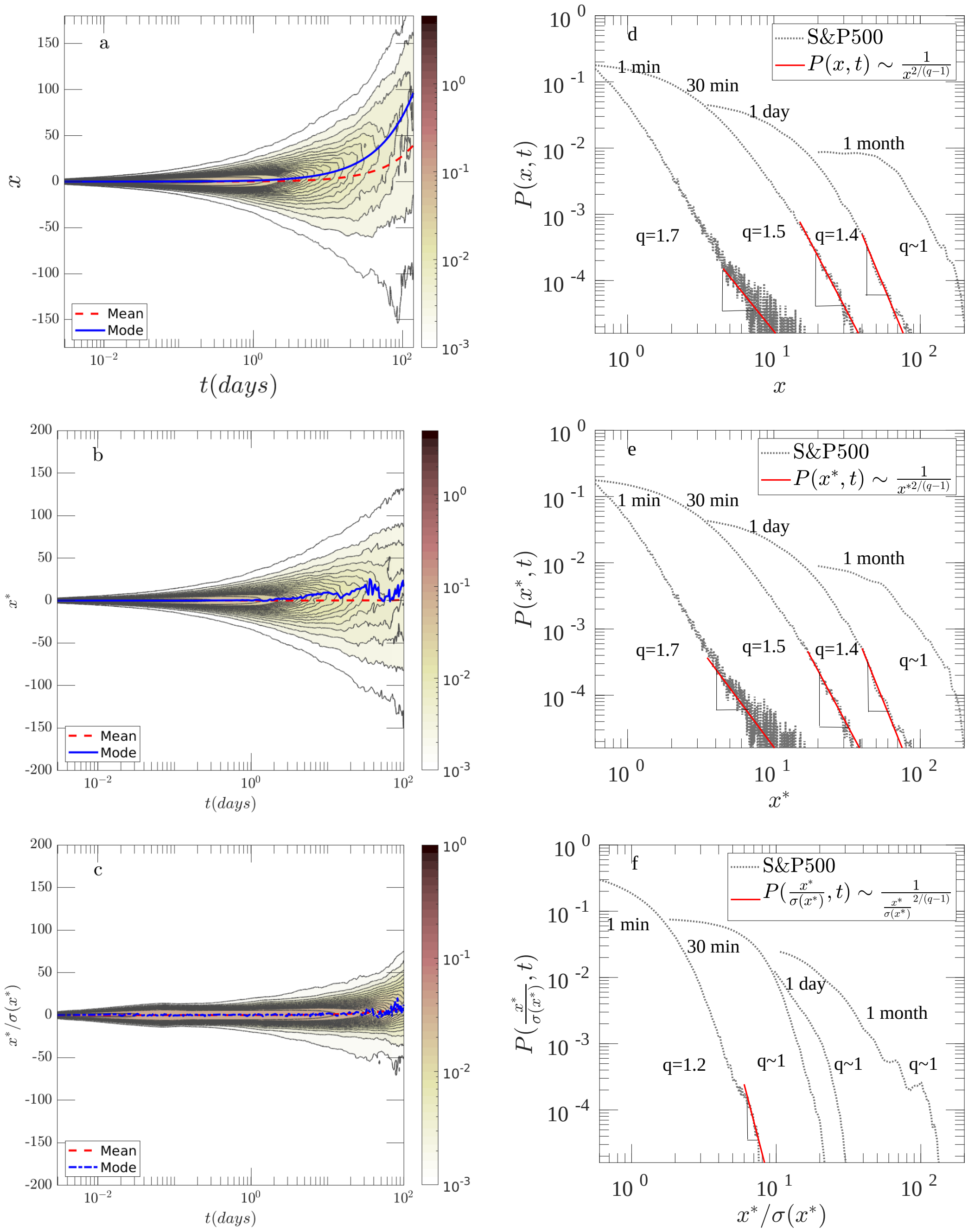


FIGURE 2.5: Representation of the time evolution of the PDF for the different types of price return displaying the asymptotic behavior (tail behavior). The construction of the PDF's evolution was made considering particular time intervals to calculate the price increments or price return. (a) Time evolution of the PDF of price return. (b) Time evolution of the PDF of detrended price return. (c) Time evolution of the PDF of the normalized price return. (d) Asymptotic behavior for the PDFs of price return at particular times. (e) Asymptotic behavior for the PDF of detrended price return at particular times. (f) Asymptotic behavior for the PDF of normalized price return at particular times. A faster convergence to Gaussian, within 30 min., is noted when the normalized price return is used.

with the time step of $t = 1, 2, 3....N$ for the index fluctuations.

The Subfigure 2.4-a presents the trend $\tilde{I}(t)$ after applying the MA analysis for a time window of 12 months (red line). The trend obtained represents a general tendency of the stock market index $I(t)$. The Subfigure 2.4-b shows the detrended price as a result of subtracting the obtained trend.

After the detrended process, the expected result is that the price return will lose asymmetry and will be modeled by the self-similar q-Gaussian distribution function (Eq. 2.5). However, the detrended price return is still non-stationary because it presents volatility clusters over the time series's full length (Subfigure 2.4-b). These clusters over the detrended price return represent a time-dependent standard deviation. Considering Eq. 2.15, the stochastic part or q-Gaussian noise is compounded by a Gaussian or stationarity noise affected by a standard deviation that varies with time. Then, the normalized price return is obtained after dividing the detrended price return by its standard deviation to obtain a stationarity time series.

The standard deviation is obtained from an overlapping or rolling window of 1 hour. Within a time period of 1 hour, the highest volume of option trading occurs, consequently the standard deviation is captured before it dissipates (Nofsinger and Prucyk 2003). The Subfigure 2.4-e shows how the clusters disappears after dividing the detrended price return by its standard deviation. Figure 2.5, presents the time evolution of the PDFs of simple price return, detrended price return, and normalized price return, respectively. The Subfigure 2.5-a shows that the simple price return has a positive trend and mode that grows with a positive rate proportional to the time interval of the price return. The Subfigure 2.5-b shows that the PDF of detrended price return has a constant mean value while its mode oscillates around zero. The Subfigure 2.5-c shows that the PDF of normalized price return has constants mean and mode values. The fat-tailed distributions of the PDFs for detrended price return represent the simple price return's stylized facts adequately. For this case, the same rate of aggregation of normality can be observed for the price return with the only difference that it is centered in zero (Subfigure 2.5-d and 2.5-e). On the other hand, the normalized price return presents a convergence to normal distribution that occurs at a faster rate (Subfigure 2.5-f). The fat-tailed distribution quickly transforms into a Gaussian one for time intervals larger than $30$ minutes.

## 2.4 Stationarity of detrended price return

In the following section, we test the detrended time series for stationarity. In statistics one of the most widely applied methods to test stationary is the Dickey-Fuller test (Babirath and Schmitl 2020; Krečar et al. 2011; Dickey and Fuller 1979. However, this method is applied for autoregressive time series with normal random noise (ARIMA) (Dickey and Fuller 1979). In Appendix-2.C we show that the detrended price return can be represented as an autoregressive model but holding a q-Gaussian noise only. As a consequence, the Dickey-Fuller test will not be applicable to the stationarity test. The proposed tests in this paper are based on the calculation of the power spectrum analysis (Witt et al. 1998). We recall the expression for the detrended price return:

$$x^*(t) = I^*(t_o + t) - I^*(t_o), \tag{2.23}$$

where $I^*(t_o)$ is the detrended stock market index at time $t_o$, and $I^*(t)$ is the detrended stock market index for any time $t > t_o$.

Looking back at the definition of normalization, we defined the normalized price return as;

$$x^{**} = \frac{x^*(t)}{\sigma(x^*)}, \tag{2.24}$$

First, we proceed to evaluate the correlation of the detrended price return $x^*$, and normalized price return $x^{**}$. The autocorrelation is defined as (Barlas 1990; Liu et al. 1999):

$$C_x(s) \equiv \frac{\langle x_t x_{t+s} \rangle}{\sigma_x^2}, \tag{2.25}$$

$$\sigma_x^2 = \langle (x_t - \mu)(x_t - \mu) \rangle.$$

Where a particular price return for a specific time is represented by $x_t$ and the time lag by $s$. The autocorrelation is evaluated for two cases after replacing $x$ by the detrended price return and the normalized price return. For both cases short-time autocorrelations are observed in Figure 2.6. The Subfigure 2.6-a represents the autocorrelation for the detrended price return. For this case, the power-law fitting of the autocorrelation holds only one order of magnitude. The autocorrelation has an exponential trend for lower values of $s$, and for higher values, the autocorrelation shows a weak but non-zero autocorrelation. A transition zone is observed between lower and higher time-lag values, and it decreases rapidly with a power law that has an exponent $\gamma = -0.60 \pm 0.32$. The Subfigure 2.6-b represents the autocorrelation for the normalized price return. For this case, the autocorrelation has an exponential trend for lower values of $s$. The autocorrelation presents negative values until the first $30$ min of lag.

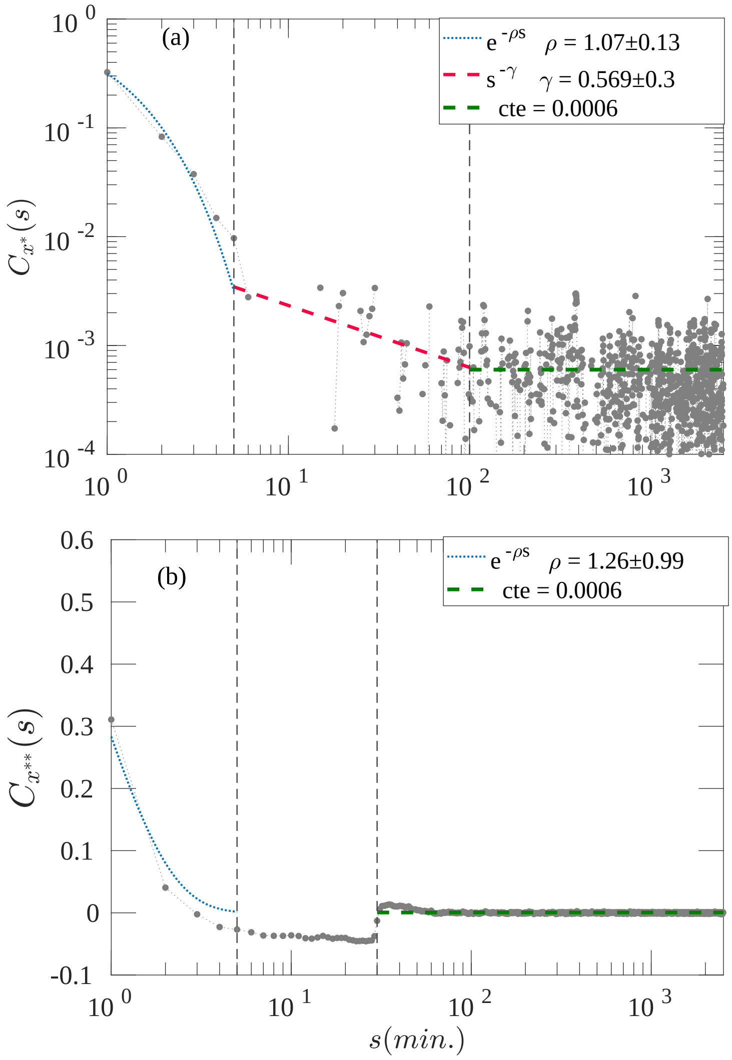


FIGURE 2.6: Autocorrelation of the detrended price return calculated as $C_x(s) \equiv \dfrac{\langle x_t x_{t+s} \rangle}{\sigma_x^2}$. Short-time correlations are observed for the first $6$ minutes. A weak long-time correlation appears after $100$ minutes.

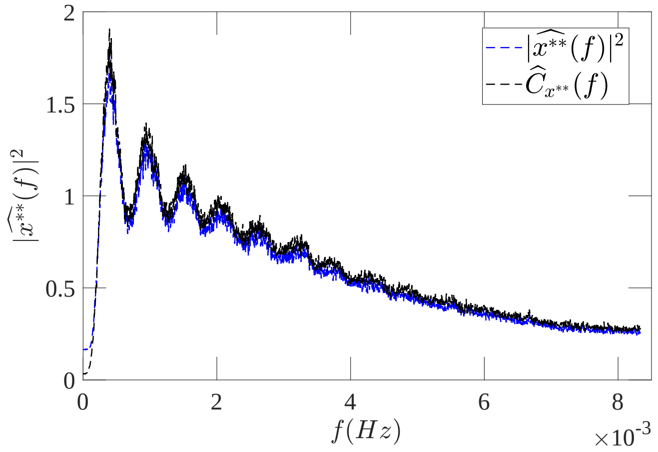


FIGURE 2.7: The Power-spectral density $|\widehat{x}(f)|^2$ of the detrended price return matches with the Fourier transform of its autocorrelation.

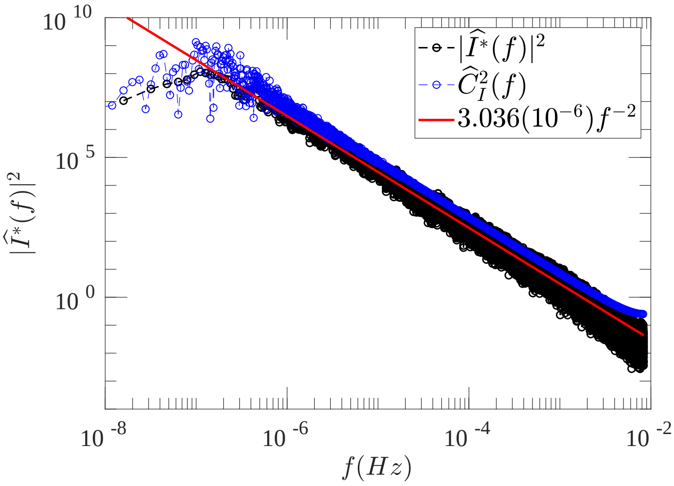


FIGURE 2.8: The power-spectral density of the detrended index $I^*(t)$ holds a power law $P(f) = M/f^2$, where $M = 3.036(10^{-6}) \pm 3(10^{-9})$. The following relation $|\widehat{I}(f)|^2 = \widehat{C}_I^2(f)$ is observed, suggesting that the Index once detrended is stationarity as well.

Then, the Stationary Test is based on the autocorrelation and the power spectrum analysis of the time series is applied. The Fourier Transformation (FT) of $x_t$ is represented as $\widehat{x}(f)$,

$$\widehat{x}(f) = \frac{1}{\sqrt{T}} \sum_{t=0}^{T} x(t) e^{-2\pi i f t}. \tag{2.26}$$

This test states that any process is stationary if the power spectrum $|\widehat{x}(f)|^2$ exists, and can be expressed as the Fourier transform of the autocorrelation $C(s)$ (Witt et al. 1998; Krenk et al.

1983),

$$|\widehat{x}(f)|^2 = \widehat{C}_x(f), \tag{2.27}$$

We determine the detrended price return as a non-stationary time series on account of the time-varying volatility and short-time correlations. The normalized price return is stationarity based on the results shown in Figure 2.7, where the match between $|\widehat{x^{**}}(f)|^2$ and $\widehat{C}_{x^{**}}(f)$ is achieved for time lags larger than 30 min. The $|\widehat{x^{**}}(f)|^2$ and the $\widehat{C}_{x^{**}}(f)$ have been smoothed by applying the Savitzky-Golay filtering. The smoothing is made with the purpose of reducing the noise of the data without distorting their tendency (Guiñón et al. 2007; Gorry 1990). The smoothing obtained by the Saviztky-Golay filter is based on the least-squares of a linear fitting across a moving window by applying the normalized convolution integers of Savitzky-Golay, $C_i$ (Guiñón et al. 2007; Gorry 1990). For this case, the length of the moving window is $3.97 \times 10^{-5}\ Hz$.

Also, the relation $|\widehat{I}(f)|^2 = \widehat{C}_I^2(f)$ is observed in Figure 2.8, suggesting that the detrended index can be represented by a red noise (Toker et al. 2020) due to its inverse proportionality to $f^2$.

## 2.5 Scaling analysis of the fractal of detrended price return

For the scaling analysis, the Hurst exponents of the detrended and normalized price returns are calculated. The Hurst exponent is a measure of long-range memory of a time series. More specifically, it measures the statistical dependence of two points of the time series with respect to the time difference between them (Kantelhardt et al. 2002b; Rangarajan and Ding 2000).

The Hurst exponent is better known as the *index of dependence*, and as such, it is a dimensionless estimator of self-similarity in a time series (Gao et al. 2003; Márton et al. 2014; Horvatic et al. 2011). The self-similarity occurs when a structure repeats itself on subintervals, so they are *scale-invariant*, which is a property that some time series possess (Márton et al. 2014).

Two types of self-similar signals exist. The monofractal signal, which presents a unique scaling behavior of complexity. The scaling behavior is obtained from the ratio of the self-similar

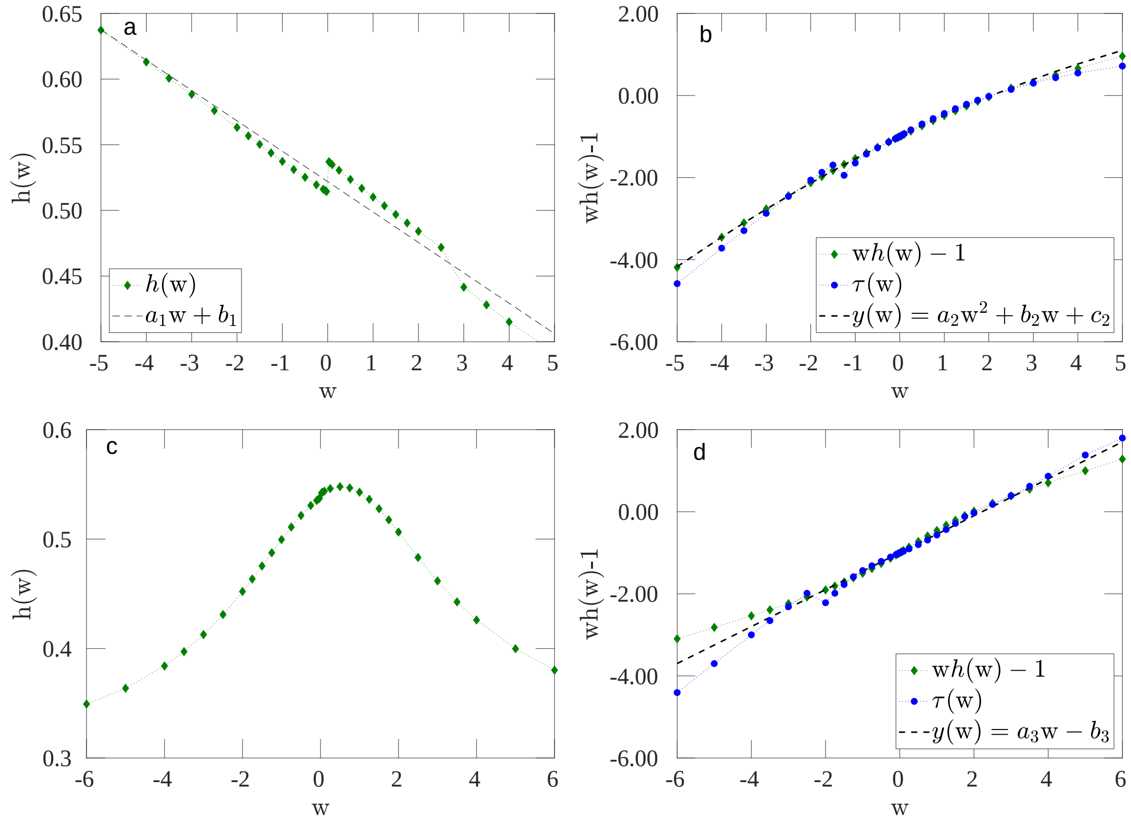


FIGURE 2.9: Evaluation of the scale exponents, $h(\mathrm{w})$, and the generalized scaling exponent, $\tau(\mathrm{w})$ for the detrended and the normalized price return. The subfigures (a) and (b) corresponds to the analysis of detrended price return and are obtained from results shown in Figure 2.12 and 2.13 respectively. The subfigures (c) and (d) correspond to the analysis of normalized price return and are obtained from results shown in Figure 2.14 and 2.15, respectively. The generalized Hurst exponent $h(\mathrm{w})$ follows Eq. (2.28) for a normalized and multifractal time series. (a) For the fitting of the generalized Hurst exponent $a_1 = -0.023 \pm 0.002$ and $b_1 = 0.522 \pm 0.004$. (b) For the fitting of the generalized scaling exponent $a_2 = -0.02157 \pm 3.8(10^{-4})$, $b_2 = 0.5270 \pm 0.0012$, $c_2 = -0.9954 \pm 0.0034$. (c) For the normalized price return the generalized Hurst exponent obeys a curve bell-shaped which points to $0.35$ when $\mid \mathrm{w} \mid > 6$. (d) For the fitting of the generalized scaling exponent, normalized price return case, $a_3 = 0.45 \pm 0.01$ and $b_3 = 0.99 \pm 0.04$.

pattern that changes with the scale at which it is measured. The second type is the multifractal signal, which has more than one scaling behavior (Kantelhardt et al. 2002b).

The Hurst exponent can be estimated by applying the detrended fluctuation analysis (DFA) (Hu et al. 2001; Løvsletten 2017) explained in the Appendix 2.C. The DFA is a technique used to demonstrate self-similarity in a time series (Ausloos 2012), and the DFA has been applied widely in scientific studies to estimate the Hurst exponent (Løvsletten 2017). Additionally, by analyzing the statistics, it is possible to characterize the time series as monofractal or multifractal if the self-similarity exists.

The first part of the DFA analysis consists in removing the trend of the original time series considering non-overlapping segments. However, our trend was removed previously in Subsection 2.3-B by applying a simple but still rigorous MA method considering overlapped time windows with an optimal size of time window $t_w$.

The second part of the DFA is based on the calculations of the *scaling function*, $F_{\mathrm{w}}(s)$, as a function of the *time segment* $s$, where $\mathrm{w}$ is the mathematical moment's order (See Appendix 2.C) (Alessio et al. 2002; Kantelhardt et al. 2002b; Kantelhardt et al. 2002a). If the *scaling function* of the time series is a power-law function and satisfies the $F_{\mathrm{w}}(s) \sim s^H$, the time series is monofractal. Then, the exponent $H$ is called the Hurst exponent (Kantelhardt et al. 2002b; Kantelhardt et al. 2001). Other time series does not have a unique, constant valued $H$. Their scaling exponent $H$ depends on the order of the moment $\mathrm{w}$ (Figure 2.12). These are classified as a multifractal time series. The generalization method of DFA (G-DFA) is tailored for multifractal time series. In the G-DFA, the *generalized statistical moments* are defined by $G_{\mathrm{w}}(s)$ in Eq. (2.36). If the series is multifractal, the exponent $\tau(\mathrm{w})$ is the so-called *generalized scaling exponent* (GSE). The multifractal time series satisfies the scaling law of $G_{\mathrm{w}}(s) \sim s^{\tau(\mathrm{w})}$. For multifractal time series the generalized scaling exponent $\tau(\mathrm{w})$ can be defined in terms of the generalized Hurst exponent $h(\mathrm{w})$ (Gu, Zhou et al. 2010; Kantelhardt et al. 2002a):

$$\tau(\mathrm{w}) = \mathrm{w}h(\mathrm{w}) - 1. \tag{2.28}$$

The Subfigure 2.9-a shows the generalized Hurst exponent of the detrended price return obtained from Figure 2.12, and its fitting. The generalized Hurst exponent is approximated to $h(\mathrm{w}) \simeq -0.023\mathrm{w} + 0.521$ for $-5.0 \leq \mathrm{w} \leq 5.0$. The Subfigure 2.9-a benefits for interpretation of the generalized Hurst exponent: $h(\mathrm{w}) \in \langle 0.5, 1\rangle$, indicates persistence (correlation) of time series (Wang et al. 2014). Subfigure 2.9-a shows persistence of time series, when $\mathrm{w} < 0$. This negative value of w represents the segments with small fluctuations (Kantelhardt et al. 2002a). On the other hand, the $h(\mathrm{w}) \in \langle 0, 0.5 \rangle$, indicates anti-persistence (no-correlation) of time series (Wang et al. 2014). Subfigure 2.9-a shows anti-persistence when $\mathrm{w} > 0$, segments with large fluctuations (Kantelhardt et al. 2002a).

Subfigure 2.9-b shows the $\tau(\mathrm{w}) = \mathrm{w}h(\mathrm{w}) - 1$ relationship, proving that the detrended price return is self-similar and multifractal (Kantelhardt et al. 2002a. Subfigure 2.9-c, shows the generalized Hurst exponent of the normalized price return obtained from Figure 2.14. The $h(\mathrm{w}) \in \langle 0, 0.5 \rangle$ indicates anti-persistence. Subfigure 2.9-d proves that the normalized price return is self-similar and multifractal such as the detrended price return but with weaker correlation that rapidly decrease. Additional analysis about the behaviour of the generalized Hurst exponent when it is linear, is displayed in the Appendix 2.D

## 2.6 Conclusions

We proposed an improved version of the Black-Scholes equations postulated in Section II of our paper, Eq (2.15). Our stochastic differential equation captures the index behavior more precisely by having a trend that fluctuates deterministically. The proposed SDE, Eq (2.15), presents its deterministic component as endogenous or exogenous predictive factors, which is associated with internal/external events that produce changes of trend direction. The stochastic part is represented by the q-Gaussian noise, which is a compound of a time-dependant standard deviation and Gaussian noise.

For the validation of our proposed SDE, the S&P500 index was detrended using a weighted average method with an overlapped time window of one year. The time window length was obtained by calculating an average Kurtosis equal to three. The aim was to achieve an optimum window size such that for a given data set the distribution in each window is as close as possible to a Gaussian distribution. However, we showed that each distribution in each window has a high varying variance within an hour, and fits better with a q-Gaussian distribution function. For the authors, these results agree with Eq (2.15), where the detrended part is a q-Gaussian noise compounded of Gaussian noise and a variance term that depends on time (volatility clusters). By calculating an optimal window size, the detrended data set is symmetric, where extreme outlier events are improbable to occur.

This paper considered three methods to prove stationary. The first one was based on previous superstatistical models, determining optimal time window length to capture local Gaussians based on the Kurtosis application. The second method was based on the DFA, which proposes an alternative approach to test stationarity for monofractal time series after removing trends that can not be normalized. The detrending price return is a multifractal time series. As a consequence, the DFA approach couldn't be used. The third method used was the Stationarity Test; this test is based on the power spectrum of the time series, which needs to be approximately equal to the Fourier transform of its autocorrelation. After the normalization of the detrended price, the Stationarity Test was applied. We obtained a match between the power spectrum and the Fourier transform of the autocorrelation after dismissing the first 30 minutes of the autocorrelations' time-lag. During these 30 minutes weak autocorrelations were detected on the normalized price return.

This paper does not provide ultimate definitive proof that the normalized price return is perfectly stationary. The authors prefer to refer to a normalized price return as a weak stationary time series, where the mean and standard deviation fluctuate around a constant value. Future work should be focused on new methods that provide a clear distinction between a deterministic trend and non-stationary stochastic noise. Additionally, further research should focus on evaluating the relationship between short time-correlated time series and volatility clustered.

## 2.A Cleansing Data

The three artifacts removed from the S&P500 data are: In 17/06/1997, at the peak of the Asian financial crisis (Corporation 2012). In 20/03/2000, when the imminent bankruptcy of many Internet companies was announced (plummets 2000). The third artifact removed was the Haiti earthquake that occurred on 11/01/2010 (Ferreira and Karali 2015). These three events introduce spurious jumps in the S&P500, producing a considerable percentage change of the Index for $1$ to $8$ minutes only. Then, the abrupt Index values return to the original. The three artifacts are shown in Figure 2.10(a-c) in chronological order.

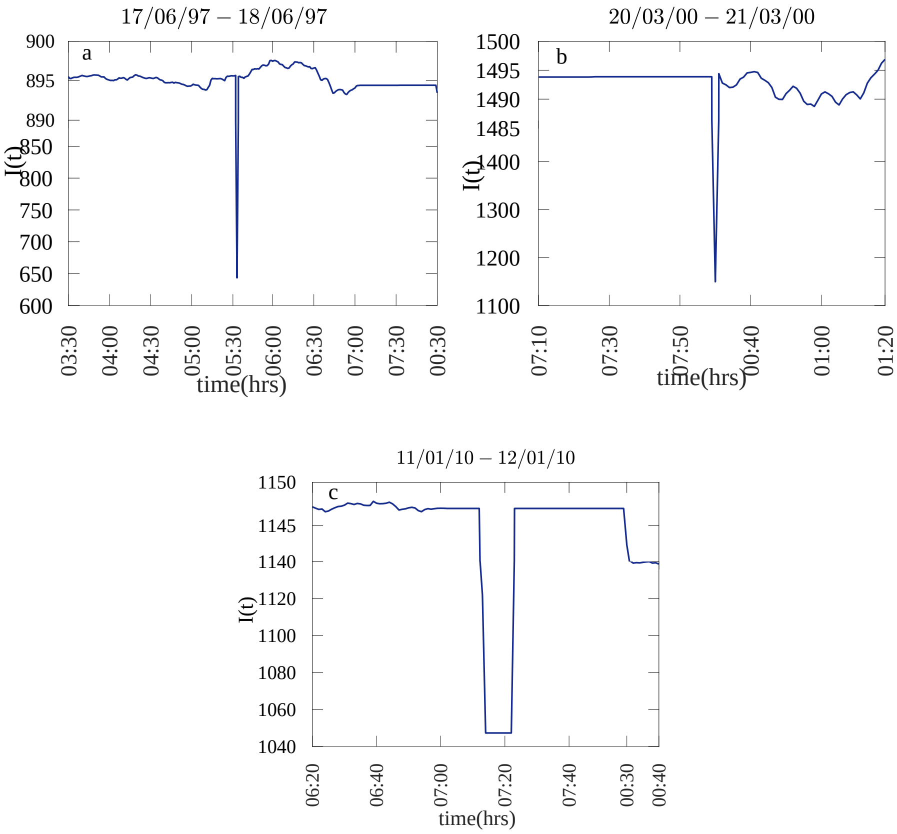


FIGURE 2.10: The three events that produce spurious jumps in S&P500 data over the past 24 years are shown in subfigures (a) the peak of the Asian financial crisis, (b) The imminent bankruptcy of many Internet companies was announced, and (c) The Haiti earthquake effect.

## 2.B Dickey-Fuller test

In statistics, the Dickey-Fuller analysis is the most popular test for determining the stationarity of time series (Babirath and Schmitl 2020; Krečar et al. 2011). The Dickey-Fuller test models autoregressive time series with random noise with the form:

$$I_t^* = \rho I_{t-1}^* + \epsilon_t, \tag{2.29}$$

where $\epsilon_t$ is a sequence of independent random variables, with mean zero following a normal distribution function. Figure 2.11 displays the linear relationship between $I_t^*$ and $I_t^*$, where $\rho \approx 1$ and $\epsilon$ obeys a $q$-Gaussian distribution. As a consequence, the Dickey-Fuller analysis will not be applicable for the stationarity test of detrended price return. Figure 2.11 presents a linear combination of two q-Gaussians. However, the solution for the PDF with two different q-values as a function of time in the previous PDE is not feasible. In Chapter 4, we address this issue by removing the data from the inactive trading period (when price change is less than 0.1 USD), and only working with the q originated from the active trading periods. While the Dickey-Fuller test can still be applied in terms of testing the non-stationarity of the time series, or the normalized time series, in this chapter (and later in Chapter 5) we adopt the physics-based method for the stationary test, the Wiener-Kinchin theorem, which has been validated with geophysical (Witt et al. 1998), physiological (Witt et al. 1998) and financial (Lim et al. 2023) data.

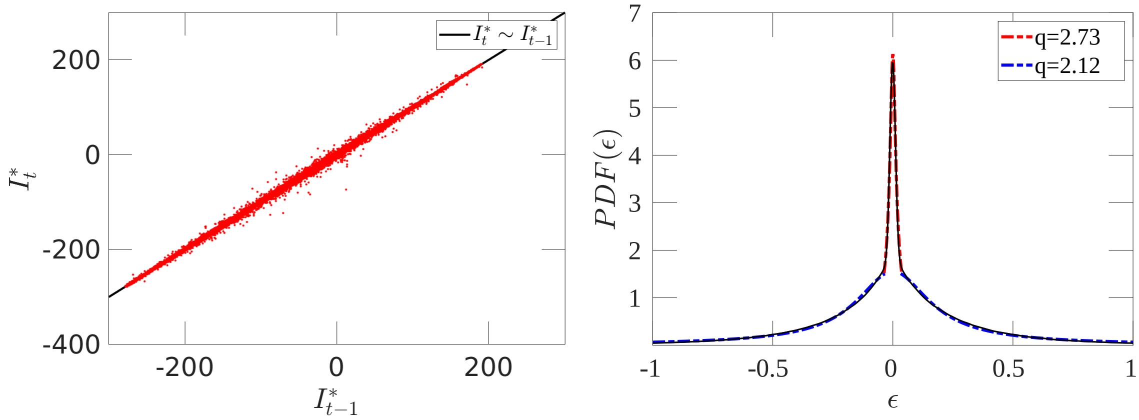


FIGURE 2.11: (a) Linear relationship between $I_t^*$ and $I_t^*$. (b) The noise obtained by removing the linear trend obeys a $q$-Gaussian distribution.

## 2.C Detrended Fluctuation Analysis (DFA)

The Detrended Fluctuation Analysis method has become a widespread technique to determine the self-similarity of a time series based on statistical functions $F_w$ (Peng et al. 1994; Kantelhardt et al. 2002b). The statistical functions $F_w$ [Eq. (2.31)] are calculated based on central moments of the time series. For that, the detrended time series is divided into equal non-overlapping segments with a length of $s$. The $s$ value represents the time segment in which the detrended time series will be analyzed.

Then, the Hurst exponent is obtained from the power law given by $F_w$ vs $s$.(Kantelhardt et al. 2002b; Kantelhardt et al. 2001).

#### 2.C.0.1 Description of the method of DFA

We will proceed to indicate the steps to adopt this method to find the Hurst exponent of the detrended price return $x(t)$. First, we focus on calculating the statistical functions $F_w$, then to the calculation of Hurst exponent $H$ (Kantelhardt et al. 2002b; Gao et al. 2003; Witt et al. 1998; Kantelhardt et al. 2001; Horvatic et al. 2011).

- *Step 1:*: The 'profile' is the cumulative sum of the time series to analyze. For this case, our profile matches with the detrended price $I^*(t)$ obtained after applying Eq. (2.19).
- *Step 2:*: The profile $I^*(t)$ is divided into non-overlapping segments $\lfloor N_s = N/s \rfloor$ with the same length $s$.
- *Step 3:*: The variance for each of the segments $v = 1, 2, 3....N_s$ is obtained by applying the following equation,

$$F^2(v,s) = \frac{1}{s}\sum_{i=1}^{s}(I^*[(v-1)s+i] - \overline{I^*}(v,s))^2, \tag{2.30}$$

where, $\overline{I^*}(v,s)$ represents the mean of each segment of $I^*(t)$.

• *Step 4:*: The statistical moments are obtained considering a range of values for the $\mathrm{w}^{\mathrm{th}}$ orders.

$$F_{\mathrm{w}}(s) = \left\{ \frac{1}{N_s} \sum_{i=1}^{Ns} [F^2(v,s)]^{\mathrm{w}/2} \right\}^{1/\mathrm{w}} \tag{2.31}$$

For detrended time series that present long-range correlations, the following power law is obtained (Kantelhardt et al. 2002b; Gao et al. 2003; Kantelhardt et al. 2002a; Rangarajan and Ding 2000):

$$F_{\mathrm{w}}(s) \sim s^{h(\mathrm{w})}. \tag{2.32}$$

For monofractal time series $h(\mathrm{w})$ is independent from $\mathrm{w}$ value due to a constant scaling behaviour over all the segments ($F^2(v,s)$ in Eq. (2.30) is cte.) (Maganini et al. 2018; Kantelhardt et al. 2002b), so $H = h(w)$. Figure 2.12 shows the results of DFA analysis, where a power law between $F_{\mathrm{w}}$ vs. $s$ is observed. However, the power laws depend on the $\mathrm{w}^{\mathrm{th}}$ order. Consequently, the Multifractal Detrending Fluctuation Analysis (MF-DFA) is applied to evaluate the dependence between the power laws and the order degree $\mathrm{w}^{\mathrm{th}}$.

For a standard multifractal analysis (MF-DFA) the scaling exponent $\tau(\mathrm{w})$ needs to be obtained. This exponent is the power law defined between the $G_{\mathrm{w}}(s)$ vs $s$. The $G_{\mathrm{w}}(s)$ is a general statistical moment based on the following relationship:

$$G_{\mathrm{w}}(s) = \sum_{v=1}^{N/s} |I^*(vs) - I^*((v-1)s)|^{\mathrm{w}}, \tag{2.33}$$

where the term $I^*(vs) - I^*((v-1)s)$ is equal to the cumulative summation of the $x(t)$ within each segment $\nu$ of size $s$.

$$\sum_{t=(v-1)s+1}^{vs} x_t = I^*(vs) - I^*((v-1)s). \tag{2.34}$$

In the standard multifractal formalism this sum is better known as the “box probability" $p_s(v)$, and it is used to find hypothetical probability values on the original profile $I^*(t)$.

$$p_s(v) = \sum_{t=(v-1)s+1}^{vs} x_t. \tag{2.35}$$

Then, by replacing Eq. (2.35) in Eq. (2.34). The “box probability" is defined in terms of the original profile, $p_s(v) = I^*(vs) - I^*((v-1)s)$. After that, we replace this equivalence in Eq. (2.33), the following relation is obtained:

$$G_{\mathrm{w}}(s) = \sum_{v=1}^{N/s} |p_s(v)|^{\mathrm{w}}, \tag{2.36}$$

where,

$$G_{\mathrm{w}}(s) \sim s^{\tau(\mathrm{w})}. \tag{2.37}$$

The $\tau(\mathrm{w})$ represents the generalized scaling exponent (GSE), and is related with $h(\mathrm{w})$ for stationary and normalized time series (Maganini et al. 2018; Kantelhardt et al. 2002b),

$$\tau(\mathrm{w}) = \mathrm{w}h(\mathrm{w}) - 1. \tag{2.38}$$

The Figure 2.9, shows a summary of the scaling exponents $h(\mathrm{w})$ and $\tau(\mathrm{w})$, respectively. The relationship between $h(\mathrm{w})$ and $\tau(\mathrm{w})$ is noticed, prooving that $x(t)$ is a multifractal stationarity time series. The Figures 2.13a and 2.13b show the results of the generalized statistical function $G_{\mathrm{w}}$ for negative and positive values of $\mathrm{w}$ respectively.

## 2.D Hurst exponent spectrum

The Legendre transformation is used to calculate the spectrum of the characteristic exponents after applying the detrending fluctuation analysis. We did the Legendre transformation of GSE as a function of $h(\mathrm{w})$. For the detrended price return the relationship between GSE and $h(\mathrm{w})$ is linear as can be observed in Subfigure 2.9a. The Legendre transform of the GSE is:

$$f(\gamma) = \gamma\mathrm{w} - \tau(\mathrm{w}) \tag{2.39}$$

where,

$$\gamma = \frac{\partial\tau(\mathrm{w})}{\partial\mathrm{w}} = h(\mathrm{w}) - \mathrm{w}\frac{\partial h}{\partial\mathrm{w}}$$

By replacing the Eq. (2.38) in Eq. (2.39), the Legendre transform of $\tau(\mathrm{w})$ is:

$$f(\gamma) = \mathrm{w}(\gamma - h(\mathrm{w})) + 1 \tag{2.40}$$

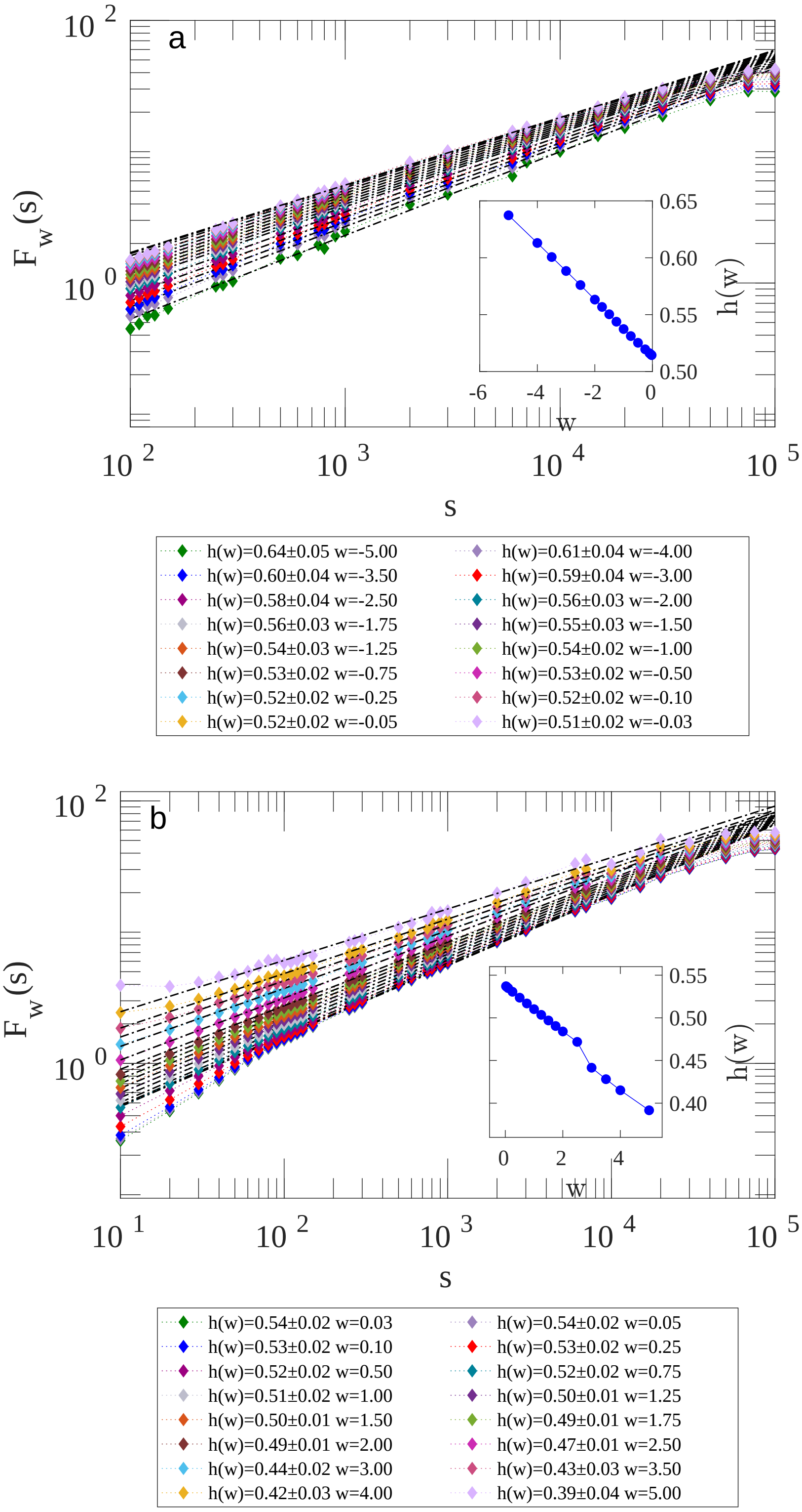


FIGURE 2.12: Detrended price return case: Calculation of the statistical function $F_w$ using Eq. (2.31). The function of $F_w$ vs $s$ display power laws $F_w(s) \sim s^{h(w)}$, where $h(w)$ depend on $w$. This feature demonstrates that the time series is a multifractal.

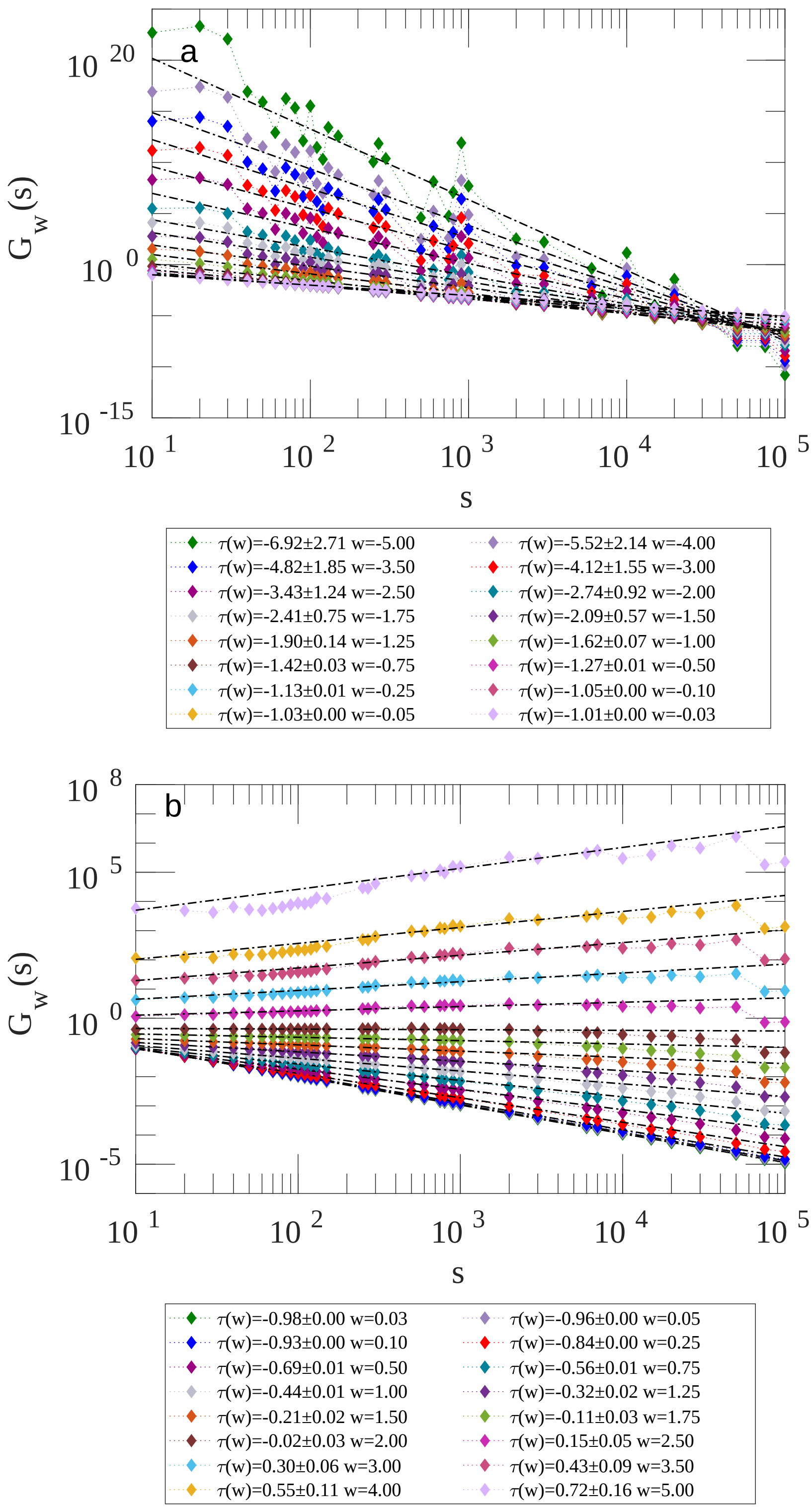


FIGURE 2.13: Detrended price return case: Calculation of the "generalized statistical functions" $G_w(s)$ vs $s$ for negative (a) and positive (b) values of order w. The "generalized statistical functions" is calculated by applying Eq. (2.36).

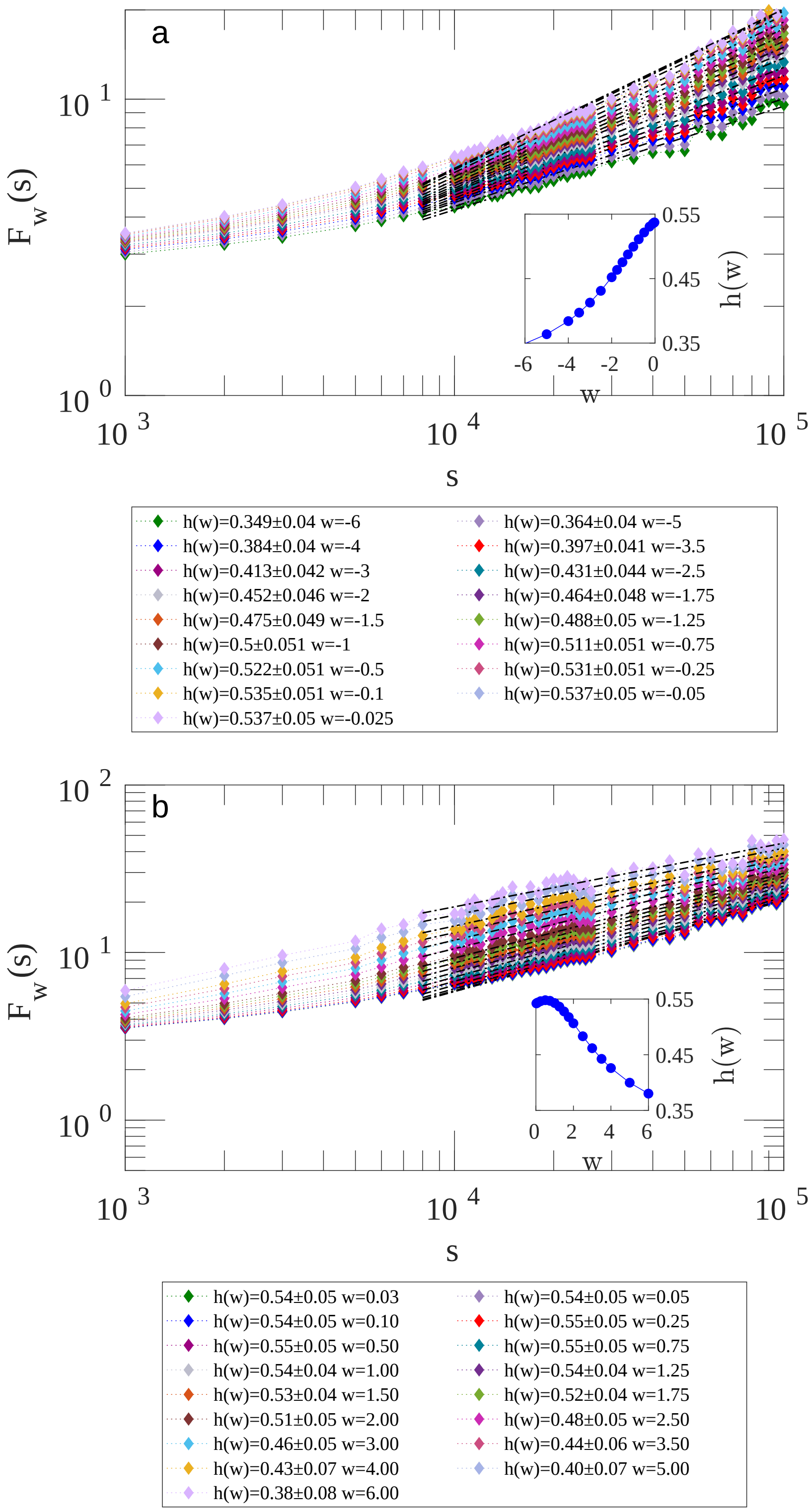


FIGURE 2.14: Normalized price return case: Calculation of the statistical function $F_w$ using Eq. (2.31). The function of $F_w$ vs $s$ display power laws $F_w(s) \sim s^{h(w)}$, where $h(w)$ depend on $w$. This feature demonstrates that the time series is multifractal.

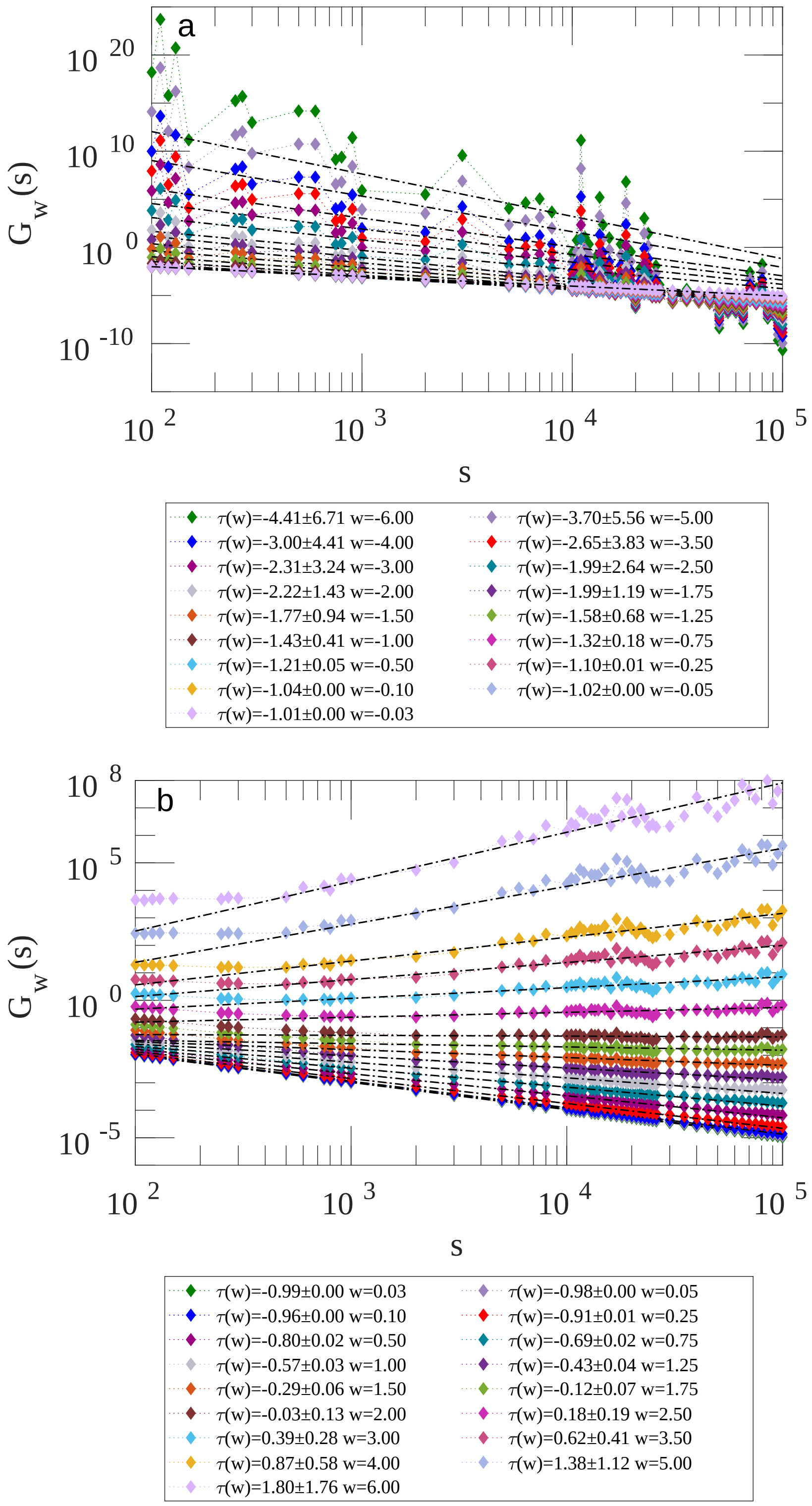


FIGURE 2.15: Normalized price return case: Calculation of the "generalized statistical functions" $G_{\rm w}(s)$ vs $s$ for negative (a) and positive (b) values of order w. The "generalized statistical functions" is calculated by applying Eq. (2.36).

For monofractal time series $h(\mathrm{w}) = cte$, implying that $\gamma = H$. On the other hand, for multifractal time series $h(\mathrm{w}) \neq cte$, then:

$$\begin{array}{ccc} monofractal & f(\gamma) = 1 & \gamma = H \\ multifractal & f(\gamma) = 0 & \gamma \neq cte \end{array}. \tag{2.41}$$

From the Subfigure 2.9a, the generalized Hurst exponent is linear $h(\mathrm{w}) = a_1 \mathrm{w} + b_1$. As a consequence the value of $\gamma = b_1 - 2a_1\mathrm{w}$, and

$$\mathrm{w} = \frac{b_1 - \gamma}{2a_1} \tag{2.42}$$

By replacing Eq. (2.42) in Eq. (2.40) the following relation is obtained:

$$f(\gamma) = 1 - \frac{1}{4a_1}(b_1 - \gamma)^2 \tag{2.43}$$

The Figure 2.16, represents how the range of probable generalized Hurst exponents values is reduced from multifractal time series to monofractal time series. At the limit of $a_1 \longrightarrow 0$, one finds that $h(\mathrm{w}) = H$ retrieving a Dirac delta function shifted representing a monofractal time series.

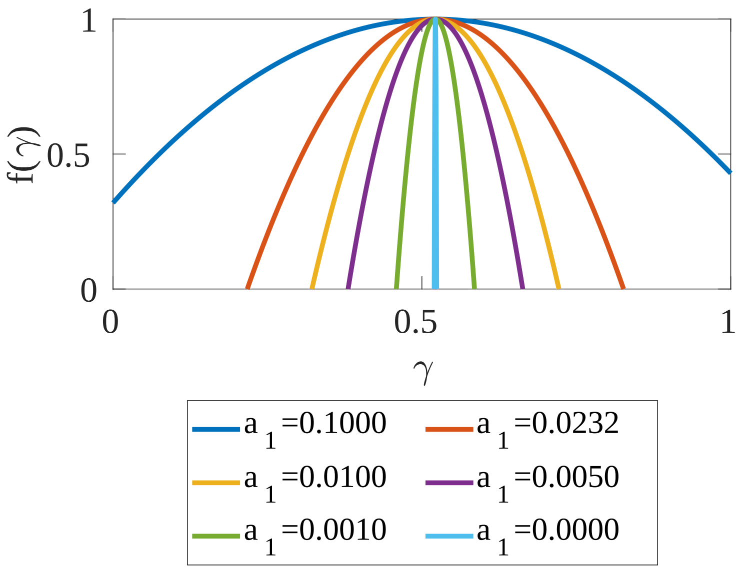


FIGURE 2.16: The range of probable generalized Hurst exponents values is reduced by making $a_1 \longrightarrow 0$ .

CHAPTER 3

# Stylized facts of high-frequency Bitcoin time series

---

In the previous chapter, we demonstrated that $q$-Gaussian distribution can be used to describe price fluctuations in conventional markets. We decomposed the financial time series into a deterministic trend and a stochastic noise. When performing the detrending process, instead of using the simple forward or backward moving average, we used a centered moving average method, where the average of the signal data points within a window of size $n$ is positioned at the center of the window. This approach is more sensitive to changes in the signal and avoids introducing a delay in the moving average relative to the signal. Comparisons were made between using symmetric and asymmetric moving windows, and it confirmed that using an asymmetric window for detrending does not affect the results for our datasets. In this chapter, our objective is to expand the empirical investigation to the stylized facts in digital assets, specifically Bitcoin cryptocurrency. Stylized facts are widely observed and acknowledged in conventional financial assets as the similarity in statistical features across different markets and times. While these stylized facts are less studied in digital assets owing to their novelty, it is crucial to examine them. Such an examination can lead to a better understanding of market dynamics in digital assets.

This chapter aims to analyze the high-frequency intraday Bitcoin dataset from 2019 to 2022 in terms of its statistical characteristics. During this time frame, the Bitcoin market index exhibited two distinct periods characterized by abrupt changes in volatility. Bitcoin price returns for both periods can be described by an anomalous diffusion process, transitioning from subdiffusion for short intervals to weak superdiffusion over longer intervals. The characteristic features related to this anomalous behavior studied in this chapter include heavy tails, which can be described using a $q$-Gaussian distribution and correlations. Autocorrelation of the absolute returns presents a power-law relationship, indicating time dependency in both periods initially. The ensemble autocorrelation of returns decays rapidly. We fitted the autocorrelation with a power-law to capture the decay and found that the second period experienced a slightly higher rate of decay. Further study involves the analysis of endogenous effects within the Bitcoin time series, examined through detrending analysis. We found that both periods are multifractal and present self-similarity in the detrended PDF. The Hurst exponent over short time intervals shifts from less than 0.5 ($\sim 0.42$) in Period 1 to be closer to 0.5 in Period 2 ($\sim 0.49$), indicating the market is more efficient at short time scales.

## 3.1 Introduction

Cryptocurrencies offer a decentralized and innovative alternative to traditional financial systems (Corbet et al. 2019). Despite not being globally accepted as digital currency, many consider cryptocurrencies valuable assets for storing and retrieving value when needed (Crosby et al. 2016). With over 2,000 distinct cryptocurrencies currently in circulation, their potential and prominence continue growing (Noam 2021). In this dynamically evolving market, Bitcoin stands out as the dominant one. Introduced by Nakamoto (Nakamoto 2008) in 2008 as the first decentralized cryptocurrency, Bitcoin has witnessed a substantial increase in its market value. Statistics from CoinMarketCap reveal that Bitcoin's market capitalization reached 567.61 billion USD as of August 3, 2023, constituting 48.09% of the aggregate market capitalization of major cryptoassets (*Global Cryptocurrency Charts* 2023). Bitcoin operates as an open accessible network, providing an emerging market free from the constraints of traditional trading hours. It captures the attention of practitioners, individuals who see value in associating Bitcoin with their addresses on the blockchain, and academics intrigued by its durability and the broader understanding of blockchain-based cryptocurrencies.

Bitcoin was created as an online payment system that enables users to engage in direct transactions without intermediaries (Nakamoto 2008). Its decentralized nature ensures independence from central banks or government authorities responsible for currency issuance (Underwood 2016; Zaghloul et al. 2020). The adoption of Bitcoin for payments of goods and services has experienced substantial growth. Some argue that businesses find it advantageous to accept Bitcoin, citing lower transaction fees compared to the typical 2-3% imposed by credit card processors (Hong 2017). Conversely, investors perceive Bitcoin as an alternative investment avenue, as indicated by an analysis of transactions from 2011 to 2014 (Baur et al. 2015). Bitcoin has sometimes been referred to as the 'digital gold' (Popper 2016), attracting individual investors seeking portfolio diversification as a replacement for gold as a hedge against inflation (Henriques and Sadorsky 2018). This investment interest extends beyond individual investors to various institutional players, including the Global Advisors Bitcoin Investment Fund, Pantera Capital, and Falcon Global Capital, which initiated Bitcoin investments as early as 2013 (Hong 2017). Various types of institutions that hold Bitcoin have emerged, including the Bitcoin Exchange-Traded Funds (ETFs) that track the value of Bitcoin. These ETFs attract investors and speculators by facilitating transactions through traditional stock market exchanges rather than cryptocurrency trading platforms. Presently, a significant portion of Bitcoin is under institutional ownership, ranging from ETFs to sovereign governments like El Salvador (Genç 2023). Institutional investment in Bitcoin takes various forms, encompassing direct ownership, participation in mining companies, Bitcoin futures ETFs, or integration into retirement strategies (Genç 2023).

The peer-to-peer characteristic of Bitcoin is underpinned by blockchain technology, which functions as a shared public ledger of all transactions and digital events among participants (Underwood 2016; Crosby et al. 2016; Zaghloul et al. 2020). This technology has demonstrated its versatility by finding applications in both financial and non-financial domains. Financial institutions and banks actively explore innovative blockchain applications, with a focus on areas such as private securities and insurance (Crosby et al. 2016). A notable example is Decentralized Finance (DeFi), which represents a groundbreaking financial paradigm built on blockchain, providing services like loans, insurance, and financial assets exchange without reliance on a central authority (Auer et al. 2023). DeFi is gaining attention from investment banks and central banks, with initiated programs to explore the potential applications of digital assets (Genç 2023). The non-financial applications of blockchain technology also hold considerable promise. Serving as a decentralized storage system, blockchain facilitates the storage of various file types. This technology can verify the existence of diverse documents, including legal documents, health records, loyalty payments, and licenses across various industries. By storing the fingerprint of the asset instead of the asset itself, blockchain ensures enhanced privacy and anonymity (Crosby et al. 2016).

With an increasing number of users adopting Bitcoin, and despite its meaningful fluctuations, high volatility, and dependence on evolving technology, this emerging asset continues to gain importance in our economy. Previous studies have extensively explored various aspects of Bitcoin, including its market efficiency (Urquhart 2016; Kurihara and Fukushima 2017; Jiang et al. 2018; Caporale et al. 2018; Noda 2021; Bariviera et al. 2017; Mnif et al. 2020; Mnif and Jarboui 2021; Fernandes et al. 2022; Montasser et al. 2022; Kakinaka and Umeno 2022), regulatory requirements (Brito et al. 2014; Böhme et al. 2015; Hendrickson and Luther 2017; Marian 2013; Gross et al. 2017), market dynamics and its correlations with various asset classes (Conrad et al. 2018; Ciaian et al. 2018; Klein et al. 2018; Eross et al. 2019; Ariya et al. 2020; Arias-Calluari et al. 2021; Hu et al. 2019; De Sousa Filho et al. 2021; Cremaschini et al. 2023; Ghosh et al. 2023; Bariviera et al. 2017; De Sousa Filho et al. 2021; Wen et al. 2022; Zhang et al. 2018a), with the intent to quantify Bitcoin price fluctuations and evaluate their proximity to stock market prices mechanisms. Given that the Bitcoin pricing mechanism differs from conventional stock market price indexes, we propose initiating the analysis by examining robust patterns or *'stylized facts'* of Bitcoin price fluctuations. This analysis is based on 'tick-by-tick' recorded data from Reuters Datascope. The motivation lies in unveiling precise time-scale properties of Bitcoin time series, allowing comparisons with the widely acknowledged stylized facts from stock market data (Cont 2001), e.g. fat tails, volatility clustering, short-time correlations, and self-similarity measurements. To do this we analyze the intraday data of the BTC/USD exchange, spanning the years 2018 to 2022. The dataset has a frequency of 10 minutes, and trading occurs continuously throughout the 24-hour day.

The paper is organized as follows: Section 3.2 recalls well-known stylized facts observed in financial time series. Section 3.3 presents a background of the Bitcoin cryptocurrency, essential for understanding the dynamics of Bitcoin transactions. In Section 3.4, we provide the governing equations adapted from our closest model obtained for stock market prices for this study, along with the notations used in this paper. In Section 3.5, we divide the Bitcoin time series into different time periods characterized by the abrupt change in the volatility, and then we examine the stylized facts for each period, respectively. Finally, we provide a summary of our findings based on the comparative analysis of the S&P 500 and Bitcoin.

## 3.2 Stylized facts of financial markets

For the evaluation of financial models and the development of econometric theories, researchers focus on studying persistent statistical characteristics of the market, commonly referred to as *'stylized facts'*.

Stylized fact is a widely adopted concept in economics, referring to the common statistical properties observed across datasets spanning different timeframes (Cont 2001; Chakraborti et al. 2011). The concept of stylized facts, initially introduced in macroeconomics to describe statistical patterns characterizing macroeconomic growth over extended periods and across diverse countries (Kaldor 1961), has undergone extensive examination in traditional financial instruments. In stock markets, widely recognized stylized facts include phenomena such as fat-tailed distribution, volatility clustering, self-similarity of market returns, and seasonality in time series (Bollerslev et al. 1994; Cont 2001; Chakraborti et al. 2011; Nystrup et al. 2015; Shakeel and Srivastava 2018; Arias-Calluari et al. 2021). Analyzing stylized facts is crucial for establishing the foundation for the development of theoretical forecasting models (Rydén et al. 1998; Liesenfeld and Jung 2000; Andersson 2001; Carnero 2004; Bulla and Bulla 2006; Malmsten and Teräsvirta 2010; Chakraborti et al. 2011). A substantial body of evidence suggests that cryptocurrency markets exhibit the key stylized characteristics observed in foreign exchange markets (Segnon and Bekiros 2020; Bariviera et al. 2017). These findings motivate a careful analysis of the most well-known stylized facts in stock markets before seeking future modeling approaches. In this section, we dedicate ourselves to recalling each of these well-known stylized facts along with their corresponding descriptions, as listed below:

(1) **fat-tailed distribution of returns**: This phenomenon was initially recognized by Mandelbrot (Mandelbrot 1963), based on empirical distributions of financial returns (and log-returns) that exhibit heavy-tailed distributions, deviating from the Gaussian

distribution (Cont 2001; Chakraborti et al. 2011). The presence of heavy tails indicates a higher likelihood of extreme events than predicted by a normal distribution (Stoyanov et al. 2011). Within a self-similar fat-tailed distribution, the tails can be characterized by a power law relation denoted as $P(x,t) \sim t^{-H}F(xt^{-H})$, where $P(x,t)$ represents the probability distribution function (PDF) of the price return $x$. $F$ was widely assumed to follow a distribution known as a Levy distribution from the 1990s, $F(x) = L_\alpha(x)$, $H = 1/\alpha$ where $\alpha \in (0,2]$ (Lévy 1954; Mantegna and Stanley 1994; Mantegna and Stanley 1999). After the 2000, $F$ was considered as a q-Gaussian distribution, $F(x) = g_q(x)$, $H = 1/\alpha$ , where $\alpha = \frac{3-q}{\xi}$ with $q \in (1,3)$ and $\xi$ as a constant parameter(Borland and Bouchaud 2004; Queirós 2005; Malamud 2003; Alonso-Marroquin et al. 2019). More recently $F$ is viewed as the solution of a general porous media equation solved through local derivatives $H(t) = 1/\alpha(t)$, where $\alpha(t) = \frac{3-q(t)}{\xi(t)}$ (Gharari et al. 2021; Tang et al. 2024b).

(2) **short-time autocorrelation of returns**: The autocorrelation function (ACF) quantifies the relationship between the current data and historical data, showing the extent to which there is some form of 'memory' in the market (Vilela et al. 2013; Nounou and Bakshi 2000). The memory is commonly defined as the critic shifted time for the autocorrelation process $\tau_c = 1/ACF(0)\int_0^\infty ACF(\tau)d\tau$ (Kasdin 1995). In terms of financial data analysis, ACF is evaluated using price returns and describes a rapid decay during very small intraday time scales, before decaying to zero value (Cont 2001; Chakraborti et al. 2011). This trend aligns with the efficient market hypothesis (De Sousa Filho et al. 2021; Cont 2001), signifying a finite memory; it retains correlation with values closer back in time only.

(3) **volatility clustering**: Volatility in finance measures the extent to which actual returns deviate from average returns over a designated time span (Kumar 2016). It is related to the risk management of assets, with higher volatility implying a greater chance of substantial losses (De Silva et al. 2017). Volatility is commonly quantified as the standard deviation ($\sigma$) of the returns, and it plays an important role as an estimation tool in empirical investigations in financial studies, especially when examining new and emerging assets (Ghosh et al. 2023). Regarding stylized facts,

volatility clustering is a widely observed phenomenon, particularly in speculative return time series. Mandelbrot initially identified this pattern (Mandelbrot 1963), denoting the tendency for substantial changes to be succeeded by similarly substantial changes, and minor changes to be succeeded by comparably minor changes. This underscores the empirical reality that price fluctuations are non-stationary processes as the fluctuations are not identically distributed and the distributions experience temporal shifts (Chakraborti et al. 2011).

(4) **self-similarity and fractality**: Broadly defined, a fractal refers to a geometric shape that exhibits fragmented characteristics, with each fragment (at least approximately) resembling a reduced-scale replica of the whole structure (Chen et al. 2016a). A fractal can be described by its scale-invariant fractal dimension (Mandelbrot 1982), which is directly related to the Hurst exponent, $H$. Fractals have been studied extensively in finance and economics, including the stock market (Lee et al. 2017), gold (Mali and Mukhopadhyay 2014), electricity (Wang et al. 2013), crude oil (Gu et al. 2010), and shipping markets (Chen et al. 2016a). In the domains of finance and economics, substantial research has explored the concept of fractals and scaling laws (Önalan 2004). Scaling laws establish a connection between price returns computed over various sampling intervals, highlighting that the shape of PDF of price return remains consistent as the time scale varies, $P(x,t) \sim t^{-H}F(xt^{-H})$ (Gharari et al. 2021), where a self-similar time series denotes $\sqrt{\langle x^2 \rangle} \propto t^H$. Fractal analysis techniques such as rescaled range analysis (R/S) and Detrended Fluctuation Analysis (DFA) have been pivotal in these investigations (Lahmiri and Bekiros 2018). Both methods yield a spectrum of Hurst exponent, enabling the determination of the fractality of the time series. However, the R/S statistic is susceptible to outlier influence, potentially leading to a biased estimation of the Hurst exponent (Gu et al. 2010). Therefore, in this study, we adopt the multifractal detrended fluctuation analysis (MF-DFA) method, which is a generalization of the DFA, owing to its proficiency in handling nonstationary time series (Lahmiri and Bekiros 2018).

Besides these well-acknowledged facts, financial markets exhibit other widely observed statistical characteristics, one of which is the anomalous diffusion in the peak of the PDF of returns. Bachelier's (Bachelier 1900) original work on market fluctuations also introduced the first option pricing model grounded in Brownian motion, associating this motion with price return fluctuations. Later the Black-Scholes equation was proposed to improve the Brownian motion model to prevent the possibility of negative prices (Black and Scholes 1973). The Black-Scholes model is alternately referred to as the geometric Brownian model. However, these models fall short of effectively characterizing numerous dynamic processes (Weron and Magdziarz 2009). This limitation arises from the fact that the mean squared displacement of the price return scales with time exhibiting a fractional exponent deviating from conventional Brownian motion (Sposini et al. 2022a), $H \neq 0.5$ and is not a unique value $H(t) = 1/\alpha(t)$; this deviation is known as anomalous diffusion. Anomalous diffusion is widely observed within financial data and is expressible through a power law relation $P_{max} \sim t^{-1/\alpha(t)}$, where $P_{max}$ represents the peak of the PDF of the future price return, and $t$ represents the predicted time (Alonso-Marroquin et al. 2019). Here, $\alpha = 2$ indicates normal (Brownian) diffusion, $\alpha < 2$ implies superdiffusion, and $\alpha > 2$ denotes subdiffusion (Sposini et al. 2022a). Moreover, the value of $\alpha$ is intricately tied to the Hurst exponent ($H$) through the relation $H = 1/\alpha(t)$ (Gharari et al. 2021; Sposini et al. 2022a; Ghosh et al. 2023). For example, this relationship is valid in fraction Brownian motion, which is a self-similar Gaussian stochastic process characterized by stationary power-law correlated increments (Gharari et al. 2021).

The aforementioned statistical properties are typically observed in traditional markets. This paper seeks to evaluate these properties in the context of Bitcoin, drawing comparisons with conventional markets. Given the distinctive framework of Bitcoin compared to traditional markets, the following section will offer a brief overview of its characteristics.

## 3.3 Bitcoin's operational framework

Cryptocurrencies are decentralized digital assets that rely on encryption to verify transactions. Bitcoin, being the first, largest, and most well-known cryptocurrency, operates differently from centralized money systems. For centralized money, currency is issued by central banks and transactions involve intermediaries like banks. In contrast, Bitcoin employs a decentralized digital infrastructure called “blockchain" for peer-to-peer transactions and value storage. This allows Bitcoin to operate independently of any government, company, or financial institution. The concept of blockchain was initially proposed in 1991 (Haber and Stornetta 1991) and further developed by Satoshi Nakamoto (Nakamoto 2008). A blockchain is a public ledger of all transactions and digital events shared among participating parties since the creation of Bitcoin (Underwood 2016; Crosby et al. 2016). The blockchain maintains a certain and verifiable record of every single transaction and ownership and once lodged, the transaction can never be erased (Crosby et al. 2016; Vujičić et al. 2018). Additionally, blockchain technology prevents double-spending, enhancing the security level of Bitcoin cryptocurrency (Kuo Chuen et al. 2018). This technology creates a network of traders, with each node in the network retaining a copy of the ledger record (Vujičić et al. 2018).

Transferring Bitcoin from one owner to another relies on blockchain technology, where Bitcoin owners execute transactions using their private and public keys. The private key serves as a digital signature, while the public key is used for verifying transactions. During a transaction, Bitcoins are sent from one address to another, requiring the sender’s private key for validation. The transaction details must include the Bitcoin address, amount to be transferred, and the public key of the next owner (Vujičić et al. 2018). Subsequently, the transaction is broadcast to the Bitcoin network, rapidly disseminating across connected nodes to notify them of its occurrence. However, before being added to the blockchain, this transaction undergoes a validation process known as Bitcoin mining. Miners engage in a competition, a ‘proof-of-work puzzle’, to include the transaction in a block. The winning miner then broadcasts the block to all nodes, allowing them to expand and update their copies of the blockchain (Zaghloul et al. 2020). Only miners possess the capability to add a transaction to the digital ledger, transitioning it from pending to confirmed.

Miners play a crucial role in Bitcoin systems, assembling a special transaction known as a coinbase transaction, which relates to the creation of new coins in the network. Bitcoin operates independently of a centralized authority responsible for issuing new coins, and instead, coins are automatically generated by the Bitcoin blockchain system as a reward for the first miner who successfully completes the proof-of-work consensus mechanism (Nakamoto 2008).

The initiation of a new coin is triggered by the first transaction in a block, and ownership of this coin is attributed to the creator of the block (Nakamoto 2008). This incentive structure motivates miners to validate transactions, thereby injecting coins into circulation. The mining process involves solving a mathematical puzzle, with miners rewarded for finding the solution, resulting in the creation of a new block that is updated to the blockchain (Tschorsch and Scheuermann 2016). The design of the Bitcoin network aims to produce one block roughly every ten minutes. As computational power increases, the network maintains a relatively stable block creation time by progressively elevating the difficulty of generating new blocks (Vujičić et al. 2018). While mining remains the exclusive means of generating new coins, it comes with a significant energy consumption. Furthermore, individual miners may face a notably low likelihood of achieving successful returns. To address this, solo miners collaborate by uniting their mining capabilities and forming mining pools. Eventually, these pools evolve into substantial organizations with considerable computational prowess, enabling them to contend with other major entities. Rewards are then distributed among participants based on their individual contributions (Zaghloul et al. 2020).

One fundamental characteristic of Bitcoin is its deliberate limitation on coin supply. The initial Bitcoin coin reward was established at 50 coins, which is the total amount of Bitcoin when it was first created. This reward is designed to undergo halving every 210,000 blocks, equivalent to approximately four years (Vujičić et al. 2018). With a fixed total supply of 21 million Bitcoin, currently, approximately 93% of this total has been brought into existence. Even after the full issuance of coins, Bitcoin will remain exchangeable among owners, with rewards shifted to the verification of transactions.

Bitcoin offers a 24/7 market accessible globally. Its unique attributes enable transactions to occur at a significantly accelerated pace compared to fiat currency, which leads to a notably more volatile market compared to conventional financial markets.

## 3.4 Governing equations

A common approach for analyzing option pricing is related to the well-known Black-Scholes equation (BSE) as the governing equation for modeling price return. We recall our governing equation from (Arias-Calluari et al. 2022) which is used to model stock market indexes. This equation allows prices to fluctuate with a trend and a stochastic noise. This stochastic noise can be well-described by a $q$-Gaussian distribution. The time evolution of the PDF of stochastic processes can be presented using a Fokker-Planck equation (FPE). In our analysis, we use fractional FPE to describe the time evolution of the PDF of price return, and use the local Katugampola fractional operators for the fractional $q$-Gaussian process. The anomalous diffusion is defined in terms of the second moment of the PDF. The autocorrelation is presented in an integral form.

(1) **Governing equations of stock market**: The market index of any given stock market data is denoted as $I(t)$, and the simple price return in a time interval from current time $t_0$ to future time $t$ is defined as

$$X(t_0, t) = I(t_0 + t) - I(t_0). \tag{3.1}$$

The stock market index fluctuates over time in a random process. In this analysis, it is assumed that the stock market index $I(t)$ can be decomposed to a deterministic trend $\bar{I}(t)$ and a stochastic noise $\hat{I}(t)$

$$I(t) = \overline{I}(t) + \hat{I}(t). \tag{3.2}$$

The price return $X(t)$ can also be divided into two parts: a deterministic component $\bar{X}(t)$ and a stochastic $q$-Gaussian noise $x(t)$

$$X(t) = \overline{X}(t) + x(t), \tag{3.3}$$

where $\overline{X}(t) = \overline{I}(t_0 + t) - \overline{I}(t_0)$, and $x(t) = \hat{I}(t_0 + t) - \hat{I}(t_0)$. The increment of the price return is calculated by the difference between the consecutive points of the price return, written as

$$\begin{aligned} X^*(t) &= I(t+1) - I(t) \\ x^*(t) &= \hat{I}(t+1) - \hat{I}(t) \end{aligned}. \tag{3.4}$$

From here onward, $t$ represents the normalized time obtained by $t = time/\Delta t$, where $time$ is the time in minutes and $\Delta t = 10\, mins$ is the frequency of the Bitcoin price index.

The main interest in financial market forecasting focuses on predicting the price return at a future time $t_0 + t$. In this context, we employ a probability approach, where we assume that the simple price return $X$ is a random variable characterized by a time-dependent PDF $P(x, t)$. Then our primary goal is to establish the governing equation that describes the evolution of $P(x, t)$.

Eq. 3.3 can be expressed as a stochastic derivative that is different from the standard derivative, where the quantity $x(t)$ is stochastic and, therefore, not differentiable, written as

$$\frac{dX}{dt} = \frac{d\bar{X}}{dt} + \frac{dx}{dt}. \tag{3.5}$$

That is conveniently written as from a stochastic Itô-Langevin equation of the form

$$\frac{dX}{dt} = \mu(X, t) + \sigma(X, t)\eta(t), \tag{3.6}$$

where $\mu$ is the trend of the time series, $\sigma$ is the volatility, $\eta(t)$ is a white noise with $< \eta >= 0$. Using the Itô's lemma (Itô 1951), it is possible to derive the partial differential equation that describes the temporal evolution of the probability density function $P(X, t)$ of the stochastic variable $X(t)$, presented as

$$\frac{\partial P}{\partial t} = -\frac{\partial}{\partial X}(\mu(X, t)P) + \frac{1}{2}\frac{\partial^2}{\partial X^2}(\sigma^2(X, t)P). \tag{3.7}$$

For a detrended price return, $\mu(X, t) = 0$, and the evolution of PDF is reduced to

$$\frac{\partial P(x, t)}{\partial t} = \frac{1}{2}\frac{\partial^2}{\partial x^2}(\sigma^2(x, t)P(x, t)). \tag{3.8}$$

The work of Borland suggests that the volatility depends on the PDF so that the diffusion process becomes non-linear (Borland 1998). Based on our earlier empirical analysis of the S&P500 stock market index, we have found that (Alonso-Marroquin et al. 2019)

$$\frac{\partial P(x,t)}{\partial \tau} = D_0 \frac{\partial^2 P^{2-q}(x,t)}{\partial x^2}, \tag{3.9}$$

where $D_0$ is a diffusion constant, $\tau = t^{\xi}$, being $0 < \xi \leq 1$ an empirical exponent obtained from the empirical data. The solution of Eq. 3.9 with the Dirac's delta as initial condition $P(x, t = 0) = \delta(x)$ is given by (Alonso-Marroquin et al. 2019)

$$P(x,t) = \frac{1}{(D_0 t)^H} \left[ g_q \left( \frac{x}{(D_0 t)^H} \right) \right], \tag{3.10}$$

where $H = 1/\alpha = \xi/(3-q)$ and $g_q(x)$ is the normalized $q$-Gaussian distribution distribution defined by

$$g_q(x) = \frac{1}{C_q} \left[ 1 - (1-q)x^2 \right]^{\frac{1}{1-q}}. \tag{3.11}$$

This is a generalization of the Gaussian distribution; if $q = 1$ the Gaussian distribution is recovered. The normalization constant $C_q$ for $1 < q < 3$ is given by

$$C_q = \sqrt{\frac{\pi}{q-1}} \frac{\Gamma((3-q)/(2(q-1)))}{\Gamma(1/(q-1))}. \tag{3.12}$$

(2) **Fractional diffusion equations**: Now we present the diffusion equation in the fractional form. Eq. 3.9 can be rewritten into two different formats. The first case is to convert it into a Fokker-Plank Equation with time-dependent volatility. This is performed by using the rule $d\tau = t^{\xi-1}dt$ to convert it into

$$\frac{\partial P(x,t)}{\partial t} = D_0 t^{\xi-1} \frac{\partial P^{2-q}(x,t)}{\partial x^2}, \tag{3.13}$$

and by comparing Eq. 3.8 and 3.9, we obtain the expression for the volatility as

$$\sigma(x,t) = \sqrt{2D_0} t^{\frac{1-\xi}{2}} P^{\frac{1-q}{2}}(x,t). \tag{3.14}$$

In a more recent work (Gharari et al. 2021), it has been proposed that Eq. 3.9 can be written as a local fractional differential equation with Katugampola fractional operator. The Katugampola fractional derivative for $0 < \xi \leq 1$ is defined by

$$\frac{d^{\xi} f}{d^{\xi} t} := \lim_{\epsilon \to 0} \frac{f(te^{\epsilon t^{-\xi}}) - f(t)}{\epsilon}. \tag{3.15}$$

The Katugampola fractional derivative has the property of

$$\frac{d^{\xi} f}{d^{\xi} t} = t^{1-\xi} \frac{df}{dt}. \tag{3.16}$$

Using the above properties, we can derive the fractional form of Eq. 3.9 as

$$\frac{\partial^{\xi} P(x,t)}{\partial^{\xi} t} = D_0 \frac{\partial^2 P^{2-q}(x,t)}{\partial x^2}. \tag{3.17}$$

This proves that Eqs. 3.13 and 3.17 are the same equations.

(3) **Anomalous diffusion**: In the following, we connect the expression for anomalous diffusion with the second moment of the time series. For a wide range of diffusion processes, the PDF follows the scaling solution and can be written in a generalized form as (Tang et al. 2024b)

$$P(x,t) = \frac{1}{\phi(t)} F\left[\frac{x}{\phi(t)}\right]. \tag{3.18}$$

In this study, $F$ is the normalized $q$-Gaussian distribution function. The anomalous diffusion can be calculated using the second moment of the time series

$$\begin{aligned} < x^2 > &= \int_{-\infty}^{\infty} x^2 P(x,t)\, dx \\ &= \int_{-\infty}^{\infty} \frac{x^2}{\phi(t)} F\left[\frac{x}{\phi(t)}\right] dx. \end{aligned} \tag{3.19}$$

By changing variable $\frac{x}{\phi(t)} = y$, the above equation can be rewritten as

$$\begin{aligned} < x^2 > &= \phi(t)^2 \int_{-\infty}^{\infty} y^2 F(y)\, dy \\ &= \phi(t)^2 \sigma_0^2. \end{aligned} \tag{3.20}$$

For a normalized distribution, $\sigma_0$ can be ignored. Therefore the nature of anomalous diffusion is calculated as

$$< x^2 >= \phi(t)^2 \propto t^{2H}. \tag{3.21}$$

The PDF is assumed to satisfy the scaling relation given by Eq. 3.18. Replacing $x = 0$ into Eq. 3.18 we obtain $P(0,t) = F(0)/\phi(t)$. Assuming that the PDF peaks at $x = 0$ (i.e. $P_{max}(t) = P(0,t)$ and using Eq. 3.21 the second moment is reduced to

$$\sqrt{< x^2 >} = \phi(t) \propto t^H \sim 1/P_{max}(t) \tag{3.22}$$

In other words, the exponent of the anomalous diffusion can be obtained from the time evolution of the peak of the PDF.

(4) **Autocorrelation Function (ACF)**: The autocorrelation function can be derived from the SDE. For a fractional Brownian motion, the correlation function can be expressed as

$$\begin{aligned} &E[X(t)X(t+\tau)] \\ &= \int_0^{t+\tau} \int_0^t E[W(t)W(t+\tau)]dtd(t+\tau), \end{aligned} \tag{3.23}$$

where $W(t) = dX/dt$. From Eq. 3.6, we can represent the time series as

$$X(t) = \int_0^t (\mu(X,t) + \sigma(X,t)\eta(t))\ dt. \tag{3.24}$$

Assuming the time series is detrended, then $\mu(X,t) = 0$. We can write the autocorrelation as

$$\begin{aligned} &\langle X(t)X(t+\tau)\rangle \\ &= \left\langle \int_0^t \sigma(X,t')\eta(t')\, dt' \int_0^{t+\tau} \sigma(X,t'')\eta(t'')\, dt'' \right\rangle \\ &= \int_0^t \int_0^{t+\tau} \langle \sigma(X,t')\eta(t')\sigma(X,t'')\eta(t'')\rangle\ dt'dt''. \end{aligned} \tag{3.25}$$

From Eq. 3.6, assuming $\sigma(x,t)$ and $\eta(t)$ are known, one can solve the integral to obtain the analytical expression of the autocorrelation.

## 3.5 Stylized facts of Bitcoin market index

Financial time series exhibit diverse stylized facts over time. Consequently, segmenting the entire time series into distinct periods for detailed investigation becomes crucial. Our initial step involves identifying these different sections within the Bitcoin price index. We collected Bitcoin price index data from March 9, 2017, to December 31, 2022, with a 10-minute frequency. Using this dataset, we computed the simple price return $X^*(t)$ (Eq. 3.4) and volatility $\sigma(t)$. The latter was calculated as the standard deviation of $X^*(t)$ on a rolling window of one hour. The results are shown in Figure 3.1 (a-c) for the price index $I(t)$, simple price return $X^*(t)$, and volatility $\sigma(t)$ respectively, providing a reference for segmenting the dataset. Data preceding April 2, 2019, was deemed spurious due to unrealistic jumps of the order of 100 USDs and was, therefore, excluded from further analysis. Figure 3.1(a) illustrates the price index, revealing a substantial upsurge in price since 2021. This significant rise coincides with Elon Musk's purchase of $1.5 billion worth of Bitcoin and Tesla's announcement to accept Bitcoin as payment. This marked a significant turning point, necessitating the recognition of data from 2021 onward as a distinct period. Consequently, data points spanning from April 2, 2019, to December 31, 2020, constitute an independent segment denoted as Period 1 in this study. A notable shift in market dynamics unfolded between 2021 and May 2022. During this period, cryptocurrency prices surged significantly. However, a significant change occurred post-May 2022. This period witnessed a series of crises impacting multiple cryptocurrencies and trading platforms. The collapse of LUNA from Terraform Labs resulted in a total loss of market value of over $400 billion. Concurrently, the decision by Elon Musk to discontinue Bitcoin acceptance for Tesla car purchases contributed to an environment characterized by an increased frequency of substantial market downturns. Consequently, the data recorded after May 2022 warrants categorization as a distinct time period. Therefore, we label the dataset from January 1, 2021, to May 9, 2022, as Period 2 in this study. Figure 3.1 (b&c) depicts the simple price return and volatility respectively, illustrating that Period 2 exhibits notably higher returns and volatility compared to Period 1.

### 3.5.1 Anomalous diffusion and fat-tailed distribution

Our analysis commences with an examination of the PDF of simple price return $X(t_0, t)$ as shown in Eq. 3.1. For both Period 1 and Period 2, we calculate the PDFs across various time intervals $t = t - t_0$, i.e. we plot the relative diffusion time instead of the absolute time, ranging

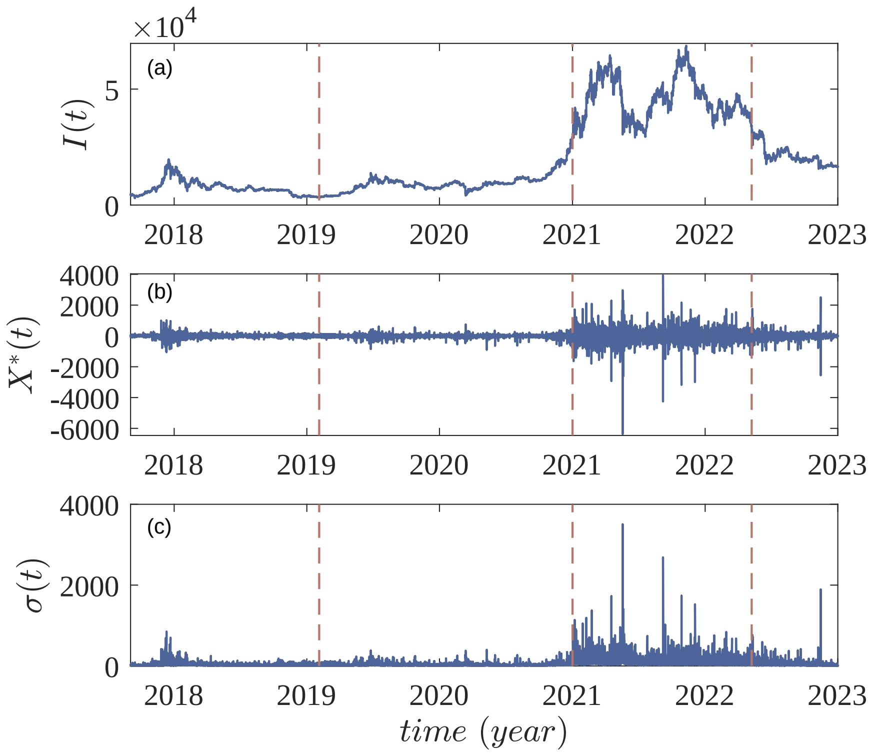


FIGURE 3.1: (a) Bitcoin market index $I(t)$ from 03/09/2017 to 31/12/2022. (b) Simple price return $X^*(t)$ obtained from $\hat{I}(t)$ following Eq. 3.4. (c) The standard deviation $\sigma(t)$ of simple price return calculated by using a 1-hour moving window, where $\sigma(t) = \sqrt{\frac{1}{N-1}\sum_{t=1}^{N}(X^*(t)-\mu)^2}$, $X_i^*$ indicates a specific segment of the price return, and $\mu$ is the mean value of that segment.

from the smallest diffusion interval $t = 1$ to a year's diffusion period $t = 326\, days$. The kernel density estimator, known for its capacity to provide a smooth and accurate estimation of PDFs (Węglarczyk 2018), is employed with a kernel bandwidth set to 0.001. This ensures that the bandwidth is sufficiently small to capture the detailed structures of the PDFs. To compute the PDFs, we calculate the price return using Eq. 3.1 for each time interval $t$ and then use the price return to calculate $P(X, t)$.

In Figure 3.2 (a), we present the peak of the PDF $P_{max}$ for Periods 1 and 2 respectively in relation to time $t$. Notably, both time periods exhibit a power-law relation between the peak of the PDF and time, expressed as $P_{max} \sim t^{-H}$. Linear curve fitting is applied to the data of Periods 1 and 2 respectively to measure the power-law slope ($H = 1/\alpha$). We note a transition in the $H$ values for both datasets is observed, signifying a shift in the diffusion mode. For Period 1, the Hurst exponent $H$ is $0.415 \pm 0.006$ at small time intervals and $0.610 \pm 0.007$ at large time intervals, corresponding to the values of $\alpha = 2.41 \pm 0.03$ and $\alpha = 1.64 \pm 0.02$, respectively. For Period 2, the slope is $H = 0.478 \pm 0.004$ at small time intervals and $H = 0.646 \pm 0.004$ at large time intervals, corresponding to the respective values of $\alpha = 2.09 \pm 0.01$ and $\alpha = 1.54 \pm 0.01$. The anomalous diffusion exponent $\alpha$ is used to distinguish normal (Brownian, $\alpha = 2, H = 0.5$) from anomalous diffusion ($\alpha \neq 2, H \neq 0.5$). The regimes of super- and subdiffusion correspond to $\alpha > 2, H < 0.5$ and $0 < \alpha < 2, H > 0.5$, respectively (Sposini et al. 2022b). These results suggest that both periods of the Bitcoin time series undergo a transition from a weak subdiffusion regime to a weak superdiffusion regime over an extended period.

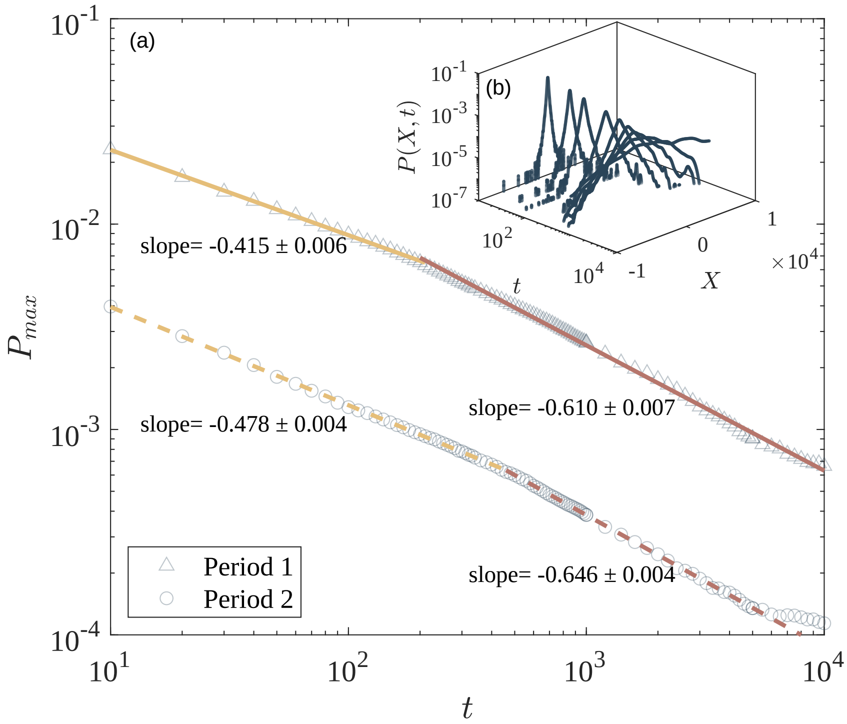


FIGURE 3.2: (a) Time evolution of the peak of the PDF for Period 1 and 2 in the log-log scale shown in Black markers. Two well-defined slopes can be observed for each period. The colored lines show the fitted slope of the power-law relation. Both periods experience a transition from a weak subdiffusion regimen to a weak superdiffusion regime over time. (b) Time evolution of the PDF for Period 2 from 10 mins to 1000 mins. The PDFs present distinctive peaks and heavy tails at small time intervals and become flat as the time interval increases.

Figure 3.2 (b) illustrates the time evolution of the PDF from 10 minutes to 1000 minutes (approximately 16.5 hours) of trading time. The PDF at the minimal time interval $t = 1$ exhibits a heavy-tailed non-Gaussian distribution, gradually flattening and broadening as time progresses. To further explore the fat-tailed distribution of the PDF, it is essential to determine the tail slope of the PDF at the minimum time interval, $P(X^*, t = 1)$. This slope, denoted as $\alpha$, is crucial for characterizing the type of distribution. The tail exponent for Lévy distribution is calculated as $P(x, t) \sim x^{-(1+\alpha)}$, where $0 < \alpha < 2$ (Lévy 1954; Mantegna and Stanley 1994). The exponent for the $q$-Gaussian distribution is $P(x, t) \sim x^{\alpha}$, where $\alpha = \frac{2}{1-q}$, and $1 < q < 3$ (Alonso-Marroquin et al. 2019). In Figure 3.3, we present the calculated tail slopes of the PDF for each period. The slopes of the tails for Period 1 and Period 2 are $\alpha = 3.95 \pm 0.18$ and $\alpha = 4.04 \pm 0.12$ respectively. By comparing these values with the corresponding exponents of Lévy and $q$-Gaussian distribution, we find that the slopes fall outside the Lévy regime and instead fit well into the $q$-Gaussian regime. The values of $q$ calculated based on the derived tail slopes using the aforementioned relation are $q = 1.51 \pm 0.02$ and $q = 1.50 \pm 0.02$ for Period 1 and 2, respectively.

Upon examining the fat-tailed distribution, we discerned that the PDF at the minimum time interval ($t = 1$) can be characterized by a $q$-Gaussian distribution. To substantiate this observation, we conducted a calibration to the $q$-Gaussian distribution for the PDFs corresponding to both Period 1 and Period 2. The outcomes of this calibration process are depicted in Figure 3.4. This calibration procedure was conducted in a semi-logarithmic scale by applying the relationship described in Eq. 3.10. This method involved taking the natural logarithm of the PDF and fitting it to the simple price return using a linear scale. Figure 3.4 (a) plots the right branch of the PDF using a log-log scale and Figure 3.4 (b) illustrates both branches of the PDF in semi-logarithmic scale. In these figures, the grey dotted curves represent the PDF of the simple price return, while the Black curves represent the fitted $q$-Gaussian distribution. Notably, the fitted distribution captures both the central and tail portions of the PDFs. The $q$ values derived from the semi-logarithmic fitting were determined as $q = 1.53$ for Period 1 and $q = 1.57$ for Period 2. Importantly, these values align with the $q$ values fitted from the power-law tail slope, affirming the consistency of the results that the diffusion is $q$-Gaussian.

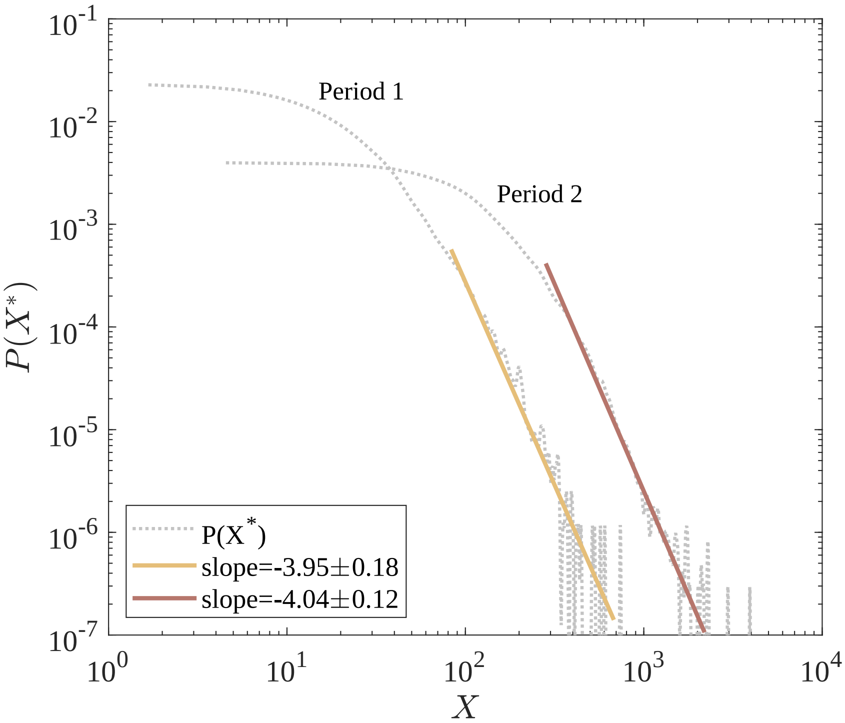


FIGURE 3.3: Tail slope of PDF at the minimum time interval $t_0$ for Period 1 and 2 respectively in log-log scale. The dotted grey lines are the PDFs of price return, and the colored lines show the fitted slope of the tail for each time period. The fitted slopes show that the tail slope is outside the Lévy regime, and fits to a $q$-Gaussian distribution.

## 3.5.2 Volatility clustering

We use the autocorrelation function (ACF) to quantify volatility clustering in the time series. The ACF is calculated on the incremental price return $X^*(t)$ using two methods: sample autocorrelation and chopping autocorrelation. The detailed definitions for each method are presented below.

The time lag of the autocorrelation is denoted as $s$, representing real-time intervals in minutes for this study. For each $s$, the sample autocorrelation is defined as

$$C(s) = \frac{\sum_{t=1}^{n-s}(X^*_{t+s} - \bar{X}^*)(X^*_t - \bar{X}^*)}{\sum_{t=1}^{n}(X^*_t - \bar{X}^*)^2}, \tag{3.26}$$

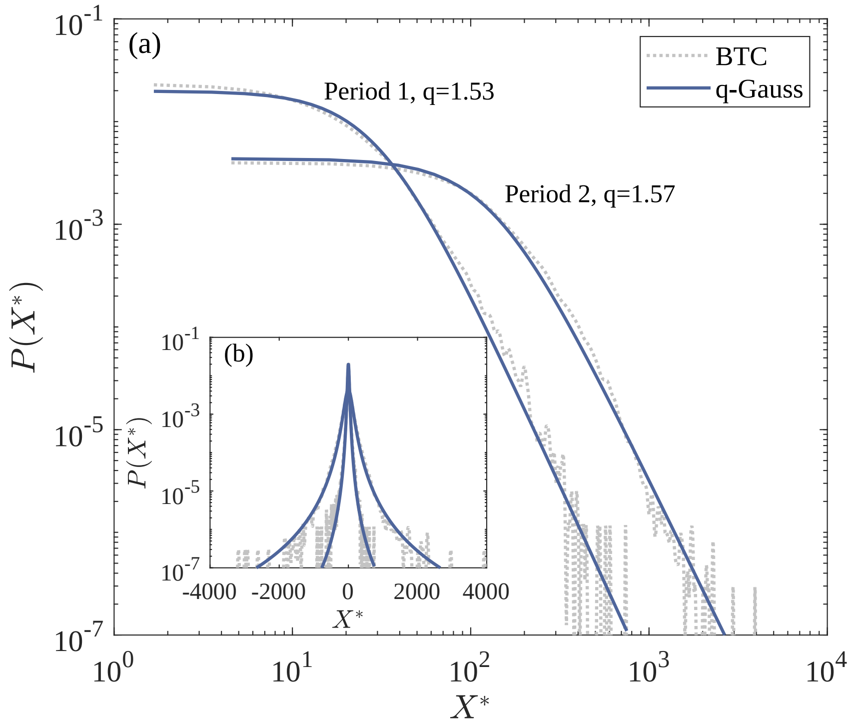


FIGURE 3.4: $q$-Gaussian fitting conducted in semi-log scale for PDFs of simple price return at $t_0$ for both Period 1 and 2. The grey dotted curves are the PDFs and the Black curves are the fitted $q$-Gaussian distribution. (a) The right branch of the PDFs for Period 1 and 2 are plotted in log-log scale respectively. (b) The full PDF and the fitted distribution are plotted in a semi-log scale.

where $X^*$ is the simple price return, $X^*_{t+s}$ is the price return shifted by $s$ minutes, and $\bar{X}^*$ is the mean value of the price return, calculated as

$$\bar{X}^* = \frac{1}{n}\sum_{t=1}^{n} X^*_t.$$

We also computed the chopping autocorrelation of the price return for both periods, following the concept of calculating the ensemble autocorrelation. In the context of stochastic processes, the ensemble represents the statistical population of the process, where each member of the ensemble is one possible realization of the process (McCauley 2008; Lahiri 2016). For finance data where only a singular historical time series exists, constructing this ensemble involves decomposing the time series into an ensemble of sub-intervals of the data. Here, each trading day effectively constitutes one realization of the dataset, given the recurring nature

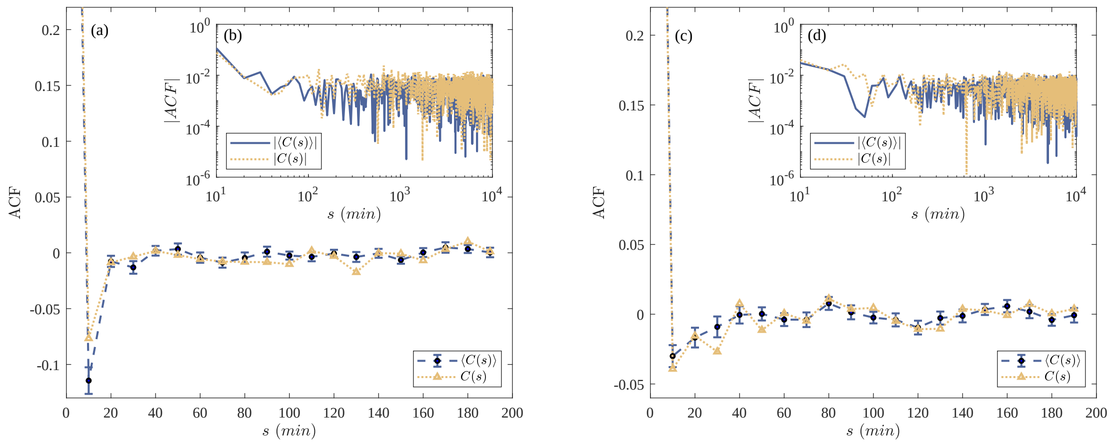

FIGURE 3.5: Sample and chopping autocorrelation with fitting for Periods 1 and 2. For both periods, anti-correlation is observed for short times, and weak long-term autocorrelation is presented. (a) For Period 1, chopping ACF is plotted in blue, and sample ACF is plotted in yellow. Anti-correlation is observed in short times with periodicity. (b) Absolute sample and chopping ACF of Period 1 plotted in log-log scale, representing a power-law relation. A linear fitting in the log-log scale measures the slope of the power-law relation as -1.17. (c) For Period 2, chopping ACF is plotted in blue, and sample ACF is plotted in yellow. Anti-correlation is also observed in short times with periodicity. (d) Absolute sample and chopping ACF of Period 2 plotted in log-log scale, with a power-law relation at initial times. A linear fitting in the log-log scale measures the slope of the power-law relation as -1.07.

of market statistics on a daily basis (Bassler et al. 2007). To build the ensemble in our study, we partitioned the data into discrete segments, where each segment serves as an independent realization of the time series. The total length of the time series for the price return is denoted as $N$, while the length of each segment is represented as $S$, and thus the number of segments is $N_s = N/S$. The chopping autocorrelation is formulated as

$$\langle C_s \rangle = \frac{C_s^i}{N_s}, \tag{3.27}$$

where $C_s^i$ corresponds to the $i^{\text{th}}$ segment within the ensemble. In the typical practice of establishing the ensemble, each segment is often delineated based on individual trading days. However, due to the continuous nature of the Bitcoin market, we chose to employ calendar weeks as the partitioning markers for our dataset. Given that our data is recorded at 10-minute intervals, resulting in 6 data points recorded per hour and $1,008$ data points accumulated each week. We rounded this to 1,000 data points for the length of each segment. Subsequently, we computed the autocorrelation for each segment and averaged it over the ensemble. The error associated with the ensemble autocorrelation was calculated as the standard error within the ensemble.

The results of the ACF calculated with both methods are presented in Figure 3.5 for Periods 1 and 2, respectively. The sample autocorrelation is plotted in yellow, while the chopping autocorrelation is in blue. The absolute sample autocorrelation functions are illustrated in Figure 3.5 (b) and (d) using a log-log scale, corresponding to Periods 1 and 2 respectively. In both time periods, a noticeable power-law relationship emerges, particularly evident at short time intervals (below 100 minutes). Over the longer term, the absolute autocorrelation exhibits a modest yet non-negligible value, persisting notably beyond the 200-minute mark ($C(s) = 0.002$ for larger $s$). To quantitatively assess this power-law behavior, we conducted linear fitting, obtaining slope values of $-1.17$ for Period 1 and $-1.07$ for Period 2. This slope of absolute autocorrelation is related to the Hurst exponent ($H$), a relationship established as $C(s) \sim s^{-2-2H}$ (Kantelhardt et al. 2002c). By calculating the Hurst exponent from the power-law slope of the absolute autocorrelation, we obtain the respective values of the Hurst exponent for Periods 1 and 2 as $H = 0.415$ and $H = 0.486$. Notably, these values align with the findings detailed in Section 3.5.1. To further examine the behavior of the short-time autocorrelation, we plot the ACF for the first 200 minutes in Figure 3.5 (a) and (c). Both sample and chopping autocorrelation show negative values at short time lags, indicating an anti-correlated relationship in short time frames. Additionally, ACFs manifest oscillations around 0 from 30 minutes to 200 minutes (approximately 2.5 hours). While both the sample autocorrelation and chopping autocorrelation exhibit similar characteristics in general, they differ in terms of magnitude. Although there are disparities between the two, these differences are not substantial enough to definitively conclude whether they indicate non-ergodic behavior in the time series or are simply a result of statistical noise.

### 3.5.3 Self-similarity of detrended PDF of price return

While the previous section focused on the stylized facts within the trended time series, it is important to note that the underlying trend inherent in financial data can potentially influence these characteristics. To address this, we now redirect our attention to exploring the stylized facts in the detrended time series. In previous sections, we found that for the Bitcoin market index, the market characteristics for Periods 1 and 2 are similar. From here, we focus the analysis on Period 2 only.

Self-similarity in the evolution of the PDF of price return is another important stylized fact in the stock market. We first tested the self-similarity of the trended time series, yet it does not present clear self-similar behavior. Thus, the detrending process is required following the relation described in Eq 3.3.

#### 3.5.3.1 Detrending time series

The detrending process was conducted using the Moving Average (MA) method. In MA, a time window is shifted from the start to the end of the time series, and the arithmetic average is used for each time window to record the trend. The two parameters that are vital to the MA are the size of the time window $t_w$ and the step in which each time window is shifted forward. In this analysis, we used a continuous sliding window with overlaps, thus the step is 1. These time windows are extended from a segment of $[t,\ \ t+t_w]$ to the consecutive window of $[t+1,\ \ t+t_w+1]$. To achieve an effective detrending result, it is necessary to select an optimal time window $t_w$ for detrending. In this study, the criteria for choosing the optimal time window are set so that the PDFs of the detrended price return $P(x^*, t)$ show the best convergence to a Gaussian distribution at large time intervals $t$ and the goodness of fit ($R^2$) indicates a valid fitting ($R^2 \geq 0.95$) for all PDFs.

We tested the time window for detrending from 1 hour to 26 weeks in order to find the best time window that meets the criteria. The optimal time window $t_w$ of 1 week is chosen for detrending, and for each time window, the arithmetic average of the index $I(t)$ from $[t,\ \ t+t_w]$ is used as the trend at time $t$. Considering at the beginning and the end of the time series where

$t < \frac{t_w}{2}$ and $t > N - \frac{t_w}{2}$ ($N$ is the total length of the time series), the size of the time window is truncated, we define the sliding window with three pieces:

• For $t < \frac{t_w}{2}$:

$$\overline{I}(t) = \frac{2}{t_w + 2t} \sum_{k=-t+1}^{\lceil (t_w-1)/2 \rceil} I(t+k), \tag{3.28}$$

• For $\frac{t_w}{2} < t < N - \frac{t_w}{2}$:

$$\overline{I}(t) = \frac{1}{t_w} \sum_{k=-\lfloor (t_w-1)/2 \rfloor}^{\lceil (t_w-1)/2 \rceil} I(t+k), \tag{3.29}$$

• For $t > N - \frac{t_w}{2}$:

$$\overline{I}(t) = \frac{2}{2N - 2t + t_w} \sum_{k=-\lfloor (t_w-1)/2 \rfloor}^{\lceil N-t \rceil} I(t+k), \tag{3.30}$$

with the time step of $t = 1, 2, 3....N$ for the index fluctuations.

The results of detrending are shown in Figure 3.6. Subfigure 3.6-a presents the trended market index $I(t)$ as the blue curve and the trend $\bar{I}(t)$ in red after applying MA analysis using the optimal time window of 1 week. Subfigure 3.6-b shows the detrended price as a result of subtracting the trend, following Eq 3.2. Subfigure 3.6-c shows the detrended price return by taking the difference of the adjacent terms in the detrended price, using Eq. 3.4

$$x^*(t) = \hat{I}(t+1) - \hat{I}(t).$$

#### 3.5.3.2 Self-similarity in PDF of detrended price return

We then test the self-similarity on the detrended price return. Recall the expression of the PDF to be:

$$P(x,t) = \frac{1}{(Dt)^H} \left[ g_q \left( \frac{x}{(Dt)^H} \right) \right]$$

where $(Dt)^H$ is the scaling factor, and $H = 1/\alpha$ is the Hurst exponent, and is related to the parameter characterizing the anomalous diffusion. Taking the result of $H = 0.478$ in Section 3.5.1 for time series Period 2, we conducted the $q$-Gaussian fitting to the detrended PDFs at

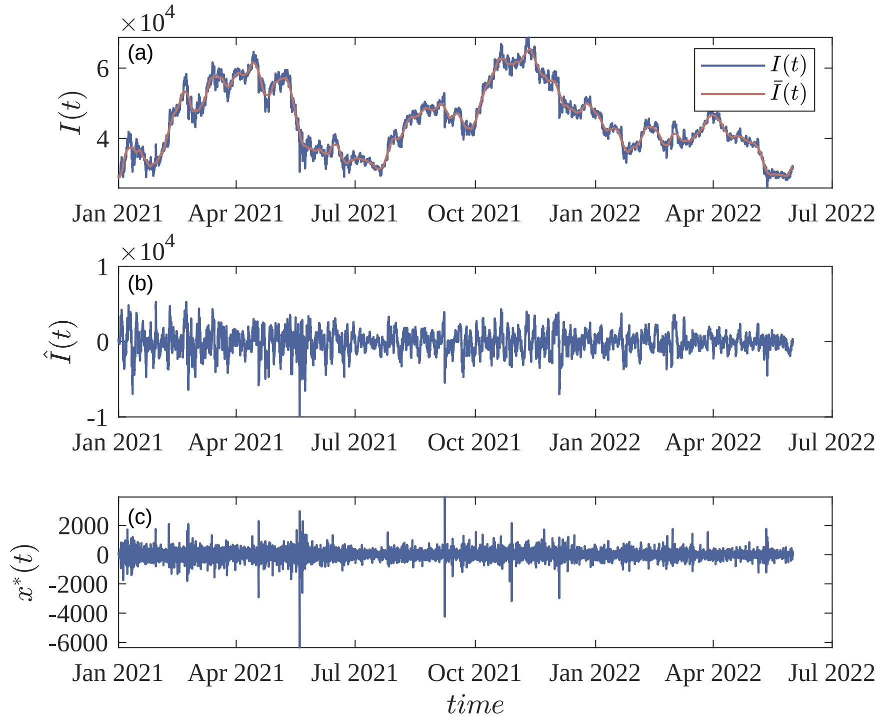


FIGURE 3.6: Results from detrending analysis for Period 2. (a) Trended price index $I(t)$ is shown as the blue curve, and the trend $\bar{I}(t)$ obtained from the MA is shown as the red curve. (b) The detrended price index $\hat{I}(t)$ was obtained by subtracting the trend from the price index. (c) Detrended price return $x^*(t)$ calculated from the detrended price index.

each time $t$ of price return in a semi-log scale, with two fitting parameters $q$ and $\beta = (Dt)^{1/\alpha}$ to find the scaling factor. The PDFs are rescaled using these factors, and the resultant PDFs were collapsed onto each other as shown in the grey curves in Figure 3.7. The collapsed PDF shows a good agreement with the $q$-Gaussian distribution with $q = 1.51$, shown as the blue curve.

### 3.5.4 Scaling analysis on the fractality of price return

In the preceding sections, we have demonstrated the presence of self-similarity in Bitcoin price returns, suggesting a fractal nature of the time series. In this section, we aim to establish whether the time series is monofractal or multifractal by performing a scaling analysis. In the

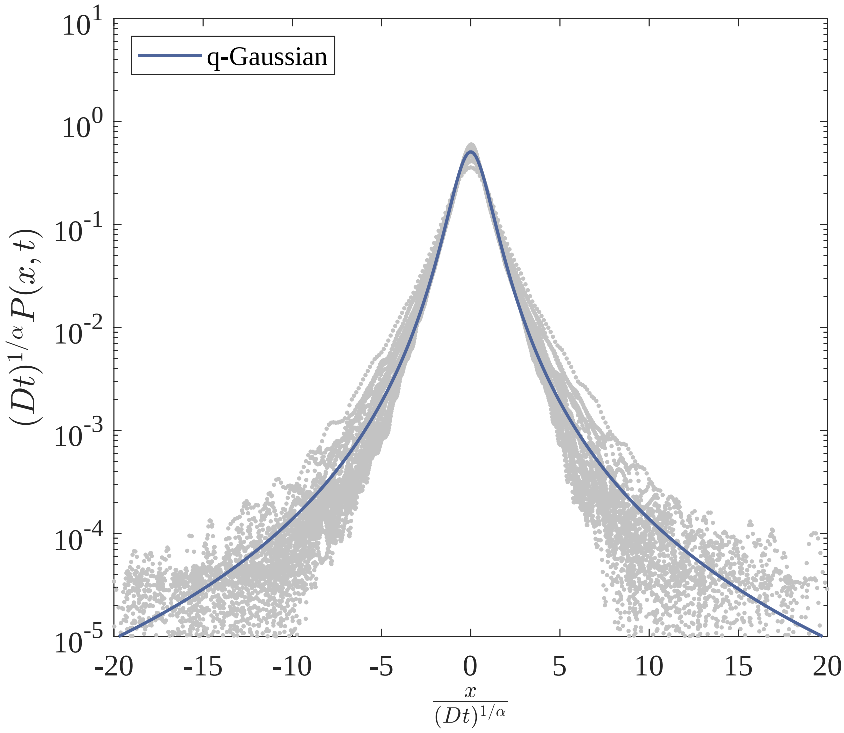


FIGURE 3.7: (Grey curves) Collapse of the PDF of detrended price return for Bitcoin Period 2. The collapsed PDFs are fitted with a $q$-Gaussian distribution (blue curve) with $q = 1.51$.

latter scenario, self-similarity is preserved, but the Hurst exponent is not unique. Instead, it exhibits a range of values forming a Hurst exponent profile.

Various methods can demonstrate the fractality of a time series, with commonly used approaches including rescaled range (R/S) analysis and detrended fluctuation analysis (DFA). Currently, DFA is becoming a more favored method because of its effectiveness in handling nonstationary time series. In our study, we applied DFA to Bitcoin Period 2 to determine fractality and calculate the Hurst exponent. DFA was performed on the trended time series. The first step of DFA involves removing the trend of the original time series by assuming the trend is the linear fitting of each non-overlapping segment.

- *Step 1*: For the trended price return with length $N$, the process of the DFA starts with defining the 'profile' of the time series by calculating the mean-centered cumulative sum of the simple price return ($X$):

$$I^*(t) = \sum_{k=1}^{i} \left[X_k - \langle X \rangle\right], i = 1, ..., N. \tag{3.31}$$

where $\langle X \rangle$ is the mean value of the time series.

The second part of DFA aims to calculate the scaling function $F_w(s)$ as a function of the time segment $s$, and $w$ is the order of the mathematical moment. This is achieved by applying the following steps:

- *Step 2*: Divide the profile $I^*(t)$ into non-overlapping segments with the same length $s$. The number of segments $N_s$ is calculated as $N_s = \lfloor N/s \rfloor$.
- *Step 3*: Calculate the local trend for each segment by a linear least-square fitting of the time series. Then the variance of each segment $v$ from $1, 2, 3....N_s$ is calculated using the equation:

$$F^2(v, s) = \frac{1}{s}\sum_{i=1}^{s}(I^*[(v-1)s + i] - \overline{I^*}(v, s))^2, \tag{3.32}$$

where $\overline{I^*}(v, s)$ is the mean of each segment of $I^*(t)$.
- *Step 4*: The statistical moments are calculated utilizing different values of order $w$:

$$F_{\mathrm{w}}(s) = \left\{\frac{1}{N_s}\sum_{i=1}^{Ns}[F^2(v, s)]^{\mathrm{w}/2}\right\}^{1/\mathrm{w}} \tag{3.33}$$

For detrended time series that present long-range correlations, the following power law is obtained: $F_w(s) \sim s^{h(w)}$. If the time series is monofractal, $h(w)$ is independent of $w$ value thus a constant is obtained where $H = h(w)$ is the Hurst exponent. For multifractal time series, $h(w)$ is dependent on $w$ and can be a linear or quadratic function.

Results of the DFA are shown in Figure 3.8 for positive and negative range of $w$ respectively. A linear fitting is conducted for each order of $w$ to obtain the power law and plotted as the dashed black lines. It is clear that the slope of $h(w)$ varies for different $w$, indicating that the time series is multifractal. Figure 3.9 plots the resultant spectrum for the Hurst exponent.

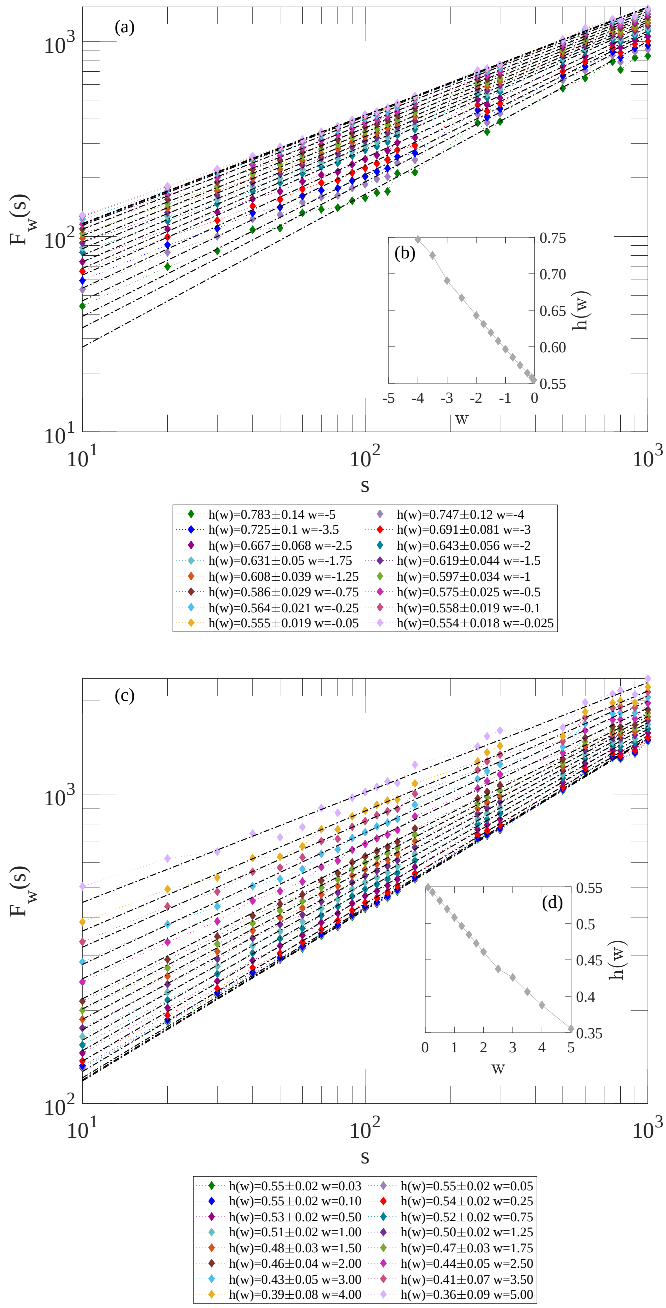


FIGURE 3.8: Calculation of the statistical function $F_w$ on Bitcoin price return for Period 2 using Eq. (3.33). The function of $F_w$ vs $s$ display power laws $F_w(s) \sim s^{h(w)}$, where $h(w)$ depend on $w$. This feature demonstrates that the time series is multifractal. (a) Calculated $F_w(s)$ function with a negative range of $w$, each $w$ value presents a power-law relationship. (b) Profile of $h(w)$ for negative $w$ values. (c) Calculated $F_w(s)$ function with a positive range of $w$, each $w$ value presents a power-law relationship. (d) Profile of $h(w)$ for positive $w$ values.

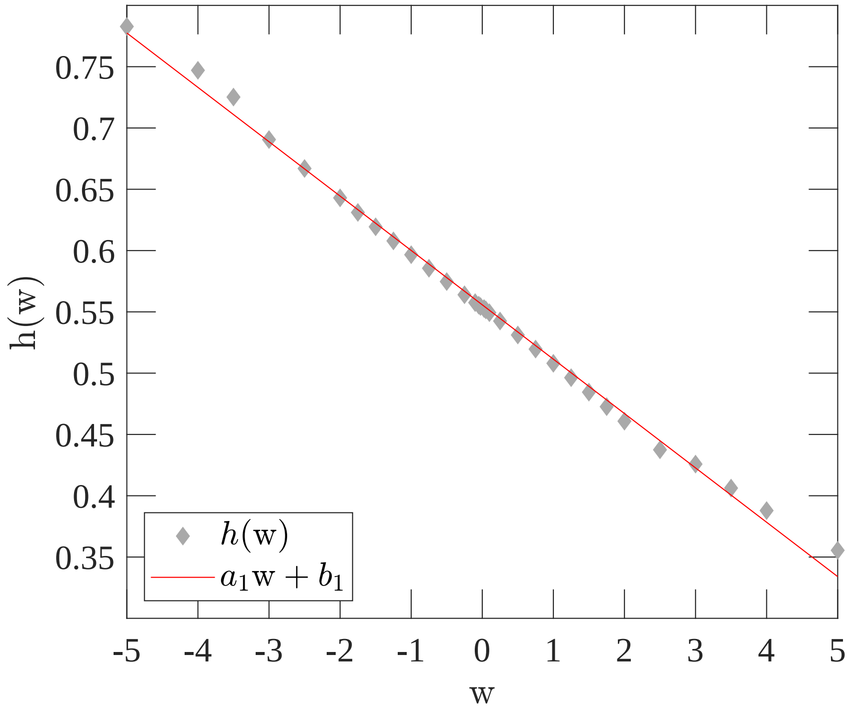


FIGURE 3.9: Evaluation of the scale exponents $h_w$ of detrended Bitcoin price return for Period 2. This profile of scale exponent can be described using a linear relationship, with $a1 = -0.044 \pm 0.006$, and $b1 = 0.556 \pm 0.002$.

## 3.6 Discussion

TABLE 3.1: Summary of stylized facts

| Stylized Facts | Period 1 | Period 2 | S&P500 |
| --- | --- | --- | --- |
| Fat-tailed Distribution<br>$P(x,t) \sim x^{\frac{2}{1-q}}$ for large $x$ | $q = 1.51$ | $q = 1.50$ | $q = 1.50$ |
| Anomalous Diffusion<br>$P(x=0,t) \sim t^{-H}, H = 1/\alpha$ | $H = 0.415$<br>$\alpha = 2.41$ | $H = 0.478$<br>$\alpha = 2.09$ | $H = 0.79$<br>$\alpha = 1.26$ |
| $q$-Gaussian Diffusion<br>$P(x,t) = \frac{1}{(Dt)^H}\left[g_q\left(\frac{x}{(Dt)^H}\right)\right]$ | $q = 1.53$ | $q = 1.57$ | $q = 1.71$<br>$q = 2.73$ |
| Volatility Clustering<br>$C(s) \sim (cs)^{2H-2}\cos(bs)$ | $H = 0.415$ | $H = 0.465$ | $C(s) \sim e^{-\rho s}$<br>$\rho = 1.07$ |
| Scaling Analysis<br>$F_w(s) \sim s^{h(w)}, H = h(2)$ | / | $H = 0.461$ | $H = 0.48$ |

We investigated the stylized facts of the Bitcoin time series from 2019 to 2022. The Bitcoin price index was divided into two periods based on changes in volatility. Table 3.1 summarizes the stylized facts observed in the Bitcoin price index. Here we compare the results of the Bitcoin price index to the well-studied conventional market S&P500 for the period from January 1996 to May 2018.

The prevalence of a heavy-tailed distribution is a characteristic feature in traditional financial markets, such as the S&P500. In line with this, we found fat-tailed distribution for both time periods of Bitcoin price return. This finding aligns with previous studies on cryptocurrencies, where the majority of types of cryptocurrencies exhibit heavy-tailed non-Gaussian distributions (Zhang et al. 2018a). Our study extends previous findings by illustrating that the PDF of Bitcoin's price return is best captured by a $q$-Gaussian distribution, making these results directly comparable with our previous results for the S&P500. Specifically, we find $q = 1.51 \pm 0.02$ for Period 1 and $q = 1.50 \pm 0.02$ for Period 2.

In comparison to the S&P500 index, the anomalous diffusion of Bitcoin presents distinctive characteristics. While Bitcoin and the S&P500 have undergone a shift in diffusion behavior, their respective diffusion patterns differ. For the S&P500 price return, research has shown that it displays a strong superdiffusion regime with $\alpha = 1.26 \pm 0.04\,(H = 0.79)$ for short time intervals, and in the long term, it exhibits a weak superdiffusion regime with $\alpha = 1.79 \pm 0.01\,(H = 0.56)$ (Alonso-Marroquin et al. 2019). In contrast, Bitcoin price returns exhibit a transition in diffusion behavior in both periods, shifting from a subdiffusion regime to a weak superdiffusion regime. In Period 1, $\alpha = 2.41 \pm 0.02\,(H = 0.415)$ for short time intervals, and $\alpha = 1.64 \pm 0.02\,(H = 0.610)$ for extended time intervals. In Period 2, short time intervals reveal $\alpha = 2.09 \pm 0.01, (H = 0.478)$, while extended time intervals exhibit $\alpha = 1.54 \pm 0.01, (H = 0.646)$. Notably, the diffusion parameters indicate that Period 1 of Bitcoin demonstrates a more pronounced subdiffusion than Period 2 for short time intervals. The anomalous diffusion of Bitcoin can be described by a $q$-Gaussian diffusion process, similar to the findings of S&P500. However, the values of the $q$ parameter are different between the two markets. For S&P500, the $q$-Gaussian exponents are $q = 1.71 \pm 0.01$ and $q = 2.73 \pm 0.005$ for the two diffusion regimes, respectively (Alonso-Marroquin et al. 2019). Conversely, for Bitcoin, the $q$-Gaussian exponents are notably lower, at approximately $q = 1.55 \pm 0.02$ for both Periods 1 and 2.

The autocorrelation functions are calculated based on the price returns of Bitcoin. Regarding the ACF for absolute returns, it demonstrates a power-law decay, with the calculated Hurst exponents shifting from less than 0.5 in Period 1 ($H = 0.415$) to slightly closer to 0.5 in Period 2 ($H = 0.486$). In terms of the ACF of price returns, both time periods exhibit short-term negative autocorrelation. The autocorrelation in small intraday time scales (less than $20$ minutes) can be attributed to the microstructure effects of the market (Cont 2001). This negative autocorrelation aligns with the findings on feedback traders in Bitcoin (Karaa et al. 2021), confirming that the high volatility and positive trading strategy can yield significant anti-autocorrelations in market dynamics. The ACF pattern observed in Bitcoin price return differs from the observations in S&P500; in the case of S&P500, the ACF presents an exponential pattern at short times, then transitions to a power-law relationship (Arias-Calluari et al. 2022).

From the scaling analysis, we found that both time periods of the Bitcoin price index are multi-fractal, which aligns with other studies on the fractality of the Bitcoin market (Takaishi 2018; Shrestha 2021). This multi-fractality characteristic is similar to the observations in the traditional financial markets and other complex systems (Lee et al. 2017; Mali and Mukhopadhyay 2014; Wang et al. 2013; Gu et al. 2010; Chen et al. 2016a). The multi-fractal nature of Bitcoin can be attributed to the presence of volatility clusters varying across different time scales and fat-tail distributions, as these aspects make essential contributions to multi-fractality in a given time series (Lahmiri and Bekiros 2018).

## 3.A Fitting for detecting self-similarity

In this chapter and the previous chapter, the diffusion coefficients are defined in a constant order, and the $q$-Gaussian diffusion is formulated with $q$ and $\beta$. When exploring the self-similarity in the PDF of the detrended price return and producing Figure 3.7, we rescaled the PDF at different time intervals to obtain a $q$-Gaussian fitting for all the rescaled PDFs. This process is conducted by assuming the self-similarity exponent is constant, and for each time $t$, we fit the PDF with parameters $q$ and $\beta$. Then we collapse all the PDFs at different times and fit them with a $q$-Gaussian function to describe the collapsed PDFs.

CHAPTER 4

# Variable order porous media equations: Application on modeling the S&P500 and Bitcoin price return

In the previous chapter, we examined the statistical characteristics of the Bitcoin cryptocurrency market in comparison to the conventional financial market of S&P500. The nonlinear fractional Fokker-Planck equations are used as the model describing the market fluctuations. We found that the market experienced a $q$-Gaussian diffusion process. Here the diffusion coefficients are defined in a constant order. From the analysis in the previous chapters, as well as other empirical evidence, we found that the parameters characterizing the PDFs experience time dependence. For example, $\alpha$ and $q$ changes with time, and the type of anomalous diffusion experience transitions. Therefore, in this chapter, we aim further than fitting the price return for a specific time. Our objective is to understand the mechanism of the evolution of $q(t)$ and, at the same time, how this influences other scaling parameters. In this chapter, we derive the variable order diffusion equation as an improvement to the model describing the market dynamics.

This chapter reveals a specific category of solutions for the $1+1$ Variable Order (VO) nonlinear fractional Fokker-Planck equations. These solutions are formulated using VO $q$-Gaussian functions, granting them significant versatility in their application to various real-world systems. We validate the VO model using datasets from both the conventional stock market and cryptocurrency. Data sets used in this chapter are at different frequencies. For the S&P500, the dataset is at 1-minute time intervals, and for Bitcoin, the data is every 10 minutes. The VO $q$-Gaussian functions provide a more robust expression for the distribution function of price returns in real-world systems. Additionally, we analyzed the temporal evolution of the anomalous characteristic exponents derived from our study, which are associated with the long-term (power-law) memory in time series data and autocorrelation patterns.

## 4.1 Introduction

Anomalous diffusion has manifested itself in various fields of science, such as physics (Solomon et al. 1993; Chechkin et al. 2005; Umarov and Steinberg 2009), chemistry (Magin et al. 2008; Metzler et al. 2014), biology (Santamaria et al. 2006; Guigas and Weiss 2008), and socioeconomic systems such as stock markets (Alonso-Marroquin et al. 2019; Gharari et al. 2021). Although it was proposed for transport and wave propagation paradigms (Richardson 1926; Gennes et al. 1976; West and Nonnenmacher 2001), now its relation with other phenomena is well-established, including but not limited to fractals and percolation in porous media (Puech and Rammal 1983; Mardoukhi et al. 2015), cell nucleus, plasma membrane and cytoplasm in biology (Saxton 2007). Anomalous diffusion is manifested in the process where the mean squared displacement of the random walker scales with time exhibiting a fractional exponent, as a result of the correlations in the stochastic process (Sokolov and Klafter 2005; Pekalski and Sznajd-Weron 1999). Under specific assumptions, a fractional version of the Fokker-Planck equation (FPE) can be employed to describe the time evolution of these systems' probability density function (PDF). Non-local fractional derivatives are relevant when dealing with the Levy process, for example (Yanovsky et al. 2000; Anderson and Moradi 2018). Intuitively, a non-local operator requires information from a whole interval when operating on a function, in contrast to local operators that only need information from a single point in their immediate vicinity (Almeida et al. 2016; Gharari et al. 2021), for a comprehensive review, see Ref. (Teodoro et al. 2019) and the references therein. This fractionalization can occur in the *time* and the *space* derivatives of the FPE. While the linear fractional FPE is suitable for describing a wide range of systems with anomalous diffusion, its non-linear version has been implemented in more diverse domains, including biological systems (Murray 1993), thermostatistics (Umarov and Tsallis 2007; Quirós and Vazquez 1999; Gilding and Peletier 1976; Pamuk 2005; Plastino and Wedemann 2020), and stock markets (Gell-Mann and Tsallis 2004; Alonso-Marroquin et al. 2019; Gharari et al. 2021). It was also shown that the PDF of the detrended price return of the S&P500 index is governed by the porous media equation (PME)— which is a non-linear FPE— through a curve fitting analysis of the PDFs after collapsing self-similar $q$-Gaussian functions (Alonso-Marroquin et al. 2019; Arias Calluari 2014; Gharari et al. 2021).

Despite the relative success of the $q$-Gaussian distributions in explaining the time evolution of the PDF of many stochastic systems, some studies show that the numerically estimated exponents exhibit slow time dependence. The stock market is an example where the PDF of price return does not follow a constant order (CO) non-linear FPE, or at least has a limited validity (Frame et al. 1970), as the price returns of stock market indexes exhibit characteristic exponents that depend on time (Arias-Calluari et al. 2021), aligned with the central limit theorem (CLT). More specifically, the stochastic fluctuations in the price return of the S&P500 index can be modeled using superdiffusive self-similar $q$-Gaussian functions and the anomalous diffusion exponent $\alpha$, which has initial values ($\alpha > 2$, $q > 1$), and then slowly converge to $\alpha \to 2, q \to 1$ corresponding to the Gaussian (normal) distribution as required by CLT (the same happens to the diffusion coefficient $D$) (Arias-Calluari et al. 2021). The diffusion process in a porous medium is another example, where if the medium structure or external field changes over time, the CO fractional diffusion is not applicable (Atangana and Bildik 2013; Hantush and Jacob 1955). This characteristic poses fundamental challenges and introduces the need to reconsider the governing equation, considering the time dependence of these exponents. To address this limitation, using “variable order" (VO) fractional diffusion equations has been proposed (Frame et al. 1970; Atangana and Bildik 2013; Hantush and Jacob 1955). In many complex systems, the inclusion of VO fractional derivatives can provide a more accurate representation of their underlying dynamics (Li and Chen 2004; Yang 2016; Almeida 2017; Atangana 2015; Alkahtani et al. 2016).

This paper considers the VO fractional porous media equation (FPME) with local fractional derivative operators, where the characteristic exponents can change slowly with time. The formalism is kept as general as possible to include a general time dependence of the exponents. By proposing a separable form for the solutions, we identify an important class of solutions that yield the ordinary $q$-Gaussian solution in the static (CO) limit. These solutions are not self-similar (SS), but the self-similarity is retrieved once we take the CO limit. In the second part of the paper, we relate these solutions to the PDF of price return in the traditional stock markets and the cryptocurrency. We assess the VO $q$-Gaussian function and inspect how this system approaches the normal diffusion counterparts over extended periods.

The paper is organized as follows: the constant order (CO) fractional diffusion process will be presented in the following section. Section 4.3 is devoted to the time-dependent variable order (VO) exponents and their solutions with and without drift. The application to the stock markets is studied in Section 4.4.

## 4.2 Constant Order (CO) fractional diffusion process

The anomalous diffusion is a diffusion process with a non-linear relationship between the mean squared displacement and time with an anomalous diffusion exponent $\alpha$. For any $d$-dimensional space, it is characterized by the following scaling relation

$$R(t) \equiv \sqrt{\langle r^2(t) \rangle} \propto t^H, \tag{4.1}$$

where $r(t)$ is the end to end distance at time $t$, $\langle ... \rangle$ is the ensemble average and $H = 1/\alpha$ is the corresponding Hurst exponent. For a normal diffusion $\alpha = 2$, while for the super- (sub-) diffusion $\alpha < 2$ ($\alpha > 2$). The anomalous diffusion can be due to time correlations, as well as the fractal structure of the *space*. An important primitive example of anomalous diffusion was given by Havlin and Ben-Avraham for random walks on fractal objects, the PDF of which is given by (Havlin and Ben-Avraham 1987)

$$P(x,t) \propto R(t)^{-d_f} \exp\left[-c\left(\frac{x}{R(t)}\right)^{\frac{\alpha}{\alpha-1}}\right], \tag{4.2}$$

where $d_f$ is the fractal dimension of the space in which the random walker is doing an exploration process. Other types of distributions with the same scaling relation between $x$ and $R(t)$ are proposed to describe anomalous diffusion processes in different physical systems, which are special solutions of the FPEs. These modifications of the FPE may include the fractionalization of the space as well as the time derivative operators, and non-linearization depending on the system that the FPE is going to describe. Various fractional diffusion equations have been introduced each of which has its own advantages and weaknesses (Umarov and Steinberg 2009; Magin et al. 2008; Chechkin et al. 2005). A fractionalization of the derivative can be either local or non-local depending on the (temporal and spatial) nature of the system (Arias-Calluari et al. 2022). The examples are the Schneider and Wyss time-derivative fractionalization (Schneider and Wyss 1989), O'Shaugnessy and Procaccia space-derivative fractionalization (O'Shaughnessy and Procaccia 1985), Giona and Roman space-time-derivative fractionalization (Giona and Roman 1992), and more general cases (Metzler et al. 1994).

An important feature in Eq. 4.2 is related to its scaling behavior. This equation suggests that for a $d$-dimensional system, $r = |\mathbf{x}|$ (where $\mathbf{x}$ shows the position of a random walker) scales with a general function of time $\phi(t)$, so that

$$\mathbf{x} \to \lambda \mathbf{x}\ ,\ \phi(t) \to \lambda \phi(t)\ ,\ P \to \lambda^{-d} P \tag{4.3}$$

(see Appendix 4.A for more details). Here $\phi(t)$ is a time-dependent function characterizing the anomalous diffusion. This suggests the following scaling solution

$$P(\mathbf{x}, t) = \frac{1}{\phi(t)^d} F\left[\frac{\mathbf{x}}{\phi(t)}\right]. \tag{4.4}$$

The nature of anomalous diffusion is directly calculated using

$$R^2 = \left\langle r(t)^2 \right\rangle \propto \int \mathrm{d}^d\mathbf{x} |\mathbf{x}|^2 F\left[\frac{\mathbf{x}}{\phi(t)}\right] \propto \phi(t)^2. \tag{4.5}$$

The scaling properties of the time series are associated with the form of $\phi(t)$. In fact, for the solution of Eq. 4.1 we have $\phi(t) = \phi_{\mathrm{SS}}(t)$ where the index "SS" points out the self-similarity law, given by (Gharari et al. 2021; Alonso-Marroquin et al. 2019)

$$\phi_{\mathrm{SS}}(t) \propto t^{1/\alpha}. \tag{4.6}$$

Combining Eq. 4.5 and Eq. 4.6, one reaches Eq. 4.1.

An important well-known example is the fractional Brownian motion (fBm), in which the PDF follows a Gaussian distribution with a self-similar structure. For a good review see Appendix 4.B and (Beran 1994; Mandelbrot and Van Ness 1968). The Levy-stable distribution is another example of a self-similar system that has vast applications in stochastic processes, including the stock markets. The heavy-tail behavior observed in stock market price fluctuations has been a cornerstone for many scientists in supporting the use of Levy-stable distributions for modeling the stochastic behavior of the price return (Bielinskyi et al. 2019b; Chang 2020; Montillet and Yu 2015; Bielinskyi et al. 2019a; Scalas and Kim 2006; Bucsa et al. 2014; Arias-Calluari et al. 2021).

There are, however, some pieces of evidence indicating that Levy-stable distributions are not sufficient to describe the stylized facts of the price return. Recent observations of the PDF of price returns for the S&P500 have shown that they follow more general distributions (Alonso-Marroquin et al. 2019). The Levy-stable distribution provides only an estimation of the stock market fluctuations at low frequencies where the correlations can be neglected. However, correlations during the first minutes on the price fluctuations were observed at high frequencies, making the Levy regime no longer applicable. Additionally, the characteristic exponents employed to model the power-law tails in the PDF of price increments for one-minute time intervals lie outside the Levy regime (Gharari et al. 2021). This divergence highlights a common occurrence in the modeling of complex systems, which can be attributed to the nonlinear nature of the governing physical phenomena.

In nonlinear systems, the principles of homogeneity and superposition do not hold. These systems exhibit a distinctive property known as *non-extensivity*, meaning that their corresponding entropy is not additive (Tsallis 1988). A notable example of non-extensive systems is observed in the PME, which possesses broad applications in stochastic processes, including the analysis of stock markets. More accurate models can be created by introducing a fractional version of the PME. This extension offers a powerful theoretical framework with the potential to effectively describe a wide range of stochastic systems. The local fractional PME reads

(Gharari et al. 2021)

$$\frac{\partial^\xi}{\partial t^\xi}P(x,t) = D\frac{\partial^2}{\partial x^2}P(x,t)^\nu, \tag{4.7}$$

where $\xi$, $D$, and $\nu \equiv 2-q$ are the constant parameters to be found by fitting the data with the time series under investigation. $D$ is the diffusion coefficient in the limit $q$, $\xi \to 1$ where the normal diffusion is retrieved. Eq. 4.7 admits solutions in terms of $q$-Gaussian and generalized $q$-Gaussian functions (Alonso-Marroquin et al. 2019; Gharari et al. 2021), which forms an important class of functions with a wide range of applications (Alonso-Marroquin et al. 2019; Borland 2002b), shown as

$$P(x,t) = \frac{1}{C_q \phi_{\text{SS}}(t)} e_q\left[-\left(\frac{x}{\phi_{\text{SS}}(t)}\right)^2\right], \tag{4.8}$$

where

$$e_q(x) \equiv (1+(1-q)x)^{\frac{1}{1-q}} \tag{4.9}$$

is $q$-exponential function (a generalization of the exponential function), and $C_q$ is a normalization factor, given by

$$C_q = \begin{cases} \frac{2\sqrt{\pi}\Gamma\left(\frac{1}{1-q}\right)}{(3-q)\sqrt{1-q}\Gamma\left(\frac{3-q}{2(1-q)}\right)} & -\infty < q < 1 \\ \sqrt{\pi} & q = 1 \\ \frac{\sqrt{\pi}\Gamma\left(\frac{3-q}{2(q-1)}\right)}{\sqrt{q-1}\Gamma\left(\frac{1}{q-1}\right)} & 1 < q < 3 \end{cases}. \tag{4.10}$$

In this relation, $\Gamma(x)$ is the standard Gamma function. The self-similar time part reads

$$\phi_{\text{SS}}(t) \equiv (D't)^{1/\alpha}, \tag{4.11}$$

where the parameter $\alpha = \frac{3-q}{\xi}$ is the anomalous diffusion exponent associated with the self-similarity of the time series and $D' \equiv (D/\xi)^{1/\xi}$ is the modified diffusion parameter to be estimated using the real data analysis. The evolution equation of the price return's PDF can be constructed based on the $q$-Gaussian fitting. Originally conceived for studying fluid propagation in porous media, PME has significantly broadened its scope over time. Now PME is used to investigate any diffusion process where the diffusion coefficient depends on the state variable, the most important of which is the stock market with $q$-Gaussian PDF (Alonso-Marroquin et al. 2019; Adams and Gelhar 1992). In our previous studies, we investigated the fractional PME with local and non-local fractional derivatives, focusing solely on its solutions for describing the PDF of S&P500 market index. Considering both cases, the results obtained from the non-local derivatives were found to be more accurate (Gharari et al. 2021).

Despite the fact that a generalized form of $q$-Gaussian PDFs better describes the PDFs of S&P500 data at any time, the exponents have been shown to vary over time (Arias-Calluari et al. 2021). Solving Eq. 4.7 with “time-dependent exponents" introduces a contradiction because the time dependence of the exponents should have been considered in the governing equation from the outset. Such governing equations with time-dependent exponents are referred to as VO governing equations. The very important question we should answer is: *Which is the generalized non-linear fractional Fokker-Planck equation that governs the PDF with variable orders?*

Variable exponents are observed in complex diffusion processes (Fedotov and Falconer 2012; Wang and Zheng 2019; Liu et al. 2016; Fang et al. 2020; Kian et al. 2018). The diffusion properties of homogeneous media are usually modeled by CO time-fractional diffusion processes, for example, see (Carcione et al. 2013). However in complex media where heterogeneous regions are present the CO fractional dynamic models are not robust over long time scales. Additionally, when considering diffusion processes in porous media where the medium structure or external field changes with time, the use of CO fractional dynamic models may not yield satisfactory results (Atangana and Bildik 2013; Hantush and Jacob 1955). In such cases, the VO time-fractional model emerges as a more suitable approach for describing space-dependent anomalous diffusion processes (Sun et al. 2009). Previous works on VO diffusion models have made substantial contributions to the modeling and analysis of complex systems (Fedotov and Falconer 2012; Frame et al. 1970; Wang and Zheng 2019; Kian et al. 2018; Fang et al. 2020; Liu et al. 2016). Building upon these works, this paper aims to generalize the PME by incorporating variable exponents. The investigation focuses on systematically exploring the problem with variable exponents and solving a time variable order porous media equation

(VO-PME). The VO-PME reads

$$\frac{\partial^{\xi(t)}}{\partial t^{\xi(t)}} P(x,t) = D(t) \frac{\partial^2}{\partial x^2} P^{\nu(t)}(x,t), \tag{4.12}$$

where $\xi(t)$, $D(t)$, and $\nu(t) \equiv 2 - q(t)$ now vary with time. Some properties of the CO equations cannot be extrapolated to the VO counterpart. For example, while one may be tempted to derive the effective time-dependent Hurst exponent as $H(t) \equiv \frac{\xi(t)}{3-q(t)}$, it is crucial to exercise caution when utilizing this expression. The reason is that the definition of the Hurst exponent is based on the autocorrelation function, which has not been explicitly obtained for the VO-PME in this study. Therefore, the aforementioned expression should be interpreted with care. In the following sections, we find an important class of solutions for the VO-PME.

## 4.3 A local variable order non-linear time diffusion equation

In this section, we consider a time-dependent VO-PME as follows

$$\frac{\partial^{\xi(t)}}{\partial t^{\xi(t)}} P(x,t) = D(t) \frac{\partial^2}{\partial x^2} P^{\nu(t)}(x,t), \tag{4.13}$$

where $\xi(t)$ and $\nu(t) = 2 - q(t)$ are VO exponents and $D(t)$ is a slow-varying time-dependent diffusion coefficient. In this equation the time derivative is fractionalized using a Katugampola derivative, see Appendix 4.C for the details. Note that in the limit $\xi, \nu, D$ are constant, the solution given by Eq. 4.8 is retrieved, i.e. the $q$-Gaussian distribution. In the analogy of Eq. 4.4 ($d = 1$), we consider the factorized solution $P(x,t) = \frac{1}{\phi(t)} F\left(\frac{x}{\phi(t)}\right)$. This approach enables us to use the method of separating variables, where $\phi(t)$ satisfies a time-fractional equation. By inserting Eq. 4.4 into Eq. 4.13, we find that (also see Appendix 4.C)

$$-\frac{\phi^{\nu(s)}(s)}{D(s)} \frac{\partial^{\xi(s)}\phi(s)}{\partial s^{\xi(s)}} = \left(\frac{d}{dz}[zF]\right)^{-1} \frac{d^2}{dz^2} F^{\nu(s)}, \tag{4.14}$$

where we make the change of variables $(x,t) \to (z \equiv \frac{x}{\phi(t)}, s \equiv t)$. To simplify the calculations, we assume that the function $q(s)$ is a slow-varying function so that the derivatives of $q(s)$ with respect to $s$ can be neglected as a first-order approximation. Thus, the right-hand side is a sole function of $z$, while the left-hand side is a sole function of $s$. Then we find

$$\begin{cases} \frac{\phi^{\nu(s)}(s)}{D(s)} \frac{\partial^{\xi(s)}\phi(s)}{\partial s^{\xi(s)}} = k & \text{(I)} \\ \left(\frac{d}{dz}[zF]\right)^{-1} \frac{d^2}{dz^2} F^{\nu(s)} = -k & \text{(II)} \end{cases} \tag{4.15}$$

where $k$ is a real number, which serves as a free parameter. Using the properties of VO-K derivative (K stands for Katugampola, see Appendix 4.C) we find that

$$\frac{\partial^{\xi(s)}\phi(s)}{\partial s^{\xi(s)}} = \frac{1}{s^{\xi(s)-1}} \phi'(s), \tag{4.16}$$

where (here and throughout of the paper) $f'(s)$ shows the first derivative of $f(s)$ with respect to the argument $s$. Therefore, Eq. 4.15-(I) leads to

$$\phi^{\nu(s)}(s)\phi'(s) = kD(s)s^{\xi(s)-1}. \tag{4.17}$$

To solve this equation, taking a similar approach from Eq. 4.6, we assume

$$\phi(s) = \phi_0 s^{1/\tilde{\alpha}(s)}, \tag{4.18}$$

where $\tilde{\alpha}(s)$ is a slow VO exponent, and $\phi_0$ is a constant. Note that, in the constant order case $\tilde{\alpha}(s)$ is identical to $\alpha$. Substituting this into Eq. 4.17 we find ($q_s \equiv q(s)$, $\nu_s \equiv \nu(s)$, $\xi_s \equiv \xi(s)$, $\tilde{\alpha}_s \equiv \tilde{\alpha}(s)$ and $D_s \equiv D(s)$)

$$\phi_0^{\nu_s+1} s^{\frac{\nu_s+1}{\tilde{\alpha}_s}} \frac{d}{ds}\left(\frac{\ln s}{\tilde{\alpha}_s}\right) = kD_s s^{\xi_s-1}, \tag{4.19}$$

or in terms of a new variable $y \equiv (\nu_s+1)\frac{\ln s}{\tilde{\alpha}(s)}$ (so that $e^y = \left(\frac{\phi(s)}{\phi_0}\right)^{\nu_s+1}$) we have

$$(\nu_s+1)e^y \frac{d}{ds}\left(\frac{y}{\nu_s+1}\right) = k\tilde{D}_s s^{\xi_s-1}, \tag{4.20}$$

where

$$\tilde{D}_s \equiv \frac{(\nu_s+1)}{\phi_0^{\nu_s+1}} D_s. \tag{4.21}$$

When $\nu_s$ is a smooth function of $s$, by considering that $\nu_s = 2 - q_s$, we can ignore its first derivative, so one can easily cast the equation to the form

$$\frac{d}{ds}e^y = k\tilde{D}_s s^{\xi_s - 1}, \tag{4.22}$$

and the solution with initial condition $y_0 \equiv y(s_0)$ is

$$e^y = e^{y_0} + kG(s, s_0). \tag{4.23}$$

In Eq. 4.23 we define

$$G(s, s_0) \equiv \int_{s_0}^{s} \tilde{D}_t t^{\xi_t - 1} dt \equiv \int_{s_0}^{s} g(t)dt, \tag{4.24}$$

where

$$g(t) \equiv \frac{D_t(\nu_t + 1)}{\phi_0^{\nu_t + 1}} t^{\xi_t - 1}. \tag{4.25}$$

Equation 4.23 can be written in the following form

$$\phi(s) = \phi_0 \left[k_1 + kG(s, s_0)\right]^{\frac{1}{\nu_s + 1}}, \tag{4.26}$$

where $k_1 \equiv \left(\frac{\phi(s_0)}{\phi_0}\right)^{\nu_{s_0} + 1}$. Note that for the solution to be real, we should always have the condition

$$G(s, s_0) \geq -\frac{k_1}{k}. \tag{4.27}$$

By choosing

$$k > 0, \tag{4.28}$$

we see that this condition is satisfied given that $k_1 \geq 0$. Note $k_1$ is a location parameter, and it is related to the initial condition, i.e. it sets the initial width of the PDF. When $k_1 = 0$, the PDF is initially the Dirac delta function, and the solution of the equation will correspond to the Green Function. In applications where the initial condition is not given, we can set $k_1$ to zero. The constant $k$ is a scale parameter so that without loss of generality we can set $k = 1$. Equations 4.18 and 4.26 the exponent $\tilde{\alpha}(s)$ is obtained as

$$\frac{1}{\tilde{\alpha}_s} = \frac{\ln\left[k_1 + kG(s, s_0)\right]}{(\nu_s + 1)\ln s}. \tag{4.29}$$

The initial time $s_0$ can be set to zero. One can easily demonstrate that, when considering fractional constant exponents, $\nu_s = \nu$, $\xi_s = \xi$, Eq. 4.26 coincides with the result of ordinary PME, that is

$$\tilde{\alpha}_s \to \alpha,\ \phi(s) \to \phi_{\rm ss}(s), \tag{4.30}$$

which is given in Eq. 4.11. Specifically, in the limit $D_s \to D = \text{const.}$, $\nu_s \to 1$, $\xi_s \to 1$ and $k_1 = 0$, one retrieves the normal diffusion (ND), for which

$$\phi(s) \to \phi_{\rm SS}^{(ND)} \equiv a s^{\alpha_{\rm ND}},\ \tilde{\alpha}_s \to \alpha_{\rm ND} = \frac{1}{2}, \tag{4.31}$$

where $a = k\sqrt{2D}$.

In the next step, we find the solution of $F$. From now on we set $k = 1$ and $k_1 = 0$, bearing in mind that the formulas can be generalized by considering other values of these parameters. We recall Eq. 4.15-II

$$\frac{d}{dz}[zF] = -\frac{d^2}{dz^2}F^{\nu_s}. \tag{4.32}$$

Let us consider the following trial special solution as a standard form

$$F(z,s) = \left(c + \eta_s z^2\right)^{\frac{1}{\nu_s - 1}}, \tag{4.33}$$

where $c$ is a constant, and $\eta_s$ is a pure function of $s$ to be determined. Before going into the details, let us comment on the real-positivity of this solution. To guarantee this, one has to impose

$$c + \eta_s z^2 \geq 0. \tag{4.34}$$

This inequality is satisfied, for any value of $z$, only when

$$\eta_s \geq 0, \tag{4.35}$$

and at the same time $c \geq 0$, which we arbitrarily set it to $c = 1$ (which can be done using a normalization). For the trial solution Eq. 4.33, one has

$$\frac{d}{dz}[F^{\nu_s}] = \frac{2\nu_s \eta_s}{\nu_s - 1} zF. \tag{4.36}$$

After incorporating this expression into Eq. 4.32, we obtain

$$\eta_s = \frac{1-\nu_s}{2\nu_s}, \tag{4.37}$$

which completes the solution. After all, the Eq. 4.35 has to be satisfied, for which we should satisfy the following inequality

$$\frac{q_s-1}{2-q_s} \geq 0. \tag{4.38}$$

Noting that

$$\frac{q_s-1}{2-q_s} \begin{cases} \geq 0 & \text{if } 1 \leq q_s < 2 \\ < 0 & \text{if } q_s < 1 \text{ or } q_s > 2, \end{cases} \tag{4.39}$$

we find a physically relevant interval where the Eq. 4.34 is fulfilled: $1 \leq q < 2$. Outside of this range, the solutions become imaginary. Finding another set of solutions is beyond the scope of the present paper as the study cases of price return in the stock market are restricted to the interval $1 < q \leq 2$; therefore, the lower branch in Eq 4.39 is applicable. Note that for $k \neq 1$ we should satisfy $\frac{q_s-1}{k(2-q_s)} \geq 0$, which is automatically satisfied for $1 \leq q < 2$ given the Eq. 4.28.

Altogether, we realize that $F(z)$ and $\phi(t)$ are positive functions, and eventually

$$P(x,t) \propto \frac{A_q(t)}{\phi(t)} \left[1 + \eta_t \left(\frac{x}{\phi(t)}\right)^2\right]^{\frac{1}{\nu_t - 1}}, \tag{4.40}$$

where $A_q(t)$ is a normalization factor (independent of $x$). Now defining $\eta_{q_t} = \frac{\eta_t}{q_t-1} = \frac{1}{2(2-q_t)}$, we find that

$$P(x,t|x_0,t_0) = \frac{A_q(t)}{\phi(t)} e_{q_t} \left[-\eta_{q_t} \left(\frac{x}{\phi(t)}\right)^2\right],$$

where $e_q(x)$ is given in Eq. 4.9. To make the notation more compact, we define

$$\Phi(t) \equiv \frac{\phi(t)}{\sqrt{\eta_{q_t}}}. \tag{4.41}$$

which gives

$$P(x,t) = \frac{1}{C_{q_t}\Phi(t)} e_{q_t}\left[-\left(\frac{x}{\Phi(t)}\right)^2\right]. \tag{4.42}$$

where $C_{q_t} = \sqrt{\eta_{q_t}} A_q^{-1}(t)$ is the new normilization factor, given in Eq. 4.10 with respect to VO parameter $q_t$. For the most applications $1 < q_t < 3$, leading to (see Eq. 4.10)

$$C_{q_t} = \frac{\sqrt{\pi}\Gamma\left(\frac{3-q_t}{2(q_t-1)}\right)}{\sqrt{(q_t-1)}\Gamma\left(\frac{1}{q_t-1}\right)}. \tag{4.43}$$

$\Phi(t)$ is an important function that gives the time-scaling properties of the model. Using Eq. 4.26 we find the explicit form

$$\Phi(t) = \phi_0\sqrt{2(2-q_t)}\left(\int_{t_0}^{t} g(s)ds\right)^{\frac{1}{3-q_t}}. \tag{4.44}$$

For example the standard deviation is

$$\sqrt{\langle x^2 \rangle} = \Phi(t). \tag{4.45}$$

If we represent

$$\Phi(t) \equiv \Phi_0 t^{\frac{1}{\alpha_t}}, \tag{4.46}$$

which defines the new exponent $\alpha(t)$, then using Eq. 4.18 one finds

$$\frac{t^{1/\tilde{\alpha}_t}}{\sqrt{\eta_{q_t}}} = Ct^{1/\alpha_t} \to \frac{1}{\alpha_t}\ln t = \frac{1}{\tilde{\alpha}_t}\ln t - \frac{1}{2}\ln\left(\eta_{q_t}\right) - \ln C, \tag{4.47}$$

where $C \equiv \frac{\Phi_0}{\phi_0}$. Using Eq. 4.47, we can calculate $\alpha_t$ if $\tilde{\alpha}_t$ and $\eta_t$ are provided and vice versa. In the practical situations, one calculates $\alpha_t$ using Eq. 4.46, and the $\tilde{\alpha}_t$ can be obtained from Eq. 4.47. A similar formulation for the case with drift is presented in Appendix 4.D.

In the rest of this section, we provide some results for the VO $q-$Gaussians for various functions $q(t)$, $\xi(t)$ and $D(t)$. Figure 4.1 displays the behavior of Eq. 4.40 and compares it with the solutions of normal diffusion and porous media processes, respectively. Figure 4.1-a shows the solution of the diffusion equation or Fick's second law, i.e. Eq. 4.7 for $q = 1$ and $\xi = 1$ with $D = 0.3$, in Figures 4.1-b and 4.1-c we can observe $q = 1$ and $\Phi = \sqrt{4Dt}$ respectively. Figure 4.1-d exhibits the solution of $P(x,t)$ with respect to time and space for a

PME, see (Eq. 4.7), applicable for $1 < q < 3$. For this example we use the values of $q = 1.5$, $\xi = 3/4$, and $D = 0.3$ in Figures 4.1-e and 4.1-f we can observe that $q = 1.5$, remains constant, and $\Phi = (Dt)^{1/\alpha}$ with $\alpha = \frac{3-q}{\xi}$ respectively. Finally, Figure 4.1-g represents the VO $q$-Gaussian presented in Eq. 4.40 and applicable for $1 < q \leq 2$ with $k = 1$, $k_1 = 0$, $q_0 = 1.7$, $\xi_0 = 1.3$, and $D_0 = 1.3$. The value of $q(t) = (q_0 - 1)e^{-at} + 1$, with $a = 0.0003$, and $\Phi(t)$, see Eq. 4.44, are shown in Figures 4.1-h and 4.1-i, respectively.

## 4.4 Application to stock markets and cryptocurrency

In this section, we apply the VO $q$-Gaussian diffusion model to describe the evolution of PDF of stock market price return. Our empirical investigation focuses on two prominent market indices: the S&P500 stock market index and the Bitcoin cryptocurrency. The S&P500 dataset encompasses the period from January 2nd, 2018, to August 9th, 2022, per minute. For the Bitcoin currency, we analyze data spanning from January 1st, 2021, to May 9th, 2022, with data points collected at ten-minute intervals. Prior to conducting our price return analysis, we undertake a pre-processing step to remove time frames characterized by trading amounts falling below $0.10$ USD. These instances predominantly occur approximately one hour before the stock market closes, specifically observed in the context of the S&P500.

The price return is defined as (Arias-Calluari et al. 2021)

$$X(t) = I(t_0 + t) - I(t_0), \tag{4.48}$$

where $I(t)$ is the index at time $t$, and $t_0$ is some reference time. By decomposing the price return $X(t)$ into a deterministic component $\bar{X}(t)$ and a stationary fluctuating component $x(t)$, we have

$$X(t) = \bar{X}(t) + x(t). \tag{4.49}$$

The trend $\bar{X}(t)$ was obtained by calculating the moving average of the index over a specific time window, $t_w$in the S&P500 and Bitcoin datasets, following the methodology described in (Arias-Calluari et al. 2022). For the S&P500 price return, a three-month optimal time window was used, while a one-week optimal time window was employed for the Bitcoin

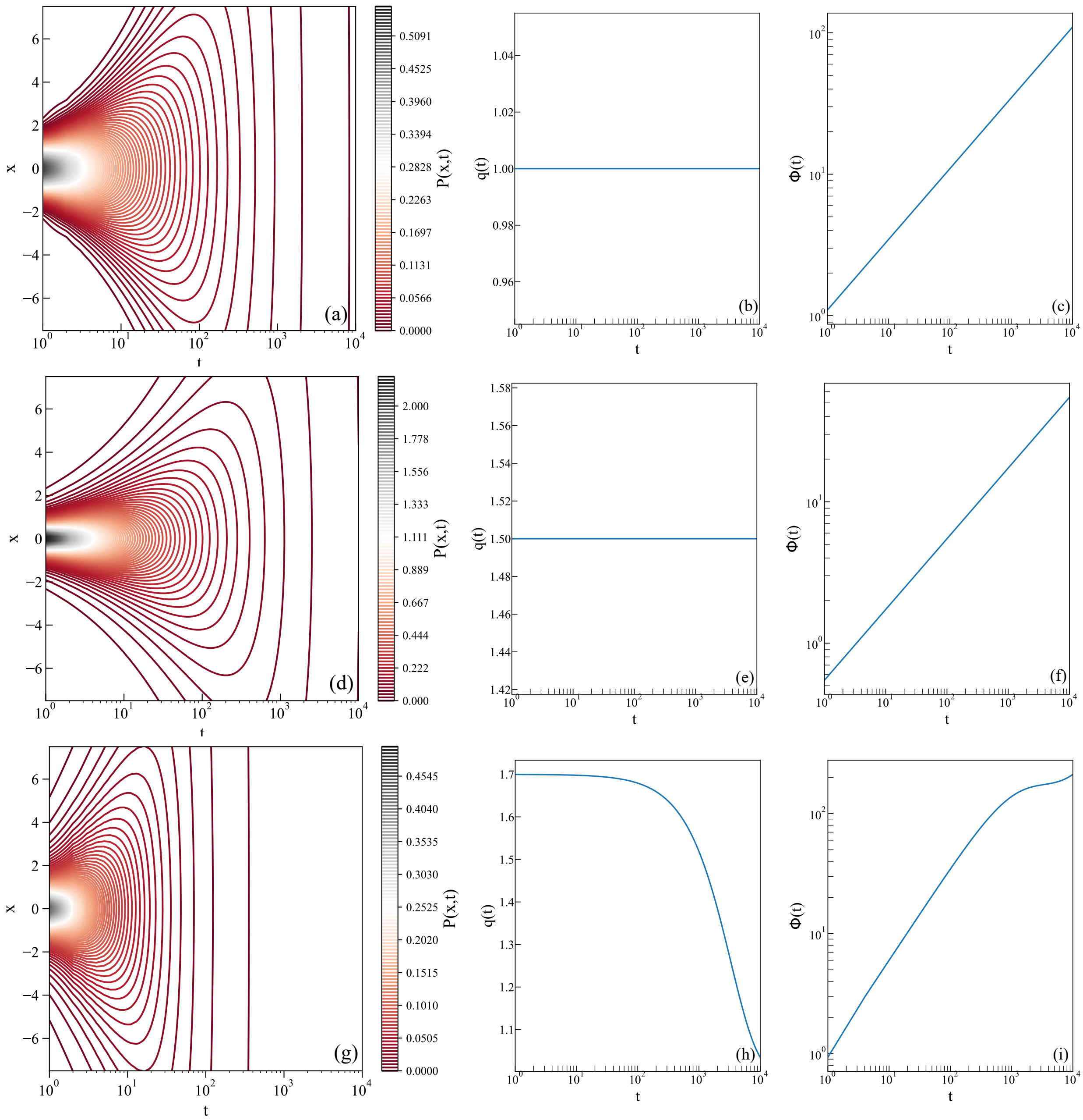

FIGURE 4.1: Summary of PMEs' solutions. (a) The time evolution of the diffusion equation or Fick's second law is described by $q = 1$ and $\Phi = \sqrt{4Dt}$ presented at (b) and (c), respectively. (d) Time evolution of $P(x, t)$ with respect to time and space for the PME presented in Eq. 4.7 for $q = 1.50$ and $\Phi = (Dt)^{1/\alpha}$ shown at (e) and (f), respectively. (g) Time evolution of VO $q$-Gaussian for a $q(t) = (q_0 - 1)e^{-at} + 1$ with $a = 0.0003$ and $q_0 = 1.7$, at panel (h). Panel (i) displays the variation of $\Phi(t)$ according to Eq. 4.44.

dataset. These specific time windows were carefully chosen to ensure that the fluctuations around the trend show stationary behavior. To confirm the validity of the observed stationary behavior, we experimented with different window sizes for detrending and ultimately selected the one that allowed the PDF to show the closest convergence to a Gaussian distribution for large times. The PDFs were calculated for $x(t)$ of S&P500 and Bitcoin at the time range $t \in [1,\ 47000]$min. By an error-minimization process, we found that the VO $q$-Gaussian diffusion described in Eq. 4.42 provides the closest match to the observed time-dependent evolution of the PDF $P(x,t)$ for both S&P500 and Bitcoin.

Figure 4.2 presents the results of the calibration process, displaying the functions $q(t)$, $\Phi(t)$, and $P_{\text{max}}(t)$ obtained by curve fitting the PDFs derived from the datasets to Eq. 4.42. We observed that the PDFs of S&P500 and Bitcoin converge to a Gaussian distribution function as time $t$ increases, and this convergence is positively correlated with the chosen optimal time window $t_w$. Figures 4.2-a and 4.2-d present the converge of $q$ towards 1 as $t$ approaches $t_w$, indicating a Gaussian distribution function with $\sigma^2 = 1/2$, and $\mu = 0$. The convergence to the normal distribution is expected given the fact that for large enough times, the conditions for the central limit theorem are satisfied. We observe also that $q(t)$ for S&P500 and Bitcoin can be effectively modeled using the following relationship

$$q(t) = (q_0 - 1)\left(1 - \frac{1}{\pi}\arctan(at)\right) + 1,$$

where $q_0$ represents the initial value of $q$ at $t_0$ and $a$ is a parameter obtained through fitting. The fitting parameters for the S&P500 are $q_0 = 1.414$ and $a = 1.28 \times 10^{-4}$, while for Bitcoin, the fitted values are $q_0 = 1.514$ and $a = 2.0 \times 10^{-3}$. The black curves in Figures 4.2-a and 4.2-d represent the results of this fitting process. It is notable that the Bitcoin time series exhibits a closer fit to this relationship compared to the S&P500 time series. Specifically, for S&P500, the fitted values of $q(t)$ remain constant $q(t) = 1.4$ for approximately the first three days of trading, followed by a rapid convergence to $q(t) = 1$. Conversely, for Bitcoin, the transition takes place over a shorter duration of around 16 hours, with $q(t)$ stabilizing at $q(t) = 1$ for larger values of $t$. These findings highlight the varying dynamics and characteristics between the S&P500 and Bitcoin markets, with Bitcoin demonstrating a more pronounced adherence to the modeled relationship for $q(t)$. Figures 4.2-b and 4.2-e present the parameter $\Phi(t)$ obtained

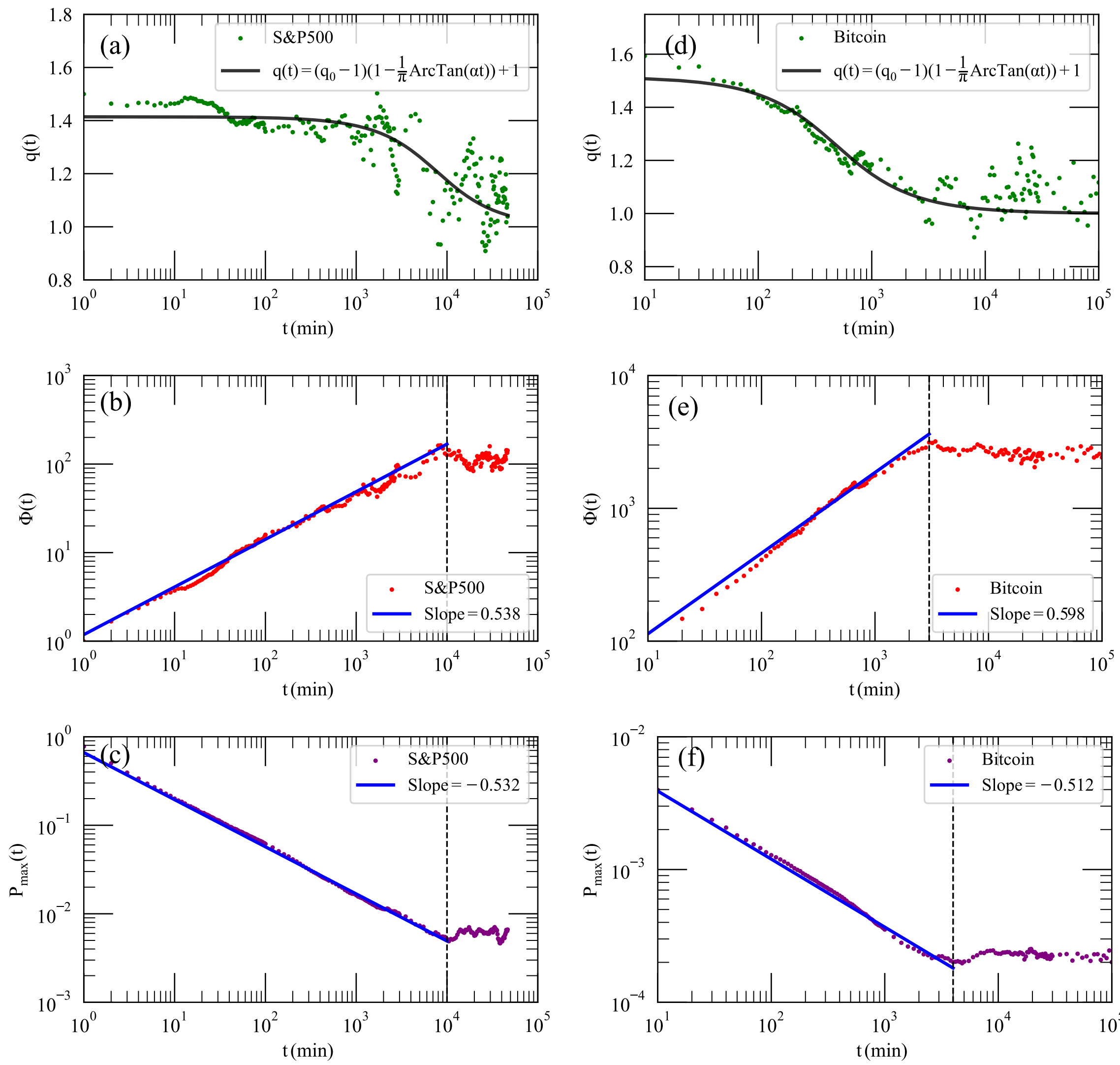


FIGURE 4.2: Results of fitting VO $q$-Gaussian to the PDFs for S&P500 and Bitcoin. The vertical dashed line indicates the point from where $\Phi(t)$ and the peak of the PDFs oscillate around a constant value. (a) Fitting parameter $q(t)$ for S&P500, which presents a constant of 1.5 initially and slowly converges to 1. (b) Fitting parameter $\Phi(t)$ for S&P500, with a slope of $1/\alpha = 0.538$. (c) The peak of the PDFs ($P_{max}(t)$) for S&P500 with a slope of $-0.532$. (d) Fitting parameter $q(t)$ for Bitcoin, initially at 1.5 and converges to 1 faster than S&P500. (e) Fitting parameter $\Phi(t)$ for Bitcoin, with a slope of $1/\alpha = 0.598$. (f) The peak of PDF ($P_{max}(t)$) for Bitcoin with a slope of $-0.512$.

from the $q$-Gaussian fitting for S&P500 and Bitcoin respectively. $\Phi(t)$ showcases a distinct slope and remains constant at large times. These slopes correspond to the anomalous diffusion, where $\Phi(t) \propto t^{1/\alpha(t)}$ (Eq. 4.6). The average slopes obtained for S&P500 and Bitcoin are

$1/\alpha = 0.54$ and $1/\alpha = 0.60$ respectively, while the local slopes depend on time. Moreover, as time $t$ increases, a constant value for $\Phi(t)$ becomes evident. This behavior is a consequence of the detrending process applied during the analysis.

An important feature of the VO diffusion is that the anomalous diffusion cannot be always derived from the temporal evolution of the peak of the PDF, it has been done in previous analyses of the S&P500 index Mantegna and Stanley 1995; Alonso-Marroquin et al. 2019. Figure 4.2-c and Figure 4.2-f shows the height of the PDF of price return ($P_{\max}(t)$) for S&P500 and Bitcoin respectively. This term is obtained as the value of the PDF at $x = 0$. For both stock markets, $P_{\max}(t)$ exhibits a slope initially and remains constant over a large time. A linear fitting is conducted and the slopes obtained are $-0.532$ and $-0.512$ for S&P500 and Bitcoin, respectively. This slope is consistent with the anomalous diffusion exponents for the S&P500 but not in the Bitcoin data. As in the case of Bitcoin, the exponent obtained from $\Phi(t)$ is $\alpha = 1.672$ and does not correspond to the exponent $1.953$ obtained from $P_{\max}$. This apparent discrepancy can be understood in the light of Eq. 4.42. There one can derive the relationship $P_{\max}(x = 0, t) = \frac{1}{C_{q_t}\Phi(t)}$, where $C_{q_t}$ is a time-dependent parameter associated with $q$ as shown in Eq. 4.43. It is noteworthy that the absolute value of the slopes in $\Phi(t)$ and $P_{\max}(t)$ shows a better agreement for S&P500 than for Bitcoin. This disparity can be attributed to the distinction in the time-dependent term $q(t)$ for both markets. In the case of S&P500, the value of $q(t)$ remains approximately constant for a longer period than for Bitcoin. As a result, $C_{q_t}$ closely approximates a constant value, leading to a relationship of $P_{max}(t) \propto 1/\Phi(t)$, which aligns with the results. Whilst for Bitcoin, where $q(t)$ varies with time, the effect of $C_{q_t}$ becomes more significant.

We now realize that neither $P_{\max}(t)$ nor $\Phi(t)$ obtained from curve fitting are reliable methods to derive the exponent of the anomalous diffusion in VO diffusion processes. In fact, the function $\Phi(t)$ obtained in Figures 4.2-b and 4.2-e present $\Phi(t)$ calculated as a fitting parameter of the PDF to the $q$-Gaussian distribution. The results of $\Phi(t)$ shown have some fluctuations and the fitting of the slope is not perfect. These fluctuations and deviations arise due to errors in the fitting process, as fitting to the $q$-Gaussian distribution may not always be perfect. Therefore,

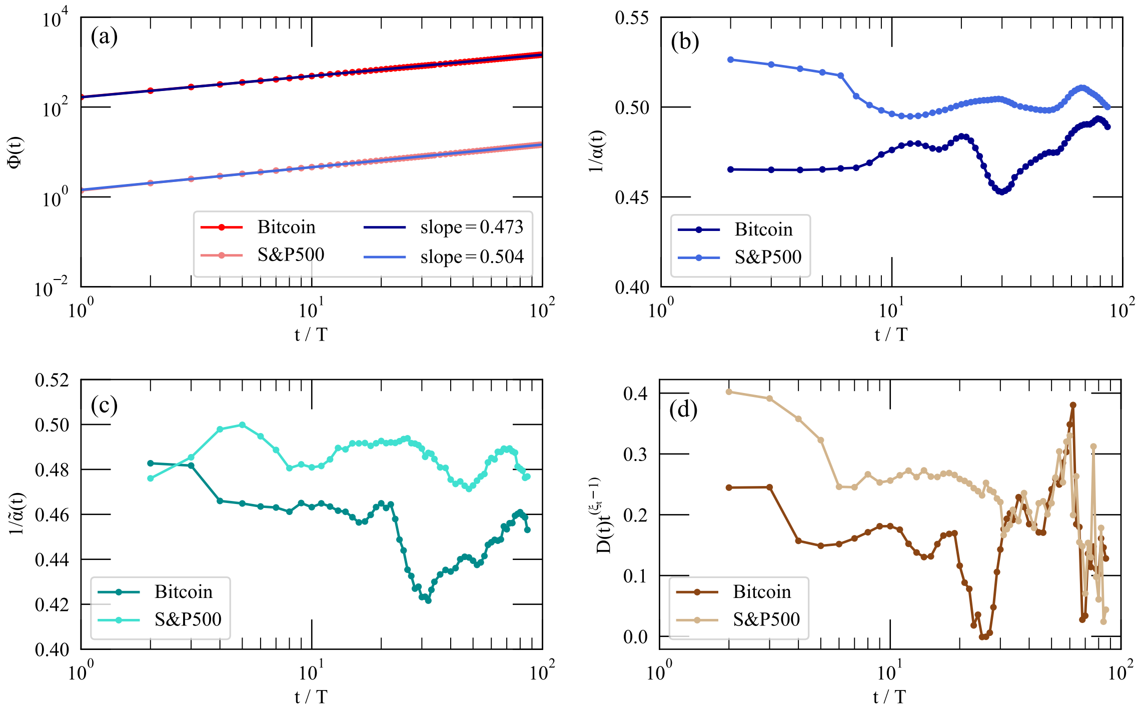


FIGURE 4.3: (a) $\Phi(t)$ calculated for both S&P500 and Bitcoin price return based on the second moment, both present clear slopes. (b) $1/\alpha(t)$ calculated as the localized slope of $\Phi(t)$. Both S&P500 and Bitcoin present a convergence to 0.5, yet at a different pace. S&P500 converges to 0.5 faster than Bitcoin. (c) $1/\tilde{\alpha}(t)$ calculated following Eq. 4.47 for S&P500 and Bitcoin. (d) Parameter $D_t t^{\xi_t - 1}$ calculated for both time series based on the relationship in Eq. 4.25.

to get rid of systematic fluctuations it is more reliable to use the variance formula (Eq. 4.45) to estimate $\Phi(t)$ and the associated exponent $\alpha_t$ as we do in the rest of this section.

The power-law relation obtained using Eq. 4.45 is presented in Figure 4.3-a. An adjustment was performed on the time series of both S&P500 and Bitcoin by rescaling the price return using the data frequency ($T$). Specifically, for the S&P500, $T = 1$ minute, while for Bitcoin, $T = 10$ minutes. The slopes of $\Phi(t)$ were computed for both S&P500 and Bitcoin. The results reveal that $\Phi(t)$ for S&P500 price return has a slope of $0.50(4)$, whereas for Bitcoin, the slope of $0.47(3)$. This shows that the slope of $\Phi(t)$ is related to the type of diffusion process. However, these exponents are the averaged ones over time, and the local slopes show different behaviors, i.e., they change over time which needs a "variable order" analysis.

We calculate the local slope of $\Phi(t)$ to determine $1/\alpha_t$ based on the aforementioned relation in Eq. 4.46, and the results are shown in Figure 4.3-b. The light-blue curve is the local slope of S&P500, indicating superdiffusion at small time scales ($t$) with $1/\alpha(t) > 0.5$, transitioning towards normal diffusion at large $t$ with $1/\alpha(t) \rightarrow 0.5$. On the other hand, the dark blue curve in Figure 4.3-b represents the local slope of the Bitcoin time series, displaying subdiffusion at small times $t$ with $1/\alpha(t) < 0.5$, and gradually converging towards normal diffusion. Upon comparing the two curves, we observe that the S&P500 slope exhibits a slow decrease in $1/\alpha$ at small $t$, while for Bitcoin, it remains relatively constant at approximately $0.46$. As time progresses, the S&P500 local slope converges to $0.5$ faster than Bitcoin, indicating a quicker convergence to Gaussian diffusion. In contrast, the local slope of Bitcoin fluctuates between $0.46$ and $0.5$, gradually converging to normal diffusion over an extended time period. The difference in the rate of convergence to a normal diffusion process between the S&P500 and Bitcoin (Figure 4.3-b) can be attributed to several key factors. Firstly, the high volatility of Bitcoin contributes to its distinct diffusion characteristics. Additionally, the high decentralization of Bitcoin allows it to be influenced by investor sentiment, which further impacts its diffusion dynamics. Lastly, the regulatory framework surrounding cryptocurrency, or rather its absence within traditional regulatory frameworks, adds to the unique behavior observed in Bitcoin.

A numerical estimation of the value of $1/\tilde{\alpha}_t$ was made using Eq. 4.47, which is shown in Fig. 4.3-c. Using this function, one is able to calculate $G(t, t_0)$ using and 4.29, and $g(t)$ as its time drivative (Eq. 4.24). Here we applied an approximation in the derivative to the Bitcoin time series to eliminate the negative values. As the final step, we are able to estimate the variable order exponents using the relation in Eq. 4.24. More precisely, the parameter $D_t t^{\xi_t - 1}$ is calculated for both time series and plotted in Figure 4.3-d. Apart from the stochastic fluctuations, we observe that this parameter decreases with time in the small time regime, showing that the diffusion process becomes slower over time as becomes constant for a time period. The decrease of the diffusion coefficient with time is consistent with previous analysis of the S&P500 data (Arias-Calluari et al. 2021). Note that the PDF of the detrended data becomes constant when the time reaches the detrended time window. Thus, the diffusion coefficient should also become zero when the time reaches the time windows used to detrend the time series. The explanation of this trend of the diffusion coefficient is elusive, but there is no reason to expect that the diffusion coefficient remains constant in VO diffusion processes.

## 4.5 Discussion

We have proposed a variable-order differential equation to describe nonlinear fractional diffusion processes with anomalous diffusion, applicable for the regime $1 \leq q < 2$. In the variable-order equation, the analytical solution is self-similar in the broad sense, with $x \sim \phi(t)$ as the scaling variable, which is given in terms of the $q-$Gaussian distribution. In the constant-order equation, the scaling variable reduces to $x \sim t^H$, where $H = 1/\alpha$ is the Hurst exponent and $\alpha$ defines whether the diffusion process is either normal or super/sub diffusive. The variable-order exponents $\alpha(t)$ and $q(t)$ are related to time correlations and non-linear diffusion. The time-dependency of the exponents allows them to comply with the Central Limit Theorem, which requires $\alpha(t) \to 2$ and $q(t) \to 1$ as $t \to \infty$. Typically, alpha is related to the Hurst exponent ($H = 1/\alpha$) of the time series associated with the diffusion process. This can be discussed in light of the fBm, which is a self-similar Gaussian stochastic process characterized by stationary power-law correlated increments. In the fBm, the Hurst exponent provides a crucial link between the diffusion coefficient $\alpha$ through the relation $H = 1/\alpha$ (Gharari et al. 2021). This exponent measures the long-range memory in time series data and can also be associated with autocorrelation patterns. Specifically, for $0 < H < 0.5$ (or $\alpha > 2$) the time series exhibits anti-correlated behavior. In the case of $H = 0.5$ (or $\alpha = 2$), the time series is uncorrelated. Finally, for $0.5 < H < 1$ (or $\alpha < 2$), the time series displays positively correlated behaviour (Kantelhardt et al. 2002d). Moreover, in positive long-range correlated series, the autocorrelation function follows a power-decay pattern described by $C(s) \sim s^{-\gamma}$ where $\gamma = 2 - 2H$ (Kantelhardt et al. 2002d).

The dynamics of the market ecosystem suggest that traders' behavior can influence autocorrelation patterns. In the stock market, traders employ various strategies, including positive feedback traders where they buy after price increases and sell when prices decline, and negative traders who follow the 'buy-low sell-high approach (Koutmos and Saidi 2001). Sentana and

Wadhwani (Sentana and Wadhwani 1992) explored the connection between volatility, returns autocorrelation, and trading strategies using a GARCH model. They conducted empirical investigations using the Dow Jones index data and discovered that positive traders can lead to negative autocorrelation, while negative traders can result in positive autocorrelation. Furthermore, they found that in an index comprising numerous securities with different trading frequencies, positive cross-autocorrelation emerges, contributing to positive autocorrelation within the index. This finding aligns with our study, specifically in the context of the S&P500 market index.

In our analysis, the variable order exponents are observed in both stock markets and cryptocurrencies. In the S&P500 market $\alpha(t) < 2$ while gently increasing to the value $\alpha(t) = 2$ for large times. This behavior is consistent with the ecology of this market, consisting of short to moderate-time investors that lead to short-time correlations. The behavior is different in the Bitcoin index where $\alpha(t)$ oscillates slightly above 2, indicating anticorrelation in the time series. This behavior is consistent with the peculiar ecology of the cryptocurrencies mainly dominated by speculators who are frequently changing their strategy to maximize utilities. For large times, the time series of price returns become uncorrelated, leading to the expectation that $\alpha$ converges to 2 in this limit.

The underlining mechanism of the values of the exponent $q(t)$ may be attributed to the interaction between the equities of the stock market, This can be understood from the Langevin equation of the non-linear FPE (Eq. 4.7) that is converted by using the property of the Katugampola derivative $d^\xi/dt^\xi = t^{1-\xi}d/dt$ to (Katugampola 2014)

$$\frac{\partial P(x,t)}{\partial t} = Dt^{\xi-1}\frac{\partial^2 P(x,t)^{2-q}}{\partial x^2}. \tag{4.50}$$

The corresponding Langevin equation describing the stochastic dynamics of the price return $X(t)$ has been derived by Borland (Borland 1998)

$$X(t+dt) = X(t) + \eta(t)(Dt^{1-\xi}P(X(t),t)^{1-q})^{1/2}dt, \tag{4.51}$$

where $\eta(t)$ is the white noise signal. Let us consider the case of an idealized gas of particles experiencing Brownian-like motion, For $q = 1$ and $\xi = 1$ the stochastic dynamic corresponds to the classical random walk that describes ideal gases. For more dense situations, $q$ may take values larger than zero, indicating that the random walk of each particle is influenced by the local density of the particles around its location. This physical picture can be extrapolated to financial markets as follows: Assuming that $X(t)$ is the index of a particular stock, the dependency of the fluctuations on its probability density functions may be attributed to the interaction between different equities in the stock market. In fact, the S&P500 index is calculated based on the 500 largest companies in the US, and it should be noted that the performance of these companies cannot be assumed to be independent. The exponent $q \approx 1.4$ is observed for price returns calculated within $t = 10^3$ minutes (roughly 3 days). For larger times $q$ converges to 2 since the CLT requires the PDF of the price return to converge to a Gaussian distribution when $t \to \infty$. In the case of Bitcoin, the exponent $q$ is larger ($q \approx 1.5$) and it converges to $q = 2$ faster (in the order of hours), which may be directly related to the transaction between different crypto-currencies. In both cases, the CLT is guaranteed since the standard deviation of the $q-$Gaussian distribution is finite for $q < 5/3$. Further investigation of these peculiar dynamic features from microscopic models such as agent-based models or order book models would provide some light on the underlines mechanism of the time evolution of these exponents.

## 4.A Dimensional analysis

In this appendix, we describe the scaling properties of the PDFs. From the dimensional analysis of the normality condition, one realizes that the dimension of any PDF $P(\mathbf{x})$ is $[P(\mathbf{x})] = [\mathbf{x}]^{-d}$, where $[Q]$ shows the *space* dimension of the quantity $Q$. To see this more explicitly, we apply the scaling transformation $\mathbf{x} \to \mathbf{y} \equiv \lambda\mathbf{x}$, and using the conservation of probability $P(x)d^dx = P(y)d^dy$, one finds

$$P(\lambda x) = \lambda^{-d} P(x). \tag{4.52}$$

For a stochastic process, where $P$ changes with time, we use the root mean displacement relation $r \equiv |\mathbf{x}|$

$$\left\langle r^2 \right\rangle \propto \phi(t)^2 \tag{4.53}$$

to predict the form of the PDF, where $\phi(t)$ is a function of time the form of which determines the anomalous diffusion nature. In this case, the equation 4.52 generalizes to

$$P(\lambda\mathbf{x}, \lambda\phi(t)) = \lambda^{-d} P(\mathbf{x}, \phi(t)), \tag{4.54}$$

which is realized using the normality condition

$$\begin{aligned} &\int_{-\infty}^{\infty} P(\mathbf{x}, \phi(t)) d^d x = \lambda^d \int_{-\infty}^{\infty} P(\lambda\mathbf{x}, \lambda\phi(t)) d^d x = 1 \\ &\rightarrow P(\lambda\mathbf{x}, \lambda\phi(t)) = \lambda^{-d} P(\mathbf{x}, \phi(t)). \end{aligned} \tag{4.55}$$

A solution of this equation is a factorized form as follows

$$P(\mathbf{x}, t) = \frac{1}{\phi(t)^d} F\left[\phi(t)^{-1}\mathbf{x}\right], \tag{4.56}$$

where the function $F$ is a well-behaved one to be determined using the governing equation. Note that $F$ is invariant under $\mathbf{x} \rightarrow \lambda\mathbf{x}$, $\phi(t) \rightarrow \lambda\phi(t)$, and also

$$\left\langle r^2 \right\rangle = \frac{\int \mathrm{d}^d x r^2 F\left[\frac{\mathbf{x}}{\phi(t)}\right]}{\int \mathrm{d}^d x F\left[\frac{\mathbf{x}}{\phi(t)}\right]} = \left[\frac{\int \mathrm{d}^d z |\mathbf{z}|^2 F[\mathbf{z}]}{\int \mathrm{d}^d z F[\mathbf{z}]}\right] \phi(t)^2, \tag{4.57}$$

where $\mathbf{z} \equiv \frac{\mathbf{x}}{\phi(t)}$. The scaling properties of the time series are associated with the form of $\phi(t)$. In fact, for the solution of the Eq. 4.7 we have $\phi(t) = \phi_{\text{SS}}(t)$ where the index "SS" points out the self-similarity law, given by Gharari et al. 2021; Alonso-Marroquin et al. 2019

$$\phi_{\text{SS}}(t) \propto t^{1/\alpha} \equiv t^{-H}, \tag{4.58}$$

where $\alpha$ is a self-similarity exponent, and $H$ is the Hurst exponent. Combining Eq. 4.5 and Eq. 4.58, one reaches the Eq. 4.1.

## 4.B Relationship between fBm, time fractional FPE and SDE

This short appendix is devoted to some scaling properties of the fBm, especially by focusing on its Langevin equation, and the corresponding FPE. Our primary objective is to explore the relationship between time-fractional generalized Lagevine and FPE equations for fBm. This example sheds light on the essential difference between the driving processes of Brownian motion (Bm) as an example of semi-martingales and fBm as a representative of non-semi-martingales. The complexity of the latter case arises mainly from the presence of correlations, resulting in sub- or super-diffusion. This also shows the consequences of the presence of non-local effects (Gharari et al. 2021).

The classical FPE establishes a relationship between the stochastic differential equation (SDE) driven by Bm and its associated partial differential equation. The fBm $B^H := \{B^H(t), t \geqslant 0\}$ is a family of stochastic processes indexed by the Hurst index $H \in (0, 1)$. For each $H$, the process $B^H$ is defined as a weighted moving average of a Bm process

$$B^H(t) = \int_0^t (t-\tau)^{H-1/2} dB(\tau), \tag{4.59}$$

where $B := \{B(t), t \geqslant 0\}$ is a Bm and $H$ is the Hurst parameter. The fBm with variance $\sigma(t)$ is the solution of the following fractional SDE (Di Paola and Pirrotta 2022)

$$\frac{d^\xi X}{dt^\xi} = \sigma(t)\eta(t), \tag{4.60}$$

where $\eta(t) = dB/dt$ is the normalized white noise, $1/2 < \xi = H + 1/2 \leq 1.5$ and $d^\xi/dt^\xi$ is the Riemann–Liouville fractional operator that is defined as

$$\frac{d^\xi f}{dt^\xi} = \frac{1}{\Gamma(\xi)} \int_0^t (t-\tau)^{\xi-1} f(\tau) d\tau. \tag{4.61}$$

Further, the fractional FPE of the fBm process is given by (Di Paola and Pirrotta 2022)

$$\frac{d^{2H} P_X(x,t)}{dt^{2H}} = \frac{\Gamma(2H)}{2\Gamma^2(H+1/2)} \sigma(t) \frac{\partial^2 P_X(x,t)}{\partial x^2}. \tag{4.62}$$

There are two main differences between the fBm and the fractional $q$-Gaussian process investigated in this paper. Firstly, the FPE of the fBm is linear and its solution is expressed in terms of Gaussian distribution, while the latter is nonlinear and the solution is given in terms of the $q$-Gaussian distribution. Secondly, the fractional FPE of the fBm involves non-local fractional derivatives while the fractional $q$-Gaussian process involves local (Katugampola) fractional operators. Yet in both cases, one can recover the Bm by either taking $H = 1/2$ in the fBm or $q = 1$ and $\alpha = 1$ in the fractional $q$-Gaussian diffusion.

On the other hand, discussing the relationship between the fractional FPE (or the governing equation) and the SDE of their associated time series are equivalent to discussing the relation between the auto-correlation of the time series and the fractionalization scheme in the governing equation. The key point is the scaling properties of the governing equation describing a self-similar time series. If $\{X(t)\}_{t\in\mathbb{Z}}$ denotes a self-similar time series with the property

$$\sqrt{\langle X^2 \rangle} \propto t^H. \tag{4.63}$$

Then, the corresponding governing equation should have the same symmetry. It means the invariance of the PDF (of the governing equation) up to a scaling factor, i.e.

$$P(X,t) = t^{-H} F(X/t^H), \tag{4.64}$$

where $F$ is a function to be fixed by the governing equation. Fractional Brownian motions are described by Eq. (4.64) when $F$ is an exponential function

$$P\left(X,t\right) \propto t^{-H} \exp\left[-\frac{1}{2}\left(\frac{X}{t^H}\right)^2\right]. \tag{4.65}$$

In fact, the governing equation for a self-similar time series should include fractional operators, or one should use a space- or time-dependent diffusion coefficient with power-law dependence. The symmetry of the system can easily be found in the corresponding PDF of the time series, and also by calculating the second moment of $X$, which $X$ denotes a self-similar time series. This means the fractionalization exponent is manifest in the PDF.

Consider a general $H$-self-similar time series $\{X(t)\}_{t\in\mathbb{Z}}$ defined by the relation $\{X(ct)\}_{t\in\mathbb{Z}} \equiv \{c^H X(t)\}_{t\in\mathbb{Z}}$, where $c > 0$, and $H$ is the Hurst exponent. If this process has stationary increments $Y_n = X(n) - X(n-1)$, then the auto-correlation $\gamma_Y(k) \equiv \langle Y_k Y_0 \rangle - \langle Y_k \rangle \langle Y_0 \rangle$ behaves like $k^{2d-1}$ as $k \to \infty$, where $d = H - \frac{1}{2}$, and $0 < d < 1/2$, ensuring that $\sum_{k=-\infty}^{\infty} \gamma_Y(k) = \infty$.

From a spectral domain perspective, the spectral density of $\{Y_n\}$ behaves as $\omega^{-2d}$ as the frequency $\omega \to 0$. This relates self-similar time series with fractionalization which is applied to the price return time series which becomes stationary by normalizing the detrended data set (see Eq. 4.48) (Gharari et al. 2021). Let us consider the special case $\Phi(t) \sim t^{1/\alpha_t}$ in Eq. 4.45. Following these facts, we suggest a relation between the Hurst exponent $H_t = 1/\alpha_t$ given in Eq. 4.13, with a self-similar function Eq. 4.42 for the VO-nonlinear case.

## 4.C Some details of VO calculations for PME

In this appendix, we introduce and inspect a VO extension of the Katugampola fractional operator, denoted as VO-K in this paper. We outline the definition of this operator and discuss some of its key properties. For a more comprehensive understanding of the Katugampola fractional operator and its underlying principles, we recommend referring to Katugampola 2014.

A VO-K fractional operator, which is used to construct the VO-PME in Section 4.3 is defined as

$$\mathcal{D}^{\alpha(t)} f(t) = \lim_{\epsilon \to 0} \frac{f(te^{\epsilon t^{-\alpha(t)}}) - f(t)}{\epsilon}, \tag{4.66}$$

for $t > 0$ and $\alpha(t) \in (0, 1]$. If $0 \leq \alpha(t) < 1$, the VO-K operator generalizes the classical calculus properties of polynomials. Furthermore, if $\alpha(t) = 1$, the definition is equivalent to the classical definition of the first-order derivative of the function $f$. When $\alpha(t) \in (n, n+1]$ (for some $n \in \mathbb{N}$, and $f$ is an $n-$differentiable at $t > 0$), the above definition generalizes to

$$\mathcal{D}^{\alpha(t)} f(t) = \lim_{\epsilon \to 0} \frac{f^{(n)}(te^{\epsilon x^{n-\alpha(t)}}) - f^{(n)}(t)}{\epsilon}.$$

If $f$ is $(n+1)-$differentiable at $t > 0$, then we have

$$\mathcal{D}^{\alpha(t)} f(t) = t^{n+1-\alpha(t)} f^{(n+1)}(t). \tag{4.67}$$

The properties of the VO-K derivatives are a simple extension of the ordinary derivatives

$$
\begin{aligned}
\mathcal{D}^{\alpha(t)}[af+bg] &= a\mathcal{D}^{\alpha(t)}(f)+b\mathcal{D}^{\alpha(t)}(g), \;\; \forall a,b\in\mathbb{R}\\
\mathcal{D}^{\alpha(t)}[C] &= 0, \;\; C\in\mathbb{R}\\
\mathcal{D}^{\alpha(t)}[fg] &= f\mathcal{D}^{\alpha(t)}(g)+g\mathcal{D}^{\alpha(t)}(f)\\
\mathcal{D}^{\alpha(t)}[f/g] &= \frac{g\mathcal{D}^{\alpha(t)}(f)-f\mathcal{D}^{\alpha(t)}(g)}{g^2}\\
\mathcal{D}^{\alpha(t)}(f\text{o}g)(t) &= f'(g(t))\mathcal{D}^{\alpha(t)}g(t),
\end{aligned}
$$

where $f\text{o}g(t) \equiv f(g(t))$. The proof of the properties of the variable order Katugampola fractional operator (VO-K) is analogous to the proof presented in (Katugampola 2014). In our case, we replace the constant order parameter $\alpha$ with the variable order parameter $\alpha(t)$.

Throughout this paper, the notations $\mathcal{D}^{\alpha(t)}$ and $\frac{\partial^{\alpha(t)}}{\partial t^{\alpha(t)}}$ is used with the same meaning. The fractional Katugampola calculations for the VO-PME are performed, as shown in Section 4.3, between Eq. 4.4 and Eq. 4.13. Applying the properties of the VO-K derivative, we get

$$
\begin{aligned}
\frac{\partial^{\xi(t)}}{\partial t^{\xi(t)}}\left(\frac{1}{\phi(t)}F\left(\frac{x}{\phi(t)}\right)\right) &= F\left(\frac{x}{\phi(t)}\right)\left(\frac{-\mathcal{D}^{\xi(t)}\phi(t)}{\phi^2(t)}\right)\\
&+\frac{1}{\phi(t)}\left(F'\left(\frac{x}{\phi(t)}\right)\mathcal{D}^{\xi(t)}\left(\frac{x}{\phi(t)}\right)\right)\\
&= F\left(z\right)\left(\frac{-\mathcal{D}^{\xi(t)}\phi(t)}{\phi^2(t)}\right)+zF'\left(z\right)\left(\frac{-\mathcal{D}^{\xi(t)}\phi(t)}{\phi^2(t)}\right)\\
&= \frac{-\mathcal{D}^{\xi(t)}\phi(t)}{\phi^2(t)}\frac{d}{dz}[zF(z)],
\end{aligned}
\tag{4.68}
$$

where $z=\frac{x}{\phi(t)}$. Then, we get the following two equations

$$
\begin{aligned}
\frac{\partial^2}{\partial x^2}P^{\nu(t)}(x,t) &= \frac{1}{\phi^{\nu(t)+2}}\frac{d^2}{dz^2}F^{\nu(t)}\\
\frac{\partial^{\xi(t)}P(x,t)}{\partial t^{\xi(t)}} &= \frac{-1}{\phi^2(t)}\frac{\partial^{\xi(t)}\phi}{\partial t^{\xi(t)}}\left[F+z\frac{d}{dz}F\right],
\end{aligned}
\tag{4.69}
$$

so that

$$
\frac{-1}{\phi^2(t)}\frac{\partial^{\xi(t)}\phi}{\partial t^{\xi(t)}}\frac{d}{dz}[zF] = \frac{D(t)}{\phi^{\nu(t)+2}}\frac{d^2}{dz^2}F^{\nu(t)}. \tag{4.70}
$$

# 4.D The local VO fractional non-linear time diffusion equation with drift

The drift is often an inevitable part of stochastic systems, that should be analyzed in detail for every case study to control its effects. Although it is suggested to define the equations for the general drift term. For the case where it depends only on time (as is the case for many physical systems of interest), the situation becomes easier. In this case, the governing equation is

$$\frac{\partial^{\xi(t)}}{\partial t^{\xi(t)}}P(x,t) = -a(t)\frac{\partial P(x,t)}{\partial x} + D(t)\frac{\partial^2 P^{\nu(t)}(x,t)}{\partial x^2}. \tag{4.71}$$

Through a change of variable $\tau = t^{\xi(t)}$ and VO-K fractional derivative, provided $h(t) = \xi(t)\ln t$ has an inverse function, we have

$$\partial_\tau P(x,t) = -a_1(\tau)\partial_x P(x,t) + D_1(\tau)\partial_x^2 P^{\nu_1(\tau)}(x,t),$$

where $a_1(\tau) = a(t(\tau))(t\xi'(t)\ln t + \xi(t))^{-1}$, $D_1(\tau) = D(t(\tau))(t\xi'(t)\ln t + \xi(t))^{-1}$, and $\nu_1(\tau) = \nu(t(\tau))$. By using the change of variable $(s,y) = (\tau, x - x_0 - f(\tau))$, where $f(\tau) = \int_0^\tau a_1(\tau')d\tau'$, and using the fact that $\frac{\partial y}{\partial \tau} = -a_1(\tau)$ and $\partial_\tau + a_1(\tau)\partial_x = \partial_s$, one finds that the governing equation $P(y,\tau)$ is

$$\partial_\tau P(y,\tau) = D(\tau)\partial_y^2 P^{\nu(\tau)}(y,\tau),$$

for which the solution is ($x_0 \equiv 0$ and $k \equiv 1$ and $k_1 \equiv 0$)

$$\begin{aligned} P(y,\tau|y_0,\tau_0) = {} & \frac{A_q(t)}{\left(\int_{\tau_0}^{\tau} g(s)ds\right)^{\frac{1}{\nu(\tau)+1}}} \\ & \times \left(c + \frac{(\nu(\tau)-1)}{2\nu(\tau)}\frac{y^2}{\left(\int_{\tau_0}^{\tau} g(s)ds\right)^{\frac{2}{\nu(\tau)+1}}}\right)^{\frac{1}{\nu(\tau)-1}}, \end{aligned} \tag{4.72}$$

where $g(s) = D(s)(1+\nu(s))$. Let us equate $P(y,\tau)$

$$P(x,t) = \frac{\partial y}{\partial x} P(y, \tau(t)).$$

Then, we obtain

$$\begin{aligned} P(x,t|_0,t_0) &= \frac{A_q(t)}{\left(\int_{t_0}^{t} g(s)ds\right)^{\frac{1}{\nu(t)+1}}} \\ &\times \left(c + \frac{(\nu(t)-1)}{2\nu(t)} \frac{(x-f(t))^2}{\left(\int_{t_0}^{t} g(s)ds\right)^{\frac{2}{\nu(t)+1}}}\right)^{\frac{1}{\nu(t)-1}}, \end{aligned} \tag{4.73}$$

where $A_q$ is a normalization factor, and $c$ and $k$ are constant. Eq. 4.73 is a VO $q$-Gaussian solution with a drift.

CHAPTER 5

# Comparative analysis of stationarity for Bitcoin and the S&P500

In previous chapters, we proposed the governing equation for the financial market, incorporating a deterministic trend and a stochastic $q$-Gaussian noise. We started with constructing the governing equations using constant order parameters and extended them to variable order parameters. A sigmoid function is used to describe the time-dependence of $q(t)$, which allows a smooth transition between the initial $q$ value for the $q$-Gaussian distribution and the final convergence to a Gaussian distribution with $q = 1$. We approached the nonlinear fractional Fokker-Planck equations with the Katugampola fractional derivative. Similar attempts were made to construct the time-dependent solution to the fractional Fokker-Planck equation using the Riemann–Liouville fractional derivative (Bologna et al. 2000). In the constant order limit, the solution we proposed in the previous chapter coincides with the literature in some respects, yet the hyper-scaling relations between the exponents are different. The governing equation we proposed accommodates the non-stationary characteristics inherent in financial systems. We assessed the stationarity of the S&P500 price return, determining that global stationarity is achieved when detrending the time series with a 1-year window and normalizing it with a 60-minute window.

In this chapter, we aim to compare and contrast stationarity between the conventional stock market and cryptocurrency. The datasets used for the analysis are the intraday price indices of the S&P500 from 1996 to 2023 and the intraday Bitcoin indices in USD from 2019 to 2023. We adopt the definition of 'wide sense stationary', which constrains the time independence of the first and second moments of a time series. The testing method used in this paper follows the Wiener-Khinchin Theorem, i.e. that for a wide sense stationary process, the power spectral density and the autocorrelation are a Fourier transform pair. We demonstrate that localized stationarity can be achieved by truncating the time series into segments, and for each segment, detrending and normalizing the price return are required. These results show that the S&P500 price return can achieve stationarity for the full 28-year period with a detrending window of 12 months and a constrained normalization window of 10 minutes. With truncated segments, a larger normalization window can be used to establish stationarity, indicating that within the segment the data is more homogeneous. For Bitcoin price return, the segment with higher volatility presents stationarity with a normalization window of 60 minutes, whereas stationarity cannot be established in other segments.

## 5.1 Introduction

In this study, we apply a novel method to the comparative analysis of the stationarity of two univariate time series: The intraday S&P500 and the intraday Bitcoin index in USD (BTC/USD). Stationarity plays a central role in much of stochastic time series analysis, see for example prediction and non-linearity (Cheng et al. 2015; Aue et al. 2015) and the distinction between varieties of stationarity (Jentsch and Rao 2015; Dahlhaus 2012). In the absence of stationarity, temporally localized dynamics can be informative of important market dynamics, such as volatility (Bhowmik and Wang 2020; Harvey et al. 2016; Jin 2017) and other forms of market instability (Onnela et al. 2003c; Onnela et al. 2003a; Onnela et al. 2003b; Harré and Bossomaier 2009; Harré 2015; Harré 2022; Harré and Zaitouny 2023). In this sense the study and estimation of the stationarity of market dynamics has played an important role in broadening our understanding of these dynamics. Of particular interest are the transformations that translate a non-stationary processes into some form of stationarity (Gardner 1978), e.g. strict-sense, wide-sense, or locally stationary process.

In order to introduce the approach we use (please see our previous work (Arias-Calluari et al. 2018; Alonso-Marroquin et al. 2019; Arias-Calluari et al. 2021; Arias-Calluari et al. 2022; Tang et al. 2024a) for a more detailed introduction to the markets and recent results on non-linear analysis) we first introduce the notion of stationarity we will be working with and then discuss the approach we have taken. We first recall the following definitions that will be useful to us:

DEFINITION 5.1.1 (Strictly Stationary Process). A continuous time random process $\{X_t\}$ is a *Strictly Stationary Process* (SSP) if, for a finite integer $n$, subscripts $t_1, t_2, \ldots, t_n$, and a cumulative distribution function $F_X(x_{t_1}, x_{t_2}, \ldots, x_{t_n})$, the following property holds:

$$F_X(x_{t_1+\tau}, \ldots, x_{t_n+\tau}) = F_X(x_{t_1}, \ldots, x_{t_n})$$

for all $\tau, t_1, \ldots, t_n \in \mathbb{R}$ and for all $n \in \mathbb{N}_0$ ■

This definition is often too restrictive, accounting as it does for all moments of the distribution. Instead a more tractable definition is often used, accounting only for a subset of the moments, one of the most common retaining equality only of the first two moments:

DEFINITION 5.1.2 (Wide-Sense Stationary Process). A continuous time random process $\{X_t\}$ (as above) is a *Wide-Sense Stationary Process* (WSP) if it constrains the mean $\mu_X(t) \triangleq \mathbb{E}[X_t]$ and auto-covariance $K_{XX}(t_1, t_2) \triangleq \mathbb{E}[(X_{t_1} - \mu_X(t_1))(X_{t_2} - \mu_X(t_2))]$ in the following fashion:

$$\begin{aligned}
\mu_X(t) &= \mu_X(t+\tau) && \text{for all } \tau, t \in \mathbb{R} \\
K_{XX}(t_1, t_2) &= K_{XX}(t_1 - t_2, 0) && \text{for all } t_1, t_2 \in \mathbb{R} \\
\mathbb{E}[\|X_t\|^2] &< \infty && \text{for all } t \in \mathbb{R} \quad \blacksquare
\end{aligned}$$

In this chapter we use the WSP definition to establish the transformations needed to be applied to $\{X_t\}$ (defined in the following section) to establish stationarity of the time series via the Wiener-Khinchin Theorem. The purpose of this analysis is to compare and contrast the local stationarity of the S&P500 and BTC/USD. This is central to improving our understanding of the extent to which the dynamics reflect qualities desirable of a mature asset market that is not dominated by speculation or bubbles and crashes.

Our approach broadly follows that of Stărică and Granger (Stărică and Granger 2005), in their study they considered the inter-day S&P500 statistics by "identifying the intervals of homogeneity, that is, the intervals where a certain estimated stationary model describes the data well." In that approach, parameters are time-dependent co-factors to be estimated within each temporal interval. In its specifics though, our approach differs somewhat from that of Stărică and Granger though. Our alternative looks at the intra-day price returns $\{X_t\}$ and considers what (fixed) size of a moving window over which the mean and standard deviation are estimated is necessary to bring the entire time series into a stationary state, this contrasts with local parameter estimation for establishing locally stationary intervals in Stărică and Granger.

This novel extension of previous methods localizes the stationarity constraint in the sense that the entire series is then stationary, but this stationarity depends on a specific time windowing of parameter estimation, rather than using the entire time series or a large time window defining an estimation interval of years. In effect, the narrower this window, the more temporally unstable the time series, and in principle there is no obvious requirement that any fixed estimation window of, for example, the variance should necessarily be adequate to bring the entire time series into a stationary state. Ultimately we find that we still do need to consider multiple (but quite large) partitions of the whole times series, but we also find that in some cases it works for entire time series, and in others it simply is not possible to establish stationarity.

## 5.2 Methodology

We recall the definitions for the governing equations of the stock market Arias-Calluari et al. 2022, starting with defining the price return at time $t$:

$$X(t_0, t) = I(t_0 + t) - I(t_0), \tag{5.1}$$

where $I(t_0)$ is the stock market index at time $t_0$, and $I(t)$ is the stock market index for any time $t > t_0$.

It is assumed that the stock market index $I(t)$ can be decomposed into two time series, consisting of a deterministic trend $\overline{I}(t)$ and a stochastic noise $I^*(t)$:

$$I(t) = \overline{I}(t) + I^*(t). \tag{5.2}$$

Then, the price return $X(t)$ can also be decomposed into a deterministic component $\overline{X}(t)$ and a stochastic noise $x(t)$, which has been modelled as $q$-Gaussian noise (see (Arias-Calluari et al. 2018; Alonso-Marroquin et al. 2019)):

$$X(t) = \overline{X}(t) + x(t), \tag{5.3}$$

where $\overline{X}(t) = \overline{I}(t_0 + t) - \overline{I}(t_0)$ and $x(t) = I^*(t_0 + t) - I^*(t)$.

We perform the analysis on the price returns for both markets, which includes a detrending process to eliminate the mean, and a regularization process to eliminate the standard deviation. The detrending process uses the Moving Average technique, where a sliding window of size $\Delta_1 t$ is shifted forward along the time series (with total length $N$), and the arithmetic average of the index $I(t)$ from $[t, \ \ t + \Delta_1 t]$ is calculated as the trend at time $t$. For the windows at the beginning and the end of the time series where $t < \frac{\Delta_1 t}{2}$ and $t > N - \frac{\Delta_1 t}{2}$, we identify three segments for calculating the moving window with respect to the window position:

• For $t < \frac{\Delta_1 t}{2}$:

$$\overline{I}(t) = \frac{2}{\Delta_1 t + 2t} \sum_{k=-t+1}^{\lceil(\Delta_1 t - 1)/2\rceil} I(t + k), \tag{5.4}$$

• For $\frac{\Delta_1 t}{2} < t < N - \frac{\Delta_1 t}{2}$:

$$\overline{I}(t) = \frac{1}{\Delta_1 t} \sum_{k=-\lfloor(\Delta_1 t - 1)/2\rfloor}^{\lceil(\Delta_1 t - 1)/2\rceil} I(t + k), \tag{5.5}$$

• For $t > N - \frac{\Delta_1 t}{2}$:

$$\overline{I}(t) = \frac{2}{2N - 2t + \Delta_1 t} \sum_{k=-\lfloor(\Delta_1 t - 1)/2\rfloor}^{\lceil N - t\rceil} I(t + k), \tag{5.6}$$

with the time step of $t = 1, 2, 3....N$ for the index fluctuations.

From the detrended price return ($x^*(t)$), a normalization process is performed to obtain the normalized price return ($x^{**}$), given by the standard score:

$$x^{**} = \frac{x^*(t)}{\sigma(x^*)}, \tag{5.7}$$

where $\sigma(x^*)$ is the standard deviation of the time series. A sliding window is shifted forward for calculating $\sigma(x^*)$, following the same segmenting technique introduced in eq. 5.4-5.6. The size of this sliding window is denoted as $\Delta_2 t$ for this calculation.

Based on previous results (Arias-Calluari et al. 2022), the stationarity test is conducted on the normalized price return ($x^{**}$). We first calculate sample autocorrelation of a time series as (Box et al. 2015; Liu et al. 1999):

$$C_x(s) = \frac{\langle x(t)\, x(t+s)\rangle}{\sigma_x^2}, \tag{5.8}$$

where $x(t)$ denotes the time series used for calculation, $s$ is the time lag, and $\sigma_x^2 = \langle (x(t)-\mu)^2\rangle$. In this analysis, the autocorrelation is calculated on the normalized price return by replacing $x(t)$ by $x^{**}$.

The Fourier transform of a time series $x_t$ is calculated as:

$$\widehat{x}(f) = \frac{1}{\sqrt{T}} \sum_{t=0}^{T} x(t) e^{-2\pi i f t}. \tag{5.9}$$

The method for the stationarity test follows the Wiener–Khinchin theorem, where for a wide-sense-stationary stochastic process, the Fourier transform of the autocorrelation ($\widehat{C_x}(f)$) of a time series equals its power spectral density (PSD), denoted as $|\widehat{x}(f)|^2$:

$$|\widehat{x}(f)|^2 = \widehat{C_x}(f). \tag{5.10}$$

A smoothing technique of the Savitzky-Golay filtering (Schafer 2011) is applied on both $\widehat{C_x}(f)$ and $|\widehat{x}(f)|^2$ in order to reduce the noise in the data without affecting their trends. The smoothed result is based on the least squares of a linear fitting across a moving window, applying the normalized convolution integers of Savitzky-Golay, denoted as $C_i$. Here, the smoothing window size is chosen as $3.97 \times 10^{-5}$ Hz following a previous study (Arias-Calluari et al. 2022).

## 5.3 Data and Results

The dataset used in this study includes the S&P500 price index and BTC/USD exchange rate, both reported at one-minute intervals. The S&P500 index data cover the period from Jan 1st, 1996 to Dec 31st, 2023, and Bitcoin data span from Apr 2nd, 2019 to Dec 31st, 2023. We conduct a stationarity test on the S&P500 time series first before moving to Bitcoin data. Both detrending and normalizing processes are required for each dataset before the stationarity test can be performed.

The initial step is to replicate the stationarity test result for the S&P500 normalized price return in the previous study, covering the sample period from Jan 1996 to March 2021. Detrending time window of $\Delta_1 t = 1$ year is used, then the detrended price return is normalized with a regularization window $\Delta_2 t = 60$ mins to arrive at the normalized price return ($x^{**}$). Figure 5.1 presents the result of the stationarity test, with the blue curve representing the Fourier transform of autocorrelation, and the orange curve for PSD. A match between $|\widehat{x^{**}}(f)|^2$ and $\widehat{C_{x^{**}}}(f)$ is achieved for time lags larger than 30 min, indicating stationarity.

We expanded the dataset to include the more recent time period from April 2021 onwards. Applying the same parameters with $\Delta_1 t = 1$ year, and $\Delta_2 t = 60$ mins, the testing results are illustrated in Figure 5.2-a. It can be observed that $|\widehat{x^{**}}(f)|^2$ and $\widehat{C_{x^{**}}}(f)$ appear as parallel curves, indicating that stationarity does not hold with these parameters. Attempts were made to narrow the detrending time window $\Delta_1 t$ to 1 week while keeping $\Delta_2 t = 60$ mins; however, stationarity still could not be achieved. Figures 5.2-b, 5.2-c, and 5.2-d presents the test results with a gradual decline in the regularization window $\Delta_2 t$, which takes values of 40 min, 20 min, and 10 min, respectively. The gap between $|\widehat{x^{**}}(f)|^2$ and $\widehat{C_{x^{**}}}(f)$ decreases with a gradual decrease in the size of $\Delta_2 t$, indicating an increase in the degree of stationarity. The normalized price return achieves stationarity with $\Delta_2 t = 10$ min for the full data set from Jan 1996 to Dec 2023.

Since stationarity does not hold for the extended time series with the same regularization window, we truncate the time series into segments, and investigate the stationarity of each period on a local scale. We use the COVID-19 pandemic as the flagging event for dividing

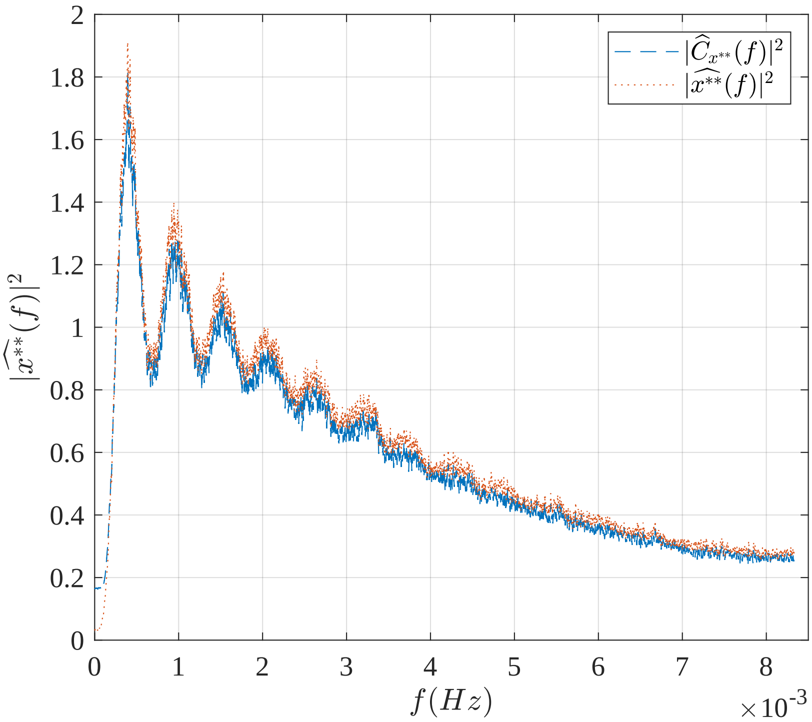


FIGURE 5.1: Reproduced results with the S&P500 price return from Jan 1996 to March 2021, detrended with a 1-year window, and normalized with a 1-hour window. The PSD aligns with the Fourier transform of autocorrelation, presenting stationarity.

the time series to explore the stationarity before and after Covid, given the higher market fluctuations observed post-pandemic. The initial impact of the pandemic on the US stock market was evident on Feb 24, 2020, when the S&P 500 and Nasdaq declined by 3% (McCabe 2020). Therefore, we consider the time series from Jan 1996 to Feb 21st, 2020 (market closed on the weekend of 23-24 Feb) as the first period. The second period is from Feb 24th, 2020 to Dec 31st, 2023. For each segment, we apply the detrending time window $\Delta_1 t = 1$ week, and the normalization window $\Delta_2 t$ is gradually narrowed down from 60 min to 40 min, 20 min, and 10 min. Results of stationarity test for each time period are shown in Figure 5.3 and Figure 5.4. In Figure 5.3, normalized price return before Covid presents stationarity with a regularization window at 60 mins, also at smaller window sizes, consistent with the results in the previous study. However, for the period after Covid, a gap is observed between $|\widehat{x^{**}}(f)|^2$ and $\widehat{C_{x^{**}}}(f)$ at $\Delta_2 t = 60$ mins, indicating non-stationarity. This gap narrows as $\Delta_2 t$ decreases, and approaches a close-to-stationary result at $\Delta_2 t = 10$ min.

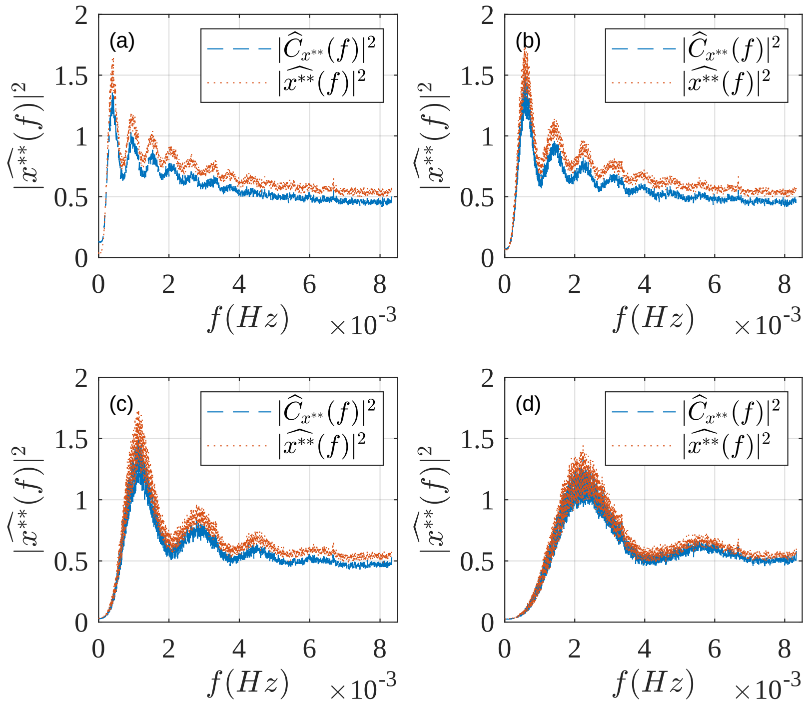


FIGURE 5.2: Stationarity test with S&P500 data from Jan 1st, 1996 to Dec 31st, 2023. (a) regularization window of 60 min. (b) regularization window of 40 min. (c) regularization window of 20 min. (d) regularization window of 10 min.

As the normalized price return after Covid did not exhibit a satisfactory level of stationarity, we further divide this period into two segments. The time series from Feb 24th, 2020, to Dec 31st, 2020, is taken as a separate segment, representing the first year of coronavirus spread. The second segment spans from Jan 1st, 2021 to Dec 31st, 2023. Stationarity tests are performed on these two time periods following the same parameters of $\Delta_1 t$ and $\Delta_2 t$, and results are presented in Figure 5.5 and Figure 5.6. By further segmenting the time series into shorter periods, both periods achieve stationarity at a better level. Figure 5.5-c present stationarity for at $\Delta_2 t = 20$ min, and an improved match is obtained at $\Delta_2 t = 10$ min. For the time period from 2021 to 2023, $|\widehat{x^{**}}(f)|^2$ and $\widehat{C_{x^{**}}}(f)$ match at $\Delta_2 t = 60$ mins, without requiring a smaller size for $\Delta_2 t$.

Testing results for the S&P500 demonstrate global non-stationarity for the full 28-year dataset. However, from a local perspective, the normalized price returns are stationary. In the following

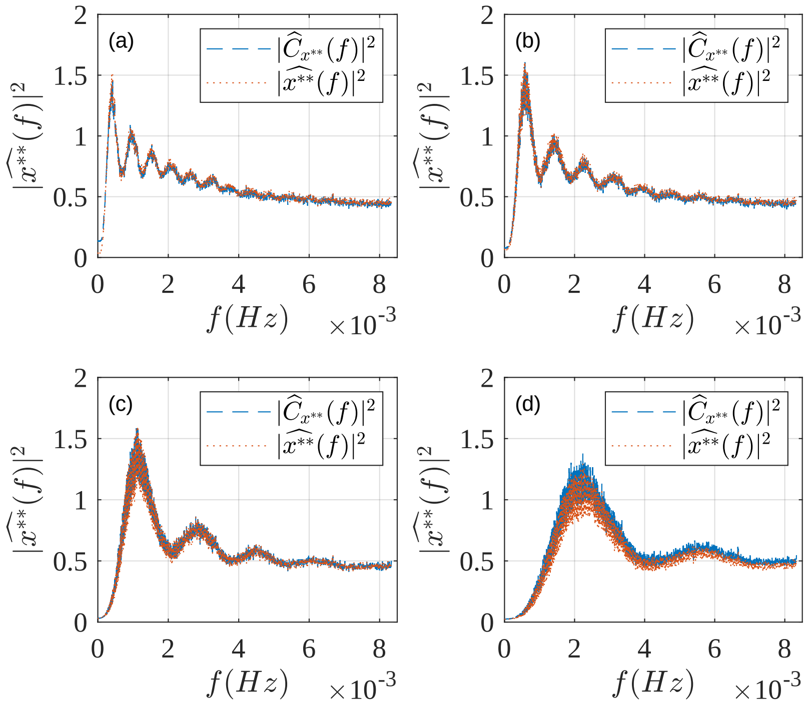


FIGURE 5.3: Stationarity test with S&P500 data from Jan 1st, 1996 to Feb 21st, 2020. (a) regularization window of 60 min. (b) regularization window of 40 min. (c) regularization window of 20 min. (d) regularization window of 10 min.

part of this paper, we focus on testing the normalized price return of Bitcoin. In our previous examination of the statistical characteristics of Bitcoin price returns, we identified two time periods for Bitcoin (Tang et al. 2024a). Here, we follow the same truncated time periods and extend the dataset to December 2023. The three segments for Bitcoin are: (1) Apr 2nd, 2019, to Dec 31st, 2020; (2) Jan 1st, 2021, to May 3rd, 2022; (3) May 4th, 2022, to Dec 31st, 2023. The price return is detrended with $\Delta_1 t = 1$ week, and the normalization window of 60 min, 40 min, 20 min, and 10 min is applied to the respective time period. Results for each period are plotted in Figure 5.7, Figure 5.8, and Figure 5.9, respectively. For Bitcoin periods 1 and 3, the detrended price return requires a smaller regularization window of 10 mins to achieve a certain level of stationarity. In contrast, for period 2, during which the price experienced larger fluctuations, a stationary result can be obtained with $\Delta_2 t = 60$ min.

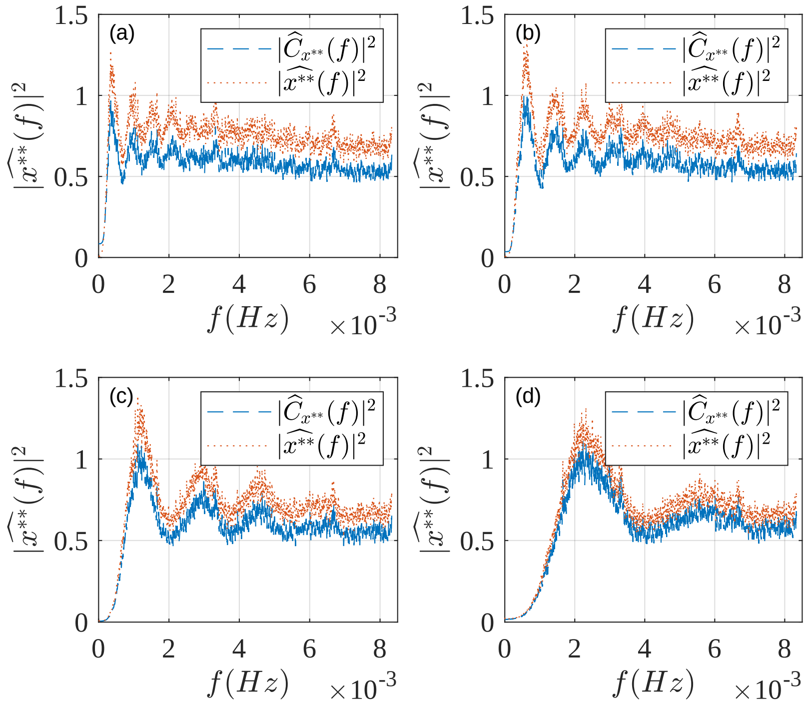


FIGURE 5.4: Stationarity test with S&P500 data from Feb 24th, 2020 to Dec 31st, 2023. (a) regularization window of 60 min. (b) regularization window of 40 min. (c) regularization window of 20 min. (d) regularization window of 10 min.

## 5.4 Discussion

In the earlier work of Stărică and Granger (Stărică and Granger 2005) they carried out a detailed analysis of the period 1957 - 2000 as they had found this was a particularly 'simple' interval in the history of the S&P500. In this 47-year period, they established that the absolute log-returns of the S&P500 was an i.i.d., non-stationary random process with time-varying unconditional variance. The model is indeed quite simple, the absolute log-returns are given by a well-studied diffusion model:

$$X(t) = \mu(t) + \sigma(t)\epsilon_t \tag{5.11}$$

that had used a test statistic given by:

$$T = \frac{X(t) - \mu(t)}{\sigma(t)} \tag{5.12}$$

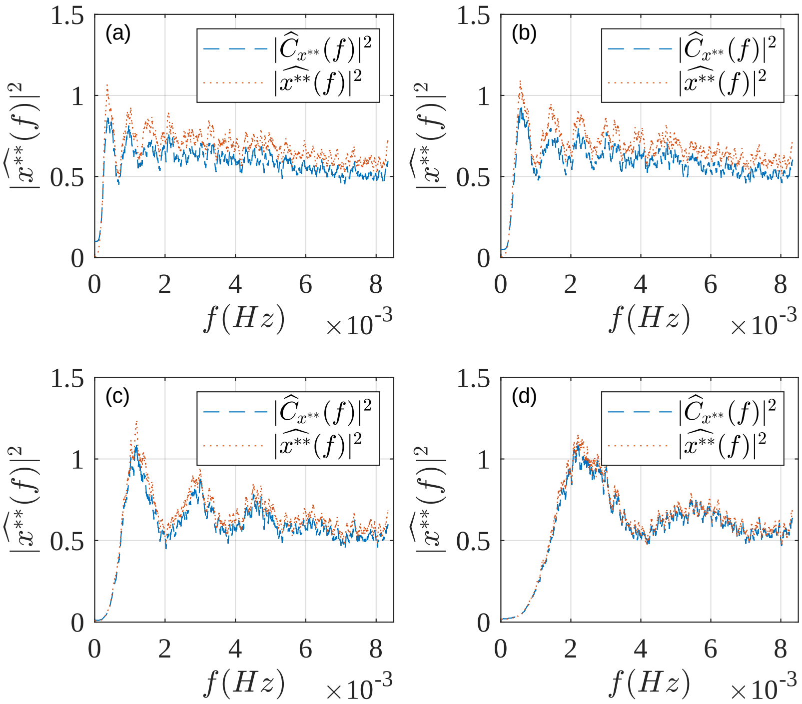


FIGURE 5.5: Stationarity test with S&P500 data from Feb 24st, 2020 to Dec 31st, 2020. (a) regularization window of 60 min. (b) regularization window of 40 min. (c) regularization window of 20 min. (d) regularization window of 10 min.

See eq. 17 in (Stărică and Granger 2005), c.f. the standard score normalization of price returns in eq. 5.7 above.

While the current study did not take advantage of the test score to validate a specific model, what it does do is standardize the distribution with an estimated time-varying mean and variance $\mu(\Delta_1 t)$ and $\sigma(\Delta_2 t)$ where $\Delta_i t$ indicates the width of the time window over which these terms are estimated (recall that $\Delta_1 t$ removes the trend, while $\Delta_2 t$ attempts to make the time series WSP). This provides an extra degree of freedom over the Stărică and Granger method while the data used provides a temporal resolution that was not possible using their inter-day data. What we have demonstrated here is a novel approach to understanding the 'complexity' of a univariate time series by seeking the maximum window size (if it exists) that allows the time series to be brought into a stationary state: the shorter this window, the more heterogeneous the time series is. Further work will develop this approach into a more

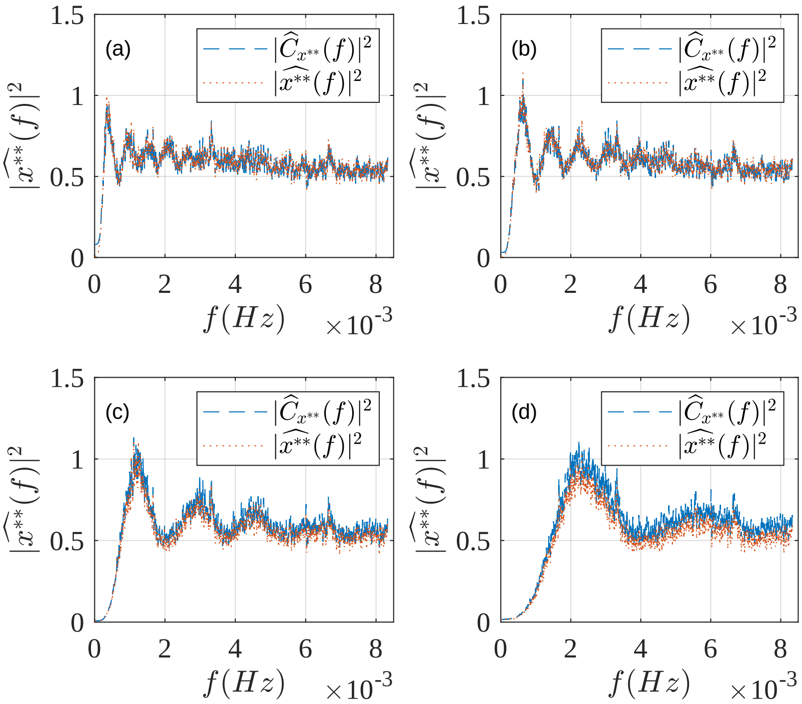


FIGURE 5.6: Stationarity test with S&P500 data from Jan 4th, 2021 to Dec 31st, 2023. (a) regularization window of 60 min. (b) regularization window of 40 min. (c) regularization window of 20 min. (d) regularization window of 10 min.

complete analytical methodology that we believe has shown here some considerable promise as a tool.

## 5.A Time window for detrending

In this chapter, when performing the detrending process, we tested with different detrending window sizes for $\Delta_1 t$ from a small time window of 1 week to the optimal time window of 1 year found in Chapter 2, and tested the detrended price return for stationarity. Results show that changing $\Delta_1 t$ does not affect the testing results of stationarity. Our results present that $\Delta_2 t$ is more sensitive to the stationarity test. Thus in this chapter, we used the detrending window size $\Delta_1 t = 1$ week and used various normalization windows for $\Delta_2 t$.

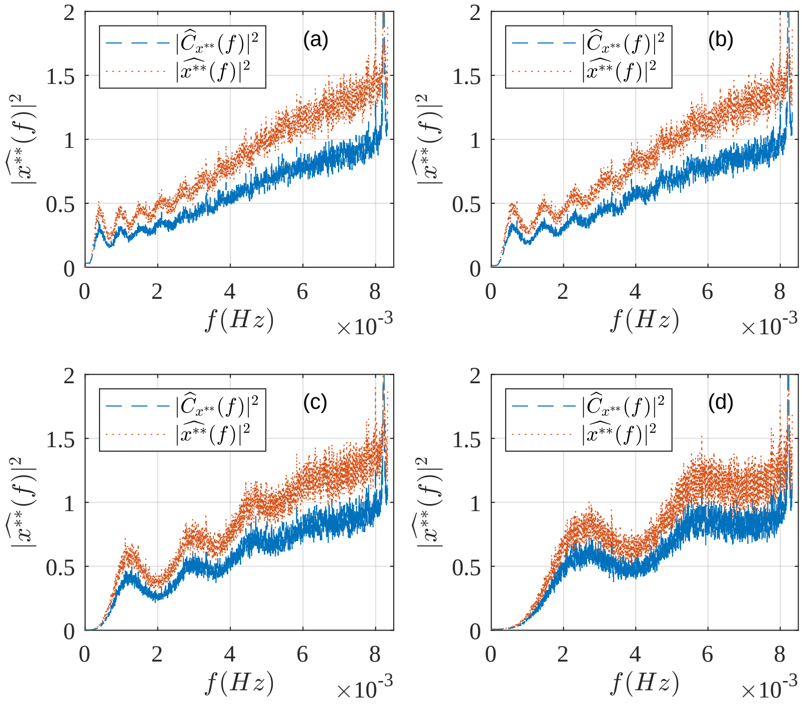


FIGURE 5.7: Stationarity test with Bitcoin data from Apr 2nd, 2019 to Dec 31st, 2020. (a) regularization window of 60 min. (b) regularization window of 40 min. (c) regularization window of 20 min. (d) regularization window of 10 min.

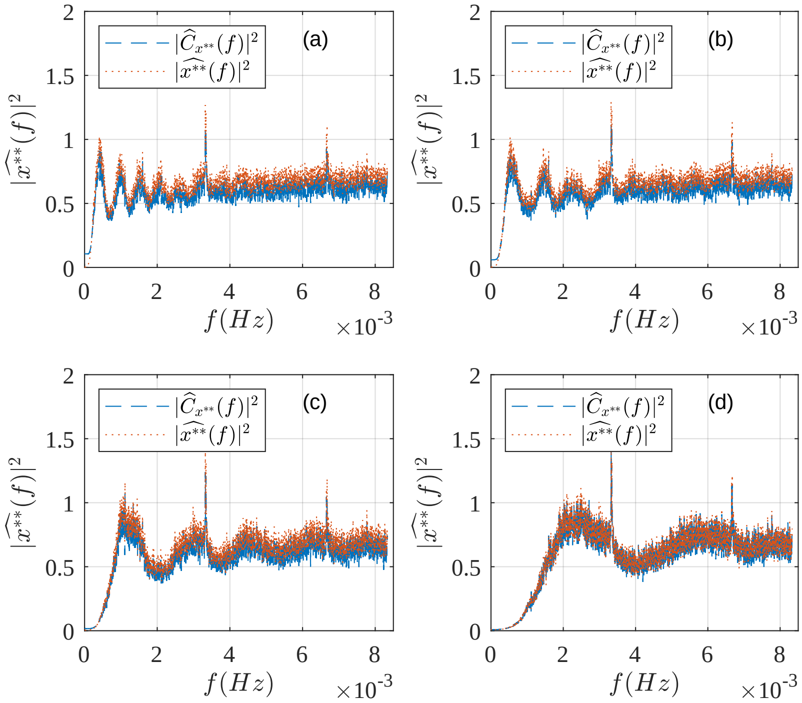


FIGURE 5.8: Stationarity test with Bitcoin data from Jan 1st, 2021 to May 3rd, 2022. (a) regularization window of 60 min. (b) regularization window of 40 min. (c) regularization window of 20 min. (d) regularization window of 10 min.

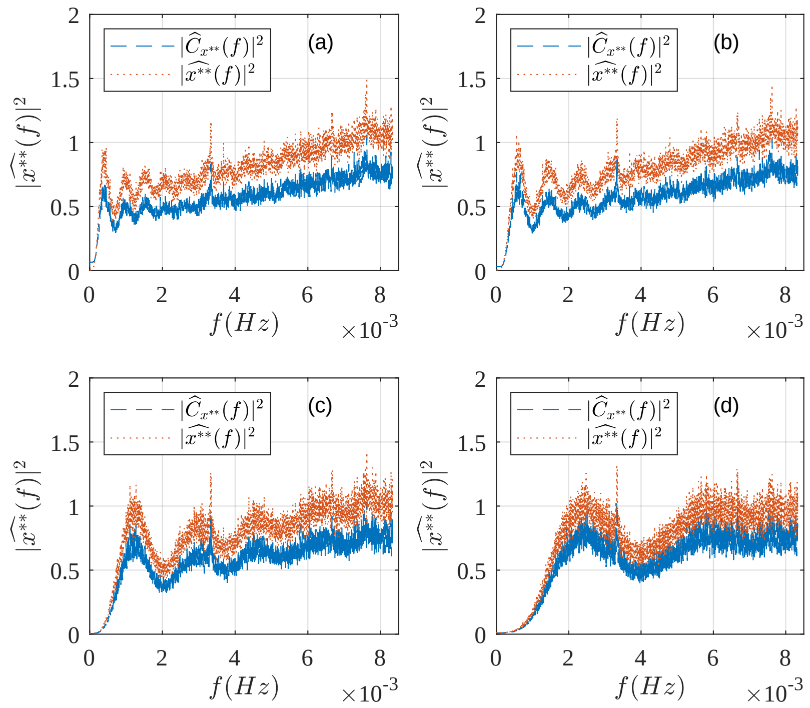


FIGURE 5.9: Stationarity test with Bitcoin data from May 4th, 2022 to Dec 31st, 2023. (a) regularization window of 60 min. (b) regularization window of 40 min. (c) regularization window of 20 min. (d) regularization window of 10 min.

CHAPTER 6

# Conclusions and Future Work

This thesis analyzed the univariate time series of both the conventional market, the S&P500, and the Bitcoin cryptocurrency. We examined the detrended price return in all chapters and extended the analysis to the normalized price return in Chapter 2 and 5 for the stationary test. We applied the detrending process to both time series to decompose the trend and the noise. The optimal time window for detrending used in this thesis varies. In Chapter 2, we determined the time window based on the kurtosis of the time series and found 13 months to be the optimal time window for the S&P500. We rounded the optimal window to one year and used this window size for the analysis in Chapter 2 and 4 for the S&P500. For Bitcoin, the optimal time window for detrending is one week, determined by the best convergence of the detrended PDF to a Gaussian distribution at large times, and this window size is used in each chapter of the thesis. Later in Chapter 5, we found that the size of the detrending window is less critical to the stationarity of the detrended price return, and we used a one-week detrending window for both time series. Moreover, in Chapter 2 and 3, a rolling standard deviation of a one-hour window is used. Larger window sizes were tested; however, this window size was chosen because the literature shows that the highest volume of options trading occurs within a one-hour period. Therefore, the standard deviation is captured before it dissipates. We used a $q$-Gaussian distribution to describe the PDF of price return for both markets, and the power-law tails are measured by the slope of the linear fittings in the log-log scale throughout the thesis. For both markets, the $q$ value for simple price returns is around 1.7, and for detrended price returns, the value drops to approximately $q = 1.4$. Multifractal detrending fluctuation analysis (MF-DFA) was performed for both time series, and both markets are multifractal, with a Hurst exponent under but close to 0.5. The Hurst exponent is also obtained from the slope of the height of the PDFs for Bitcoin, and the result agrees with the MF-DFA findings. We developed an analytical connection between $H$ and the root square of mean-squared displacement to classify anomalous diffusion regimes directly from PDF. In terms of stationarity, the S&P500 presents a higher level of stationarity than Bitcoin on local scales.

Developing an appropriate model to describe the statistical characteristics and estimate the future properties of a market has been a continuous area of interest. For over a century, consistent attempts were made to analyze univariate financial time series, leading to various models aiming to describe the evolution of financial markets over time.

This research explored the statistical analysis of univariate time series in financial markets, with a specific focus on comparing traditional markets represented by the S&P500 index with the emerging and evolving landscape of digital assets, namely Bitcoin. We qualitatively investigated the statistical characteristics of Bitcoin price return and compared them to the observations in the S&P500. The results revealed that despite the market formation and structure of cryptocurrency being very different from conventional markets, they share similar stylized facts. This convergence of statistical characteristics between digital assets and traditional markets provided evidence of the maturation of the cryptocurrency market and its potential integration into broader financial systems.

This thesis demonstrated the applicability of the $q$-Gaussian distribution from a financial economic perspective. Compared to the Gaussian distribution, Lévy-stable distribution, and fractional Brownian motion model, the $q$-Gaussian distribution is a more suitable model to describe the evolution of the market due to its ability to capture the heavy-tailed and weakly correlated features in price returns. We proposed governing equations for the markets, considering that the time series can be decomposed into a deterministic trend and stochastic fluctuations. By deriving solutions to these governing equations, we developed the $q$-Gaussian diffusion process with time-varying exponents. The $q$-Gaussian diffusion process is characterized by a fractional, non-linear diffusion equation with two exponents: the Hurst exponent ($H$), which defines the fractionality and accounts for anomalous behavior and autocorrelation, and the $q$-exponents that define the non-linearity of the diffusion and contribute to the heavy-tailed distribution. These solutions have denoted their effectiveness in capturing the underlying mechanisms driving price movements in both conventional and digital markets, supporting current developments in financial modeling.

Furthermore, by exploring non-stationary characteristics in the time series, we found that the extent to which stationarity holds shifts with time and is affected by exogenous events. In the pre-Covid period for the S&P500, stationarity can be achieved globally by removing the trend and volatility in the price return. However, the S&P500 in the post-pandemic period presents stationarity only on a localized scale, indicating that the market is still recovering from the crisis. For Bitcoin, temporal variations in stationarity are also observed. Examining stationarity in financial time series provides insight into a better understanding of market dynamics.

This thesis examined both the S&P500 price index and Bitcoin. A typical issue in dealing with indices, such as the S&P 500, is the problem of how the night gaps or weekends are considered. In Chapter 2 and 5 of this thesis, we used all the data available from the database. The dataset records both active trading periods and some inactive trading periods at the beginning and the end of a trading day. In Chapter 4, we removed the data from the inactive trading period (when a price change is less than 0.1 USD) and only worked with the dataset from the active trading periods. Whereas Bitcoin runs 24/7, so the dataset is continuously recorded without gaps. Future work could expand the analysis to other financial markets and assets for a thorough comparison.

In this thesis, we consider the $q$-Gaussian diffusion process within the range of $q \in (1, 3)$. However, for $q \in (5/3, 3)$, the solution to the $q$-Gaussian diffusion diverges and exhibits infinite variance. This issue can be mitigated by adding a non-symmetric term $(\beta' x^3)$ and a positive term $(\beta'' x^4)$ to the normalized $q$-Gaussian distribution. The introduction of asymmetry is crucial as it can lead to entropy optimization. Consequently, future research could focus on how this additional term could be beneficial when applying the $q$-Gaussian distribution model to financial markets.

We decomposed the univariate time series of financial market price fluctuations into deterministic trend variation and a stochastic process, with a greater focus on the stochastic component.

We identified changes in market dynamics related to external crises and revealed localized stationarity. Subsequent research could explore the deterministic component of the time series. Recognizing financial markets as complex systems with numerous relevant influences, it is intriguing to distinguish chaoticity from regularity in deterministic dynamical systems. Moreover, potential future research may aim to examine how market dynamics evolve in response to both exogenous and endogenous events.

Furthermore, we have provided empirical evidence that the financial price returns can achieve localized stationarity when the trend and volatility are removed. The stationarity test used in this thesis requires a Fourier transform, and potential future work can explore the possibility of using a $q$-Fourier transform for the analysis. Subsequent research could also focus on building an analytical framework for modeling the time-varying dynamics of market returns. Moreover, as volatility can be connected with the autocorrelation function of a time series using the Hurst exponent, it is promising to explore how the autocorrelation function may be different in segmented time series and how the Hurst exponent evolves in different time periods.

As we conclude, this study not only contributes to the academic understanding of financial markets but also provides practical implications for investors, policymakers, and stakeholders navigating the complexities of contemporary financial systems. As digital assets continue to gain prominence, these findings can serve as a reference for future research and decision-making in an evolving financial landscape.

## 6.1 Future outlook

Bitcoin was the first cryptocurrency introduced, holding the largest market share in the rapidly expanding cryptocurrency market. The debate over categorizing Bitcoin as a currency or an asset gained traction with its increasing prominence. Bitcoin price exhibits high volatility, closely related to its substantial market capitalization, which has been further witnessed by the significant rise since the beginning of 2024. Our findings indicate that Bitcoin behaves more like an asset and is not yet ready to replace fiat currency. The statistical characteristics of Bitcoin change significantly in different periods, indicating evolving market dynamics that point towards market inefficiency.

Furthermore, the results in this thesis support that Bitcoin is still in its infancy and has not yet reached maturity. Comparing the statistical characteristics of digital assets to mature markets such as the S&P500 provides opportunities to develop techniques that can be used to understand how the future of mature digital asset markets could unfold. These techniques can be applied to various types of digital assets, from cryptocurrency to non-fungible tokens (NFTs), potentially contributing to the development of modern digital asset management services, risk management, and portfolio optimization.

The mutual cross-fertilization between economics and other disciplines has led to the development of robust empirical observations, diverse models, and theories in understanding financial markets. The methodology used in this thesis aligns with approaches that conceptualize financial markets as complex adaptive systems. Describing markets in terms of emergence, scale-invariance, and universality allows for a better understanding of them at macroscopic levels, characterized by stylized facts and statistical regularities. This interdisciplinary perspective recognizes the need for a systemic and complex approach to economic and financial systems. Combining financial economics analysis with complex systems analysis can contribute to theories and models suitable for adaptive evolutionary systems in areas such as ecology, cognitive systems, and network science. We argue that a new science of economic and financial systems should integrate findings from various scientific fields to pave the way for a multidisciplinary complex systems science of financial markets.

# Bibliography


Adams, E Eric and Gelhar, Lynn W (1992). ‘Field study of dispersion in a heterogeneous aquifer: 2. Spatial moments analysis’. *Water Resources Research* 28.12, pp. 3293–3307.

Addison, Paul S. (1997). *Fractals and chaos: an illustrated course*. Philadelphia, Pa: Institute of Physics Pub. ISBN: 0750304006.

Ahn, Kwangwon, Choi, MooYoung, Dai, Bingcun, Sohn, Sungbin and Yang, Biao (2018). ‘Modeling stock return distributions with a quantum harmonic oscillator’. *EPL (Europhysics Letters)* 120.3, p. 38003.

Alessio, E, Carbone, A, Castelli, G and Frappietro, V (2002). ‘Second-order moving average and scaling of stochastic time series’. *The European Physical Journal B-Condensed Matter and Complex Systems* 27.2, pp. 197–200.

Ali, Ahmed H and AL-Qazaz, Qutaiba N Nayef (2020). ‘Fractional Brownian motion inference of multivariate stochastic differential equations’. *Periodicals of Engineering and Natural Sciences* 8.1, pp. 464–480.

Aljethi, Reem Abdullah and Kılıçman, Adem (2023). ‘Derivation of the Fractional Fokker–Planck Equation for Stable Lévy with Financial Applications’. *Mathematics* 11.5, p. 1102. ISSN: 2227-7390. DOI: 10.3390/math11051102. URL: https://dx.doi.org/10.3390/math11051102.

Alkahtani, Badr Saad T, Koca, Ilknur and Atangana, Abdon (2016). ‘A novel approach of variable order derivative: Theory and Methods’. *J. Nonlinear Sci. Appl* 9.6, pp. 4867–4876.

Almeida, Ricardo (2017). ‘Caputo–Hadamard fractional derivatives of variable order’. *Numerical Functional Analysis and Optimization* 38.1, pp. 1–19.

Almeida, Ricardo, Guzowska, Małgorzata and Odzijewicz, Tatiana (2016). ‘A remark on local fractional calculus and ordinary derivatives’. *Open Mathematics* 14.1, pp. 1122–1124.

Alonso-Marroquin, Fernando, Arias-Calluari, Karina, Harré, Michael, Najafi, Morteza N and Herrmann, Hans J (2019). 'Q-Gaussian diffusion in stock markets'. *Physical Review E* 99.6, p. 062313.

Anderson, Johan and Moradi, Sara (2018). 'Anomalous diffusion by the fractional Fokker-Planck equation and Lévy stable processes'. *Fractional dynamics, anomalous transport and plasma science*. Springer, pp. 77–92.

Andersson, Jonas (2001). 'On the Normal Inverse Gaussian Stochastic Volatility Model'. *Journal of Business & Economic Statistics* 19.1, pp. 44–54. ISSN: 0735-0015. DOI: 10.1198/07350010152472607. URL: https://dx.doi.org/10.1198/07350010152472607.

Arias Calluari, Karina (2014). 'Methods for forecasting stock markets'. PhD thesis. The University of Sydney.

Arias-Calluari, Karina, Alonso-Marroquin, Fernando and Harré, Michael S (2018). 'Closed-form solutions for the Lévy-stable distribution'. *Physical Review E* 98.1, p. 012103.

Arias-Calluari, Karina, Alonso-Marroquin, Fernando, Najafi, Morteza N and Harré, Michael (2021). 'Methods for forecasting the effect of exogenous risks on stock markets'. *Physica A: Statistical Mechanics and its Applications* 568, p. 125587.

Arias-Calluari, Karina, Najafi, Morteza N, Harré, Michael S, Tang, Yaoyue and Alonso-Marroquin, Fernando (2022). 'Testing stationarity of the detrended price return in stock markets'. *Physica A: Statistical Mechanics and its Applications* 587, p. 126487. ISSN: 0378-4371. DOI: https://doi.org/10.1016/j.physa.2021.126487. URL: https://www.sciencedirect.com/science/article/pii/S0378437121007603.

Ariya, Kanyawut, Naktnasukanjn, Nathee, Rattanadamrongaksorn, Tanarat, Udomwong, Piyachat, Sokantika, Saronsad and Chakpitak, Nopasit (2020). 'Cryptocurrencies Asset Pricing Analysis: Evidence from Thailand markets'. *Proceedings - 2020 15th International Joint Symposium on Artificial Intelligence and Natural Language Processing, iSAI-NLP 2020*. DOI: 10.1109/iSAI-NLP51646.2020.9376813.

Atangana, Abdon (2015). 'On the stability and convergence of the time-fractional variable order telegraph equation'. *Journal of computational physics* 293, pp. 104–114.

Atangana, Abdon and Bildik, Necdet (2013). ‘The use of fractional order derivative to predict the groundwater flow’. *Mathematical Problems in Engineering* 2013.

Aue, Alexander, Norinho, Diogo Dubart and Hörmann, Siegfried (2015). ‘On the prediction of stationary functional time series’. *Journal of the American Statistical Association* 110.509, pp. 378–392.

Auer, Raphael, Haslhofer, Bernhard, Kitzler, Stefan, Saggese, Pietro and Victor, Friedhelm (2023). *The Technology of Decentralized Finance (DeFi)*. Bank for International Settlements, Monetary and Economic Department.

Ausloos, Marcel (2012). ‘Generalized Hurst exponent and multifractal function of original and translated texts mapped into frequency and length time series’. *Physical Review E* 86.3, p. 031108.

Babirath, Julia and Schmitl, Rainer (2020). ‘Forecasting based on spectral time series analysis: prediction of the Aurubis stock price’. *Investment Management & Financial Innovations* 17.4, p. 215.

Bachelier, L. (1900). ‘Théorie de la spéculation’. *Annales scientifiques de l’École Normale Supérieure* 17, pp. 21–86. DOI: 10.24033/asens.476. URL: https://doi.org/10.24033/asens.476.

Bahri, FMZ and Sharples, JJ (n.d.). ‘Sensitivity of the Empirical Mode Decomposition to Interpolation Methodology and Data Non-stationarity’. *Environmental Modeling & Assessment* (), pp. 1–20.

Bariviera, Aurelio F., Basgall, María José, Hasperué, Waldo and Naiouf, Marcelo (2017). ‘Some stylized facts of the Bitcoin market’. *Physica A: Statistical Mechanics and its Applications* 484, pp. 82–90. ISSN: 0378-4371.

Barlas, Yaman (1990). ‘An autocorrelation function test for out put validation’. *Simulation* 55.1, pp. 7–16.

Barles, Guy and Soner, Halil Mete (1998). ‘Option pricing with transaction costs and a nonlinear Black-Scholes equation’. *Finance and Stochastics* 2.4, pp. 369–397.

Bassler, Kevin E., McCauley, Joseph L. and Gunaratne, Gemunu H. (2007). ‘Nonstationary increments, scaling distributions, and variable diffusion processes in financial markets’.

*Proceedings of the National Academy of Sciences* 104.44, pp. 17287–17290. ISSN: 0027-8424. DOI: 10.1073/pnas.0708664104. URL: https://dx.doi.org/10.1073/pnas.0708664104.

Baur, Dirk G., Lee, Adrian D. and Hong, KiHoon (2015). 'Bitcoin: Currency or Investment?' URL: https://api.semanticscholar.org/CorpusID:166527842.

Beran, Jan (1994). *Statistics for long-memory processes*. Vol. 61. CRC press.

Bhowmik, Roni and Wang, Shouyang (2020). 'Stock market volatility and return analysis: A systematic literature review'. *Entropy* 22.5, p. 522.

Bielinskyi, Andrii, Semerikov, Serhii, Solovieva, Viktoria and Soloviev, Vladimir (2019a). 'Levy's stable distribution for stock crash detecting'. *EDP Sciences*.

Bielinskyi, Andrii, Soloviev, Vladimir, Semerikov, Serhii and Solovieva, Viktoria (2019b). 'Detecting stock crashes using Levy distribution'. *CEUR Workshop Proceedings*.

Björk, Tomas and Hult, Henrik (2005). 'A note on Wick products and the fractional Black-Scholes model'. *Finance and Stochastics* 9.2, pp. 197–209.

Black, Fischer and Scholes, Myron (1973). 'The Pricing of Options and Corporate Liabilities'. *Journal of Political Economy* 81.3, pp. 637–654. ISSN: 00223808, 1537534X. URL: http://www.jstor.org/stable/1831029.

Böhme, Rainer, Christin, Nicolas, Edelman, Benjamin and Moore, Tyler (2015). 'Bitcoin: Economics, Technology, and Governance'. *Journal of Economic Perspectives* 29.2, pp. 213–238. ISSN: 0895-3309. DOI: 10.1257/jep.29.2.213. URL: https://dx.doi.org/10.1257/jep.29.2.213.

Bollerslev, Tim, Engle, Robert F and Nelson, Daniel B (1994). 'ARCH models'. *Handbook of econometrics* 4, pp. 2959–3038. ISSN: 1573-4412.

Bologna, Mauro, Tsallis, Constantino and Grigolini, Paolo (2000). 'Anomalous diffusion associated with nonlinear fractional derivative Fokker-Planck-like equation: Exact time-dependent solutions'. *Physical Review E* 62.2, p. 2213.

Borland, Lisa (1998). 'Microscopic dynamics of the nonlinear Fokker-Planck equation: A phenomenological model'. *Physical Review E* 57.6, pp. 6634–6642. ISSN: 1063-651X. DOI: 10.1103/physreve.57.6634. URL: https://dx.doi.org/10.1103/physreve.57.6634.

Borland, Lisa (2002a). 'A theory of non-Gaussian option pricing'. *Quantitative Finance* 2.6, pp. 415–431. ISSN: 1469-7688. DOI: 10.1080/14697688.2002.0000009. URL: https://doi.org/10.1080/14697688.2002.0000009.

— (2002b). 'Option pricing formulas based on a non-Gaussian stock price model'. *Physical review letters* 89.9, p. 098701.

Borland, Lisa and Bouchaud, Jean-Philippe (2004). 'A non-Gaussian option pricing model with skew'. *Quantitative Finance* 4.5. doi: 10.1080/14697680400008684, pp. 499–514. ISSN: 1469-7688. DOI: 10.1080/14697680400008684. URL: https://www.tandfonline.com/doi/abs/10.1080/14697680400008684.

Box, George E. P. (2013). *Time series analysis : forecasting and control.* eng. 4th ed. Wiley Series in Probability and Statistics. Hoboken: Wiley. ISBN: 9781118210871.

Box, George EP, Jenkins, Gwilym M, Reinsel, Gregory C and Ljung, Greta M (2015). *Time series analysis: forecasting and control*. John Wiley & Sons.

Brito, Jerry, Shadab, Houman and Castillo, Andrea (2014). 'Bitcoin Financial Regulation: Securities, Derivatives, Prediction Markets, and Gambling'. *Columbia Science and Technology Law Review* 16.1, pp. 144–221. URL: https://heinonline.org/HOL/P?h=hein.journals/cstlr16&i=144%20https://heinonline.org/HOL/PrintRequest?handle=hein.journals/cstlr16&collection=journals&div=6&id=144&print=section&sction=6.

Brown, Robert (1828a). 'Mikroskopische Beobachtungen über die im Pollen der Pflanzen enthaltenen Partikeln, und über das allgemeine Vorkommen activer Molecüle in organischen und unorganischen Körpern'. *Annalen der Physik* 90.10, pp. 294–313.

— (1828b). 'XXVII. A brief account of microscopical observations made in the months of June, July and August 1827, on the particles contained in the pollen of plants; and on the general existence of active molecules in organic and inorganic bodies'. *The philosophical magazine* 4.21, pp. 161–173.

Bucsa, Gigel, Haven, Emmanuel, Jovanovic, Franck and Schinckus, Christophe (2014). 'The practical use of the general formula of the optimal hedge ratio in option pricing: an example of the generalized model of an exponentially truncated Levy stable distribution'. *Theoretical Economics Letters* 4.9, pp. 760–66.

Bulla, Jan and Bulla, Ingo (2006). 'Stylized facts of financial time series and hidden semi-Markov models'. *Computational Statistics & Data Analysis* 51.4, pp. 2192–2209. ISSN: 0167-9473. DOI: https://doi.org/10.1016/j.csda.2006.07.021. URL: https://www.sciencedirect.com/science/article/pii/S0167947306002374.

Buonocore, RJ, Brandi, G, Mantegna, RN and Di Matteo, T (2019). 'On the interplay between multiscaling and stock dependence'. *Quantitative Finance*, pp. 1–13.

Campbell, John Y., Lo, Andrew W. and MacKinlay, A.Craig (1997). 'Introduction'. *The Econometrics of Financial Markets*. Princeton University Press, pp. 3–26. ISBN: 9780691043012. URL: http://www.jstor.org/stable/j.ctt7skm5.6 (visited on 20/02/2024).

Cao, Wen, Hurvich, Clifford and Soulier, Philippe (Sept. 2017). 'Drift in Transaction-Level Asset Price Models'. *Journal of Time Series Analysis* 38.5, pp. 769, 790. ISSN: 0143-9782.

Caporale, Guglielmo Maria, Gil-Alana, Luis A. and Plastun, Alex (2018). 'Persistence in the Cryptocurrency Market'. *SSRN Electronic Journal*. ISSN: 1556-5068. DOI: 10.2139/ssrn.3126040. URL: https://dx.doi.org/10.2139/ssrn.3126040.

Carcione, José M, Sanchez-Sesma, Francisco J, Luzón, Francisco and Gavilán, Juan J Perez (2013). 'Theory and simulation of time-fractional fluid diffusion in porous media'. *Journal of Physics A: Mathematical and Theoretical* 46.34, p. 345501.

Carnero, M. A. (2004). 'Persistence and Kurtosis in GARCH and Stochastic Volatility Models'. *Journal of Financial Econometrics* 2.2, pp. 319–342. ISSN: 1479-8409. DOI: 10.1093/jjfinec/nbh012. URL: https://dx.doi.org/10.1093/jjfinec/nbh012.

Chakraborti, Anirban, Toke, Ioane Muni, Patriarca, Marco and Abergel, Frédéric (2011). 'Econophysics review: I. Empirical facts'. *Quantitative Finance* 11.7, pp. 991–1012. ISSN: 1469-7688. DOI: 10.1080/14697688.2010.539248. URL: https://dx.doi.org/10.1080/14697688.2010.539248.

Chang, Chuo (2020). 'Dynamic correlations and distributions of stock returns on China's stock markets'. *Journal of Applied Finance and Banking* 10.1, pp. 107–140.

Chechkin, Aleksei V, Gorenflo, R and Sokolov, Igor M (2005). 'Fractional diffusion in inhomogeneous media'. *Journal of Physics A: Mathematical and General* 38.42, p. L679.

Chen, Feier, Tian, Kang, Ding, Xiaoxu, Miao, Yuqi and Lu, Chunxia (2016a). 'Finite-size effect and the components of multifractality in transport economics volatility based on multifractal detrending moving average method'. *Physica A: Statistical Mechanics and its Applications* 462, pp. 1058–1066. ISSN: 0378-4371. DOI: https://doi.org/10.1016/j.physa.2016.06.101. URL: https://www.sciencedirect.com/science/article/pii/S0378437116303764.

Chen, Wenting, Yan, Bowen, Lian, Guanghua and Zhang, Ying (2016b). 'Numerically pricing American options under the generalized mixed fractional Brownian motion model'. *Physica A: Statistical Mechanics and its Applications* 451, pp. 180–189.

Cheng, Changqing, Sa-Ngasoongsong, Akkarapol, Beyca, Omer, Le, Trung, Yang, Hui, Kong, Zhenyu and Bukkapatnam, Satish TS (2015). 'Time series forecasting for nonlinear and non-stationary processes: a review and comparative study'. *Iie Transactions* 47.10, pp. 1053–1071.

Chua, Kuang Chua, Chandran, Vinod, Acharya, U Rajendra and Lim, Choo Min (2010). 'Application of higher order statistics/spectra in biomedical signals—A review'. *Medical engineering & physics* 32.7, pp. 679–689.

Ciaian, Pavel, Rajcaniova, Miroslava and Kancs, d'Artis (2018). 'Virtual relationships: Short- and long-run evidence from BitCoin and altcoin markets'. *Journal of International Financial Markets, Institutions and Money* 52, pp. 173–195. ISSN: 1042-4431. DOI: https://doi.org/10.1016/j.intfin.2017.11.001. URL: https://www.sciencedirect.com/science/article/pii/S1042443117302858.

Clara-Rahola, Joaquim, Puertas, Antonio M, Sanchez-Granero, Miguel Angel, Trinidad-Segovia, Juan E and Nieves, F Javier de las (2017). 'Diffusive and arrested-like dynamics in currency exchange markets'. *Physical review letters* 118.6, p. 068301.

Conrad, Christian, Custovic, Anessa and Ghysels, Eric (2018). 'Long- and Short-Term Cryptocurrency Volatility Components: A GARCH-MIDAS Analysis'. *Journal of Risk and Financial Management* 11.2, p. 23. ISSN: 1911-8074. DOI: 10.3390/jrfm11020023. URL: https://dx.doi.org/10.3390/jrfm11020023.

Cont, R. (2001). 'Empirical properties of asset returns: stylized facts and statistical issues'. *Quantitative Finance* 1.2. doi: 10.1080/713665670, pp. 223–236. ISSN: 1469-7688. DOI: 10.1080/713665670. URL: https://doi.org/10.1080/713665670.

Cont, Rama. and Tankov, Peter. (2004). *Financial modelling with jump processes*. eng. Chapman & Hall/CRC financial mathematics series. Boca Raton, Fla: Chapman & Hall/CRC. ISBN: 9780203485217.

Corbet, Shaen, Lucey, Brian, Urquhart, Andrew and Yarovaya, Larisa (2019). 'Cryptocurrencies as a financial asset: A systematic analysis'. *International Review of Financial Analysis* 62, pp. 182–199. ISSN: 1057-5219. DOI: 10.1016/j.irfa.2018.09.003. URL: https://dx.doi.org/10.1016/j.irfa.2018.09.003.

Corporation, Thomson Reuters (2020). *Products and services/News and data*. URL: https://www.thomsonreuters.com/en/contact-us.html (visited on 05/08/2020).

Corporation, Zen Investor (2012). *A History Of Market Crashes*. URL: https://www.zeninvestor.org/history-market-crashes/ (visited on 05/08/2020).

Cremaschini, Alessandro, Punzo, Antonio, Martellucci, Eliano and Maruotti, Antonello (2023). 'On stylized facts of cryptocurrencies returns and their relationship with other assets, with a focus on the impact of COVID-19'. *Applied Economics* 55.32, pp. 3675–3688. ISSN: 0003-6846. DOI: 10.1080/00036846.2022.2117777. URL: https://dx.doi.org/10.1080/00036846.2022.2117777.

Crosby, Michael, Pattanayak, Pradan, Verma, Sanjeev and Kalyanaraman, Vignesh (2016). 'Blockchain technology: Beyond bitcoin'. *Applied Innovation* 2.6-10, p. 71.

Dahlhaus, Rainer (2012). 'Locally stationary processes'. *Handbook of statistics*. Vol. 30. Elsevier, pp. 351–413.

De Silva, Harindra, McMurran, Gregory M. and Miller, Megan N. (2017). '14 - Diversification and the Volatility Risk Premium'. *Factor Investing*. Ed. by Emmanuel Jurczenko. Elsevier, pp. 365–387. ISBN: 978-1-78548-201-4. DOI: https://doi.org/10.1016/B978-1-78548-201-4.50014-3. URL: https://www.sciencedirect.com/science/article/pii/B9781785482014500143.

De Sousa Filho, F. N. M., Silva, J. N., Bertella, M. A. and Brigatti, E. (2021). 'The Leverage Effect and Other Stylized Facts Displayed by Bitcoin Returns'. *Brazilian Journal of Physics*

51.3, pp. 576–586. ISSN: 0103-9733. DOI: 10.1007/s13538-020-00846-8. URL: https://dx.doi.org/10.1007/s13538-020-00846-8.

Di Paola, M and Pirrotta, A (2022). 'Fokker–Planck equation of the fractional Brownian motion'. *International Journal of Non-Linear Mechanics* 147, p. 104224.

Dickey, David A and Fuller, Wayne A (1979). 'Distribution of the estimators for autoregressive time series with a unit root'. *Journal of the American statistical association* 74.366a, pp. 427–431.

Einstein, Albert (1905). 'Über die von der molekularkinetischen Theorie der Wärme geforderte Bewegung von in ruhenden Flüssigkeiten suspendierten Teilchen'. *Annalen der physik* 4.

— (1908). 'The elementary theory of the Brownian motion'. *Zeitschrift für Elektrochemie und angewandte physikalische Chemie* 14, pp. 235–239.

— (1956). *Investigations on the Theory of the Brownian Movement*. Courier Corporation.

Eross, Andrea, McGroarty, Frank, Urquhart, Andrew and Wolfe, Simon (2019). 'The intraday dynamics of bitcoin'. *Research in International Business and Finance* 49, pp. 71–81. ISSN: 0275-5319. DOI: 10.1016/j.ribaf.2019.01.008. URL: https://dx.doi.org/10.1016/j.ribaf.2019.01.008.

Evertsz, Carl JG (1995). 'Fractal geometry of financial time series'. *Fractals* 3.03, pp. 609–616.

Fama, Eugene F. (1963). 'Mandelbrot and the Stable Paretian Hypothesis'. *The Journal of Business* 36.4, pp. 420–429. ISSN: 00219398, 15375374. URL: http://www.jstor.org/stable/2350971 (visited on 13/02/2024).

— (1970). 'Efficient Capital Markets: A Review of Theory and Empirical Work'. *The Journal of Finance* 25.2, pp. 383–417. ISSN: 00221082, 15406261. DOI: 10.2307/2325486. URL: http://www.jstor.org/stable/2325486.

Fang, Zhi-Wei, Sun, Hai-Wei and Wang, Hong (2020). 'A fast method for variable-order Caputo fractional derivative with applications to time-fractional diffusion equations'. *Computers & Mathematics with Applications* 80.5, pp. 1443–1458.

Fedotov, Sergei and Falconer, Steven (2012). 'Subdiffusive master equation with space-dependent anomalous exponent and structural instability'. *Physical Review E* 85.3, p. 031132.

Fernandes, Leonardo H. S., Bouri, Elie, Silva, José W. L., Bejan, Lucian and Araujo, Fernando H. A. de (2022). 'The resilience of cryptocurrency market efficiency to COVID-19 shock'. *Physica A: Statistical Mechanics and its Applications* 607, p. 128218. ISSN: 0378-4371. DOI: https://doi.org/10.1016/j.physa.2022.128218. URL: https://www.sciencedirect.com/science/article/pii/S0378437122007762.

Ferreira, Susana and Karali, Berna (2015). 'Do earthquakes shake stock markets?' *PloS one* 10.7, e0133319.

Frame, John D, Baldwin Jr, John M, Gocke, David J and Troup, Jeanette M (1970). 'Lassa fever, a new virus disease of man from West Africa'. *The American journal of tropical medicine and hygiene* 19.4, pp. 670–676.

Frank, Till Daniel (2005). *Nonlinear Fokker-Planck equations: fundamentals and applications*. Springer Science & Business Media.

Gao, JB, Cao, Yinhe and Lee, Jae-Min (2003). 'Principal component analysis of 1/f$\alpha$ noise'. *Physics Letters A* 314.5-6, pp. 392–400.

Gardner, W (1978). 'Stationarizable random processes'. *IEEE Transactions on information theory* 24.1, pp. 8–22.

Gay-Balmaz, François and Holm, Darryl D (2018). 'Stochastic geometric models with non-stationary spatial correlations in Lagrangian fluid flows'. *Journal of nonlinear science* 28.3, pp. 873–904.

Gell-Mann, Murray and Tsallis, Constantino (2004). *Nonextensive entropy: interdisciplinary applications*. Oxford University Press.

Genç, Ekin (Mar. 2023). *How are institutions and companies investing in crypto?* URL: https://www.coindesk.com/learn/how-are-institutions-and-companies-investing-in-crypto/.

Gennes, Pierre Gilles de et al. (1976). 'La percolation: un concept unificateur'. *La recherche* 7.72, pp. 919–927.

Gharari, Fatemeh, Arias-Calluari, Karina, Alonso-Marroquin, Fernando and Najafi, Morteza N (2021). 'Space-time fractional porous media equation: Application on modeling of S&P500 price return'. *Physical Review E* 104.5, p. 054140.

Ghosh, Bikramaditya, Bouri, Elie, Wee, Jung Bum and Zulfiqar, Noshaba (2023). 'Return and volatility properties: Stylized facts from the universe of cryptocurrencies and NFTs'. *Research in International Business and Finance* 65, p. 101945. ISSN: 0275-5319. DOI: https://doi.org/10.1016/j.ribaf.2023.101945. URL: https://www.sciencedirect.com/science/article/pii/S0275531923000715.

Gilding, BH and Peletier, LA (1976). 'On a class of similarity solutions of the porous media equation'. *Journal of mathematical analysis and applications* 55.2, pp. 351–364.

Giona, Massimiliano and Roman, H Eduardo (1992). 'Fractional diffusion equation for transport phenomena in random media'. *Physica A: Statistical Mechanics and its Applications* 185.1-4, pp. 87–97.

*Global Cryptocurrency Charts* (2023). https://coinmarketcap.com/charts/. Accessed: 2023-08-03.

Gnedenko, Boris Vladimirovich and Kolmogorov, Andreĭ. Nikolaevich. (1968). *Limit distributions for sums of independent random variables*. eng. Rev. Addison-Wesley series in statistics. Reading, Mass: Addison-Wesley.

Gneiting, Tilmann and Schlather, Martin (2004). 'Stochastic Models That Separate Fractal Dimension and the Hurst Effect'. *SIAM Review* 46.2, pp. 269–282. ISSN: 0036-1445. DOI: 10.1137/s0036144501394387. URL: https://dx.doi.org/10.1137/s0036144501394387.

Gopikrishnan, Parameswaran, Meyer, Martin, Amaral, LA Nunes and Stanley, H Eugene (1998). 'Inverse cubic law for the distribution of stock price variations'. *The European Physical Journal B-Condensed Matter and Complex Systems* 3.2, pp. 139–140. ISSN: 1434-6028.

Gopikrishnan, Parameswaran, Plerou, Vasiliki, Amaral, Luis A Nunes, Meyer, Martin and Stanley, H Eugene (1999). 'Scaling of the distribution of fluctuations of financial market indices'. *Physical Review E* 60.5, p. 5305.

Gorry, Peter A (1990). 'General least-squares smoothing and differentiation by the convolution (Savitzky-Golay) method'. *Analytical Chemistry* 62.6, pp. 570–573.

Granero, MA Sánchez, Segovia, JE Trinidad and Pérez, J García (2008). 'Some comments on Hurst exponent and the long memory processes on capital markets'. *Physica A: Statistical Mechanics and its applications* 387.22, pp. 5543–5551.

Gross, Andrew, Hemker, Jeff, Hoelscher, Jamie and Reed, Brad (2017). 'The role of secondary sources on the taxation of digital currency (Bitcoin) before IRS guidance was issued'. *Journal of Accounting Education* 39, pp. 48–54. ISSN: 0748-5751. DOI: https://doi.org/10.1016/j.jaccedu.2017.02.001. URL: https://www.sciencedirect.com/science/article/pii/S0748575116302159.

Gu, Gao-Feng and Zhou, Wei-Xing (2006). 'Detrended fluctuation analysis for fractals and multifractals in higher dimensions'. *Physical Review E* 74.6, p. 061104.

Gu, Gao-Feng, Zhou, Wei-Xing et al. (2010). 'Detrending moving average algorithm for multifractals'. *Physical Review E* 82.1, p. 011136.

Gu, Rongbao, Chen, Hongtao and Wang, Yudong (2010). 'Multifractal analysis on international crude oil markets based on the multifractal detrended fluctuation analysis'. *Physica A: Statistical Mechanics and its Applications* 389.14, pp. 2805–2815. ISSN: 0378-4371. DOI: https://doi.org/10.1016/j.physa.2010.03.003. URL: https://www.sciencedirect.com/science/article/pii/S0378437110002013.

Guigas, Gernot and Weiss, Matthias (2008). 'Sampling the cell with anomalous diffusion—the discovery of slowness'. *Biophysical journal* 94.1, pp. 90–94.

Guiñón, José Luis, Ortega, Emma, García-Antón, José and Pérez-Herranz, Valentín (2007). 'Moving average and Savitzki-Golay smoothing filters using Mathcad'. *Papers ICEE* 2007, pp. 1–4.

Haber, Stuart and Stornetta, W. Scott (1991). 'How to Time-Stamp a Digital Document'. *Advances in Cryptology-CRYPTO' 90*. Ed. by Alfred J. Menezes and Scott A. Vanstone. Springer Berlin Heidelberg, pp. 437–455. ISBN: 978-3-540-38424-3.

Hansun, S. (2013). 'A new approach of moving average method in time series analysis'. *2013 Conference on New Media Studies (CoNMedia)*, pp. 1–4.

Hantush, Mahdi Salih and Jacob, C Ei (1955). 'Non-steady radial flow in an infinite leaky aquifer'. *Eos, Transactions American Geophysical Union* 36.1, pp. 95–100.

Harré, M and Bossomaier, Terence (2009). 'Phase-transition–like behaviour of information measures in financial markets'. *Europhysics Letters* 87.1, p. 18009.

Harré, Michael (2015). 'Entropy and transfer entropy: the Dow Jones and the build up to the 1997 Asian crisis'. *Proceedings of the International Conference on Social Modeling and Simulation, plus Econophysics Colloquium 2014*. Springer International Publishing, pp. 15–25.

Harré, Michael S (2022). 'Entropy, Economics, and Criticality'. *Entropy* 24.2, p. 210.

Harré, Michael S and Zaitouny, Ayham (2023). 'Detecting criticality in complex univariate time-series: A case study of the US housing market crisis and other markets'. *Expert Systems with Applications* 211, p. 118437.

Harvey, David I, Leybourne, Stephen J, Sollis, Robert and Taylor, AM Robert (2016). 'Tests for explosive financial bubbles in the presence of non-stationary volatility'. *Journal of Empirical Finance* 38, pp. 548–574.

Havlin, Shlomo and Ben-Avraham, Daniel (1987). 'Diffusion in disordered media'. *Advances in physics* 36.6, pp. 695–798.

He, Xinjiang and Chen, Wenting (2014). 'The pricing of credit default swaps under a generalized mixed fractional Brownian motion'. *Physica A: Statistical Mechanics and its Applications* 404, pp. 26–33.

Hendrickson, Joshua R. and Luther, William J. (2017). 'Banning bitcoin'. *Journal of Economic Behavior & Organization* 141, pp. 188–195. ISSN: 0167-2681. DOI: https://doi.org/10.1016/j.jebo.2017.07.001. URL: https://www.sciencedirect.com/science/article/pii/S0167268117301798.

Henriques, Irene and Sadorsky, Perry (2018). 'Can Bitcoin replace gold in an investment portfolio?' *Journal of Risk and Financial Management* 11.3, p. 48. ISSN: 1911-8074.

Hong, KiHoon (2017). 'Bitcoin as an alternative investment vehicle'. *Information Technology and Management* 18.4, pp. 265–275. ISSN: 1573-7667. DOI: 10.1007/s10799-016-0264-6. URL: https://doi.org/10.1007/s10799-016-0264-6.

Horvatic, Davor, Stanley, H Eugene and Podobnik, Boris (2011). 'Detrended cross-correlation analysis for non-stationary time series with periodic trends'. *EPL (Europhysics Letters)* 94.1, p. 18007.

Hu, Albert S., Parlour, Christine A. and Rajan, Uday (2019). 'Cryptocurrencies: Stylized facts on a new investible instrument'. *Financial Management* 48.4, pp. 1049–1068. ISSN: 0046-3892. DOI: 10.1111/fima.12300.

Hu, Kun, Ivanov, Plamen Ch, Chen, Zhi, Carpena, Pedro and Stanley, H Eugene (2001). 'Effect of trends on detrended fluctuation analysis'. *Physical Review E* 64.1, p. 011114.

Huang, Wei, Shen, Zheng, Huang, Norden E and Fung, Yuan Cheng (1998). 'Engineering analysis of biological variables: an example of blood pressure over 1 day'. *Proceedings of the National Academy of Sciences* 95.9, pp. 4816–4821.

Hurst, Harold Edwin (1951). 'Long-term storage capacity of reservoirs'. *Transactions of the American society of civil engineers* 116.1, pp. 770–799.

Ihlen, Espen (2012). 'Introduction to Multifractal Detrended Fluctuation Analysis in Matlab'. *Frontiers in Physiology* 3. ISSN: 1664-042X. DOI: 10.3389/fphys.2012.00141. URL: https://www.frontiersin.org/articles/10.3389/fphys.2012.00141.

Itô, Kiyosi (1951). 'On a formula concerning stochastic differentials'. *Nagoya Mathematical Journal* 3.none, pp. 55–65, 11.

Ivanov, Plamen Ch, Ma, Qianli DY, Bartsch, Ronny P, Hausdorff, Jeffrey M, Amaral, Luís A Nunes, Schulte-Frohlinde, Verena, Stanley, H Eugene and Yoneyama, Mitsuru (2009). 'Levels of complexity in scale-invariant neural signals'. *Physical Review E* 79.4, p. 041920.

Jentsch, Carsten and Rao, Suhasini Subba (2015). 'A test for second order stationarity of a multivariate time series'. *Journal of Econometrics* 185.1, pp. 124–161.

Jiang, Yonghong, Nie, He and Ruan, Weihua (2018). 'Time-varying long-term memory in Bitcoin market'. *Finance Research Letters* 25, pp. 280–284. ISSN: 1544-6123. DOI: https://doi.org/10.1016/j.frl.2017.12.009. URL: https://www.sciencedirect.com/science/article/pii/S1544612317306682.

Jin, Xiaoye (2017). 'Time-varying return-volatility relation in international stock markets'. *International Review of Economics & Finance* 51, pp. 157–173.

Johnson, Neil F., Jefferies, Paul. and Hui, Pak Ming. (2003). *Financial market complexity*. eng. New York: Oxford University Press. ISBN: 0198526652.

Jondeau, Eric, Poon, Ser-Huang and Rockinger, Michael (2007). *Financial Modeling Under Non-Gaussian Distributions*. eng. Springer Finance. London: Springer London. ISBN: 9781846284199.

Kakinaka, Shinji and Umeno, Ken (2022). 'Cryptocurrency market efficiency in short- and long-term horizons during COVID-19: An asymmetric multifractal analysis approach'. *Finance Research Letters* 46, p. 102319. ISSN: 1544-6123. DOI: https://doi.org/10.1016/j.frl.2021.102319. URL: https://www.sciencedirect.com/science/article/pii/S1544612321003469.

Kaldor, Nicholas (1961). 'Capital Accumulation and Economic Growth'. Palgrave Macmillan UK, pp. 177–222. DOI: 10.1007/978-1-349-08452-4_10. URL: https://dx.doi.org/10.1007/978-1-349-08452-4_10.

Kale, M. and Butar Butar, Ferry (2011). 'Fractal analysis of time series and distribution properties of Hurst exponent'. *Journal of Mathematical Sciences and Mathematics Education* 5, pp. 8–19.

Kamaruzaman, Anis Farhan, Zain, Azlan Mohd, Yusuf, Suhaila Mohamed and Udin, Amirmudin (2013). 'Levy flight algorithm for optimization problems-a literature review'. *Applied mechanics and materials* 421, pp. 496–501. ISSN: 1662-7482.

Kantelhardt, Jan W, Ashkenazy, Yosef, Ivanov, Plamen Ch, Bunde, Armin, Havlin, Shlomo, Penzel, Thomas, Peter, Jörg-Hermann and Stanley, H Eugene (2002a). 'Characterization of sleep stages by correlations in the magnitude and sign of heartbeat increments'. *Physical Review E* 65.5, p. 051908.

Kantelhardt, Jan W, Koscielny-Bunde, Eva, Rego, Henio HA, Havlin, Shlomo and Bunde, Armin (2001). 'Detecting long-range correlations with detrended fluctuation analysis'. *Physica A: Statistical Mechanics and its Applications* 295.3-4, pp. 441–454.

Kantelhardt, Jan W, Zschiegner, Stephan A, Koscielny-Bunde, Eva, Havlin, Shlomo, Bunde, Armin and Stanley, H Eugene (2002b). 'Multifractal detrended fluctuation analysis of nonstationary time series'. *Physica A: Statistical Mechanics and its Applications* 316.1-4, pp. 87–114.

— (2002c). 'Multifractal detrended fluctuation analysis of nonstationary time series'. *Physica A: Statistical Mechanics and its Applications* 316.1-4, pp. 87–114. ISSN: 0378-4371. DOI:

10.1016/s0378-4371(02)01383-3. URL: https://dx.doi.org/10.1016/s0378-4371(02)01383-3.

— (2002d). 'Multifractal detrended fluctuation analysis of nonstationary time series'. *Physica A: Statistical Mechanics and its Applications* 316.1-4, pp. 87–114. ISSN: 0378-4371. DOI: 10.1016/s0378-4371(02)01383-3. URL: https://dx.doi.org/10.1016/s0378-4371(02)01383-3.

Karaa, Rabaa, Slim, Skander, Goodell, John W., Goyal, Abhinav and Kallinterakis, Vasileios (2021). 'Do investors feedback trade in the Bitcoin—and why?' *The European Journal of Finance*. doi: 10.1080/1351847X.2021.1973054, pp. 1–21. ISSN: 1351-847X. DOI: 10.1080/1351847X.2021.1973054. URL: https://doi.org/10.1080/1351847X.2021.1973054.

Kasdin, N Jeremy (1995). 'Discrete simulation of colored noise and stochastic processes and 1/f/sup/spl alpha//power law noise generation'. *Proceedings of the IEEE* 83.5, pp. 802–827.

Katugampola, Udita N (2014). 'A new fractional derivative with classical properties'. *arXiv preprint arXiv:1410.6535*.

Kendall, M. G. and Hill, A. Bradford (1953). 'The Analysis of Economic Time-Series-Part I: Prices'. *Journal of the Royal Statistical Society. Series A (General)* 116.1, pp. 11–34. ISSN: 00359238. URL: http://www.jstor.org/stable/2980947 (visited on 13/02/2024).

Kian, Yavar, Soccorsi, Eric and Yamamoto, Masahiro (2018). 'On time-fractional diffusion equations with space-dependent variable order'. *Annales Henri Poincaré*. Vol. 19-12. Springer, pp. 3855–3881.

Klein, Tony, Pham Thu, Hien and Walther, Thomas (2018). 'Bitcoin is not the New Gold – A comparison of volatility, correlation, and portfolio performance'. *International Review of Financial Analysis* 59, pp. 105–116. ISSN: 1057-5219. DOI: 10.1016/j.irfa.2018.07.010. URL: https://dx.doi.org/10.1016/j.irfa.2018.07.010.

Kleinow, Torsten (2002). 'Testing continuous time models in financial markets'. PhD thesis. Humboldt-Universität zu Berlin, Wirtschaftswissenschaftliche Fakultät. DOI: http://dx.doi.org/10.18452/14770.

Koponen, Ismo (July 1995). 'Analytic approach to the problem of convergence of truncated Lévy flights towards the Gaussian stochastic process'. *Phys. Rev. E* 52 (1), pp. 1197–1199. DOI: 10.1103/PhysRevE.52.1197. URL: https://link.aps.org/doi/10.1103/PhysRevE.52.1197.

Koutmos, Gregory and Saidi, Reza (2001). 'Positive feedback trading in emerging capital markets'. *Applied Financial Economics* 11.3, pp. 291–297.

Krečar, Nikola, Gubina, Andrej F and Božič, Gregor (2011). 'A method for calibration of a fundamental model of electricity price'. *2011 8th International Conference on the European Energy Market (EEM)*. IEEE, pp. 105–109.

Krenk, Steen, Madsen, Henrik O and Madsen, Peter H (1983). 'Stationary and transient response envelopes'. *Journal of Engineering Mechanics* 109.1, pp. 263–277.

Kristoufek, Ladislav and Vosvrda, Miloslav (2014a). 'Commodity futures and market efficiency'. *Energy Economics* 42, pp. 50–57.

— (2014b). 'Measuring capital market efficiency: long-term memory, fractal dimension and approximate entropy'. *The European Physical Journal B* 87.7. ISSN: 1434-6028. DOI: 10.1140/epjb/e2014-50113-6. URL: https://dx.doi.org/10.1140/epjb/e2014-50113-6.

Kumar, Rajesh (2016). '2 - Risk and return'. *Valuation*. Ed. by Rajesh Kumar. San Diego: Academic Press, pp. 47–72. ISBN: 978-0-12-802303-7. DOI: https://doi.org/10.1016/B978-0-12-802303-7.00002-4. URL: https://www.sciencedirect.com/science/article/pii/B9780128023037000024.

Kuo Chuen, David LEE, Guo, Li and Wang, Yu (2018). 'Cryptocurrency: A New Investment Opportunity?' *The Journal of Alternative Investments* 20.3, pp. 16–40. DOI: 10.3905/jai.2018.20.3.016.

Kurihara, Yutaka and Fukushima, Akio (2017). 'The market efficiency of Bitcoin: a weekly anomaly perspective'. *Journal of Applied Finance and Banking* 7.3, p. 57. ISSN: 1792-6580.

Labit, B, Furno, I, Fasoli, A, Diallo, A, Müller, SH, Plyushchev, G, Podestá, M and Poli, FM (2007). 'Universal statistical properties of drift-interchange turbulence in TORPEX plasmas'. *Physical review letters* 98.25, p. 255002.

Lahiri, Avijit (2016). 'Chapter 7 - Optical Coherence: Statistical Optics'. *Basic Optics*. Ed. by Avijit Lahiri. Amsterdam: Elsevier, pp. 605–696. ISBN: 978-0-12-805357-7. DOI: https://doi.org/10.1016/B978-0-12-805357-7.00007-1. URL: https://www.sciencedirect.com/science/article/pii/B9780128053577000071.

Lahmiri, Salim and Bekiros, Stelios (2018). 'Chaos, randomness and multi-fractality in Bitcoin market'. *Chaos, Solitons & Fractals* 106, pp. 28–34. ISSN: 0960-0779. DOI: https://doi.org/10.1016/j.chaos.2017.11.005. URL: https://www.sciencedirect.com/science/article/pii/S0960077917304605.

Lan, Boon Leong, Yeoh, Ee Von and Ng, Jin Aun (2010). 'Distribution of detrended stock market data'. *Fluctuation and Noise Letters* 9.03, pp. 245–257.

Langevin, Paul (1908). 'Sur la théorie du mouvement brownien'. *Compt. Rendus* 146, pp. 530–533.

Le Tran, Vu and Leirvik, Thomas (2020). 'Efficiency in the markets of crypto-currencies'. *Finance Research Letters* 35, p. 101382.

Lee, Minhyuk, Song, Jae Wook, Park, Ji Hwan and Chang, Woojin (2017). 'Asymmetric multi-fractality in the U.S. stock indices using index-based model of A-MFDFA'. *Chaos, Solitons & Fractals* 97, pp. 28–38. ISSN: 0960-0779. DOI: https://doi.org/10.1016/j.chaos.2017.02.001. URL: https://www.sciencedirect.com/science/article/pii/S0960077917300280.

Lévy, Paul (1954). *Theorie de l'addition des variables aleatoires.* fre. 2me ed. Monographies des probabilités : calcul des probabilités et ses applications. Paris: Gauthier-Villars.

Li, Chunguang and Chen, Guanrong (2004). 'Chaos and hyperchaos in the fractional-order Rössler equations'. *Physica A: Statistical Mechanics and its Applications* 341, pp. 55–61.

Liesenfeld, Roman and Jung, Robert C. (2000). 'Stochastic Volatility Models: Conditional Normality versus Heavy-Tailed Distributions'. *Journal of Applied Econometrics* 15.2, pp. 137–160. ISSN: 08837252, 10991255. URL: http://www.jstor.org/stable/2678528.

Lim, Seonkyu, Park, Jaehyeon, Kim, Seojin, Wi, Hyowon, Lim, Haksoo, Jeon, Jinsung, Choi, Jeongwhan and Park, Noseong (2023). 'Long-term Time Series Forecasting based on

Decomposition and Neural Ordinary Differential Equations'. *2023 IEEE International Conference on Big Data (BigData)*. IEEE, pp. 748–757.

Liu, Yanhui, Gopikrishnan, Parameswaran, Stanley, H Eugene et al. (1999). 'Statistical properties of the volatility of price fluctuations'. *Physical review e* 60.2, p. 1390.

Liu, Zhenhai, Zeng, Shengda and Bai, Yunru (2016). 'Maximum principles for multi-term space-time variable-order fractional diffusion equations and their applications'. *Fractional Calculus and Applied Analysis* 19.1, pp. 188–211.

Lo, Andrew W (1991). 'Long-term memory in stock market prices'. *Econometrica: Journal of the Econometric Society*, pp. 1279–1313.

Løvsletten, Ola (2017). 'Consistency of detrended fluctuation analysis'. *Physical Review E* 96.1, p. 012141.

Lux, Thomas (1996). 'The stable Paretian hypothesis and the frequency of large returns: an examination of major German stocks'. *Applied financial economics* 6.6, pp. 463–475. ISSN: 0960-3107.

Maganini, Natália Diniz, Da Silva Filho, Antônio Carlos and Lima, Fabiano Guasti (2018). 'Investigation of multifractality in the Brazilian stock market'. *Physica A: Statistical Mechanics and its Applications* 497, pp. 258–271.

Magin, Richard L, Abdullah, Osama, Baleanu, Dumitru and Zhou, Xiaohong Joe (2008). 'Anomalous diffusion expressed through fractional order differential operators in the Bloch–Torrey equation'. *Journal of Magnetic Resonance* 190.2, pp. 255–270.

Malamud, Bruce (Dec. 2003). 'Tails of natural hazards'. *Physics World* 17, pp. 31–35. DOI: 10.1088/2058-7058/17/8/35.

Mali, Provash and Mukhopadhyay, Amitabha (2014). 'Multifractal characterization of gold market: A multifractal detrended fluctuation analysis'. *Physica A: Statistical Mechanics and its Applications* 413, pp. 361–372. ISSN: 0378-4371. DOI: https://doi.org/10.1016/j.physa.2014.06.076.

Malkiel, Burton G. (1989). 'Efficient Market Hypothesis'. Palgrave Macmillan UK, pp. 127–134. DOI: 10.1007/978-1-349-20213-3_13. URL: https://dx.doi.org/10.1007/978-1-349-20213-3_13.

Malmsten, Hans and Teräsvirta, Timo (2010). 'Stylized facts of financial time series and three popular models of volatility'. *European Journal of pure and applied mathematics* 3.3, pp. 443–477. ISSN: 1307-5543.

Mandelbrot, B.B. (2001). 'Scaling in financial prices: IV. Multifractal concentration'. *Quantitative Finance* 1.6, pp. 641–649. DOI: 10.1088/1469-7688/1/6/306. eprint: https://doi.org/10.1088/1469-7688/1/6/306. URL: https://doi.org/10.1088/1469-7688/1/6/306.

Mandelbrot, Benoît (1963). 'The Variation of Certain Speculative Prices'. *The Journal of Business* 36. URL: https://EconPapers.repec.org/RePEc:ucp:jnlbus:v:36:y:1963:p:394.

Mandelbrot, Benoit (1967). 'The Variation of Some Other Speculative Prices'. *The Journal of Business* 40.4, pp. 393–413. ISSN: 00219398, 15375374. URL: http://www.jstor.org/stable/2351623 (visited on 14/02/2024).

Mandelbrot, Benoit and Taylor, Howard M. (1967). 'On the Distribution of Stock Price Differences'. *Operations Research* 15.6, pp. 1057–1062. ISSN: 0030364X, 15265463. URL: http://www.jstor.org/stable/168611 (visited on 13/02/2024).

Mandelbrot, Benoit B (1982). *The fractal geometry of nature*. Vol. 1. WH freeman New York.

— (1997). 'Discontinuity and scaling: their scope and likely limitations'. *Fractals and Scaling in Finance: Discontinuity, Concentration, Risk. Selecta Volume E*, pp. 50–78.

— (1999). 'A multifractal walk down Wall Street'. *Scientific American* 280.2, pp. 70–73.

Mandelbrot, Benoit B and Hudson, Richard L (2010). *The (mis) behaviour of markets: a fractal view of risk, ruin and reward*. Profile books.

Mandelbrot, Benoit B and Van Ness, John W (1968). 'Fractional Brownian motions, fractional noises and applications'. *SIAM review* 10.4, pp. 422–437.

Mantegna, Rosario N and Stanley, H Eugene (1999). *Introduction to econophysics: correlations and complexity in finance*. Cambridge university press. ISBN: 1139431226.

— (1994). 'Stochastic Process with Ultraslow Convergence to a Gaussian: The Truncated Lévy Flight'. *Physical Review Letters* 73.22, pp. 2946–2949. ISSN: 0031-9007. DOI: 10.1103/physrevlett.73.2946. URL: https://dx.doi.org/10.1103/physrevlett.73.2946.

Mantegna, Rosario N. and Stanley, H. Eugene (1995). 'Scaling behaviour in the dynamics of an economic index'. *Nature* 376.6535, pp. 46–49. ISSN: 0028-0836. DOI: 10.1038/376046a0. URL: https://dx.doi.org/10.1038/376046a0.

— (1996). 'Turbulence and financial markets'. *Nature* 383.6601, pp. 587–588. ISSN: 1476-4687. DOI: 10.1038/383587a0. URL: https://doi.org/10.1038/383587a0.

— (1997). 'Econophysics: Scaling and its breakdown in finance'. *Journal of Statistical Physics* 89.1, pp. 469–479. ISSN: 1572-9613. DOI: 10.1007/BF02770777. URL: https://doi.org/10.1007/BF02770777.

Marano, Giuseppe Carlo (2019). 'Non-stationary stochastic modulation function definition based on process energy release'. *Physica A: Statistical Mechanics and its Applications* 517, pp. 280–289.

Marathe, Rahul R and Ryan, Sarah M (2005). 'On the validity of the geometric Brownian motion assumption'. *The Engineering Economist* 50.2, pp. 159–192.

Mardoukhi, Yousof, Jeon, Jae-Hyung and Metzler, Ralf (2015). 'Geometry controlled anomalous diffusion in random fractal geometries: looking beyond the infinite cluster'. *Physical Chemistry Chemical Physics* 17.44, pp. 30134–30147.

Marian, Omri (2013). 'Are Cryptocurrencies Super Tax Havens? Commentaries'. *Michigan Law Review First Impressions* 112, pp. 38–48.

Márton, LF, Brassai, ST, Bakó, L and Losonczi, L (2014). 'Detrended fluctuation analysis of EEG signals'. *Procedia Technology* 12, pp. 125–132.

Matacz, Andrew (1997). *Financial Modeling and Option Theory with the Truncated Levy Process*. arXiv: cond-mat/9710197 [cond-mat.stat-mech].

McCabe, Caitlin (2020). *Dow Industrials Close 1,000 Points Lower as Coronavirus Cases Mount*. URL: https://www.wsj.com/articles/stocks-fall-as-coronavirus-spread-accelerates-outside-china-11582533308 (visited on 23/02/2024).

McCauley, Joseph L. (2008). 'Time vs. ensemble averages for nonstationary time series'. *Physica A: Statistical Mechanics and its Applications* 387.22, pp. 5518–5522. ISSN: 0378-4371. DOI: 10.1016/j.physa.2008.05.057. URL: https://dx.doi.org/10.1016/j.physa.2008.05.057.

Meng, Xiangyi, Zhang, Jian-Wei and Guo, Hong (2016). 'Quantum Brownian motion model for the stock market'. *Physica A: Statistical Mechanics and its Applications* 452, pp. 281–288.

Meng, Xiangyi, Zhang, Jian-Wei, Xu, Jingjing and Guo, Hong (2015). 'Quantum spatial-periodic harmonic model for daily price-limited stock markets'. *Physica A: Statistical Mechanics and its Applications* 438, pp. 154–160.

Metzler, Ralf, Barkai, Eli and Klafter, Joseph (1999). 'Anomalous diffusion and relaxation close to thermal equilibrium: A fractional Fokker-Planck equation approach'. *Physical review letters* 82.18, p. 3563.

Metzler, Ralf, Glöckle, Walter G and Nonnenmacher, Theo F (1994). 'Fractional model equation for anomalous diffusion'. *Physica A: Statistical Mechanics and its Applications* 211.1, pp. 13–24.

Metzler, Ralf, Jeon, Jae-Hyung, Cherstvy, Andrey G and Barkai, Eli (2014). 'Anomalous diffusion models and their properties: non-stationarity, non-ergodicity, and ageing at the centenary of single particle tracking'. *Physical Chemistry Chemical Physics* 16.44, pp. 24128–24164.

Metzler, Ralf and Klafter, Joseph (2000). 'The random walk's guide to anomalous diffusion: a fractional dynamics approach'. *Physics reports* 339.1, pp. 1–77.

Michael, Fredrick and Johnson, MD (2003). 'Derivative pricing with non-linear Fokker–Planck dynamics'. *Physica A: Statistical Mechanics and its Applications* 324.1-2, pp. 359–365.

Mnif, Emna and Jarboui, Anis (2021). 'COVID-19, bitcoin market efficiency, herd behaviour'. *Review of Behavioral Finance* 13.1, pp. 69–84. ISSN: 1940-5979. DOI: 10.1108/rbf-09-2020-0233. URL: https://dx.doi.org/10.1108/rbf-09-2020-0233.

Mnif, Emna, Jarboui, Anis and Mouakhar, Khaireddine (2020). 'How the cryptocurrency market has performed during COVID 19? A multifractal analysis'. *Finance Research Letters* 36, p. 101647. ISSN: 1544-6123. DOI: https://doi.org/10.1016/j.frl.2020.101647. URL: https://www.sciencedirect.com/science/article/pii/S1544612320306346.

Montasser, Ghassen El, Charfeddine, Lanouar and Benhamed, Adel (2022). 'COVID-19, cryptocurrencies bubbles and digital market efficiency: sensitivity and similarity analysis'. *Finance Research Letters* 46, p. 102362. ISSN: 1544-6123. DOI: https://doi.org/10.1016/j.frl.2021.102362. URL: https://www.sciencedirect.com/science/article/pii/S1544612321003652.

Montillet, Jean-Philippe and Yu, Kegen (2015). 'Modeling Geodetic Processes with Levy alpha-Stable Distribution and FARIMA'. *Mathematical geosciences* 47.6, pp. 627–646.

Mukhopadhyay, Ujan, Skjellum, Anthony, Hambolu, Oluwakemi, Oakley, Jon, Yu, Lu and Brooks, Richard (2016). 'A brief survey of cryptocurrency systems'. *2016 14th annual conference on privacy, security and trust (PST)*. IEEE, pp. 745–752.

Müller, Ulrich A, Dacorogna, Michel M, Olsen, Richard B, Pictet, Olivier V, Schwarz, Matthias and Morgenegg, Claude (1990). 'Statistical study of foreign exchange rates, empirical evidence of a price change scaling law, and intraday analysis'. *Journal of Banking & Finance* 14.6, pp. 1189–1208. ISSN: 0378-4266.

Murray, James D. (1993). 'Epidemic Models and the Dynamics of Infectious Diseases'. Springer Berlin Heidelberg, pp. 610–650. DOI: 10.1007/978-3-662-08542-4_19. URL: https://dx.doi.org/10.1007/978-3-662-08542-4_19.

Mynhardt, H. R., Plastun, Alex and Makarenko, Inna (2014). 'Behavior of Financial Markets Efficiency During the Financial Market Crisis: 2007-2009'. *Corporate Ownership and Control* 11.2F, pp. 531–546.

Nakamoto, Satoshi (2008). *A peer-to-peer electronic cash system*. URL: https://bitcoin.org/en/bitcoin-paper.

Nava, Noemi, Di Matteo, Tiziana and Aste, Tomaso (2016). 'Time-dependent scaling patterns in high frequency financial data'. *The European Physical Journal Special Topics* 225.10, pp. 1997–2016.

Ncheuguim, Emmanuel Kengni, Appiah-Kubi, Seth and Ofori-Dankwa, Joseph (2014). 'The Truncated Levy Flight Model: A Comparative Analysis of Its Utility in Modeling the Standard and Poor's 500 and the Ghana Stock Exchange'. *Advancing research methodology in the African Context: Techniques, methods, and designs*. Emerald Group Publishing Limited, pp. 215–233.

Niu, Hongli and Wang, Jun (2013). 'Volatility clustering and long memory of financial time series and financial price model'. *Digital Signal Processing* 23.2, pp. 489–498.

Noam, Eli (2021). *The Macro-Economics of Crypto-Currencies: The Role of Private Moneys in Monetary Policy*. 23rd ITS Biennial Conference, Online Conference / Gothenburg 2021. Digital societies and industrial transformations: Policies, markets, and technologies in a post-Covid world 238043. International Telecommunications Society (ITS). URL: https://ideas.repec.org/p/zbw/itsb21/238043.html.

Noda, Akihiko (2021). 'On the evolution of cryptocurrency market efficiency'. *Applied Economics Letters* 28.6, pp. 433–439. ISSN: 1350-4851. DOI: 10.1080/13504851.2020.1758617. URL: https://dx.doi.org/10.1080/13504851.2020.1758617.

Nofsinger, John R and Prucyk, Brian (2003). 'Option volume and volatility response to scheduled economic news releases'. *Journal of Futures Markets: Futures, Options, and Other Derivative Products* 23.4, pp. 315–345.

Nounou, Mohamed N. and Bakshi, Bhavik R. (2000). 'Chapter 5 - Multiscale Methods for Denoising and Compression'. *Wavelets in Chemistry*. Ed. by Beata Walczak. Vol. 22. Data Handling in Science and Technology. Elsevier, pp. 119–150. DOI: https://doi.org/10.1016/S0922-3487(00)80030-1. URL: https://www.sciencedirect.com/science/article/pii/S0922348700800301.

Nystrup, Peter, Madsen, Henrik and Lindström, Erik (2015). 'Stylised facts of financial time series and hidden Markov models in continuous time'. *Quantitative Finance* 15.9, pp. 1531–1541. ISSN: 1469-7688. DOI: 10.1080/14697688.2015.1004801. URL: https://dx.doi.org/10.1080/14697688.2015.1004801.

O'Shaughnessy, Ben and Procaccia, Itamar (1985). 'Analytical solutions for diffusion on fractal objects'. *Physical review letters* 54.5, p. 455.

Oh, Gabjin, Kim, Seunghwan and Eom, Cheoljun (2008). 'Long-term memory and volatility clustering in high-frequency price changes'. *Physica A: Statistical Mechanics and its Applications* 387.5, pp. 1247–1254. ISSN: 0378-4371. DOI: https://doi.org/10.1016/j.physa.2007.08.061. URL: https://www.sciencedirect.com/science/article/pii/S0378437107011351.

Oldham, Keith and Spanier, Jerome (1974). *The Fractional Calculus Theory and Applications of Differentiation and Integration to Arbitrary Order*. 1st ed. Vol. v.Volume 111. Mathematics in science and engineering. San Diego: Elsevier Science & Technology. ISBN: 9780125255509.

Oliveira, Fernando A., Ferreira, Rogelma M. S., Lapas, Luciano C. and Vainstein, Mendeli H. (2019). 'Anomalous Diffusion: A Basic Mechanism for the Evolution of Inhomogeneous Systems'. *Frontiers in Physics* 7. ISSN: 2296-424X. DOI: 10.3389/fphy.2019.00018. URL: https://www.frontiersin.org/articles/10.3389/fphy.2019.00018.

Oliveira Filho, FM, Cruz, JA Leyva and Zebende, GF (2019). 'Analysis of the EEG biosignals during the reading task by DFA method'. *Physica A: Statistical Mechanics and its Applications* 525, pp. 664–671.

Önalan, Ömer (2004). 'Self-similarity and multifractality in financial asset returns'. *1st International Conference on Computational Finance and its Applications*. Bologna, Italy, pp. 289–295.

Onnela, J-P, Chakraborti, Anirban, Kaski, Kimmo and Kertesz, Janos (2003a). 'Dynamic asset trees and Black Monday'. *Physica A: Statistical Mechanics and its Applications* 324.1-2, pp. 247–252.

Onnela, J-P, Chakraborti, Anirban, Kaski, Kimmo, Kertesz, Janos and Kanto, Antti (2003b). 'Dynamics of market correlations: Taxonomy and portfolio analysis'. *Physical Review E* 68.5, p. 056110.

Onnela, Jukka-Pekka, Chakraborti, Anirban, Kaski, Kimmo, Kertesz, Janos and Kanto, Antti (2003c). 'Asset trees and asset graphs in financial markets'. *Physica Scripta* 2003.T106, p. 48.

Pamuk, Serdal (2005). 'Solution of the porous media equation by Adomian's decomposition method'. *Physics Letters A* 344.2-4, pp. 184–188.

Pekalski, Andrzej and Sznajd-Weron, Katarzyna (1999). *Anomalous diffusion: From basics to applications*. Springer.

Peng, C-K, Buldyrev, Sergey V, Havlin, Shlomo, Simons, Michael, Stanley, H Eugene and Goldberger, Ary L (1994). 'Mosaic organization of DNA nucleotides'. *Physical review e* 49.2, p. 1685.

Plastino, A.R. and Plastino, A. (1995). 'Non-extensive statistical mechanics and generalized Fokker-Planck equation'. *Physica A: Statistical Mechanics and its Applications* 222.1, pp. 347–354. ISSN: 0378-4371. DOI: https://doi.org/10.1016/0378-4371(95)00211-1. URL: https://www.sciencedirect.com/science/article/pii/0378437195002111.

Plastino, Angel R and Wedemann, Roseli S (2020). 'Nonlinear Fokker–Planck equation approach to systems of interacting particles: thermostatistical features related to the range of the interactions'. *Entropy* 22.2, p. 163.

Plerou, Vasiliki, Gopikrishnan, Parameswaran, Amaral, Luis A Nunes, Meyer, Martin and Stanley, H Eugene (1999). 'Scaling of the distribution of price fluctuations of individual companies'. *Physical review e* 60.6, p. 6519.

plummets, MicroStrategy (2000). *Shares fall more than 60 percent on earnings, revenue restatement*. URL: https://money.cnn.com/2000/03/20/companies/microstrategy/ (visited on 11/08/2020).

Politi, Mauro, Millot, Nicolas and Chakraborti, Anirban (2012). 'The near-extreme density of intraday log-returns'. *Physica A: Statistical Mechanics and its Applications* 391.1-2, pp. 147–155.

Ponta, Linda, Trinh, Mailan, Raberto, Marco, Scalas, Enrico and Cincotti, Silvano (2019). 'Modeling non-stationarities in high-frequency financial time series'. *Physica A: Statistical Mechanics and its Applications* 521, pp. 173–196.

Popper, N. (2016). *Digital Gold: Bitcoin and the Inside Story of the Misfits and Millionaires Trying to Reinvent Money*. HarperCollins. ISBN: 9780062572066. URL: https://books.google.com.au/books?id=rafFCwAAQBAJ.

Puech, L and Rammal, R (1983). 'Fractal geometry and anomalous diffusion in the backbone of percolation clusters'. *Journal of Physics C: Solid State Physics* 16.35, p. L1197.

Queirós, S. M. Duarte (2005). 'On non-Gaussianity and dependence in financial time series: a nonextensive approach'. *Quantitative Finance* 5.5. doi: 10.1080/14697680500244403, pp. 475–487. ISSN: 1469-7688. DOI: 10.1080/14697680500244403. URL: https://doi.org/10.1080/14697680500244403.

Quirós, Fernando and Vazquez, Juan Luis (1999). 'Asymptotic behaviour of the porous media equation in an exterior domain'. *Annali della Scuola Normale Superiore di Pisa-Classe di Scienze* 28.2, pp. 183–227.

Rangarajan, Govindan and Ding, Mingzhou (2000). 'Integrated approach to the assessment of long range correlation in time series data'. *Physical Review E* 61.5, p. 4991.

Rao, BLS Prakasa (2016). 'Pricing geometric Asian power options under mixed fractional Brownian motion environment'. *Physica A: Statistical Mechanics and its Applications* 446, pp. 92–99.

Rejichi, Imen Zgueb and Aloui, Chaker (2012). 'Hurst exponent behavior and assessment of the MENA stock markets efficiency'. *Research in International Business and Finance* 26.3, pp. 353–370. ISSN: 0275-5319. DOI: https://doi.org/10.1016/j.ribaf.2012.01.005. URL: https://www.sciencedirect.com/science/article/pii/S0275531912000062.

Ren, Louie, Ren, Peter and Glasure, Yong (2018). 'On the different forms of returns from moving average buy-sell trading rule in the stock market'. *Benchmarking: An International Journal* 25.1, pp. 253–258.

Renn, Jüregen. (2005). 'Einstein's invention of Brownian motion'. *Annalen der Physik* 14.S1. istex:ED68F05FAEF2D9DCE416DA47E8916FD4B4908D02, pp. 23–37. ISSN: 0003-3804. DOI: 10.1002/andp.200410131.

Richardson, Lewis Fry (1926). 'Atmospheric diffusion shown on a distance-neighbour graph'. *Proceedings of the Royal Society of London. Series A, Containing Papers of a Mathematical and Physical Character* 110.756, pp. 709–737.

Risken, Hannes (1996). 'Fokker-Planck Equation'. *The Fokker-Planck Equation: Methods of Solution and Applications*. Ed. by Hannes Risken. Berlin, Heidelberg: Springer Berlin Heidelberg, pp. 63–95. ISBN: 978-3-642-61544-3. DOI: 10.1007/978-3-642-61544-3_4. URL: https://doi.org/10.1007/978-3-642-61544-3_4.

Roman, HE, Porto, M and Dose, C (2008). 'Skewness, long-time memory, and non-stationarity: application to leverage effect in financial time series'. *EPL (Europhysics Letters)* 84.2, p. 28001.

Ross, Bertram (1974). *Fractional calculus and its applications: proceedings of the international conference held at the University of New Haven, June 1974*. Vol. 457. Springer.

Ruiz, G and Marcos, AF de (2018). 'Evidence for criticality in financial data'. *The European Physical Journal B* 91, pp. 1–5.

Rydén, Tobias, Teräsvirta, Timo and Åsbrink, Stefan (1998). 'Stylized Facts of Daily Return Series and the Hidden Markov Model'. *Journal of Applied Econometrics* 13.3, pp. 217–244. ISSN: 08837252, 10991255. URL: http://www.jstor.org/stable/223228.

Salinas, Silvio (2001). *Introduction to statistical physics*. Springer Science & Business Media.

Samko, Stefan G, Kilbas, Anatoly A, Marichev, Oleg I et al. (1993). *Fractional integrals and derivatives*. Vol. 1. Gordon and breach science publishers, Yverdon Yverdon-les-Bains, Switzerland.

Samorodnitsky, Gennady et al. (2007). 'Long range dependence'. *Foundations and Trends® in Stochastic Systems* 1.3, pp. 163–257.

Sánchez-Granero, M. J., Fernández-Martínez, M. and Trinidad-Segovia, J. E. (2012). 'Introducing fractal dimension algorithms to calculate the Hurst exponent of financial time series'. *The European Physical Journal B* 85.3. ISSN: 1434-6028. DOI: 10.1140/epjb/e2012-20803-2. URL: https://dx.doi.org/10.1140/epjb/e2012-20803-2.

Santamaria, Fidel, Wils, Stefan, De Schutter, Erik and Augustine, George J (2006). 'Anomalous diffusion in Purkinje cell dendrites caused by spines'. *Neuron* 52.4, pp. 635–648.

Saxton, Michael J (2007). 'A biological interpretation of transient anomalous subdiffusion. I. Qualitative model'. *Biophysical journal* 92.4, pp. 1178–1191.

Scalas, Enrico and Kim, Kyungsik (2006). 'The art of fitting financial time series with Levy stable distributions'. *arXiv preprint physics/0608224*.

Schafer, Ronald W (2011). 'What is a Savitzky-Golay filter?[lecture notes]'. *IEEE Signal processing magazine* 28.4, pp. 111–117.

Schmidt, Anatoly B. (2011). *Financial markets and trading an introduction to market microstructure and trading strategies*. eng. 1st edition. Wiley finance ; 637. Hoboken, N.J: Wiley. ISBN: 1-118-09365-8.

Schneider, Walter R and Wyss, Walter (1989). 'Fractional diffusion and wave equations'. *Journal of Mathematical Physics* 30.1, pp. 134–144.

Segnon, Mawuli and Bekiros, Stelios (2020). 'Forecasting volatility in bitcoin market'. *Annals of Finance* 16.3, pp. 435–462.

Sentana, Enrique and Wadhwani, Sushil (1992). 'Feedback Traders and Stock Return Autocorrelations: Evidence from a Century of Daily Data'. *The Economic Journal* 102.411, pp. 415–425. ISSN: 00130133, 14680297. DOI: 10.2307/2234525. URL: http://www.jstor.org/stable/2234525.

Shakeel, Moonis and Srivastava, Bhavana (2018). 'Stylized Facts of High-frequency Financial Time Series Data'. *Global Business Review* 22.2, pp. 550–564. ISSN: 0972-1509. DOI: 10.1177/0972150918811701. URL: https://doi.org/10.1177/0972150918811701.

Shrestha, Keshab (2021). 'Multifractal detrended fluctuation analysis of return on Bitcoin'. *International Review of Finance* 21.1, pp. 312–323. ISSN: 1369-412X.

Smoluchowski, M Von (1916). 'Drei vortrage uber diffusion, brownsche molekularbewegung und koagulation von kolloidteilchen'. *Z. Physik.* 17, pp. 585–599.

Sokolov, Igor M and Klafter, Joseph (2005). 'From diffusion to anomalous diffusion: a century after Einstein's Brownian motion'. *Chaos: An Interdisciplinary Journal of Nonlinear Science* 15.2, p. 026103.

Solomon, TH, Weeks, Eric R and Swinney, Harry L (1993). 'Observation of anomalous diffusion and Lévy flights in a two-dimensional rotating flow'. *Physical Review Letters* 71.24, p. 3975.

Sornette, Didier (2003). 'Critical market crashes'. *Physics reports* 378.1, pp. 1–98.

Sposini, Vittoria, Krapf, Diego, Marinari, Enzo, Sunyer, Raimon, Ritort, Felix, Taheri, Fereydoon, Selhuber-Unkel, Christine, Benelli, Rebecca, Weiss, Matthias, Metzler, Ralf and

Oshanin, Gleb (2022a). 'Towards a robust criterion of anomalous diffusion'. *Communications Physics* 5.1. ISSN: 2399-3650. DOI: 10.1038/s42005-022-01079-8. URL: https://dx.doi.org/10.1038/s42005-022-01079-8.

— (2022b). 'Towards a robust criterion of anomalous diffusion'. *Communications Physics* 5.1, p. 305. ISSN: 2399-3650. DOI: 10.1038/s42005-022-01079-8. URL: https://doi.org/10.1038/s42005-022-01079-8.

Stanley, H.E., Gopikrishnan, P, Plerou, V and Amaral, LAN (2000). 'Quantifying fluctuations in economic systems by adapting methods of statistical physics'. *Physica A: Statistical Mechanics and its Applications* 287.3-4, pp. 339–361. ISSN: 0378-4371.

Stanley, HE, Amaral, LAN, Buldyrev, Sergey V, Gopikrishnan, P, Plerou, V and Salinger, MA (2002). 'Self-organized complexity in economics and finance'. *Proceedings of the National Academy of Sciences* 99.suppl. 1, pp. 2561–2565. ISSN: 0027-8424.

Stărică, Cătălin and Granger, Clive (2005). 'Nonstationarities in stock returns'. *Review of economics and statistics* 87.3, pp. 503–522.

Stoyanov, Stoyan V., Rachev, Svetlozar T., Racheva-Yotova, Boryana and Fabozzi, Frank J. (2011). 'Fat-Tailed Models for Risk Estimation'. *The Journal of Portfolio Management* 37.2, pp. 107–117. ISSN: 0095-4918. DOI: 10.3905/jpm.2011.37.2.107. URL: https://dx.doi.org/10.3905/jpm.2011.37.2.107.

Sun, HongGuang, Chen, Wen and Chen, YangQuan (2009). 'Variable-order fractional differential operators in anomalous diffusion modeling'. *Physica A: Statistical Mechanics and its Applications* 388.21, pp. 4586–4592.

Takaishi, Tetsuya (2018). 'Statistical properties and multifractality of Bitcoin'. *Physica A: Statistical Mechanics and its Applications* 506, pp. 507–519. ISSN: 0378-4371. DOI: https://doi.org/10.1016/j.physa.2018.04.046. URL: https://www.sciencedirect.com/science/article/pii/S0378437118304771.

Tang, Yaoyue, Arias-Calluari, Karina, Harré, Michael S. and Alonso-Marroquin, Fernando (2024a). *Stylized Facts of High-Frequency Bitcoin Time Series*. arXiv: 2402.11930 [q-fin.ST].

Tang, Yaoyue, Gharari, Fatemeh, Arias-Calluari, Karina, Alonso-Marroquin, Fernando and Najafi, M. N. (Feb. 2024b). 'Variable-order porous media equations: Application on modeling the S&P500 and Bitcoin price return'. *Phys. Rev. E* 109 (2), p. 024310. DOI: 10.1103/PhysRevE.109.024310. URL: https://link.aps.org/doi/10.1103/PhysRevE.109.024310.

Telesca, Luciano, Lapenna, Vincenzo and Macchiato, Maria (2004). 'Mono-and multi-fractal investigation of scaling properties in temporal patterns of seismic sequences'. *Chaos, Solitons & Fractals* 19.1, pp. 1–15.

Teodoro, G Sales, Machado, JA Tenreiro and De Oliveira, E Capelas (2019). 'A review of definitions of fractional derivatives and other operators'. *Journal of Computational Physics* 388, pp. 195–208.

Thäle, Christoph (2009). 'Further remarks on mixed fractional Brownian motion'. *Applied Mathematical Sciences* 38, pp. 1885–1901.

Toker, Daniel, Sommer, Friedrich T and D'Esposito, Mark (2020). 'A simple method for detecting chaos in nature'. *Communications biology* 3.1, pp. 1–13.

Tsallis, Constantino (1988). 'Possible generalization of Boltzmann-Gibbs statistics'. *Journal of Statistical Physics* 52.1, pp. 479–487. ISSN: 1572-9613. DOI: 10.1007/BF01016429. URL: https://doi.org/10.1007/BF01016429.

— (2017). 'Economics and Finance: q-Statistical stylized features galore'. *Entropy* 19.9, p. 457.

Tsallis, Constantino, Anteneodo, Celia, Borland, Lisa and Osorio, Roberto (2003). 'Nonextensive statistical mechanics and economics'. *Physica A: Statistical Mechanics and its Applications* 324.1-2, pp. 89–100. ISSN: 0378-4371.

Tsallis, Constantino and Arenas, Zochil Gonzalez (2014). 'Nonextensive statistical mechanics and high energy physics'. *EPJ Web of Conferences*. Vol. 71. EDP Sciences, p. 00132.

Tsallis, Constantino and Bukman, Dirk Jan (1996). 'Anomalous diffusion in the presence of external forces: Exact time-dependent solutions and their thermostatistical basis'. *Physical Review E* 54.3, R2197.

Tsay, Ruey S. (2005). *Analysis of Financial Time Series*. eng. Hoboken, NJ, USA: John Wiley & Sons, Inc. ISBN: 9780471690740.

Tschorsch, Florian and Scheuermann, Bjorn (2016). 'Bitcoin and Beyond: A Technical Survey on Decentralized Digital Currencies'. *IEEE Communications Surveys & Tutorials* 18.3, pp. 2084–2123. ISSN: 1553-877X. DOI: 10.1109/comst.2016.2535718. URL: https://dx.doi.org/10.1109/comst.2016.2535718.

Turcotte, Donald L. (2003). 'Tectonophysics'. *Encyclopedia of Physical Science and Technology (Third Edition)*. Ed. by Robert A. Meyers. New York: Academic Press, pp. 499–511. ISBN: 978-0-12-227410-7. DOI: https://doi.org/10.1016/B0-12-227410-5/00763-8. URL: https://www.sciencedirect.com/science/article/pii/B0122274105007638.

Umarov, Sabir and Constantino, Tsallis (2022). *Mathematical Foundations of Nonextensive Statistical Mechanics*. World Scientific.

Umarov, Sabir and Steinberg, Stanly (2009). 'Variable Order Differential Equations with Piecewise Constant Order-Function and Diffusion with Changing Modes'. *Zeitschrift für Analysis und ihre Anwendungen* 28.4, pp. 431–450.

Umarov, Sabir and Tsallis, Constantino (2007). 'On multivariate generalizations of the q-central limit theorem consistent with nonextensive statistical mechanics'. *AIP Conference Proceedings*. Vol. 965-1. American Institute of Physics, pp. 34–42.

Umarov, Sabir, Tsallis, Constantino, Gell-Mann, Murray and Steinberg, Stanly (2010). 'Generalization of symmetric $\alpha$-stable Lévy distributions for q> 1'. *Journal of mathematical physics* 51.3.

Umarov, Sabir, Tsallis, Constantino and Steinberg, Stanly (2008). 'On a q-central limit theorem consistent with nonextensive statistical mechanics'. *Milan journal of mathematics* 76.1, pp. 307–328.

Underwood, Sarah (2016). 'Blockchain beyond bitcoin'. *Communications of the ACM* 59.11, pp. 15–17. ISSN: 0001-0782. DOI: 10.1145/2994581. URL: https://dx.doi.org/10.1145/2994581.

Urquhart, Andrew (2016). 'The inefficiency of Bitcoin'. *Economics Letters* 148, pp. 80–82. ISSN: 0165-1765. DOI: https://doi.org/10.1016/j.econlet.2016.09.019. URL: https://www.sciencedirect.com/science/article/pii/S0165176516303640.

Vainstein, Mendeli H, Costa, Ismael VL and Oliveira, FA (2006). 'Mixing, Ergodicity and the Fluctuation-Dissipation Theorem in complex systems'. *Jamming, Yielding, and Irreversible Deformation in Condensed Matter*, pp. 159–188.

Vasconcelos, Giovani L (2004). 'A guided walk down wall street: an introduction to econophysics'. *Brazilian Journal of Physics* 34.3B, pp. 1039–1065.

Vilela, Marco, Halidi, Nadia, Besson, Sebastien, Elliott, Hunter, Hahn, Klaus, Tytell, Jessica and Danuser, Gaudenz (2013). 'Chapter Nine - Fluctuation Analysis of Activity Biosensor Images for the Study of Information Flow in Signaling Pathways'. *Fluorescence Fluctuation Spectroscopy (FFS), Part B*. Ed. by Sergey Y. Tetin. Vol. 519. Methods in Enzymology. Academic Press, pp. 253–276. DOI: https://doi.org/10.1016/B978-0-12-405539-1.00009-9. URL: https://www.sciencedirect.com/science/article/pii/B9780124055391000099.

Vogl, Markus (2023). 'Hurst exponent dynamics of S&P 500 returns: Implications for market efficiency, long memory, multifractality and financial crises predictability by application of a nonlinear dynamics analysis framework'. *Chaos, Solitons & Fractals* 166, p. 112884. ISSN: 0960-0779. DOI: https://doi.org/10.1016/j.chaos.2022.112884.

Voit, Johannes. (2005). *The Statistical Mechanics of Financial Markets*. eng. 3rd ed. 2005. Theoretical and Mathematical Physics. Berlin, Heidelberg: Springer Berlin Heidelberg. ISBN: 3-540-26289-X.

Vujičić, D., Jagodić, D. and Ranđić, S. (2018). 'Blockchain technology, bitcoin, and Ethereum: A brief overview'. *2018 17th International Symposium INFOTEH-JAHORINA (INFOTEH)*, pp. 1–6. DOI: 10.1109/INFOTEH.2018.8345547.

Walker, Andrew (2020). *US oil prices turn negative as demand dries up*. URL: https://www.bbc.com/news/business-52350082#:~:text=The%20price%20of%20US%20oil,world%20have%20kept%20people%20inside. (visited on 21/04/2020).

Wang, Fang, Liao, Gui-ping, Li, Jian-hui, Li, Xiao-chun and Zhou, Tie-jun (2013). 'Multifractal detrended fluctuation analysis for clustering structures of electricity price periods'. *Physica A: Statistical Mechanics and its Applications* 392.22, pp. 5723–5734. ISSN: 0378-4371. DOI: https://doi.org/10.1016/j.physa.2013.07.039.

URL: https://www.sciencedirect.com/science/article/pii/S0378437113006493.

Wang, Hong and Zheng, Xiangcheng (2019). 'Wellposedness and regularity of the variable-order time-fractional diffusion equations'. *Journal of Mathematical Analysis and Applications* 475.2, pp. 1778–1802.

Wang, Jing, Shang, Pengjian and Cui, Xingran (2014). 'Multiscale multifractal analysis of traffic signals to uncover richer structures'. *Physical Review E* 89.3, p. 032916.

Węglarczyk, Stanisław (2018). 'Kernel density estimation and its application'. *ITM Web of Conferences* 23, p. 00037. ISSN: 2271-2097. DOI: 10.1051/itmconf/20182300037. URL: https://dx.doi.org/10.1051/itmconf/20182300037.

Wen, Zhuzhu, Bouri, Elie, Xu, Yahua and Zhao, Yang (2022). 'Intraday return predictability in the cryptocurrency markets: Momentum, reversal, or both'. *The North American Journal of Economics and Finance* 62, p. 101733. ISSN: 1062-9408. DOI: https://doi.org/10.1016/j.najef.2022.101733. URL: https://www.sciencedirect.com/science/article/pii/S1062940822000833.

Weron, A. and Magdziarz, M. (2009). 'Anomalous diffusion and semimartingales'. *Europhysics Letters* 86.6, p. 60010. ISSN: 0295-5075. DOI: 10.1209/0295-5075/86/60010. URL: https://dx.doi.org/10.1209/0295-5075/86/60010.

West, Bruce J and Nonnenmacher, Theo (2001). 'An ant in a gurge'. *Physics Letters A* 278.5, pp. 255–259.

Witt, Annette, Kurths, Jürgen and Pikovsky, A (1998). 'Testing stationarity in time series'. *physical Review E* 58.2, p. 1800.

Xu, Dan and Beck, Christian (2016). 'Transition from lognormal to $\chi$2-superstatistics for financial time series'. *Physica A: Statistical Mechanics and its Applications* 453, pp. 173–183.

Xu, Limei, Ivanov, Plamen Ch, Hu, Kun, Chen, Zhi, Carbone, Anna and Stanley, H Eugene (2005). 'Quantifying signals with power-law correlations: A comparative study of detrended fluctuation analysis and detrended moving average techniques'. *Physical Review E* 71.5, p. 051101.

Yang, Xiao-Jun (2016). 'Fractional derivatives of constant and variable orders applied to anomalous relaxation models in heat-transfer problems'. *arXiv preprint arXiv:1612.03202*.

Yanovsky, VV, Chechkin, AV, Schertzer, D and Tur, AV (2000). 'Lévy anomalous diffusion and fractional Fokker–Planck equation'. *Physica A: Statistical Mechanics and its Applications* 282.1-2, pp. 13–34.

Zaghloul, E., Li, T., Mutka, M. W. and Ren, J. (2020). 'Bitcoin and Blockchain: Security and Privacy'. *IEEE Internet of Things Journal* 7.10, pp. 10288–10313. ISSN: 2327-4662. DOI: 10.1109/JIOT.2020.3004273.

Zhang, Wei, Wang, Pengfei, Li, Xiao and Shen, Dehua (2018a). 'Some stylized facts of the cryptocurrency market'. *Applied Economics* 50.55, pp. 5950–5965. ISSN: 0003-6846.

— (2018b). 'The inefficiency of cryptocurrency and its cross-correlation with Dow Jones Industrial Average'. *Physica A: Statistical Mechanics and its Applications* 510, pp. 658–670. ISSN: 0378-4371.

Appendix A

# Amendment to Figures

---

This appendix revises some figures in this thesis.

Figure A.1-a is a revised version of Figure 2.6-a, correcting fitting parameter $\gamma$ to $\gamma = 0.60 \pm 0.32$.

Figure 2.6-b is correct, also shown in Figure A.1-b. Here we add a comment that a jump in the correlation function is observed at $s = 30$ min. We classify this as a transition from q-Gaussian to Gaussian from 30 min to 1 hr due to the standardization process divided by sigma. We tried different window sizes for standardization and found that the rate of convergence to Gaussian is related to the window size.

Figure A.2 is a correction of Figure 2.13 in terms of the expression of errors in the fitting.

Figure A.3-a is a correction of Figure 2.14-a in terms of the expression of errors in the fitting.

Figure A.4 is a correction of Figure 2.15 in terms of the expression of errors in the fitting.

Figure A.5-a and A.5-b is a correction of Figure 3.8-a and 3.8-b in terms of the expression of errors in the fitting.

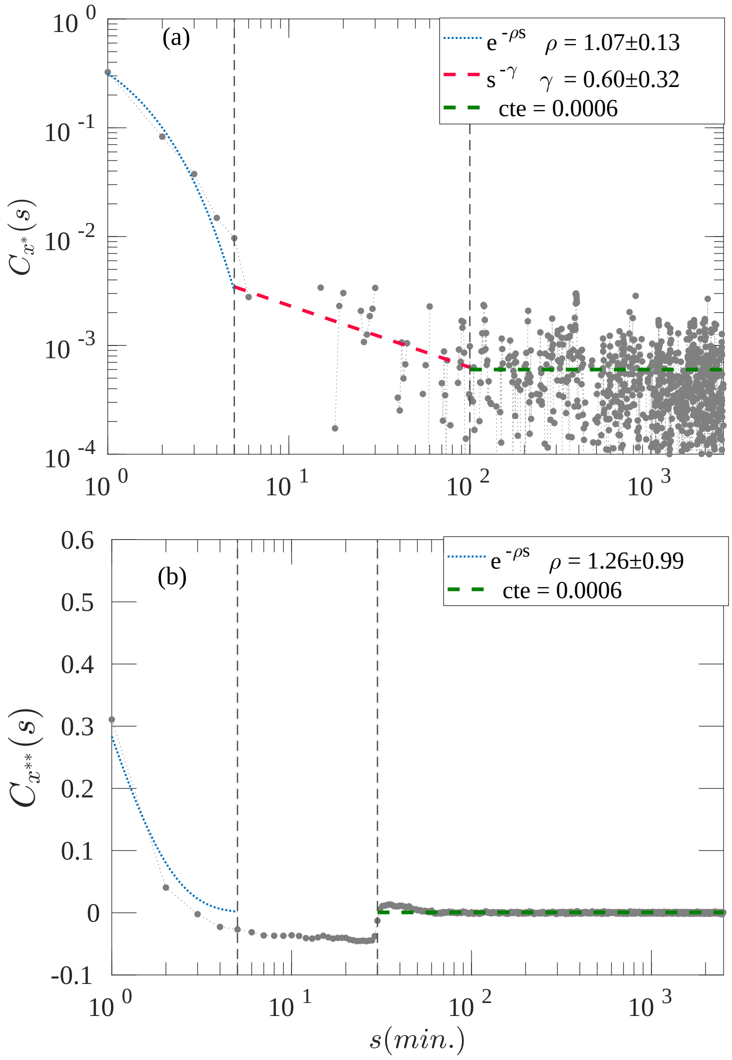


FIGURE A.1: Autocorrelation of the detrended price return calculated as $C_x(s) \equiv \dfrac{\langle x_t x_{t+s} \rangle}{\sigma_x^2}$. Short-time correlations are observed for the first $6$ minutes. A weak long-time correlation appears after $100$ minutes.

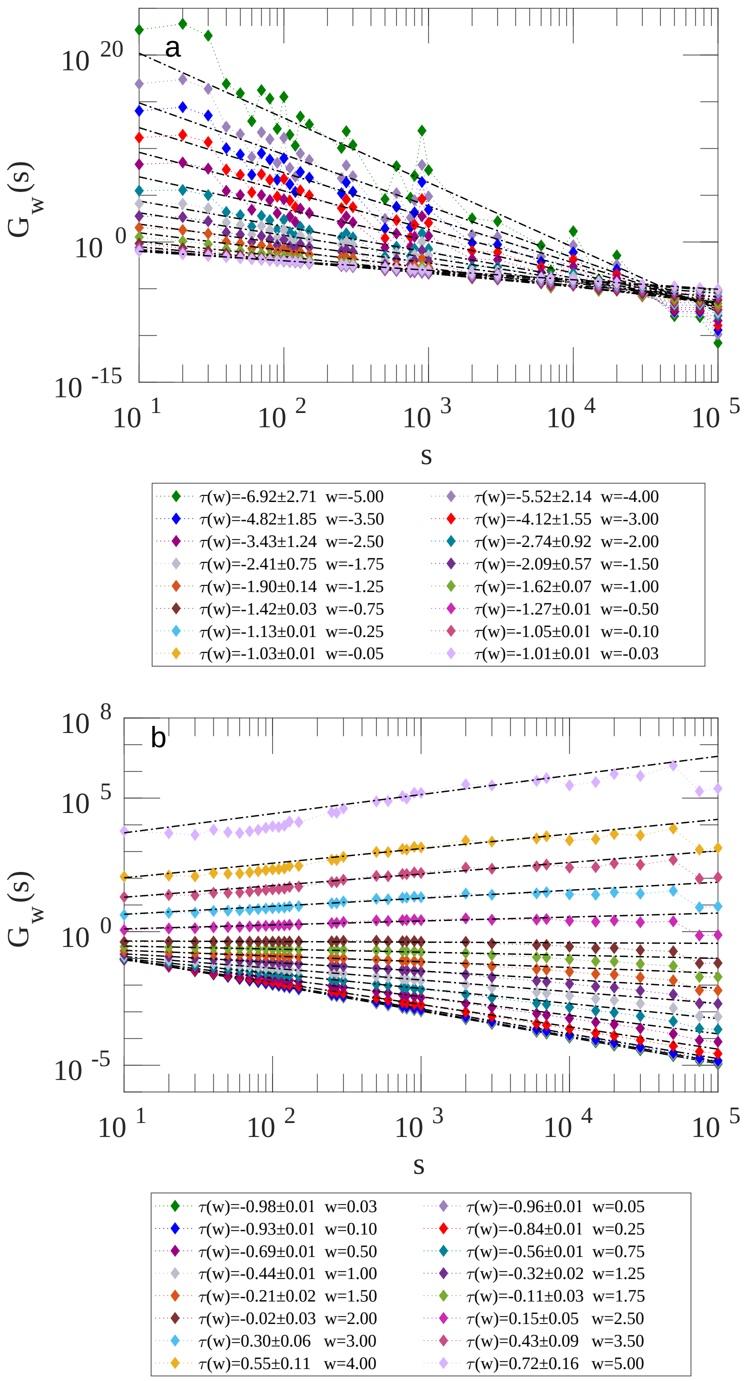


FIGURE A.2: Detrended price return case: Calculation of the “generalized statistical functions" $G_w(s)$ vs $s$ for negative (a) and positive (b) values of order w. The “generalized statistical functions" is calculated by applying Eq. (2.36).

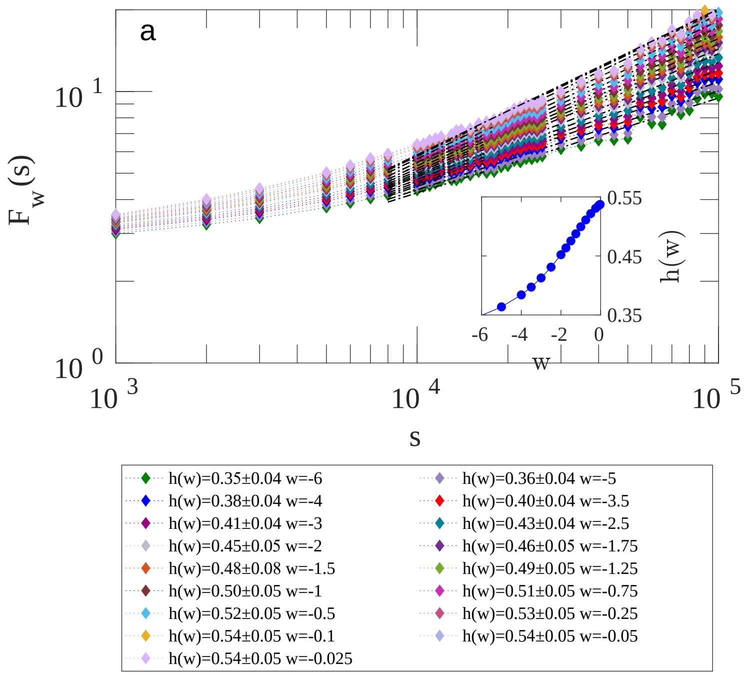


FIGURE A.3: Normalized price return case: Calculation of the statistical function $F_w$ using Eq. (2.31). The function of $F_w$ vs $s$ display power laws $F_w(s) \sim s^{h(w)}$, where $h(w)$ depend on $w$. This feature demonstrates that the time series is multifractal.

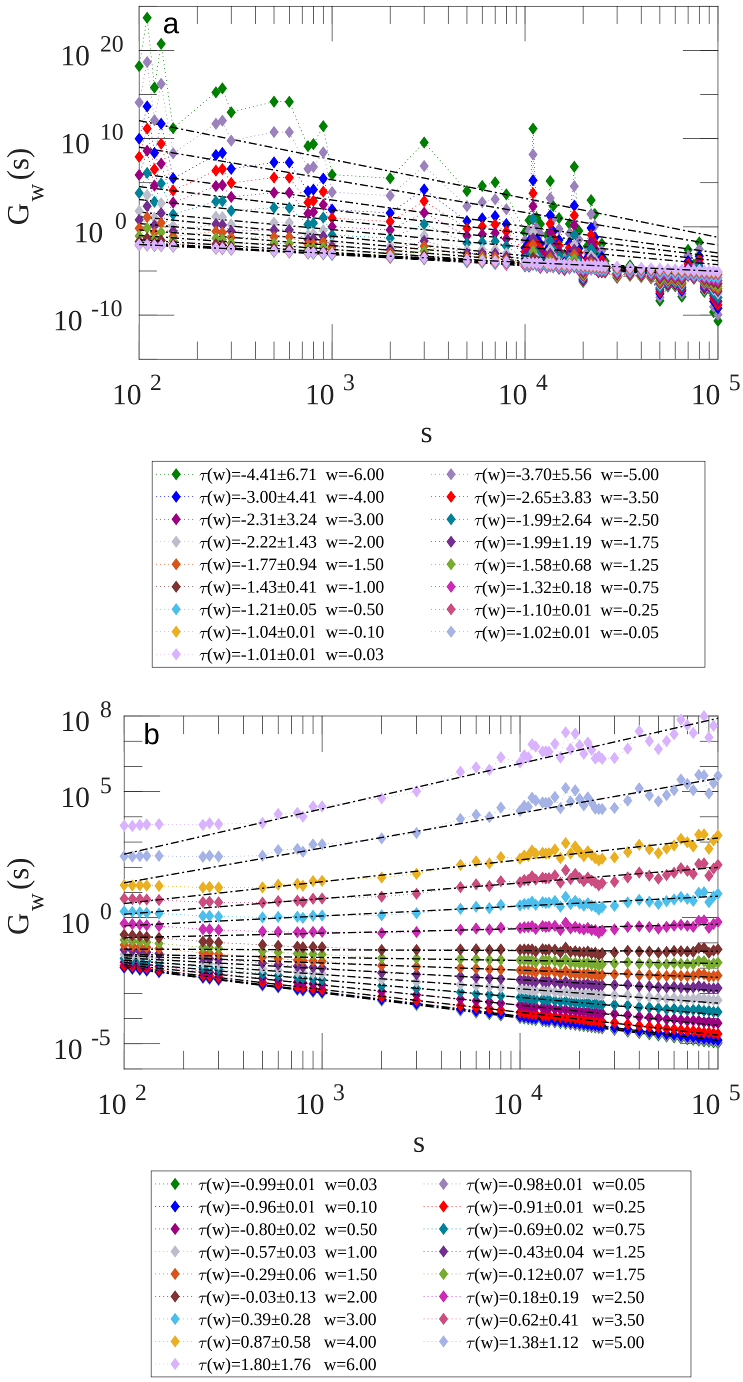


FIGURE A.4: Normalized price return case: Calculation of the “generalized statistical functions" $G_{\mathrm{w}}(s)$ vs $s$ for negative (a) and positive (b) values of order w. The “generalized statistical functions" is calculated by applying Eq. (2.36).

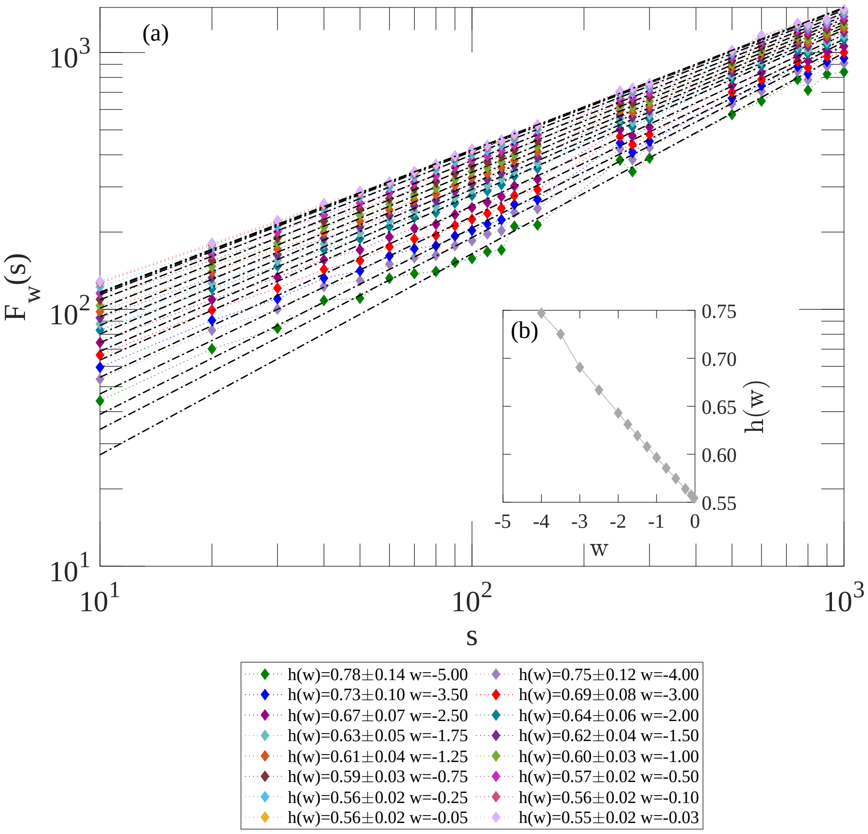


FIGURE A.5: Calculation of the statistical function $F_w$ on Bitcoin price return for Period 2 using Eq. (3.33). The function of $F_w$ vs $s$ display power laws $F_w(s) \sim s^{h(w)}$, where $h(w)$ depend on $w$. This feature demonstrates that the time series is multifractal. (a) Calculated $F_w(s)$ function with a negative range of $w$, each $w$ value presents a power-law relationship. (b) Profile of $h(w)$ for negative $w$ values.